

**Provenance study of the Early Iron Age  
Knobbed ware in Troia, NW Turkey  
and the Balkans.  
Petrographic and geochemical evidence**

Dissertation

zur Erlangung des Grades eines Doktors der Naturwissenschaften

der Geowissenschaftlichen Fakultät  
der Eberhard-Karls-Universität Tübingen

vorgelegt von  
Farkas Pintér  
aus Budapest

2005

Tag der mündlichen Prüfung: 20. 07. 2005

Dekan: Prof. Klaus G. Nickel, Ph.D.

1. Berichterstatter: Prof. Dr. Muharrem Satır

2. Berichterstatter: Prof. Dr. Ernst Pernicka

# TABLE OF CONTENTS

<b>Summary</b>	<b>7</b>
<b>Zusammenfassung</b>	<b>9</b>
<b>Összefoglalás</b>	<b>11</b>
<b>Acknowledgements</b>	<b>13</b>
<b>1. ARCHAEOLOGICAL EVIDENCE</b>	<b>16</b>
<b>2. IMPORTANCE AND AIM OF THE STUDY</b>	<b>21</b>
<b>3. OVERVIEW OF THE PREVIOUS RESEARCH IN POTTERY ANALYSES</b>	<b>22</b>
<b>3.1. Archaeometrical ceramic studies in Troia</b>	<b>25</b>
<b>4. SAMPLING AND ANALYTICAL METHODS</b>	<b>26</b>
<b>4.1. Sampling</b>	<b>26</b>
<b>4.2. Analytical methods</b>	<b>30</b>
4.2.1. Mineral separation	31
4.2.2. Petrographic analyses and cathodoluminescence investigation (CL)	32
4.2.3. X-ray diffractometry (XRD)	36
4.2.4. X-ray fluorescence spectroscopy (XRF)	38
4.2.5. Radiogenic isotopes ( $^{87}\text{Sr}/^{86}\text{Sr}$ , $^{143}\text{Nd}/^{144}\text{Nd}$ )	42
4.2.6. Electron microprobe analysis (EMPA)	45
4.2.7. Neutron Activation Analysis (NAA)	46
<b>5. MAIN GEOLOGICAL FEATURES OF THE STUDY AREAS</b>	<b>47</b>
<b>5.1. Introduction</b>	<b>47</b>
<b>5.2. The Troad</b>	<b>48</b>
<b>5.3. The Avşa Island and surrounding areas</b>	<b>51</b>
<b>5.4. The Thrace basin and its southern coast at the Sea of Marmara (Menekşe Çataği)</b>	<b>51</b>
<b>5.5. The south-western Strandja Massive (north Turkish Thrace and Ovcarovo)</b>	<b>53</b>
<b>5.6. The south-eastern Rhodope Mts. (Chal)</b>	<b>55</b>
<b>5.7. The southern Balkanides (Diadovo, Pshenitsevo, and Kirilovo)</b>	<b>57</b>
<b>5.8. The north-eastern Moesian platform (Sboriano)</b>	<b>59</b>
<b>6. RESULTS</b>	<b>62</b>
<b>6.1. Petrography, mineralogy and phase analysis</b>	<b>62</b>
<b>6.1.1. Petrographic analysis of the sherds and comparative materials</b>	<b>62</b>
6.1.1.1. <i>Troia</i>	65
6.1.1.1.1. Petrography of the comparative materials	65
6.1.1.1.2. Petrography of the sherds; Petrographic group 1	68
6.1.1.2. <i>The Avşa Island</i>	77
6.1.1.2.1. Petrography of the sherd; Petrographic group 2	77
6.1.1.3. <i>Menekşe Çataği East (MCE) and West (MCW)</i>	78
6.1.1.3.1. Petrography of the sherds; Petrographic group 3	78
6.1.1.4. <i>North Turkish Thrace</i>	83
6.1.1.4.1. Petrography of the comparative material	83
6.1.1.4.2. Petrography of the sherds; Petrographic group 4	83
6.1.1.5. <i>Ovcarovo</i>	88
6.1.1.5.1. Petrography of the sherds; Petrographic group 5	88

6.1.1.6. <i>Chal</i>	90
6.1.1.6.1. Petrography of the comparative material	90
6.1.1.6.2. Petrography of the sherds; Petrographic group 6	90
6.1.1.7. <i>Diadovo, Pshenitsevo, and Kirilovo</i>	92
6.1.1.7.1. Petrography of the comparative materials	92
6.1.1.7.2. Petrography of the sherds; Petrographic group 7	92
6.1.1.8. <i>Sborianovo</i>	96
6.1.1.8.1. Petrography of the sherds; Petrographic group 8	96
<b>6.1.2. Cathodoluminescence investigation</b>	<b>97</b>
<b>6.1.3. X-ray diffractometry</b>	<b>98</b>
6.1.3.1. <i>Sherds from Troia (TR-7, 12, 19, and 25)</i>	99
6.1.3.2. <i>Sherds from the Avşa Island and Menekşe Çataği (A-1, MCW-6, and MCE-1)</i>	100
6.1.3.3. <i>Sherds from north Turkish Thrace (AT-2, DH-2, HM, and YK-3)</i>	100
6.1.3.4. <i>Sherds from Chal (CH-1 and 3)</i>	101
6.1.3.5. <i>Sherds from Ovcarovo and Sborianovo (OVC-1, 4, and SBO-3)</i>	102
6.1.3.6. <i>Sherds from Diadovo, Pshenitsevo and Kirilovo (DIA-6, 13, PSH-2, and KIR-2)</i>	103
<b>6.2. Geochemical analyses</b>	<b>104</b>
<b>6.2.1. Geochemical composition of comparative sediments and the sherds</b>	<b>104</b>
6.2.1.1. <i>Comparative sediments and the sherds from Troia</i>	106
6.2.1.2. <i>Comparative sediments and the sherds from Menekşe Çataği</i>	113
6.2.1.3. <i>Comparative sediments and the sherds from north Turkish Thrace</i>	116
6.2.1.4. <i>Comparative sediments and the sherds from Ovcarovo</i>	119
6.2.1.5. <i>Comparative sediments and the sherds from Chal</i>	121
6.2.1.6. <i>Comparative sediments and the sherds from Diadovo-Pshenitsevo, and Kirilovo</i>	123
6.2.1.7. <i>Comparative sediments and the sherds from Sborianovo</i>	126
<b>6.2.2. Radiogenic isotopes</b>	<b>128</b>
6.2.2.1. <i>Troia</i>	128
6.2.2.2. <i>Menekşe Çataği</i>	129
6.2.2.3. <i>North Turkish Thrace</i>	129
6.2.2.4. <i>Chal</i>	129
6.2.2.5. <i>Diadovo-Pshenitsevo</i>	130
6.2.2.6. <i>Sborianovo</i>	131
<b>6.2.3. Electron microprobe analysis (EMPA)</b>	<b>132</b>
6.2.3.1. <i>Sample MCE-1 (Menekşe Çataği)</i>	132
6.2.3.2. <i>Sample AT-2 (north Turkish Thrace)</i>	134
<b>6.2.4. Neutron activation analysis (NAA)</b>	<b>139</b>
6.2.4.1. <i>The sherd from Troia (Tr-20)</i>	139
6.2.4.2. <i>Intermediate volcanite fragments from the sherd MCE-1 and the rock sample Mc-8 (Menekşe Çataği)</i>	140
<b>7. SUMMARY AND INTERPRETATION OF THE RESULTS</b>	<b>142</b>
<b>7.1. The origin of the Knobbed ware</b>	<b>143</b>
<b>7.1.1. Summary and interpretation of the petrographic and cathodoluminescence results</b>	<b>143</b>
7.1.1.1. <i>Troia</i>	143
7.1.1.2. <i>The Avşa Island</i>	146
7.1.1.3. <i>Menekşe Çataği</i>	147
7.1.1.4. <i>North Turkish Thrace</i>	148
7.1.1.5. <i>Ovcarovo</i>	148

7.1.1.6. <i>Chal</i>	149
7.1.1.7. <i>Diadovo-Pshenitsevo, Kirilovo</i>	149
7.1.1.8. <i>Sborianovo</i>	150
<b>7.1.2. Summary and interpretation of the chemical data of comparative sediments and the sherds</b>	<b>151</b>
7.1.2.1. <i>Troia</i>	151
7.1.2.2. <i>Menekşe Çatağı</i>	155
7.1.2.3. <i>North Turkish Thrace</i>	156
7.1.2.4. <i>Ovcarovo</i>	158
7.1.2.5. <i>Chal</i>	159
7.1.2.6. <i>Diadovo-Pshenitsevo, Kirilovo</i>	160
7.1.2.7. <i>Sborianovo</i>	161
<b>7.1.3. Summary and interpretation of the radiogenic isotope results</b>	<b>163</b>
<b>7.1.4. Summary and interpretation of the EMPA results</b>	<b>166</b>
<b>7.1.5. Summary and interpretation of the NAA results</b>	<b>168</b>
<b>7.1.6. The grouping of the sherds on the basis of their origin</b>	<b>169</b>
<b>7.2. The production technology of the Knobbed ware</b>	<b>170</b>
7.2.1. Possible raw materials used for the pottery production	170
7.2.2. Firing atmosphere of the sherds	172
7.2.3. Maximum firing temperatures of the sherds	173
<b>8. CONCLUSION AND DISCUSSION</b>	<b>176</b>
8.1. General conclusions	176
8.2. Archaeological discussion of the results	178
8.3. General observations concerning the provenance analysis of coarse wares	179
8.4. Open questions resulting from this study	180
<b>LITERATURE</b>	<b>182</b>
<b>APPENDICES</b>	
Appendix 1. Archaeological description and photographs of the sherds from Troia, Chal, Diadovo, Pshenitsevo, and Kirilovo.	192
Appendix 2. Geological samples analysed in this study.	200
Appendix 3. Petrographic modal composition of the Knobbed ware sherds analysed in this study	202
Appendix 4. Textural features of the Knobbed ware sherds analysed in this study	205
Appendix 5. Measured elements, number of the standards applied, standard deviation ( $3\sigma$ ), detection limit, and standard concentrations of the X-ray fluorescence (XRF) analysis	211
Appendix 6. X-ray fluorescence (XRF) data of geological samples	212
Appendix 7. X-ray fluorescence (XRF) data of the sherds	214
Appendix 8. Radiogenic isotope data of geological samples and the sherds analysed in this study	217
Appendix 9. Data of the electron microprobe analysis (EMPA) of the sherds MCE-1 and AT-2	218
Appendix 10. Data of the neutron activation analysis (NAA) of the sherd TR-20, the volcanite fragments in the sherd MCE-1, and the basalt sample Mc-8	220
Curriculum vitae	221



## Summary

At the beginning of the Early Iron Age in Troia, in the settlement phase VIIb2 (ca. 1100-1000 B.C.), new vessel forms (Knobbed ware or in German Buckelkeramik) of hand-made pottery appeared. The same vessel forms, with similar decoration can be found in several archaeological localities in Turkish Thrace and the Balkans (Bulgaria, SE-Romania). In this geoarchaeological work the primary question is whether there is a possible common origin of the pottery from different regions? Was the Knobbed ware in Troia transported from the Balkans, or do we have to do it with transfer of technological solutions, and the vessels were made on the spot from local material? Moreover, which raw materials and technique (firing temperatures, etc.) were used in producing the ceramics?

In order to answer these questions samples of 90 ceramic fragments and 69 comparative geological materials (clayey, silty, sandy sediments, rock fragments, etc.) have been collected from the most important archaeological sites and survey areas of the occurrence of the Knobbed ware: Troia, the Avşa Island, Menekşe Cataği, north Turkish Thrace (near Edirne) in Turkey, and Chal, Ovcarovo, Diadovo, Pshenitsevo, Kirilovo, and Sborianovo in Bulgaria. A complex analytical procedure employed in this study included optical microscopy (petrographic modal and cathodoluminescence), chemical (XRF, NAA, EMPA) radiogenic isotopes of  $^{87}\text{Sr}/^{86}\text{Sr}$  and  $^{143}\text{Nd}/^{144}\text{Nd}$ , and XRD (X-ray diffractometry) analyses.

In the first step the sherds have been grouped into eight petrographic groups and several subgroups based on their non-plastic inclusion (temper) composition.

Using the major and trace elements Mg, K, Rb, Ba, Sr, Nb, Ti, Y, Zr, Fe, V, Cr and Ni, bivariate plots and PAAS-normalised (post-Archaeon average Australian Shale) multi-element diagrams were edited in order to determine the local sediment patterns of the different areas based on clayey and sandy sediments (local reference materials), sampled near the archaeological sites.

Comparing the PAAS-normalised XRF data from the sherds to those of the local sediment patterns, using petrographic data as well as geological information of the different areas, I can conclude that most sherds seem to have affinities to local sediments in Troia and most archaeological sites discussed in this study. With the help of radiogenic isotopes I could chemically differentiate some more production locations, which could not be exactly identified using the XRF data. Neutron activation and electron microprobe analyses were used to analyse single rock or mineral fragments (temper) found in the sherds in order to compare their chemical properties to the results of former geochemical studies. Thus the results could be directly applied to those rocks and several effects (e.g. firing, alteration of a pottery), which might influence the results of the provenance analysis could be excluded.

The results of the provenance analysis, corresponding with several former archaeological studies, show that petrographic and chemical signals of 82 out of 90 vessel fragments fit well the natural properties of possible local raw materials at the archaeological places of this study, indicating that these potteries were, with high probability, locally produced. Three of six sherds from south Bulgaria

(Ovcarovo) show clear affinities with north Bulgarian (Sborianovo) vessel fragments and sediments, thus I assume that their place of origin was north Bulgaria and they were transported from there to the South. Complex archaeometrical analyses proved that five other fragments from north Turkish Thrace and Menekşe Cataği were not locally produced. In most cases, due to the absence of the comparative chemical and petrographic data, I could not determine the exact place of origin of the analysed sherds unequivocally, but several places could be excluded or, on the contrary, taken into consideration.

One of largest problems posed in this work was to filter the chemical influence of temper on chemical and isotope geochemical composition. I could show that sherds containing non-plastic inclusions or added temper rich in trace elements (e.g. volcanites, magmatites), can influence the whole chemical composition of the (clayey) raw material of the sherds, and thus complicate the interpretation of the data. Consequently, in case of coarse wares, only the combined use of petrographic and geochemical analyses can give the effective provenance.

On the basis of microscopic textural analysis I can establish that raw materials used for the ceramic production were mainly silty-sandy clays and/or river sediments. The use of very fine-grained clays or levigated materials can be excluded. By means of the clay mineral content (XRD data) analysed sherds were grouped into three groups, indicating each one different, but relatively low maximum firing temperature: in case of chlorite content: (550) 600-650 °C, 10Å phyllosilicate and calcite content: 700-750 °C, and 10Å phyllosilicate content: 800-850 °C. Firing-cooling procedure took place mostly under reducing atmosphere, the fact reflected by the greyish-black colour of the samples.

## Zusammenfassung

Am Anfang der Früheisenzeit tauchen in Troia in der Siedlungsphase VIIb2 (ca. 1100-1000 v.Chr.) neue Gefäßformen handgemachter Keramik (Buckelkeramik) auf. Dieselben Gefäßformen mit ähnlicher Dekoration kann man in zahlreichen archäologischen Plätzen in türkisch Thrakien und auf dem Balkan (Bulgarien, SO-Rumänen) finden. In dieser geoarchäologischen Arbeit ist die wichtigste Frage, ob eine gemeinsame Herkunft der Buckelkeramik aus verschiedenen Regionen möglich ist? Ist die Buckelkeramik aus dem Balkan nach Troia transportiert worden, haben wir es nur mit dem Transfer der Herstellungstechnik zu tun, oder ist die Keramik vor Ort aus lokalen Materialien produziert worden? Eine andere Frage dieser Arbeit ist, welche Rohmaterialien und Technik (Brenntemperatur, usw.) für die Keramikherstellung benutzt wurden?

Um diese Fragen zu beantworten wurden 90 Keramikfragmente und 69 geologische Proben (hauptsächlich sandige Tone und Schlamm) von den wichtigsten archäologischen Orten, wo Buckelkeramik gefunden sind (Troia, Insel Avşa, Menekşe Cataği, nördliche Türkischthrakien in der Türkei bzw. Chal, Ovcarovo, Diadovo, Pshenitsevo, Kirilovo and Sborianovo in Bulgarien), gesammelt. Die in der Arbeit durchgeführten Untersuchungen umfassen die folgenden Methoden: mikroskopische (modale) Analyse und Kathodolumineszenz, chemische Analysen (Röntgenfluoreszenz-Analyse (RFA), Neutronaktivierungs-Analyse (NAA), Mikrosonde-Analyse (EMPA) und radiogene Isotopen Untersuchungen ( $^{87}\text{Sr}/^{86}\text{Sr}$  und  $^{143}\text{Nd}/^{144}\text{Nd}$ ), bzw. Röntgendiffraktometrie (XRD).

Als erster Schritt wurden die untersuchten Scherben, anhand ihrer Magerung, in acht petrographische Gruppen und mehrere Subgruppen klassifiziert.

Mit der Hilfe der Elemente Mg, K, Rb, Ba, Sr, Nb, Ti, Y, Zr, Fe, V, Cr und Ni bezogen auf PAAS (post-Archaean average Australian Shale) wurden Multielement-Diagramme erstellt, um die lokale chemischen Eigenschaften der geologischen Proben (Tone, Sande, usw.) verschiedenen archäologischen Orten und ihren Umgebung identifizieren zu können

Zusätzlich und ergänzend zu den petrographischen Ergebnissen wurden chemische Daten von Sedimenten und Scherben verglichen, dadurch konnten Informationen über die Herkunft des archäologischen Materials erhalten werden. Die Unterschiede in der Konzentration und Verteilung mancher Elementen (z.B. K, Rb, Sr, Ba, usw.) kann mit dem Verhalten (Mobilität/Immobilität, Löslichkeit) sowie mit sekundären Prozessen (z.B. Alteration) erklärt werden. Radiogene Isotopenverhältnisse von Sr und Nd können weitere wichtige Ergebnisse zur Differenzierung der Scherben geben.

Anhand der chemischen und der Isotopendaten, sowie der petrographischen Ergebnisse der Scherben, verglichen mit den Ergebnissen der lokalen Rohmaterialien, kann abgeleitet werden, dass 82 von 90 der Gefäßen (mit großer Wahrscheinlichkeit) lokal produziert sind. Drei Scherben aus Südbulgarien

(Ovcarovo) zeigen eindeutige Affinität zu den lokalen Sedimenten, sowie den Scherben aus Nordbulgarien (Sborianovo). Damit kann abgeleitet werden, dass diese Gefäßstücke aus dem Norden Bulgariens nach Süden transportiert wurden. Zusätzliche Untersuchungen zeigten auch, dass weitere fünf Scherben aus Nord Thrakien und Menekşe Cataği sicherlich nicht lokal produziert sind. Sowohl petrographische als auch geochemische Untersuchungen ergeben keine zuverlässigen Informationen über ihren Herkunftsort. Dies könnte entweder mit ähnlichem geologischem Aufbau der untersuchten Regionen, oder mit mangelnder Probenanzahl erklärt werden.

Außerdem konnte gezeigt werden, dass spurenelementreiche Magerung (z.B. von Vulkaniten, Magmatiten), die gesamtchemische Zusammensetzung des tonigen Materials der Scherben signifikant beeinflussen und die Interpretation der Daten erschweren kann. Deshalb können im Falle von Grobwaren, nur die kombinierte Anwendung petrographischer und chemischer Analysen aussagekräftige Information über Herkunftsbestimmung liefern.

Anhand des Tonmineral-Gehaltes (XRD Daten) der analysierten Scherben konnten drei verschiedenen Gruppen eingeteilt werden, die alle verschiedene, aber relativ niedrige maximale Brenntemperaturen indizierten. Dies sind im Fall von Chlorit-Gehalt:  $T_{\max}$ : (550) 600-650 °C, bei Gegenwart Präsenz von 10Å Phyllosilikat (Illit-Muskovit) und Kalzit  $T_{\max}$ : 700-750 °C, mit 10Å Phyllosilikat-Gehalt  $T_{\max}$ : 800-850 °C. Das Brennen der Keramik hat am meisten unter reduzierenden Bedingungen stattgefunden, was auch die grau-schwarze Farbe der Scherben erklärt.

## Összefoglalás

A kora vaskor kezdetén a trójai (Kisázsia) VIIIb2-es településszintben (kb. Kr.e. 1100-1000) egy addig ismeretlen, kézzel formázott kerámiatípus jelenik meg (Knobbed ware, Buckelkeramik). Azonos formájú edénytöredékek, hasonló díszítéssel számos régészeti lelőhelyen megtalálhatóak az adott korból Trákia törökországi részén, valamint a Balkánon, elsősorban DK-Románia és Bulgária területén. A disszertáció elsődleges célkitűzése, hogy kiderítse van-e közös lelőhelye a különböző ásatásokról előkerült kerámia töredékeknek; a Trójában előkerült töredékek a kerámiának a Balkánról való eredetére utalnak, vagy csak a készítési technológia „vándorolt” és az edényeket helyben, helyi nyersanyagokból készítették? Továbbá milyen nyersanyagokat és technológiát (égetési hőmérséklet) alkalmaztak a készítésük során?

A feltett kérdések megválaszolására a régészetileg kiemelkedő fontosságú ásatásokról (Törökországban: Trója, Avşa-sziget, Menekşe Cataği, Észak-Trákia, valamint Bulgáriában Chal, Ovcarovo, Diadovo, Pshenitsevo, Kirilovo és Sborianovo lelőhelyekről) 90 cseréptöredéket, valamint a kémiai-petrográfiai összehasonlító vizsgálatokhoz 69 üledék- (agyagos, homokos üledékek, stb.) és kőzetmintát gyűjtöttem be. A vizsgálatok petrográfiai mikroszkópos és katódlumineszcens megfigyelésekből, kémiai analízisből (RFA, NAA, mikroszonda) radiogén izotópos mérésekből ( $^{87}\text{Sr}/^{86}\text{Sr}$  és  $^{143}\text{Nd}/^{144}\text{Nd}$ ) és röntgendiffrakciós fázisanalízisből (XRD) álltak.

A régészeti töredékeket először a kőzettani megfigyelések és soványítóanyag tartalmuk alapján, nyolc fő- és számos alcsoportba soroltam be. A kémiai összehasonlító vizsgálatok alapját a régészeti lelőhelyek környékéről begyűjtött üledékminták képezték. Tizenhárom fő- és nyomelem (Mg, K, Rb, Ba, Sr, Nb, Ti, Y, Zr, Fe, V, Cr és Ni) felhasználásával a mért adatokat kétváltozós, ill. PAAS-ra (post-Archaeon average Australian Shale) normalizált sokelemes diagramok segítségével meghatároztam a vizsgált területekre és üledékekre jellemző kémiai szignálokat.

A kerámia töredékek szintén PAAS-ra normalizált kémiai adatai a helyi üledékszignálokhoz hasonlítva, valamint a petrográfia csoportosítás eredményeivel kiegészítve alkották az eredethatározás fő gerincét. Néhány mobilis elem (K, Rb, Sr, Ba stb.) értékeiben mutatkozó eltérések és anomáliák valószínűleg másodlagos (kilúgzás, mállás, talajoldatok, stb.) és/vagy a soványító anyag befolyásoló hatására voltak visszavezethetők.

A radiogén izotóp analízis segítségével számos esetben a teljes kémiai mérések alapján létrehozott csoportosítást tudtam továbbfinomítani.

A neutronaktivációs analízist és a mikroszonda elemzés eredményeit a soványító anyag egyedi ásvány- és kőzetszemcséinek az elemzésére használtam fel, így lehetőség nyílt a kapott adatokat közvetlenül a geológiai szakirodalomban rendelkezésre álló helyi és a környéken előforduló kőzetek adataival összevetni, ami által kikerülhettem a teljesminta-elemzésben rejlő bizonytalanságokat (égetés, mállás, stb. hatása a kerámia kémiai összetételre).

Az eredethatározás vizsgálatainak az eredményei, részben jó összhangban számos korábbi régészeti tanulmánnyal, kimutatták, hogy a legtöbb régészeti minta petrográfiai és kémiai jellemzői jól illeszkednek a helyi potenciális nyersanyagok tulajdonságaikhoz, így a vizsgált 90-ből, 82 darab cseréptöredék (nagy valószínűséggel) helyben készítettnek tekinthető.

Három dél-bulgáriai (Ovcarovo) töredék egyértelmű hasonlóságot mutatott észak-bulgáriai (Sborianovo) cserepekkel és helyi üledékekkel, így feltételezem, hogy ezek a minták eredeti készítési helye Észak-Bulgáriában volt és onnan került a déli vidékekre. További 5 trákiai (Észak-Trákia és Menekşe Cataği) minta eredetével kapcsolatban is a nem helyben való készítést feltételezem a lelőhelyükről gyűjtött helyi anyagoktól való eltérő tulajdonságok miatt. Habár a nem helyi nyersanyag léte egyértelműen bizonyítható, a pontos származási helyekkel kapcsolatban csak feltételezéseim vannak, ami elsősorban a megfelelő számú (régészeti) összehasonlító anyag és az információk hiányosságával magyarázható.

A dolgozat egyik lényeges pontja a kerámiák soványító anyagának a teljes kémiai összetételre gyakorolt hatásának kiszűrése volt. A nyomelemekben gazdag (pl. vulkanit szemcsék, stb.) soványító anyagot tartalmazó töredékek bizonyos esetekben (pl. radiogén izotópösszetétel) befolyásolhatják a cserép teljeskémiai-összetételét, bizonytalanná téve az eredethatározás végeredményét. Ezért, durvaszemcsés kerámiák esetében, csak a petrográfiai és kémiai adatok együttes értelmezése vezethet megbízható eredethatározáshoz.

A mikroszkópos szöveti vizsgálatok alapján megállapítottam, hogy a kerámiakészítéshez használt lehetséges nyersanyagok legnagyobb része finom homokos iszapos agyag és fluviatilis üledék (iszap) volt, amit bizonyos esetekben homokkal vagy durvább szemcseméretű törmelékkel soványíthattak.

A röntgendiffrakciós vizsgálatok és a cserepek agyagásvány-tartalma alapján a vizsgált minták 3 csoportba sorolhatók a feltételezett maximális hőmérsékletük szerint. Ezek:

Kerámiatöredékek klorit tartalommal:  $T_{\max}$ : (550) 600-650 °C, 10Å-ös filloszilikát (illit, muszkovit) és kalcit tartalommal:  $T_{\max}$  700-750 °C valamint 10Å-ös filloszilikát tartalommal:  $T_{\max}$ : 800-850 °C. Az égetési-hűtési folyamat szinte minden esetben redukzív körülmények között zajlott, amire a cserepek szürkés-fekete színe is egyértelműen utal.

## Acknowledgements

The study presented in the following dissertation has been carried out for three years at the Lehrstuhl für Geochemie, Universität Tübingen, as a project in frames of the Graduiertenkolleg “Anatolien und seine Nachbarn”.

I would like to express my gratitude to Prof. Muharrem Satır, the Head of the Lehrstuhl für Geochemie and the Supervisor of my dissertation, for the constant advice and support during this time. I am also very grateful to Prof. Manfred Korfmann, the Director of the Troia Projekt, for encouraging me to study the problem of the Knobbed ware in Troia and for kindly allowing me to analyse the material from the excavations at Troia.

At this place I would also like to express my warmest thanks to the Colleagues and Friends in Tübingen, Budapest, Turkey, Bulgaria and Switzerland for their help and support.

I owe deep gratitude to Dr. György Szakmány (Department of Petrology and Geochemistry, Eötvös University, Budapest) who discussed with me the results of petrographic and chemical analyses and made very useful suggestions for this study.

Dr. Heinrich Taubald (Lehrstuhl für Geochemie, Universität Tübingen) ran the chemical analysis necessary for the study and offered his immense help in interpretation of the results. He also kindly read the text and made many useful remarks.

Dr. Wolfgang Siebel (Lehrstuhl für Geochemie, Universität Tübingen) performed the isotope analysis and discussed with me its results.

Mária Tóth (Hungarian Academy of Sciences, Institute for Geochemical Research) ran the XRD analyses and was always a great help in interpretation of the data.

Dr. Gábor Dobosi (Hungarian Academy of Sciences, Institute for Geochemical Research) carried out the electron microprobe analysis.

I would like to thank Prof. Péter Árkai (Hungarian Academy of Sciences, Institute for Geochemical Research) for the possibility of running the XRD and EMPA measurements.

Dr. Márta Balla (Radiochemistry Laboratory of the Institute of Nuclear Techniques, Budapest University of Technology and Economics) has made the necessary NAA analyses.

I would like to thank Prof. Andrea Mindszenty for the possibility of running the CL analysis at the Department of Applied Geology, Eötvös University. Dr. Zoltán Lantos (Hungarian Academy of Sciences, Geological Research Group, Eötvös University, Budapest) kindly helped to run the analysis.

I would like to offer my warm thanks to the staff of the Lehrstuhl für Geochemie, Universität Tübingen, especially to Gisela Bartholomä, Marcella Schuhmann, Gabriela Stoschek and Bernd Steinhilber. They helped me to prepare the samples and to perform series of analyses. Elmar Reitter was a great help in preparing and running the isotope analyses.

The technician of the Lehrstuhl für Geochemie, Universität Tübingen, Indra Gill-Kopp, prepared all thin sections analysed in the dissertation.

Ute Wahl and Helga Mozer the Secretaries of the Lehrstuhl für Geochemie have always offered me their kind help in matters concerning the organisation of my work in Tübingen.

Dr. Anne-Marie Wittke was of a great help in all the formalities connected with my participation in the Graduiertenkolleg Program.

Pavol Hnila (Graduiertenkolleg "Anatolien und seine Nachbarn", Universität Tübingen), who presently prepares his doctoral dissertation on the archaeological aspects of the Knobbed ware in Troia, has kindly discussed with me the archaeological problems related to the presence of the Knobbed ware and Barbarian ware in Troia and in Balkans. He was also a great help in selecting the samples for analyses from the Troian pottery material.

Dr. Marta Guzowska (Institute of Archaeology, Warsaw University) has corrected the English version of the text and discussed with me many archaeological aspects of my study.

Prof. Mehmet Özdoğan (Institute of Archaeology, Istanbul University) has kindly allowed me to analyse the material from Turkish Thrace.

Dr. Asli Erım-Özdoğan (Istanbul University) and Dr. Mehmet Akif Işın (Archaeological Museum, Tekirdağ) allowed me to analyse the material from their excavations at Menekşe Çatağı and helped me to select the samples.

Prof. Ernst Pernicka (Curt-Engelhorn-Zentrum Archäometrie, Mannheim) offered me his support at the beginning of the project. He helped me to get in touch with the Bulgarian colleagues and provided some material for analyses among the Troian sherds.

Prof. Diana Guergova (Bulgarian Academy of Sciences, Archaeological Institute), Momchil Kuzmanov (University of Sofia), and Prof. Ivelin Kuleff (Faculty of Chemistry, University of Sofia) helped me immensely to organise the trip to Bulgaria and to acquire the material for analyses from the Bulgarian archaeological sites.

Prof. Marino Maggetti (Department of Geosciences, University of Fribourg) was a great assistance during the duration of the project offering general support, sharing his knowledge and offering practical help.

To Mustafa Kibaroglu (Lehrstuhl für Geochemie, Universität Tübingen) and Gürsel Sunal (Istanbul University) I owe my thanks for many interesting discussions concerning the geology of Turkey and for practical help in acquiring data concerning the geology of the region. Mustafa Kibaroglu was also an invaluable partner in discussions on the methodology of pottery analyses.

Prof. Nikola Zidarov (Central Laboratory of Mineralogy and Crystallography, Bulgarian Academy of Sciences) provided me with lots of useful information about the geology of Bulgaria and offered practical help in acquiring the geological maps of Bulgaria.

Dr. Gebhard Bieg is an author of all photographs of the Knobbed ware sherds used in this study.

Several Friends have offered me their precious help in organising my three year stay in Tübingen and in facilitating every aspect of my life during the period of study.

Judit Zöldföldi helped me to organise my stay in Tübingen and offered her friendship and help in practical everyday matters.

István and Judit Dunkl and their family I owe many thanks for general support, friendship and good atmosphere (including numerous invitations for excellent food).

Igor Cerovský and Martin Danišik were invaluable company in the moments of leisure; I owe big thanks for the good time, trips and climbing.

Last but not least other Friends and Colleagues from Tübingen and Budapest: Dr. Thomas Wenzel, Prof. Wolfgang Frisch, Prof. Torsten Vennemann, Stephan Valley, Dr. Thomas Tütken, Dezső and Heide Varjú, Othmar and Dora Fritsch, Per Jeisecke, Petar Zidarov, Diane Thumm, Usama Chekhani, Dr. Balázs Székely, Dr. Katalin T. Biró, Dr. László Csontos, Dr. József Kovács, Dr. Zsolt Kasztovszky, Dr. Szabolcs Harangi, Katalin Gherdán, Olga Komoróczy, Csabáné Sándor M., Barnabás Korbély, and Gábor Gáti offered me their help and support during the study and my stay in Tübingen.

Special thanks must go to my Family, for their continuous support and trust.

The three year stay in Tübingen, scientific trips to Turkey and Bulgaria, participation in an archaeometry course in Fribourg, Switzerland (Archäometrie II – Keramik; 11-15.02.2002) as well as participations in conferences in Amsterdam (2002), Lisbon (2003) and Zaragoza (2004), where I have presented the partial results of the project, were financed by the Deutsche Forschungsgemeinschaft in frames of the Graduiertenkolleg Programm: „Anatolien und seine Nachbarn“ at the Universität Tübingen.

## CHAPTER 1. Archaeological evidence

The presence of the Knobbed ware in Troia was already acknowledged by Schliemann and Dörpfeld (Schliemann, 1881; Schmidt, 1902), but it was for the first time properly defined and described by Blegen (Blegen *et al.*, 1958). The German term *Buckelkeramik*, introduced by Schliemann (Schliemann, 1881; cf. also Schmidt, 1902) has been directly translated into English as Knobbed ware (Blegen *et al.*, 1958). Large amounts of Knobbed ware have been identified during the renewed excavation at Troia since 1988 (Korfmann, 1988, 1991, 1992, 1997, 2000; Koppenhöfer, 1997). The archaeological study of Knobbed ware at Troia is presently being prepared by Pavol Hnila.

Knobbed ware has drawn the attention of archaeologists because of its unique character. In Troia certain types of the wheel made pottery, which developed at the beginning of the Late Bronze Age (e.g. Grey Minyan or Tan Ware; cf. Blegen *et al.*, 1953; Bayne, 2000) share the same characteristics continuously through the beginning of the Early Iron Age. The ceramics are wheelmade on a fast wheel. Their angular shapes reminded several researchers of the metal vessels which could serve as prototypes for the clay vessels (Blegen *et al.*, 1953). Their carefully burnished surface is otherwise undecorated with rare exceptions of the incised lines or plastic appliques. They have been fired in high temperatures in a well controlled environment which resulted in production of a hard, good quality and durable ceramics.

In contrast to this pottery tradition, well established in Troia for hundreds of years, the Knobbed ware shows entirely different characteristics. The vessels are always handmade and their shape often irregular and asymmetric. The surface of the vessel is very well burnished, often to high lustre, which is the main decorative feature of the vessel. Additionally the vessels are decorated with different types of knobs and incisions. The clay used for the production for the Knobbed ware vessels is coarser than that used in the contemporary wheel made ceramics in Troia. It has been macroscopically observed by Blegen that the fabric is very friable and it contains many large admixed particles. Blegen further stated that the section and the surface vary considerably in colour, and the surface shows uneven coloration, presumably resulting from uneven firing (Blegen *et al.*, 1958).

The Knobbed vessels represent, in addition to the technological differences, also entirely different set of shapes; many new shapes unknown in Troia before the appearance of the Knobbed ware are introduced (cf. Blegen *et al.*, 1958: Fig. 218; shapes A 101, A 103, A 104, A 105, A 106, A 107, B 43, B 44, B 45, B 46, B 47, B 48, C 83, C 84).

Knobbed ware thus represents a class of hand-made pottery, appearing suddenly in a town with a 1000-year-old tradition of the use of the potter's wheel. Although Blegen stressed the inferior quality of those vessels compared to the earlier assemblages in Troia (Blegen *et al.*, 1958), the careful execution and finishing of the Knobbed vessels may suggest that in Troian households it played a role of tableware, alongside with the wheel made vessels of Troian tradition. The new shapes associated

with Knobbed ware in Troia are mainly connected with direct consumption or serving of food. The assumption of the tableware character of the Knobbed ware was further supported by the functional analysis of several domestic assemblages in Troia (Guzowska *et al.*, 2003).

In Troia the Knobbed ware has been observed to appear first in the VIIb2 phase, following a destruction, most probably of a warlike character, which the town suffered at the end of the VIIa period and the appearance of the Coarse or Barbarian ware in VIIb1 phase (Blegen *et al.*, 1958). As there is no overall destruction horizon dividing the VIIb settlement into two phases (cf., however, Mountjoy, 1999 for the destruction of several houses at the end of VIIb1 phase), the division into VIIb2 and VIIb2 has been based on pottery; the VIIb2 phase (Fig. 1) has been identified as such by the very appearance of the Knobbed ware (Blegen *et al.*, 1958).

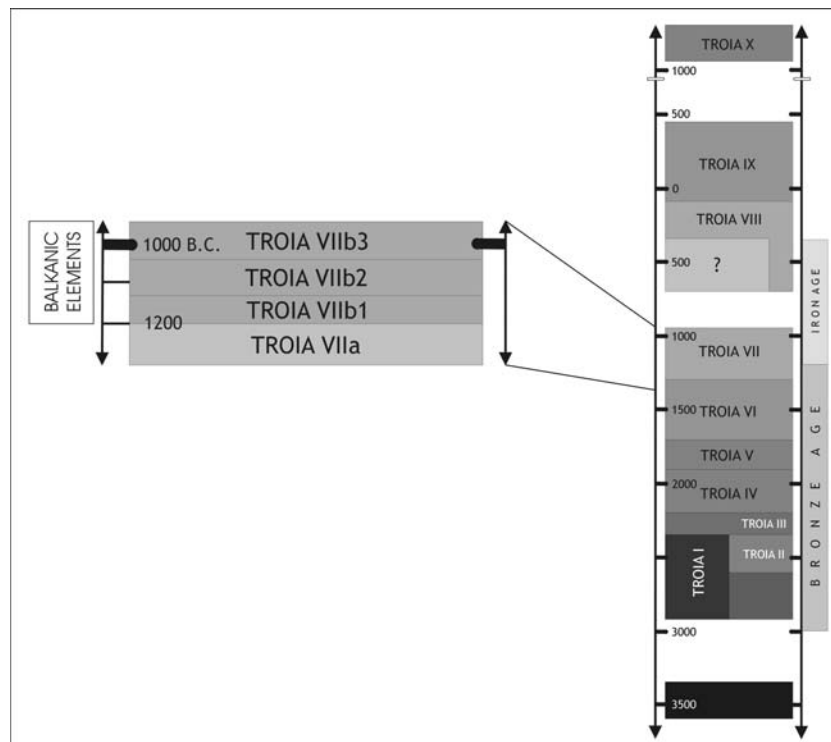


**Fig. 1 Absolute chronology of the appearance of the Balkanic elements (Knobbed ware) in Troia (after Wagner *et al.*, 2003).**

The absolute chronology of the appearance of the Knobbed ware in Troia can be thus only established by the link to the Aegean. The *terminus post quem*, defined by the Mycenaean pottery can be - very approximately - the beginning of the LH III C middle (Mountjoy, 1997).

The *terminus ante quem* is more difficult to establish and can be, with caution, defined by the appearance of the Protogeometric pottery which, according to Catling's typology dates between 1025 and 950 B.C. (Catling, 1998).

The appearance of the Knobbed and Barbarian wares in Troia corresponds chronologically with the change in architecture, and replacement of large, widely spaced houses by small irregular buildings crammed alongside crooked lanes (Blegen *et al.*, 1958).

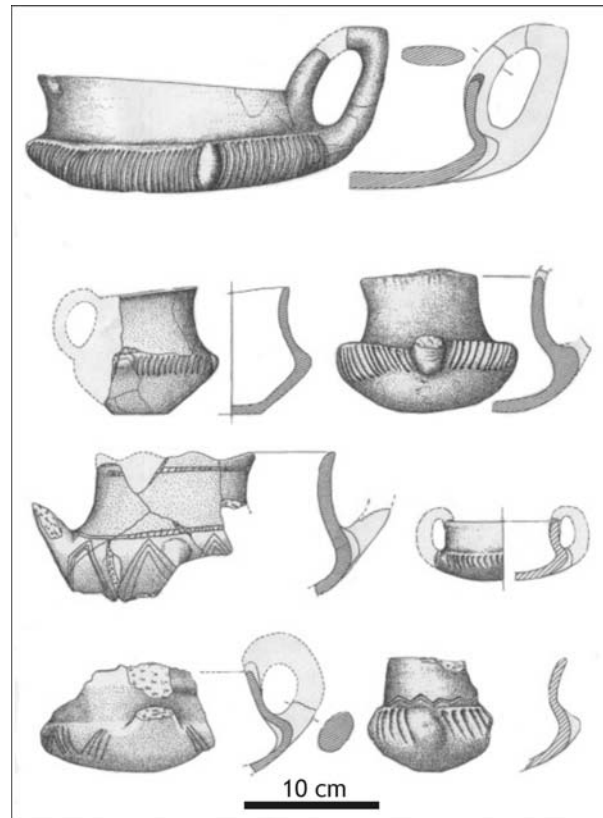


**Fig. 2 Characteristic forms and decoration of the Knobbed ware vessel in Troia (after Koppenhöfer, 1997).**

The tradition of producing handmade pottery decorated with knobs (Fig. 2) originated probably on the west coasts of the Black Sea (Fig. 3). The best analogies for the Troian Knobbed ware are represented by the potter of the Babadag group (southeast Romania), which developed from the Coslogeni culture in the present southeast Romania (Morintz, 1964; Hänsel, 1976). Other parallels come from the Chataalka culture, the Maritsa-Tundsha area, the Black Sea coast of Bulgaria, e.g., the Pshenitsevo Group (Dimitrov, 1968; 1971; Chichikova, 1968; Stefanovich, 1974; Hänsel, 1976; Koppenhöfer, 1997), the area of Macedonia (mainly Kastanas: Hochstetter, 1984) and the island Thasos (Koukouli-Chrysanthaki 1970; 1982; Fig. 3)<sup>1</sup>.

<sup>1</sup> The description, dating and analogies for the Knobbed ware in Troia presented in this dissertation are based on the previous studies of the pottery, mainly by Carl Blegen and Dietrich Koppenhöfer (Blegen *et al.*, 1958; Koppenhöfer, 1997). As it has been mentioned above, the Knobbed ware is presently an object of extensive archaeological studies for the doctoral dissertation of Pavol Hnila in frames of the Graduiertenkolleg “Anatolien und seine Nachbarn” carried out at the Universität Tübingen. This extensive study may result with new data concerning the Knobbed ware at Troia, which are not available at the moment of writing of the present dissertation. The key question of the origin of the Knobbed ware in Troia remains, however, unchanged. It is my hope that the present dissertation will provide more geological and chemical data which can be further used by archaeologists.



**Fig. 3 Distribution of the Knobbed ware in the Balkans and in Asia Minor (modified after Becks & Thumm, 2001).**

The Knobbed ware has also been identified in the Aegean, where a name Handmade Burnished Ware (HBW: French & Rutter, 1977; Deger-Jalkotzy, 1983; Pilides, 1994) is used to describe generally the coarse ware, handmade pottery with various types of decoration, which in Troia has been differentiated in two groups, Knobbed and Coarse ware (Blegen *et al.*, 1958). The HBW has been found in several locations on the Greek mainland (e.g., in Korakou – Rutter, 1975; Aigeira - Deger-Jalkotzy, 1977; Menelaion - Catling & Catling, 1981 and in smaller quantities in Athens, Perati, Delphi, Mycenae, Lefkandi & Tiryns: cf. Rutter, 1975 and Pilides, 1994, who collect and discuss the data and quote further references) as well as in Cyprus (Karageorghis, 1986; Pilides, 1994; Fig. 3) and in the Levant (Badre, 1998; Mazar, 1985). Small amounts of HBW present at various Aegean sites allows for the assumption that the pottery has been imported, although at least part of this material has been identified as locally produced (Whitbread, 1992; Pilides, 1992; 1994).

The origin of the Knobbed ware in Troia has been widely discussed over many years. A new class of pottery appearing in Troia in the VIIb settlement is connected with a totally new approach to ceramic production and use. In comparison to the pottery produced in Troia continuously since the Middle Bronze Age, the Knobbed ware is handmade and relatively low-fired, which implies entirely different technology and tradition of production. The shapes are also a break with the tradition present in Troia

for hundreds of years, implying possibly different food traditions. Many scholars, starting with Carl Blegen (Blegen *et al.*, 1958) postulated, that such drastic change in pottery traditions must be related to the change in population. The fact that the new pottery appeared in Troia after a series of destruction has been often quoted as an argument for the theory that weakened Troia was settled by the newcomers from the North (cf. also. Bloedow, 1985; Dimitrov, 1968; 1971; Koppenhöfer, 1997; Stefanovich, 1974).

It has to be strongly stressed at this point that it is impossible to answer questions about such complex event as migration basing only on the pottery data; full analysis of the problem requires extensive research on other aspects of life (architecture, dietary customs, system of beliefs, anthropological components of the local population, etc.; cf. Anthony, 1990; 1997; 2000). **Nevertheless the ability of establishing, whether the new type of pottery appearing in Troia in the Early Iron Age is locally produced or imported, adds a very important voice to the discussion on the possible population changes in Troia in particular and the area of south-eastern Balkans and north-western Anatolia in general.**

In the archaeological discussions on the Knobbed ware and the consequences of its appearance, carried out by now, the lack of hard, archaeologically unrelated data concerning the origin of the new pottery is remarkable. Important archaeological conclusions have been based solely on the ground of the archaeological analogies, creating the danger of a circular argument (cf. especially Dimitrov, 1968, 1971; Bloedow, 1985; Stefanovich, 1974).

## CHAPTER 2. Importance and aim of the study

As mentioned above, the factor of decisive importance in discussing the cultural implications of the appearance of the Knobbed ware in Troia and the surrounding area is to determine the origin of the new ware. Local production could be used as an argument supporting the theory that the people who introduced this new type of pottery indeed lived in Troia in the VIIb settlement. If, however, the Knobbed ware vessels were imported, the population change in Troia would be more disputable.

By now only limited geochemical data from pottery (Guzowska *et al.*, 2003) and no data from geological material (possible raw materials) have been available from the areas where the Knobbed ware presumably originated (i.e. today's Bulgaria and Romania). Most theories produced so far were thus mere speculations.

The aim of this study is to provide a hard set of data concerning the origin of the Knobbed ware in Troia and its possible relations to the sources of production of related potteries in northwest Turkey and in the Balkans. These data will be used in three ways:

- the results of petrographic and geochemical analyses of the selected Knobbed ware sherds from Troia, the area of the Sea of Marmara and the Balkans, compared to the data obtained from the analyses of local sediments and locally produced sherds will allow to reconsider theories of the local vs. imported origin of the Knobbed ware in Troia and other sites analysed in this study;
- the results of the petrographic and mineralogical analyses of 20 selected sherds will provide extensive information on the technology of production of the Knobbed ware vessels in Troia the area of the Sea of Marmara and the Balkans. This in turn will provide basis for the discussion on the traditions in pottery production and will allow to estimate how far the technology of production of the Knobbed ware at Troia is related vs. foreign to the local production techniques;
- the discussion of the methodology of the research in the following dissertation can help to better understand the role of non-plastic inclusions in the interpretation of the chemical data of the sherds, which can be used in the future in the provenance analysis of coarse wares.

The presented dissertation offers the first complex analysis of the Knobbed ware from Troia, Turkish Thrace and the southern Balkans. The petrographic, geochemical data as presented below are ready for the further use in archaeological and ethnological studies. Their analysis can bring us one step closer towards understanding the social role of the Knobbed ware and the ethnicity of its makers.

## CHAPTER 3. Overview of the previous research in pottery analyses

Since the first attempt (Richards, 1895) focussed on the natural composition of archaeological ceramic fragments, several working groups and studies have dealt with the scientific analysis of this very important archaeological material.

The previous studies have dealt either with the provenance analyses of the sherds or with the question which raw materials, firing temperatures and, producing techniques were used for the pottery production.

In 1956 Shepard summarised first in the book *Ceramics for the Archaeologist* the criteria of the scientific ceramic analyses. In addition to the archaeological pottery classification, she has mentioned the main analytical techniques (polarising microscopy, spectroscopy, X-ray diffractometry, etc.). In 1969 Peacock reviewed in his study the most important analytical techniques. Since that time only few summarising and general studies came out (Schneider, 1978; Schneider *et al.*, 1989; Burmeiser *et al.*, 1989; Orton *et al.*, 1993); the results of different archaeometrical studies are mostly found in proceedings of conferences or in scientific magazines like *Archaeometry*.

The two most important analytical methods used in ceramics analysis are optical microscopic (petrographic) and chemical analyses.

Petrographic investigation, which analyses qualitatively and/or quantitatively the mineral and rock fragments in the sherd, can be a powerful and cheap method, especially in case of coarse wares, used to decide whether the analysed sherd was locally produced or imported. Furthermore it can also be very useful in the interpretation of chemical data, secondary processes, and the producing technique.

One of the first analyses was carried out by Obenauer (1936) and since the middle of the 20<sup>th</sup> century petrographic investigation has become a widely-used analytical method. Maggetti (1974, 1994) showed in several studies the importance of optical microscopy. Other researchers (Arnold, 1972; Kamilli & Lamberg-Karlovsky, 1973; Hagn, 1983; Schubert, 1984, 1986, 1987; Böhm & Hagn, 1988; Thierrin-Michael, 1991; Whitbread, 1992, 2001; Goren, 1995; Szakmány, 1996, 1998; Szakmány & Kustár, 2000; Chandler, 2001; Gherdán *et al.*, 2002; Mason, 2003; Maritan, 2004, etc.) have used petrographic analysis on different ceramics, originating mostly from the Mediterranean and Alp-Carpathian regions. Whitbread (1986) characterised the argillaceous inclusions found in potteries. Mason (1995) showed new criteria in the petrographic characterisation of ceramics. Some authors (Middleton *et al.*, 1985; Szakmány, 1996) use widely the petrographic modal analysis in their studies to characterise more accurately the non-plastic inclusions (temper) in the sherds. In addition to the studies dealing with the mineral and rock fragment content of the sherds Maggetti *et al.*, (1981b) showed the importance of fossil shells found in the clayey material of the ceramics for provenance analysis.

Chemical analyses focus mainly on the whole sherd and results are compared to reference materials (either locally produced pottery or local sediments, Mommsen, 2001). Depending on the type of the analysed ceramics (fine-coarse), the reference group(s), and the lack of alteration and/or firing processes which may influence the original chemical composition, chemical analyses are the most widely used scientific methods in archaeometrical studies. Although chemical data can provide lots of useful information, their interpretation can be difficult without petrographic information (Kilka, 1992; Maggetti, 1994; Di Pierro, 2003).

For the characterisation of fine wares, like Grey Minyan Ware in Troia (Knacke-Loy, 1994) or the Roman terra sigillata (Maggetti *et al.*, 1981a), chemical analysis is the only possibility to get reliable information about their origin. Most common chemical analytical methods are: X-ray fluorescence (Birgöl *et al.*, 1977; Adan-Bayewitz & Perlman, 1985; Mazo-Gray & Alvarez, 1992; García-Heras *et al.*, 2001; Hall *et al.*, 2002) mostly for main and partially for trace elements and instrumental neutron activation analysis (NAA; Harbottle, 1976; Balla, 1981; Hancock, 1985; Gunneweg & Mommsen, 1990; Kerschner *et al.*, 1993; Glowacki *et al.*, 1995; Mommsen *et al.*, 1989; 1992; 2001; Gomez *et al.*, 2002), and prompt gamma activation analysis (PGAA; Kasztovszky *et al.*, 2004) for trace elements and REE. Other chemical analytical methods, like inductively-coupled plasma emission mass spectrometry (ICP-MS) and atomic absorption spectrometry (AAS; Hatcher & Tite, 1995) are also useful in determining the elementary composition of a sherd.

Although the use of radiogenic isotopes ratios (e.g.  $^{87}\text{Sr}/^{86}\text{Sr}$ ,  $^{143}\text{Nd}/^{144}\text{Nd}$ ,  $^{207}\text{Pb}/^{206}\text{Pb}$ , etc.) for sediment provenance studies has been a common analytical method since the first attempts (Miller & O'Nions, 1984; Nelson & DePaolo, 1988) in geological studies, the first use of the method for provenance studies on archaeological ceramics dates from the 1990's (Knacke-Loy, 1994). Other studies also proved the usability and benefit (cf. Chapter 4) of this method (Guzowska *et al.*, 2003; Carter *et al.*, 2004).

The provenance analysis of pottery is a complex scientific work requiring circumspect and efficient sampling of (geological) reference materials, sherds, and analytical methods. Several problems can only be answered with the simultaneous use of different techniques (e.g. petrography and chemistry or XRD). Very often chemistry leaves open questions, which might only be answered with optical microscopic investigation and/or the simultaneous use of the two methods (Kilka, 1992; Maggetti, 1994; Hein *et al.*, 2002). The geology of an area always determines the chemical and petrographic properties of the possible raw materials used for ceramics production (Maggetti, 1974, 1991). Difficult geological setting of the study area or mixing of different raw materials (clays) always complicates interpretation of the data, thus the determination of the origin of the analysed sherd.

The purification effect of firing (Kilikoglou *et al.*, 1988), burial (Buxeda I Garrigós *et al.*, 2001, 2002), or contact with sea water (Béarat *et al.*, 1992; Von der Crone, 1993) for the pottery is another phenomenon which must be considered in the interpretation of the chemical data. Several studies (e.g. Buxeda I Garrigós *et al.*, 2001) proved that mobile elements can be leached from high temperature-

fired ceramics during the burial. The general alteration processes of archaeological materials (bone, glass, pottery) were analysed by Rottländer (1989).

As it has already been mentioned, the presence of exotic clasts (natural or added temper) in the clayey material can strongly influence the whole chemical composition of the sherd. The influence of these clasts on the chemistry of the potteries was analysed by Marro (1978), Stimmel *et al.*, (1986) and Di Pierro (2003). They all found that in the interpretation of chemical analyses of coarse wares the presence of big amount of non-plastic inclusions or temper must be considered. Marro (1978) and Di Pierro (2003) also presented some useful mechanical methods to separate coarse temper fragments from the sherds, without influencing the chemical composition of the clayey matrix.

In order to filter the above mentioned primary or secondary chemical effects one can also measure the chemical composition of the single mineral and rock fragments in a thin section using electron microprobe analysis (EMPA). The benefit of this method is that the chemical composition of typical or rare fragments like volcanites, metamorphites, etc. can be directly compared to the data of similar rocks from the presumed place of origin. Although the EMPA is not a widely used analytical method in pottery provenance studies, some successful attempts have already been made using this method in archaeometrical provenance studies (Kamilli & Lamberg-Karlovsky, 1979; Tite & Maniatis, 1975).

Another interesting and useful method is cathodoluminescence spectroscopy. The method, widely used in marble provenance analysis (e.g. Barbin *et al.*, 1992; Zöldföldi & Satır, 2003) can be a new method in the pottery provenance analysis. Picouet *et al.* (1999) demonstrated that using cathodoluminescence spectroscopy on different types of mono- and polyquartz can be differentiated, thus the possible origin of the quartz-bearing raw material (clay, sand, etc.) can be determined.

Aside from the provenance studies the most important question in archaeometrical studies is the analysis of the production techniques of ceramics.

The most common applied analytical techniques are optical microscopy, X-ray diffractometry (XRD), scanning electron microscopy, and Mössbauer spectroscopy.

The view through the optical microscope can provide valuable information about the structure of the sherd (orientation of fragments, type of texture, roundness and sphericity of the clasts, levitation of the material, etc.; Klenk, 1987; Maggetti, 1994; Szakmány, 1996; Spataro, 2002).

Using XRD we can get information about the quality and quantities of mineral phases, which are not observable in the microscope, due to their fine grain-size (e.g. clay minerals). The importance of clay minerals lies in their sensibility to temperature changes, thus they are important temperature indicator minerals. Several authors (Maggetti, & Heimann, 1979; Maggetti & Rossmann, 1981; Maggetti, 1982; Kardos *et al.*, 1985; Klenk, 1987; Maggetti *et al.*, 1989; Nungässer *et al.*, 1992; Cultrone *et al.*, 2001) used XRD in order to analyse and follow the changes in ceramics during the firing. New mineral phases which can be formed at high temperature can also be analysed with XRD (Maggetti, & Heimann, 1979; Cultrone *et al.*, 2001) or with scanning electron microscope (Tite & Maniatis, 1975;

Tite & Bimson, 1986; Tite *et al.*, 2001) which provides large magnification and clear 3D image of the structure of the material.

Picon (1973) summarised the knowledge about the ceramics firing modes (atmosphere). He distinguished three modes (A, B and C) depending on the firing, soaking and cooling phases of the firing.

### **3.1. Archaeometrical ceramic studies in Troia**

The first geoarchaeological analysis was carried out by Felts (1942), who analysed different sherds from the settlement phase I-II, III, VI, VIII and IX from the collection of the American excavations (1932-1938). On the basis of the petrographic observations he noticed that Troian ceramics were successively, in time, produced with increasing firing temperatures, finer matrix, and decreasing porosity. He classified the sherds into different groups based on their temper composition and suggested the differences between local and imported wares.

Based on the first chemical investigation (optical emission spectral analysis; Jones, 1986) on Troian ceramics from the settlement phases I-VII, analysed at the Research Laboratory for Archaeology and the History of Arts at the Oxford University, twenty-five sherds have been grouped by means of eight major and trace elements. Three different local chemical groups were distinguished and presence of imported wares from central Greece and from Crete was also suggested, although their exact origin could not be determined because of the few elements measured and the chemical similarities between the suggested places of origin.

The first comprehensive study on Troian pottery was made by Knacke-Loy (1994) and Knacke-Loy *et al.* (1995). He analysed petrographically and chemically 120 vessel fragments from the settlement phases I to VIII, focussing mainly on the wares from the sixth settlement phase. Using petrographic grouping and especially chemical (XRF, NAA) analyses as well as statistical method (cluster analysis) he could determine the origin of most wares. In the archaeometrical pottery investigation, as a new method, the radiogenic isotopes ( $^{87}\text{Sr}/^{86}\text{Sr}$ ,  $^{143}\text{Nd}/^{144}\text{Nd}$ ,  $^{207}\text{Pb}/^{206}\text{Pb}$ ) were successfully used for distinguishing the archaeological material which was beyond the scope of the common applied methods. According to the results of Knacke-Loy most sherds seem to have been locally produced, but import wares from Cyprus and from Mycenae were also found.

Guzowska *et al.* (2003) summarised the archaeological and chemical (NAA and radiogenic isotope data) data from selected Troia VIIb fine and coarse wares. The comparing of the NAA and isotopic data of Knobbed ware with the chemical data of local sediments and locally produced ceramic suggested that, in addition to the locally produced vessels, some import Knobbed ware vessels may have also occurred in the settlement.

## CHAPTER 4. Sampling and analytical methods

The primary aim of this work is to investigate the possible origin of the Early Iron Age Knobbed ware from Troia and from different regions in the Balkans. Further goal of this study is to analyse the production technology of this pottery, in order to obtain additional information which can help to identify the origin of the pottery. To give reliable answer to these questions, extensive sampling and analytical methods have been carried out. The following subchapters briefly present sampling and methods used in the study.

### 4.1. Sampling

Ninety Knobbed ware sherds were taken as samples from the most significant archaeological sites and survey areas in western Anatolia and in the Balkans (Fig.4):

- Troia: 28 sherds (Fig. 5),
- Sea of Marmara (The Avşa Island): 1 sherd,
- the northern coast of the Sea of Marmara (Menekşe Çatağı): 10 sherds,
- north Turkish Thrace (Ağaçköprü, Araptepe, Cevizlik Mevkii, Demirlihanlı Mezarlığı, Hamam Mevkii, Yedigöz Kemeri): 17 sherds,
- southeast Bulgaria (Ovcarovo): 6 sherds,
- south Bulgaria (Chal): 6 sherds,
- central Bulgaria (Diadovo, Kirilovo, Pshenitsevo): 19 sherds,
- north Bulgaria (Sborianovo): 3 sherds.

The sherds were selected for sampling by archaeologists working at the sites and are examples of representative vessels for the period and the class of pottery. For the detailed archaeological and macroscopic description of all as well as the photographs of 24 selected Knobbed ware sherd analysed in this study cf. Appendix 1.

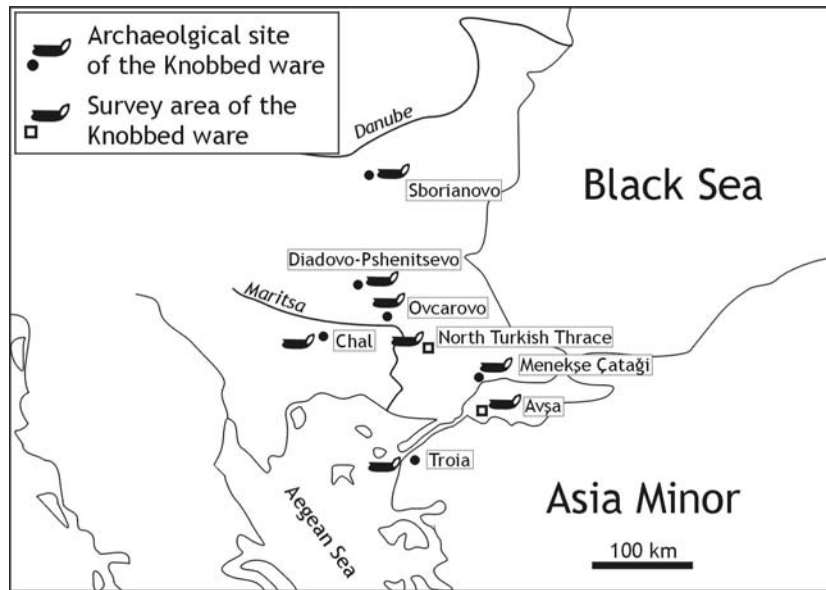


Fig. 4 Sampling sites of the sherds and geological materials.

From Troia additionally two locally produced sherds from the settlement phases I-V (Troia registration nos. *K8.911.93*: Coarse ware (451), *K8.911.94*: Brown ware (103)) and one sherd from the settlement phase V (Troia registration no. *A5/6.502.13*) as well as the fragment of a Knobbed ware vessel (*E9.158.1*), analysed by Ernst Pernicka (in Guzowska *et al.*, 2003) were also taken as comparative archaeological samples.

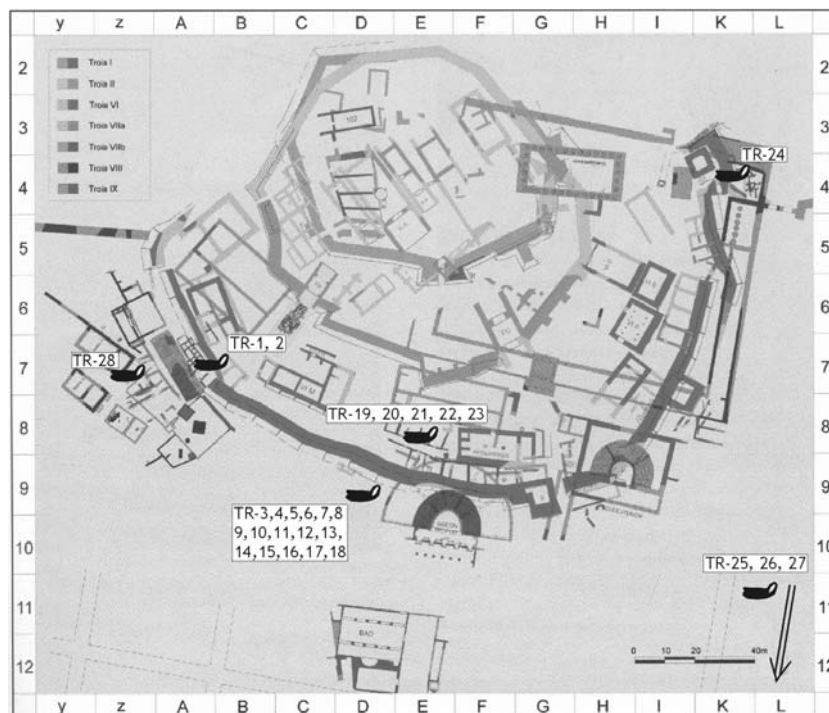
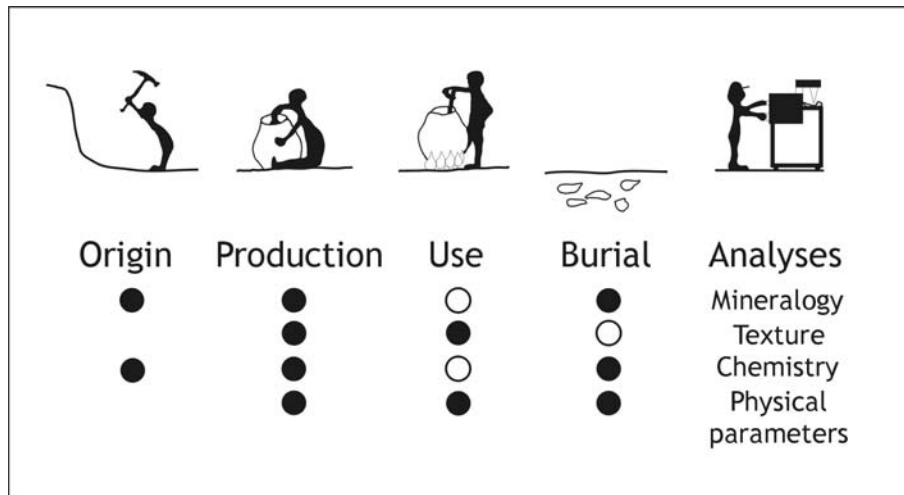


Fig. 5 Places of find of the analysed Knobbed ware fragments in Troia (modified after Korfmann, 2001).

Determining whether a sherd was locally produced from local materials, or whether it was produced in another area and transported to the habitat, needs complex research methods, knowledge of the materials, the geological patterns of the studied areas and the effects of all processes, which can influence and change the petrographic and chemical composition of the pottery fragment (Fig. 6).



**Fig. 6 Analytical methods and their significance in the investigation of the history of a sherd (dots show the application of different methods in the pottery analyses; after Maggetti, 1994).**

Raw material, used for ceramic production, reflects the geology of the catchment area (hinterland) of a river providing sediments to the sedimentary basin (Maggetti, 1994). Thus through knowing and considering the geology, geomorphology, drainage pattern and basin of the study area, valuable information can be gained for effective provenance identification. This important information can be mostly obtained from petrographic investigation.

The second step is to carry out chemical analysis on the sherds and comparing obtained data to local raw materials or undoubtedly locally produced archaeological artefacts. Comparison of the examined sherds to the local material is important for deciding about their origin. Optimally the local materials are fragments of misfired vessels (failed vessels; Mommsen *et al.*, 1988), which were immediately thrown away after the firing process, thus remained *in situ* in their environment. Destroyed kilns, made of adobe, often contain such misfired vessels. Until now in Troia and the other studied areas in Thrace and in the Balkan such misfired sherds have not been found yet.

In such case, when no misfired vessels are available, local raw materials (river sediments, clay deposits, sands, silts, silty clays, etc.) must be used and chemically characterised as reference materials.

In using local sediments as reference materials for comparative chemical analyses, several factors must be considered. In most cases there is no available evidence which raw materials, e.g. clay deposits were used in local pottery production (Schneider 1978; Buxeda I Garriós *et al.*, 2001). The factor of deliberate mixing of different clays and sediments in order to obtain raw material of better

quality, can also influence the chemical properties of a sherd, thus the interpretation of the results. Furthermore sediment accumulation during the last thousand years must also be considered. In case of Troia approximately 2 to 4 m of young fluvial sediment (Kayan, 1991, 1997), and near Edirne (Turkish Thrace) approximately 4-6 m of thick sandy-clayey piedmont deposits (M. Özdoğan, personal communication) have accumulated during the last 3000 years.

Therefore in the process of sampling of local sediments the following factors were considered:

- the lack of chemical information in the geological literature in most areas under study;
- geomorphological history of development of the area (the surface we can see now is not identical with the surface from 3000 years ago)
- selection of possible raw materials used in the local ceramic production, based on the preliminary petrographic analysis of the sherds.

Confronting these factors wide-ranging sampling of 69 different sediment and rock samples (cf. Appendix 2) from different localities and layers seem to have been the best solution to characterise petrographically and geochemically the possible raw materials (sediments) of the study areas. Therefore sampling for this study focused on the following geological materials:

- river sediments, taken directly from active and/or inactive riverbeds (coarse to fine sands, silts, silty and sandy clays, clays),
- sandy to silty deposits,
- clay deposits (Neogene to Quaternary),
- soil samples,
- rock fragments and pebbles from riverbeds.

Finer sediments (sandy-silty clays to clays) were sampled for chemical analyses to characterise the different pottery production areas on the basis of elementary features of the sediments. Samples belonging to coarser grain fractions (coarse sand, small pebbles, rock fragments) were used as comparative material in the petrographic analysis.

According to the geomorphological history of development of the Karamenderes plain and the Troad (Kayan, 1991, 1997; Kayan *et al.*, 2003) several trans- and regressional phases can be differentiated. Using the data of the geomorphologic and  $^{14}\text{C}$  absolute data, it was possible to determine the approximate present buried position of the sediments situated on the surface around 1150-1000 BC. Thus geochemical data (Knacke-Loy, 1994) from several boreholes from different depths (cf. Appendix 6), correlated with the surface sediments of the Early Iron Age and also with earlier periods were chosen as comparative material.

## 4.2. Analytical methods

The first step in the analyses was petrographic investigation and grouping of the sampled sherds. The results were compared to the microscopic observations of comparative sediment samples and locally produced sherds. According to the petrographic observations and because of the lack of the chemical data from comparative sediments from the Avşa Island, I have decided to apply the cathodoluminescence method to characterise marble fragments found in the sherd from the island.

As a second step bulk chemical composition (XRF) of the ceramic fragments as well as the sediments was determined and the samples were grouped considering the petrographic grouping.

In cases when petrographic and chemical (XRF) data did not provide sufficient results on the origin of the sherds, I have used the radiogenic isotope and rare earth element composition (NAA) of these sherds and related them to the chemical data of comparative geological and archaeological materials. Two sherds were also chosen for electron microprobe analysis (EMPA) to determine the chemical composition of some volcanic rock fragments and minerals found in their matrix, in order to get more information about their chemical composition, geological properties, and thus about their possible origin.

The final conclusion about the provenance of the archaeological material was based on the results of combined, different analytical methods and the comparison with the local materials, considering the geological setting of the studied areas (Fig.7).

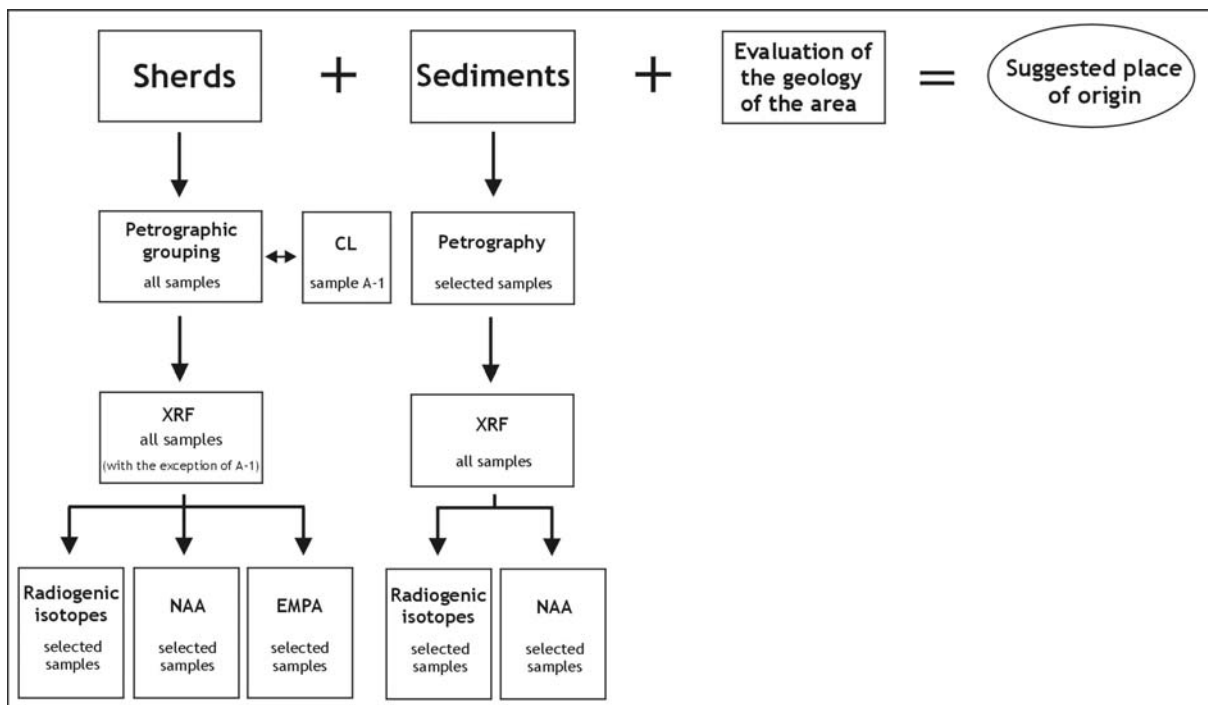
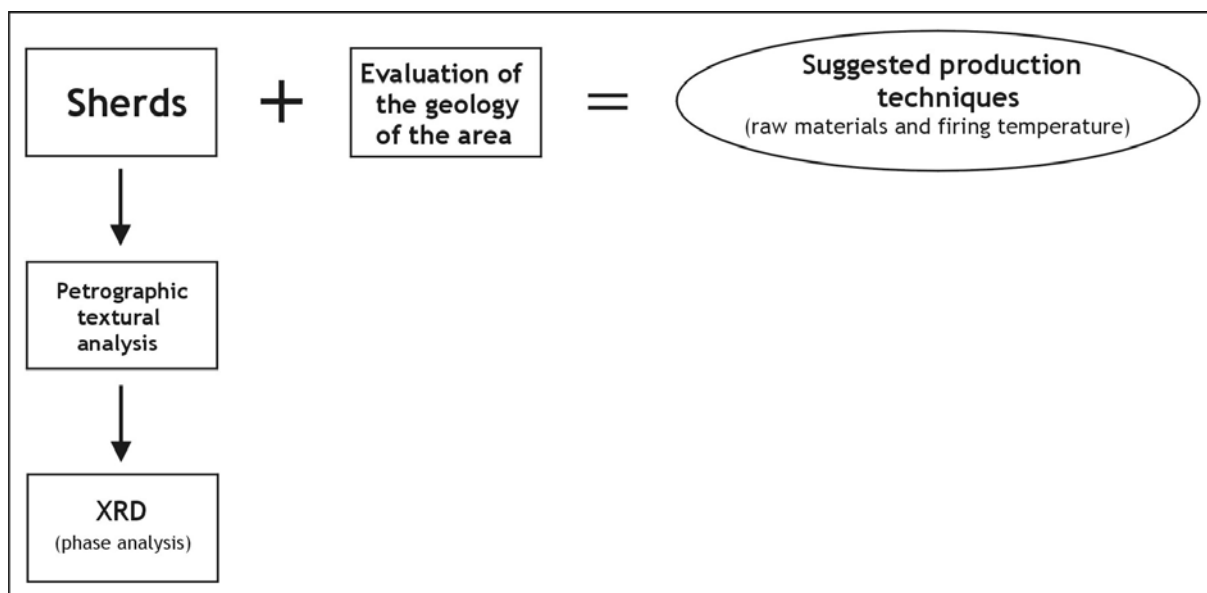


Fig. 7 The methodology used in the provenance analysis of the Knobbed ware.

To receive information about firing temperature and production technology of the Knobbed ware 20 sherds were selected for the X-ray diffractometric analysis. XRD data were also compared to the results of petrographic and textural observations (possible raw materials) and used as base for estimation of the maximum firing temperatures of the pottery (Fig. 8).



**Fig. 8** The methodology used in the analysis of the production techniques of the Knobbed ware.

#### **4.2.1. Mineral separation**

The sherds were prepared for the bulk chemical analyses (XRF, NAA) and radiogenic isotopes ( $^{87}\text{Sr}/^{86}\text{Sr}$ ,  $^{143}\text{Nd}/^{144}\text{Nd}$ ) in the following way: the surface (altered parts, secondary carbonate sinters, etc.) was mechanical cleaned using diamond drills. In order to obtain a relatively homogenous material according to the grain size distribution and (maximum) grain size of the sherds, at least 5 g of material was extracted and powdered in an agate mill. The necessary amount of the powder was used for the different (bulk) analyses.

In some chemical investigations (XRF, radiogenic isotopes, NAA) the temper or the paste of archaeological samples was analysed, thus either clayey matrix or non-plastic clasts were separated from the whole sherd. Several studies (e.g. Marro, 1978; Di Pierro, 2003) reported about the problems connected with the separation of the non-plastic inclusions (temper) from the clay and presented useful solutions (e.g. crushing,  $\text{H}_2\text{O}_2$  treatment, sieving, handpicking, etc.). The methods, however, were not used in this study for various reasons. The methods described by Marro (1978) and Di Pietro (2003) are useful in case of coarse wares (defined by an average size of their non-plastic inclusions larger than 0.2 mm; Schneider *et al.*, 1978), where temper made of one or few rock types was added to the paste. Furthermore the material requirement in the above mentioned studies is very high (30-100 g of sherd; Di Pierro, 2003). However, according to the above presented definition (Schneider *et al.*, 1978),

the Knobbed ware can also be regarded coarse ware; it was mostly produced (cf. Chapter 7) from silty-sandy clayey sediments with partially admixed coarser non-plastic inclusions. I have also had available much smaller samples of archaeological material (about 5 to 20 g).

Therefore the extraction methods used in this study were simplified, but equally effective. After the selected sherds were gently crushed in an agate mortar with an agate crusher, they were carefully grinded using a rubber tool to avoid the break-up of the smaller non-plastic (rock) fragments. Crushed samples were sieved; fractions smaller than 0.02 mm were considered as parts of the paste and collected for further analyses. Single rock and/or mineral fragments were handpicked under the binocular microscope from coarser fractions (~1 to 0.1 mm) for further analyses.

Decarbonatisation process for calcite-bearing clay samples for the radiogenic isotope analysis was carried out in the following way:

About 0.5 g powder sample was leached for 12 hours with 1 ml of 5 M acetic acid. After leaching the samples were flushed three times with deionised H<sub>2</sub>O (between flushing always mixed with Vortex). After the flushing procedure the samples were dried at 70 °C.

#### ***4.2.2. Petrographic analyses and cathodoluminescence investigation (CL)***

Petrographic observation is one of the most important analytical methods in this work, because of the great amount of the non-plastic inclusions occurring in the Knobbed ware sherds, allowing for the efficient application of this method. In case of coarse wares petrographic analysis is an indispensable method in order to understand the chemical patterns of the materials (e.g. Maggetti, 1974, 1982, 1994; Whitbread, 1992; 2001; Goren, 1995; Szakmány, 1996; 1998, Szakmány & Kustár, 2000, etc.). Petrographic properties of non-plastic inclusions can provide a lot of information which, compared to the geological information from the presumed region of origin of the ceramics and considering several factors, like the geomorphologic evaluation, the drainage pattern and basin of the area, etc. (cf. Chapter 5), can decide about identification of the pottery, thus directly about its provenance (Maggetti, 1994).

Considering these criteria detailed qualitative and quantitative petrographic analyses have been carried out.

Thin sections from the sherds and geological (sand) samples were prepared in the following way: a sample of a sherd and an adequate grain fraction of the geological samples were put into a plastic form with a diameter of 3 cm. All samples were fixed with a synthetic resin Araldite. After hardening a standard (thickness: 30 µm) thin sections were made.

### *Definitions used in the qualitative and quantitative observation*

In this work, for all mineral and rock fragments found in the sherds, the term „non-plastic inclusion“ or „clast“ was used. After Maggetti’s definition (1974, 1994) all rock and mineral fragments larger than 0.015 mm, both intentionally added by a potter to the paste and included naturally in the clay (e.g. silty-sandy clay, mud), were classified as non-plastic inclusions (Fig. 9). All non-plastic clasts smaller than 0.015 mm have been considered as belonging to the paste (clayey material). The term „temper“ (cf. Chapter 7) has been used only in cases when non-plastic inclusions were certainly intentionally added by a potter to the paste.

For the purpose of qualitative analyses, all types of clasts have been determined using a Leitz Laborlux 12 POL S polarising microscope. The quantity of the clasts as well as the ratio of matrix and non-plastic inclusions have been manually measured in all thin sections using a square grid. Although this method is very time consuming, it can provide more reliable data than other, (semi) automatised point-, line-, or ribbon-counting methods (Middleton *et al.*, 1985). Another benefit of this method is that it allows to measure separately different mineral and rock fragments.

For the purpose of quantitative measurements all clasts smaller than 0.015 mm, as well as (plastic) clay pellets, pores and paste (clay) have been identified as matrix. All mineral and rock fragments (except for the secondary pore-filling micritic carbonate) larger than 0.015 mm have been considered and measured as non-plastic inclusion (Fig. 9).

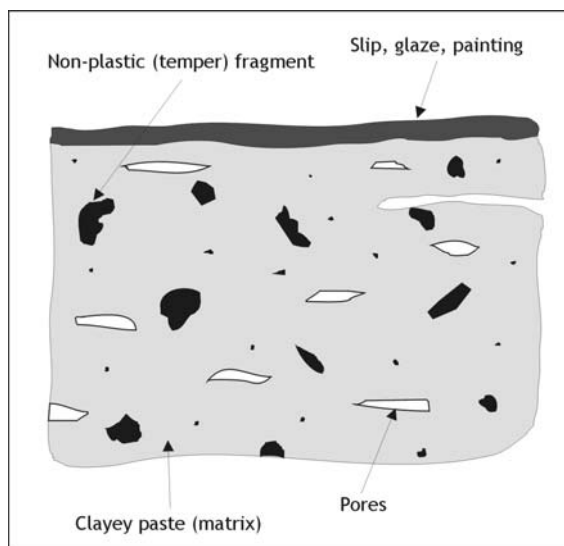


**Fig. 9 Main components of a sherd (after Maggetti, 1982).**

In addition to the percentage of matrix and non-plastic inclusions, the amount of the different types of clasts has also been given in percent by volume relative to the total amount of the non-plastic inclusions (Szakmány, 1996). For clasts with a volume smaller than 1 vol % a term „accessory (mineral)“ has been used in the description.

### *Definitions used in the fabric analysis of the sherds*

The textural properties, like colour and isotropism (optical activity) of the groundmass, type of texture, sorting of the grain size distribution, maximum grain size, roundness, and sphericity of the clasts are factors which can provide information about the type of raw materials used for pottery production, the technology of production, and post-depositional environment of the vessel (Orton *et al.*, 1993; Szakmány 1996, 1998).

The isotropism of the groundmass, observed with the technique of crossed nicols, offers information predominantly about the very fine-grained carbonate content of the clayey matrix. The primary carbonatic matter in the groundmass (anisotropic optical property) suggests two facts: the use of the calcareous clay and the firing temperature below the point of the structural damage of calcite (750-800 °C). If the matrix has isotropic optical properties, the clay is non-calcareous or calcite in the material has been burnt out (Szakmány, 1998). Isotropic groundmass may also refer to high firing temperatures (melting over 1050 °C; Maggetti, 1994).

Ceramics display considerable variability in terms of average grain size, the distribution of grain size of non-plastic fragments (sorting; type of texture: hiatal-serial; Fig 10). Amongst the microscopic analyses one of most important is the identification of purposely added temper which influences greatly the technology of production (Maggetti, 1994; Szakmány, 1998). There are 5 attributes referring to artificially added temper: 1) bimodal distribution of the non-plastic grains (hiatal texture), 2) angular outlines of the temper grains, 3) organic material (chaff), 4) use of crushed pottery fragments (grog/chamott), 5) bone (Maggetti, 1994). Because there were no rest of organic materials (chaff, bone) nor grog found among the non-plastic inclusions in the samples studied here, I only deal with the first two criteria.

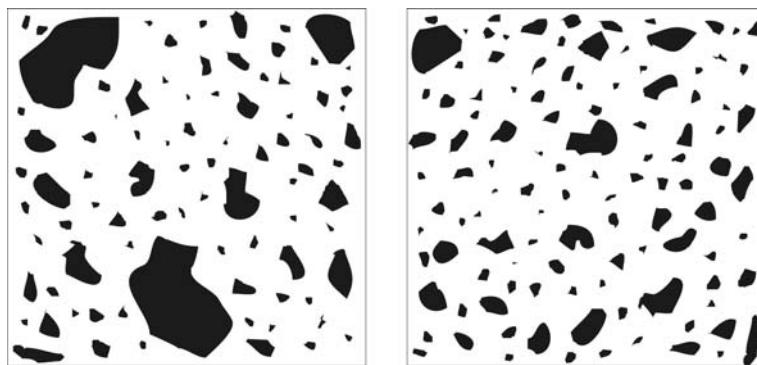


**Fig. 10 Distribution of the non-plastic (temper) fragment grain sizes in pottery: hiatal (left) and serial (right; black patches signify the non-plastic inclusions; after Maggetti, 1982).**

The colour of the groundmass signifies firing atmosphere of the vessel. Oxidising and reducing atmospheres cause different colours, well observed on the surface of the vessel or in the cross-section of the sherd. Oxidising atmosphere is signified by reddish-orange, reducing mostly by black and grey colours. The colour of a vessel is resulting from the presence of organic matter and/or very fine-

grained iron minerals in the clay. If organic material is fired in reduced atmosphere it will not burn out, but will remain in the material and will modulate the vessel into dark tone. If there is no organic matter in the raw material and the firing is reducing, iron minerals will be converted into  $\text{Fe}^{\text{II}}\text{O}$  or  $\text{FeFe}_2\text{O}_4$ , which are black in colour. The temperature can partially also influence the forming of iron-minerals. Oxidising firing causes the organic material to burn out from the clay, however, in case of very fast firing (e.g. neolithic pottery, Maggetti, 1994) there is no time for complete burn out of all organic material. Thus, in many, cases black core can be found in the middle of the sherd. Oxidising also influences the oxidation state of iron, thus  $\text{Fe}^{\text{III}}_2\text{O}_3$  will be red or orange in colour (Rye, 1981; Fig. 11).

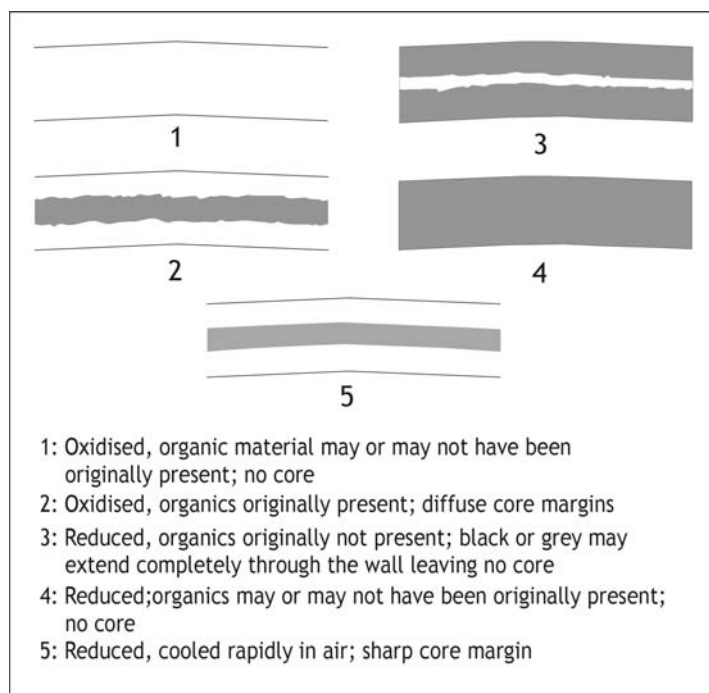


**Fig. 11 The influence of different firing atmospheres on core-forming in coarse wares (after Rye, 1981).**

The outer colour of a vessel always depends on the cooling circumstances after firing (Picon, 1973). Picon distinguished three types of firing modes. Type A combines reducing firing with oxidising cooling, type B implies reducing firing and cooling, and in type C firing and cooling take place under oxidising circumstances. In this study we are not dealing with the type C, because it is the firing mode of high-temperature fired ceramics (e.g. Roman terra sigillata).

#### *Cathodoluminescence investigation (CL)*

Luminescence is an emission of light from a solid material which is „excited“ by some form of energy. Cathodoluminescence results from excitation by electrons. CL analysis is widely used in provenance analysis and the investigation of depositional environment of carbonatic minerals and rocks (e.g. calcite, dolomite, limestone and marble). Different colours of the luminescence depend on impurities

contained in the crystal or on lattice defects. In carbonates the principal activator is manganese (inducing orange luminescence) and the main quencher is iron. Different manganese and iron content of the samples influence the colour of the luminescence. The colour of luminescence can thus be characteristic for different marble occurrences and CL analysis can be a useful method in the provenance analyses of the carbonatic rocks (Barbin *et al.*, 1992; Zöldföldi & Satır, 2003). In this study I have attempted to characterise the calcite inclusions found in the sherd A-1 (the Avşa Island) on the basis of their luminescence, in order to compare their properties with the CL properties of well-known marble sources near Marmara region.

Observations were done on polished thin section surface using a Maas-Nuclide ELM-3 Cathodoluminoscope, at the Department of Applied and Environmental Geology of the Eötvös University of Budapest.

#### **4.2.3. X-ray diffractometry (XRD)**

When investigating the firing temperature of the ceramics, analyses will focus on phyllosilicates (clay minerals) and relict or new phases in the material. In case of low-temperature fired potteries (~ 450 to 750 °C) and depending on the firing/soaking time, new phases cannot be formed, therefore the presence of clay minerals will be chiefly decisive by determination of the firing temperature. The X-ray diffractometry is a powerful method for determination of the submicroscopical (grain size < 2 $\mu$ ) clay minerals.

Besides clay minerals some other minerals (e.g. calcite) are also sensitive phases, which react to different firing temperatures with different structural changes as well as structural collapse or damage (Thorez, 1975; Brindley & Brown, 1980). These structural changes and the presence, or lack of clay minerals bear information about possible maximum firing temperature and firing circumstances (Maggetti, 1982; Cultrone *et al.*, 2001).

Several authors (cf. Chapter 3) have already reported about the possibilities and problems of the evaluation of the XRD data concerning the firing temperature of a vessel. One of most useful methods, which I could not use in this study because of the small size of the analysed sherds, is refiring of the vessel fragments and detection of changes in phases of the material. Furthermore, when investigating the maximum firing temperature of a ceramic, several effects must be considered, making the evaluation of the data more difficult. These are:

- mineral composition of the clay sources used for the pottery production,
- grain size of the non-plastic inclusions,
- CaCO<sub>3</sub> content in the matrix (calcareous clays),
- oxidising-reducing firing atmosphere,
- soaking time.

Therefore according to several author (e.g. Nemezc, 1973; Thorez, 1975; Brindley & Brown, 1980; Rye 1981; Maggetti, 1982, 1994 and Cultrone *et al.*, 2001), I have decided to present here temperature ranges of thermal decomposition of (pure) mineral phases analysed in the sherds of this study. In evaluation of the data some more factors (e.g. firing atmosphere, grain-size, mineral composition of the paste, etc.) will also be considered.

Fig. 12 shows that quartz is stable until approximately 1150 °C (change from the modification  $\alpha$  to the  $\beta$  takes place at approximately 570 °C). Plagioclase and K-feldspar are stable until 1000-1050 °C. The decomposition of the 10 Å phyllosilicates takes place at 900-950 °C (sericite-muscovite) as well as 850-900 °C (illite). The 002 reflection of the clay mineral chlorite disappears at approximately 550-600°C, its 001 reflection at 650 °C. Depending on the grain size, firing atmosphere, soaking time, etc. (cf. Chapter 8) reflection of the mineral phase calcite can be found on the diffractogram until 700-800 (850) °C. Although in the sherds of this study no new phases which were formed in solid-phase reactions during the high temperatures have been found, one can mention that CaO, which forms during the decomposition of calcite reaches stability between 700 and 1000 °C.

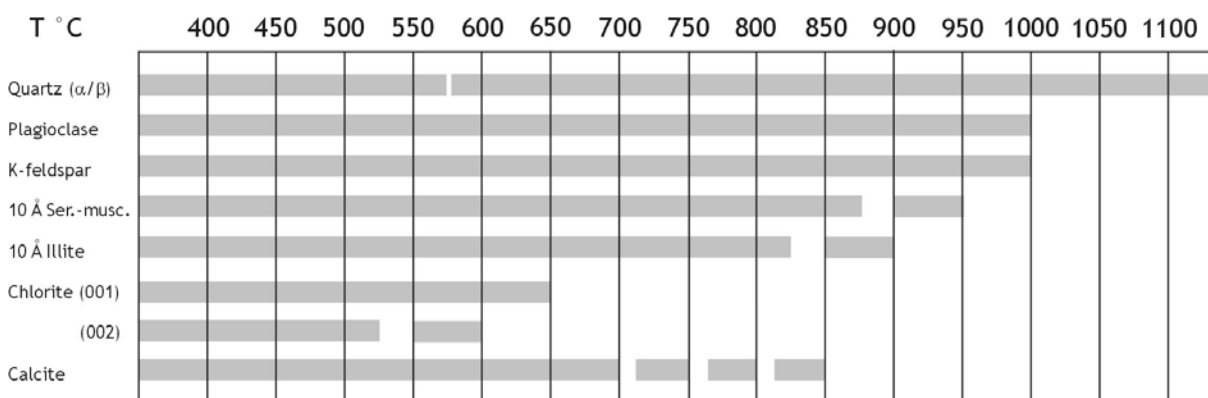


**Fig. 12 Thermal stability of some common minerals found in ceramics (after Nemezc, 1973; Brindley & Brown, 1980; Rye 1981; Maggetti, 1982, 1994 and Cultrone *et al.*, 2001).**

Because illite is less stable than muscovite (Fig. 12), its decomposition can happen, on the basis of the firing circumstances and time, at lower temperature than decomposition of muscovite. Through interpreting the XRD data on the basis of the form of 001 peak, or clay mineral diagnosis, illite and muscovite should be easily distinguished.

As we will see in case of the Knobbed ware new phases were not formed during the firing. Therefore the presence of clay minerals will be decisive for determination of the maximum firing temperature.

The data obtained from the XRD analyses were compared to the petrographic results; determination of the firing temperature was carried out by collective use of both methods.

Brief description of the XRD method is given below. Macroscopic grains are made from many elementary crystallines, which coherently diffract X-rays. Measurement is based on the detection of

the intensity of the beam diffracted in the function of the diffraction angle. The diffractogram consists of a continuous background (instrument, amorph phases) and high-intensity sharp peaks (Bragg-reflexions), which occur at characteristic angle-values. The position and the intensity of the reflexions are determined by the real crystal structure and the model of the diffraction. The position of the peaks can be described by Bragg's Law ( $n\lambda = 2d \sin\Theta$ ) which ascribe the contact between the crystal lattice, wavelength ( $\lambda$ ) and the angle of incidence ( $\Theta$ ). Using these parameters the lattice plain distance ( $d$ ) is determinable. The determination of the phases (qualitative analysis) is carried out by comparing the measured  $d$ -values and intensities with international references (**PDD – Powder Diffraction Data, ASTM – American Society for Testing Materials**).

Measurements were carried out in the Institute for Geochemical Research of the Hungarian Academy of Sciences (Budapest) with a Philips PW 1730 X-ray diffractometer (graphite monochromator and Cu tube) controlled by PC-APD software.

Although modern clay mineralogical diagnostic (Thorez, 1975; Brindley & Brown, 1980) requires grain fractions smaller than 2  $\mu$  for the exact identification of clay minerals, due to the size of the sherds, whole samples were measured. After powdering the samples in an agate mill, powder was settled with deionised water onto a glass plate and measured by XRD.

#### ***4.2.4. X-ray fluorescence spectroscopy (XRF)***

XRF analysis was used in this study in order to determine the bulk chemical composition of the geological and archaeological samples.

In X-ray fluorescence spectroscopy, the sample is exposed to a source of X-rays. As the high energy photons strike the sample, they knock electrons out of their orbits around the nuclei of the atoms. As a result, an electron from an outer orbit (shell) of the atom will fall into the orbit of the missing electron. The relocated electron has an excess of energy that is expended as an X-ray fluorescence photon. This fluorescence is unique to the chemical composition of the sample. The detector collects the spectrum of the fluorescence and converts it to electrical impulses proportional to the energies of the various X-rays in the sample's spectrum. Since each element has a different and identifiable X-ray signature, counting the pulses in that sector determines the presence and concentration of the chemical element(s) in the sample.

The quantitative analyses of the major and trace elements were carried out using the wave length dispersive XRF. Samples were powdered (grain size of the powder < 50  $\mu$ ) in an agate mortar. LOI (loss of ignition), equivalent with the loss of weight, occurring during the ignition results from the reactions of CO<sub>2</sub> (originated mostly from carbonates), H<sub>2</sub>O (structural water of the clay minerals) and Fe<sup>2+/3+</sup> conversions. LOI is calculated after heating the samples to 1000 °C for one hour

The samples (1.5000 g) were mixed with 7.5000 g of Spectromelt Fluxing agent (MERCK A12, di-Lithiumtetraborat/Lithiumteraborat (66:34)) and melted using the OxiFlux-System of the Firm CBR Analyse Service on 1200 °C to obtain homogenous tablets.

Measurements were carried out at the Department of Geochemistry of the University of Tübingen using a Bruker AXS Pioneer X-ray Spectrometer (Rh X-ray tube, 4kW). The results have been evaluated with the computer program „Traces“, which uses 32 standards for the calibration. The measured elements, the number of the standards applied, the standard deviation ( $3\sigma$ ), detection limit, and standard concentrations are presented in the Appendix 5.

It has to be mentioned, that in case of the element Nb, some samples (mostly sherds) show no value and there is also a gap in the multi-element diagrams. This is due to the type of the evaluation. In case where standard deviation ( $3\sigma$ ) is larger than the detection limit and a sample contains from an amount of a trace element near the detection limit, the program automatically defines its amount as 0.0. It means that the measured samples contain less than 9.8 ppm of Nb (cf. Appendix 5).

Chemical data of the XRF analysis were used to create bivariate diagrams and multi-element plots. The 12 following elements have been chosen for the multi-element plots (in decreasing range of incompatibility): K, Rb, Ba, Sr, Nb, Ti, Y, Zr, Fe, V, Cr, and Ni. During selecting of the elements for plots, the following factors have been considered: compatibility/incompatibility, mobility/immobility, as well as characteristic differences in distribution of the elements among the different ceramics and sediments. Values have been normalised to PAAS (Table 1; Post Archaean average Australian Shale; Mc Lennan, 1989).

<b>TiO<sub>2</sub></b>	<b>1</b>	<b>Rb</b>	<b>160</b>
<b>Fe<sub>2</sub>O<sub>3 total</sub></b>	<b>6.5</b>	<b>Sr</b>	<b>200</b>
<b>K<sub>2</sub>O</b>	<b>3.7</b>	<b>V</b>	<b>150</b>
<b>Ba</b>	<b>650</b>	<b>Y</b>	<b>27</b>
<b>Cr</b>	<b>110</b>	<b>Zr</b>	<b>210</b>
<b>Ni</b>	<b>55</b>	<b>Nb</b>	<b>19</b>

**Table 1 PAAS normalising values used in this study (after Mc Lennan, 1989).**

The PAAS has been chosen because its average chemical and mineralogical composition is near to the average chemical and mineralogical composition of clayey-sandy materials and ceramics, and differences in their chemical composition caused by various geological/geochemical processes will be easier observed and explained. Because, aside from sherds, mostly clayey sediments have been investigated in this work, the above mentioned standards seem to have been the most useful.

The cursory observation of sedimentary processes may suggest that they can equably mix all rocks found in the environment of the sedimentary basin and counteract the chemical differentiation. Main

processes and factors which affect the distribution of an element in the sediments and sedimentary systems are: ionic potential, pH, Eh, colloidal properties and adsorption (Mason & Moore, 1982).

These processes can strongly influence the final composition of the sediments and the raw materials of the pottery production; the chemistry of the sediments approximately reflects the main characteristics and the chemical properties of the rocks from which they were derived in the territory of the catchment area of the river system which provided them. This can be very helpful to distinguish different sediments and furthermore to explain and understand the chemical characteristics of the geological materials of the different areas.

According to Wedephol *et al.* (1970, 1972, 1974, 1978) the short summary of the main behaviour of the elements used in the multi-element plots are given below.

### **K**

The K content of the sediment is mainly controlled by the alteration/amount of K-feldspar. After entering the (soil) solution  $K^+$  is either used in the formation of K-minerals, such as illite, adsorbed on other clays, or removed by fluid migration. In argillaceous sediments the amount of K is a function of the clay mineral and K-feldspar content, where  $K_2O$  usually highly correlates with the clay mineral content. In coarser fractions (silts, sands, etc.) the K content is primary a function of three minerals, K-feldspar, K-mica (muscovite) and glauconite. The K content of the sediment increases with decreasing grain size.

### **Rb**

Due to the similar atomic and ionic properties to K, rubidium should be camouflaged by potassium in K-minerals and the two elements should strongly positively correlate. When a rock system undergoes some sort of differentiation Rb, is expected to be concentrated relative to K in the felsic fraction and the K/Rb ratio will decrease in a sequence from mafic to acidic rocks. In weathering Rb is closely linked to K and adsorption may play an important role in the concentration of Rb relative to K. Investigations stated, that Rb concentration was related to K only when illite formed from weathered micas and feldspars. The continuous decrease in the K/Rb ratio during weathering is probably an effect of the combination of ion exchange and adsorption.

### **Ba**

Both Ba increase and Ba decrease have been observed in the weathering products of different rocks. Among the factors which influence Ba behaviour in this process are: climate, type of clay minerals (which form during the decomposition), amount and kind of organic material present, and sulfur/sulphate content. In coarser sediments, sedimentary rocks (sands, sandstones) besides micas, feldspars are most important Ba carriers.

**Sr**

The major host minerals of the crustal strontium are feldspars (K-feldspar and plagioclase). During weathering Sr is usually less mobilised than Ca, which can be, similarly to K and Rb, camouflaged by Sr. This implies that Sr is held more tightly on clay minerals (Sr is more weakly hydrated than Ca). Different investigations have shown that strontium is rather a mobile element during rock weathering, especially under decomposition of feldspar. In case of sandy sediments and sandstones the major controlling mineral phases are, besides feldspars, carbonates. In clayey sediments and shales Sr appears to be derived either almost entirely from weathering products or represents a mixed population composed of young volcanogenic and old continental components.

**Nb**

Niobium is either released during the weathering cycle to solutions through the destruction of host species (e.g. biotite, amphibole, Ti minerals) of magmatic and metamorphic rocks, or remains behind within resistant minerals such as ilmenite, zircon, sphene, etc. These latter residual minerals and also the dissolved elements tend to be concentrated in clays.

**Ti**

The main titanium bearing phases (Ti oxides and ilmenite) are very resistant against weathering; they are transported undecomposed into sediments. If Ti-bearing silicates are decomposed, the titanium will be dissolved but is soon transformed into Ti oxide-aquate, which is transformed into anatase or rutile (TiO<sub>2</sub>). Thus Ti is locally accumulated during chemical weathering and it consists of residues, new products of weathering and diagenetic minerals. The distribution of Ti in clays on the grain size fractions varies considerably according to different sources but most of the Ti occurs on the coarser fractions.

**Y**

Scientific investigations have shown that there is no significant difference and fractionation in the Y content (lanthanides) among clastic rocks of arid environment of erosion and sedimentation. Humid conditions apparently can cause lanthanide concentrations and distribution patterns in detrital sediments. Clear sand fraction (lots of quartz) can cause the decrease of Y (and lanthanides) in clayey sediments.

**Zr**

Although the behaviour of zirconium during weathering and transportation is inadequately known, one can say generally that Zr tends to accumulate in weathering profiles, especially in the coarser (sandy) fractions, e.g. in case of fluvial sediments in high energy environments.

**Fe**

The geochemistry of iron at the Earth's surface is intimately linked to the chemistry of oxygen, sulphur and carbon. In weathering processes of Fe-bearing minerals CO<sub>2</sub>, O<sub>2</sub> and H<sub>2</sub>O play most important role. Very fine-grained ferric (Fe<sup>3+</sup>) oxides formed by weathering can be adsorbed on the large specific surface of the clay minerals, thus clays usually are richer in Fe than sands and sandstones. However, because of the great chemical fractionation which takes place during weathering, erosion, sedimentation, and diagenesis, the oxidation state and total iron content of sediments and sedimentary rocks is highly variable.

**V**

By means of several investigations it can be concluded that vanadium remains in the residual rock-forming minerals or its major proportion is dispersed and incorporated in clay minerals. Recent clays, formed under oxidising conditions, are often strongly enriched in V.

**Cr**

Because Cr<sup>3+</sup> closely resembles Al<sup>3+</sup> and Fe<sup>3+</sup> in its chemical properties and their ion size, it will behave similar to these ions during weathering processes, and will finally concentrate in clays. Thus finer fractions especially are richer in Cr than the coarser ones.

**Ni**

Nickel is easily mobilised during weathering. It is however coprecipitated with iron and manganese oxides. Similar to chromium compatible Ni also shows decrease in its content from ultramafic to acidic magmatites and their weathering products.

#### **4.2.5. Radiogenic isotopes (<sup>87</sup>Sr/<sup>86</sup>Sr, <sup>143</sup>Nd/<sup>144</sup>Nd)**

Further geological (Goldstein *et al.*, 1984; Miller & O'Nions, 1984; Nelson & DePaolo, 1988) and archaeometrical (Knacke-Loy, 1994; Knacke-Loy *et al.*, 1995; Carter *et al.*, 2004) studies have proved that radiogenic isotope geochemical investigation is a useful tool in provenance analyses of basin sediments and archaeological ceramics. The similar atomic structure of the light rare earth elements Sm (mother nuclide) and Nd (daughter nuclide) causes similar geochemical behaviour (low fractionation and high immobility) in the Sm-Nd isotopic system. Therefore the Nd isotopic composition can be effectively used in provenance studies. According to Miller & O'Nions (1984) and Goldstein & Jacobsen (1988) the averaged Nd isotopic composition of pelitic alteration products of an orogenic region can be considered as reflecting the isotopic composition of the hinterland. If sediments originated from regions of different geological history, their isotopic composition will also reflect the

difference. Analogical to basin sediments this association can also be worked in case of ceramics (Knacke-Loy, 1994).

In this study the aim of the radiogenic isotope investigations is to attempt to characterise, besides bulk chemical composition of the samples (XRF), isotopically different areas on the basis of their local sediments and locally produced ceramics. The isotopic composition of sherds with uncertain origin is compared to these local isotopic signals.

Evaluating the data some other factors have to be taken into consideration, like an influence of grain size distribution, weathering processes and metamorphism on the (Nd) isotopic composition. According to Nelson & DePaolo (1988) Sm and Nd belong to the light rare earth elements and their behavior is very similar; they are relatively immobile during metamorphic processes (up to the amphibolite-facies) and alteration. The mobilisation and fractionation of (Sr) Nd isotopes during the firing process are also irrelevant (Knacke-Loy, 1994).

Sedimentary rocks of different grain sizes (e.g. siltstone, sandstone) belonging to the same geological formation, have the same Nd isotopic composition. Thus non-plastic inclusions in the plastic matrix (clay) of the ceramics do not influence the Nd isotopic ratios, if the whole material belongs to the same formation (Nelson & DePaolo, 1988). In case of potteries where clayey material was deliberately tempered with sand, crushed rocks, etc. the isotopic composition could be influenced by other factors. However in the provenance analyses of fine wares, the radiogenic isotopes seem to be a useful method (Knacke-Loy, 1994). Due to the above mentioned factors the following study will only use data obtained from the combined use of various analysing techniques (petrography, XRF, etc.).

For isotopic analyses about 50 mg of homogenised and powderised material was used. For good dissolution, the samples were placed in an oven at 180 °C under high pressure in polytetrafluoroethylene (PTFE) reaction bombs or Teflon beakers and dissolved in HF-HClO<sub>4</sub> acids for six days.

Sr and light rare-earth elements were isolated on quartz columns by conventional ion exchange chromatography with a 5 ml resin bed of Bio Rad AG 50W-X12, 200-400 mesh. Nd and Sm were separated from other rare earth elements on quartz columns using 1.7 ml Teflon powder coated with HDEHP, di(2-ethylhexyl)orthophosphoric acid, as the cation exchange medium.

Sr was loaded with a Ta-HF activator on preconditioned W filaments and measured in single-filament (Sr-IC) mode. Nd was loaded as phosphate on preconditioned Re filaments and measurements were performed in a Re double filament configuration.

To adjust the mass fractionations, occurring during the measurements, the <sup>87</sup>Sr/<sup>86</sup>Sr ratios were normalised to <sup>86</sup>Sr/<sup>88</sup>Sr = 0.1194 and the <sup>143</sup>Nd/<sup>144</sup>Nd values to <sup>146</sup>Nd/<sup>144</sup>Nd = 0.7219.

Isotopic measurements were carried out on a Finnigan MAT 262 mass spectrometer at the Department of Geochemistry at the University of Tübingen.

### *Measurement of the $^{87}\text{Sr}/^{86}\text{Sr}$ isotopic ratio*

From the decay process of the radioactive isotope  $^{87}\text{Rb}$  (27.8 % of the natural rubidium found in nature) arises stable isotope  $^{87}\text{Sr}$  with a half-life of  $4.88 \times 10^{10}$  (years). The number of the daughters' arisen is described by the decay equation:

$$^{87}\text{Sr} = ^{87}\text{Sr}_i + ^{87}\text{Rb} (e^{\lambda t} - 1)$$

$^{87}\text{Sr}$ =	number of $^{87}\text{Sr}$ atoms per weight unit of the mineral
$^{87}\text{Sr}_i$ =	number of $^{87}\text{Sr}$ atoms per weight unit at the moment of the forming of the mineral
$^{87}\text{Rb}$ =	number of $^{87}\text{Rb}$ atoms at the moment of the measurement
$\lambda$ =	decay constant of $^{87}\text{Rb} = 1.42 \times 10^{-11} \text{a}^{-1}$
$t$ =	formation age of the mineral

Because the analysed samples are alteration products of different rocks containing different Rb-bearing minerals (e.g. K-feldspar, biotite, etc.), with different  $^{87}\text{Rb}$  content, the  $^{87}\text{Sr}/^{86}\text{Sr}$  ratios represent the mean of the components found in the sample.

### *Measurement of the $^{143}\text{Nd}/^{144}\text{Nd}$ isotopic ratio*

$^{143}\text{Nd}$  (half-life  $1.06 \times 10^{11}$  years) is produced by  $\alpha$ -decay of  $^{147}\text{Sm}$ . The decay equation describes the gain of the radiogenic  $^{143}\text{Nd}$  from the  $\alpha$ -decay of the  $^{147}\text{Sm}$ :

$$^{143}\text{Nd} = ^{143}\text{Nd}_i + ^{147}\text{Sm} (e^{\lambda t} - 1)$$

$^{143}\text{Nd}$ =	number of $^{143}\text{Nd}$ atoms per weight unit of the mineral
$^{143}\text{Nd}_i$ =	number of $^{143}\text{Nd}$ atoms per weight unit at the moment of the forming of the mineral
$^{147}\text{Sm}$ =	number of $^{147}\text{Sm}$ atoms at the moment of the measurement
$\lambda$ =	decay constant of $^{147}\text{Sm} = 6.54 \times 10^{-12} \text{a}^{-1}$
$t$ =	formation age of the mineral

The Sm/Nd ratio of the bulk Earth can be assumed to be the same as in chondritic meteorites. From the bulk Earth Sm/Nd ratio, the  $^{143}\text{Nd}/^{144}\text{Nd}$  ratio of the bulk Earth can be calculated. It is thus often more meaningful to consider variations in  $^{143}\text{Nd}/^{144}\text{Nd}$  relative to the bulk Earth, or chondritic, value. This is the purpose of  $\epsilon$  notation.  $\epsilon_{\text{Nd}}$  is simply the relative deviation of the  $^{143}\text{Nd}/^{144}\text{Nd}$  ratio from the chondritic ratio in parts in  $10^4$ :

$$\epsilon_{\text{Nd}} = \left( \frac{^{143}\text{Nd}}{^{144}\text{Nd}} - \left( \frac{^{143}\text{Nd}}{^{144}\text{Nd}} \right)_{\text{CHON}} \right) / \left( \frac{^{143}\text{Nd}}{^{144}\text{Nd}} \right)_{\text{CHON}} \times 10^4$$

The present day chondritic value of  $^{143}\text{Nd}/^{144}\text{Nd}$  is 0.512638 (when corrected for mass fractionation to a  $^{146}\text{Nd}/^{144}\text{Nd}$  ratio of 0.7219).

Most rocks have  $\epsilon_{\text{Nd}}$  values in the range of - 20 to +10.  $\epsilon_{\text{Nd}}$  provides information about the history of a rock. A negative  $\epsilon_{\text{Nd}}$  value implies that an average Sm/Nd ratio of the rock or its precursors has been lower than the chondritic ratio over the history of the Earth. This in turn implies the rare earth pattern of the rock or its precursors was light rare earth-enriched. We can draw the opposite inference from a positive  $\epsilon_{\text{Nd}}$  value. The average Nd isotopic composition of pelitic alteration products of an orogenic region reflects the isotopic composition of their parent rocks (White, 2001).

#### ***4.2.6. Electron microprobe analysis (EMPA)***

Bulk chemical analyses can carry several difficulties (e.g. “tempering effect”) used to determining the origin of coarse wares. In cases, when unique but small mineral (e.g. pyroxene, spinel, tourmaline, etc.) or rock fragments (e.g. volcanites) are present in the sherd, EMPA can be a powerful method in the provenance analysis (e.g. Kamilli & Lamberg-Karlovsky, 1979; Tite & Maniatis, 1975). Results of the measurements on solid grains can be directly compared to data obtained from rocks and geological formations of the presumed place of origin of the raw material of the sherd and thus to the presumed place of production.

EMPA is a non-destructive method for determining the chemical composition of tiny amounts of solid materials. The term „non-destructive” means that the thin section prepared from the sample and analysed with EMPA can be used for further analyses (e.g. optical microscopy, etc.).

EMPA uses a high-energy, focused beam of electrons to generate X-rays characteristic of the elements within a sample from volumes as small as 3 micrometers ( $10^{-6}\text{m}$ ) at a cross-section. The resulting X-rays are diffracted by synthetic analysing crystals (TAP, PET, LIF) and counted using gas-flow and sealed proportional detectors. Chemical composition is determined by comparing the intensity of X-rays from standards with those from unknown materials after corrections for effects of absorption and fluorescence in the sample.

The electron microprobe is designed specially for detecting and measuring characteristic X-rays. The resulting data yield quantitative chemical information in a textural context. Variations in chemical composition within a material, such as a mineral grain, can be easily determined.

The analyses were carried out in the Institute for Geochemical Research of the Hungarian Academy of Sciences (Budapest) using a JEOL JXA-733 instrument, equipped with 3 wavelength dispersive spectrometers and an Oxford Instruments INCA Energy 200 energy dispersive spectrometer. Detection limit: 0.1 wt %.

The evaluation of the measured data were carried out using the computer program MINPROG (Harangi, 1993). EMPA was carried out on the same thin sections which were used for the petrographic analyses.

#### ***4.2.7. Neutron Activation Analysis (NAA)***

Neutron activation analysis using (mostly thermal) neutrons is a useful method for the simultaneous determination of about 25 to 40 major, minor, and trace elements in small geological samples. The method allows for the highly selective determination of these elements (especially of the rare earth elements [REE], Sc, Cr, Co, Rb, Sb, Rb, Hf, Ta, W, Th, U, and others) in the ppm and ppb range. At the NAA analysis the sample is activated with neutrons. During the irradiation with neutrons, the naturally occurring stable isotopes of all elements that constitute the rock and mineral samples are transformed into higher-mass radioactive (unstable) isotopes by neutron capture reactions, and then the activated nucleus decays with a characteristic half-life.

The amount of the radioactive nuclide is determined by measuring the intensity of the characteristic gamma-ray lines in the gamma spectrum. For the measurements gamma-ray detector and specialised electronic equipment is used. Because irradiated samples contain radionuclide of different half-lives, the gamma spectra change with time and it is therefore necessary to count at different time intervals after the end of the irradiation (early in the process for rather short-lived isotopes, and later, after short-lived isotopes have decayed and therefore reduced the background, for long-lived isotopes. After taking into account different half-life corrections, decay times, counting times, and other correction factors, the results are quantified by comparison with synthetic or natural standards which have been irradiated and counted together with the samples.

The pottery samples were prepared for the analysis in a following way. Cleaned and powdered samples were fired at 600 °C for an hour to eliminate absorbed humidity and current content of organics. Other samples (non-plastic inclusions, etc.) were not fired. 50 to 100 mg of sample was measured into polyethylene irradiation capsules. For the measurements the standards NBS 1633a Coal Fly Ash and IAEA Soil-7 were used. The samples were irradiated and measured at the Radiochemistry Laboratory of the Institute of Nuclear Techniques at the Budapest University of Technology and Economics. The samples were irradiated at 100 kW reactor power, a neutron flux of  $10^{12}$  n/cm<sup>2</sup>, for a period of 8 hours. For the isotopes of shorter half-life, first measurements were carried out after 5-6 days of cooling with 5000 to 8000 s of measuring time. After one month of cooling the samples were measured again with at least 10000 s of measuring time in order to determine the amount of the isotopes with longer half-life.

## CHAPTER 5. Main geological features of the study areas

### 5.1. Introduction

Archaeological sites, survey areas, and the archaeological material they produced, researched in this study, are situated on the eastern and south-eastern part of the Balkan Peninsula and in northwest Anatolia. This vast area belongs to several major tectonic units, which have complex geological history. These units are partially made from similar geological formations, the phenomenon which, as we will see later, is reflected in the petrographic and chemical composition of the geological and archaeological materials collected in different places.

Major tectonic units in the area under discussion are orientated from the south to the north: the Sakarya Zone in north-western Anatolia, the Thrace Basin, the Strandja and Rhodope Massives in Turkish Thrace and in Bulgaria, the Balkanides and the Moesian platform in Bulgaria (Fig. 13).

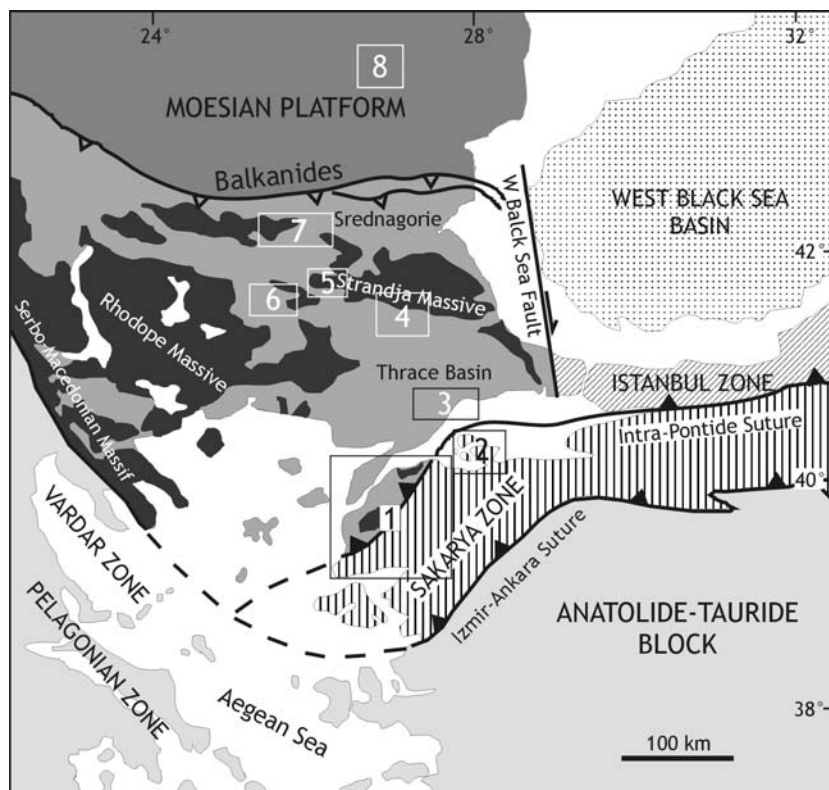


**Fig. 13** Main tectonic units of northwest Anatolia and the Balkan Peninsula. Quadrangles show the position of the detailed geological maps (1. The Troad; 2. The Ayşa Island and surrounding areas; 3. Menekşe Çatağı and its environment; 4. North Turkish Thrace; 5. The westernmost Strandja Massive; 6. The northeast Rhodope Mts.; 7. The south-eastern Balkanides; 8. The north-eastern Moesian Platform; after Okay et al., 1996, 2001).

These fragments with independent Paleozoic and Mesozoic geological histories had assembled by the Tertiary, following the closure of the intervening Tethyan oceanic basins (Foosse & Manheim, 1975; Okay *et al.*, 1996, 2001).

The aim of the following chapter is to characterise the different areas in order to obtain answers to a several petrographic and chemical questions concerning the provenance analysis. As we will see, without the knowledge of the geological backgrounds no successful provenance analyses could be carried out. The chapter contains the brief history of geological development and information on the major geological features (formations, rock types) of the wider environ of the archaeological sites.

## 5.2. The Troad

Troia is situated on the north-western Biga peninsula on the north-western spur on a Neogene erosion surface above the flood plains of the Karamenderes river in the west and the Dümrek river in the north.

Fig. 14 shows the drainage basins of the rivers Karamenderes and Dümrek. Basic raw materials of the sediments transported by these rivers are found in their catchment areas. The geology of the Biga peninsula has been studied in detail in the last decades (Bingöl *et al.*, 1973; Okay *et al.*, 1991; Okay *et al.*, 1996; Okay & Satır, 2000a-b). The Marmara region has been divided into four zones settled NE-SW (from NW to SE: the Gelibolu zone, the Ezine zone, the Ayvacik-Karabiga zone, and the Sakarya zone).

The oldest metamorphosed rocks are found in the Kazdağ Massive in the southern part of the peninsula. Their ages have been isotopically dated to Devonian and mid-Carboniferous (Okay *et al.*, 1996; Okay & Satır, 2000a). There are granitoides, gneisses and metamorphosed basement sediments of the Kazdağ Group. Gneiss, which constitutes most part of the Kazdağ Massive, consists mostly of quartz, plagioclase, biotite and hornblende. Among accessories a diopside, garnet and titanite can also be found. Medium to coarse grained, dark green amphibolites consist of plagioclase, hornblende and opaque minerals.

The Kazdağ Group belongs to the Sakarya zone, the southernmost of the four zones in this region. The zone is defined from the north by the Intra-Pontides Suture and from the south by the Izmir-Ankara Suture (Sengör & Yılmaz, 1981).

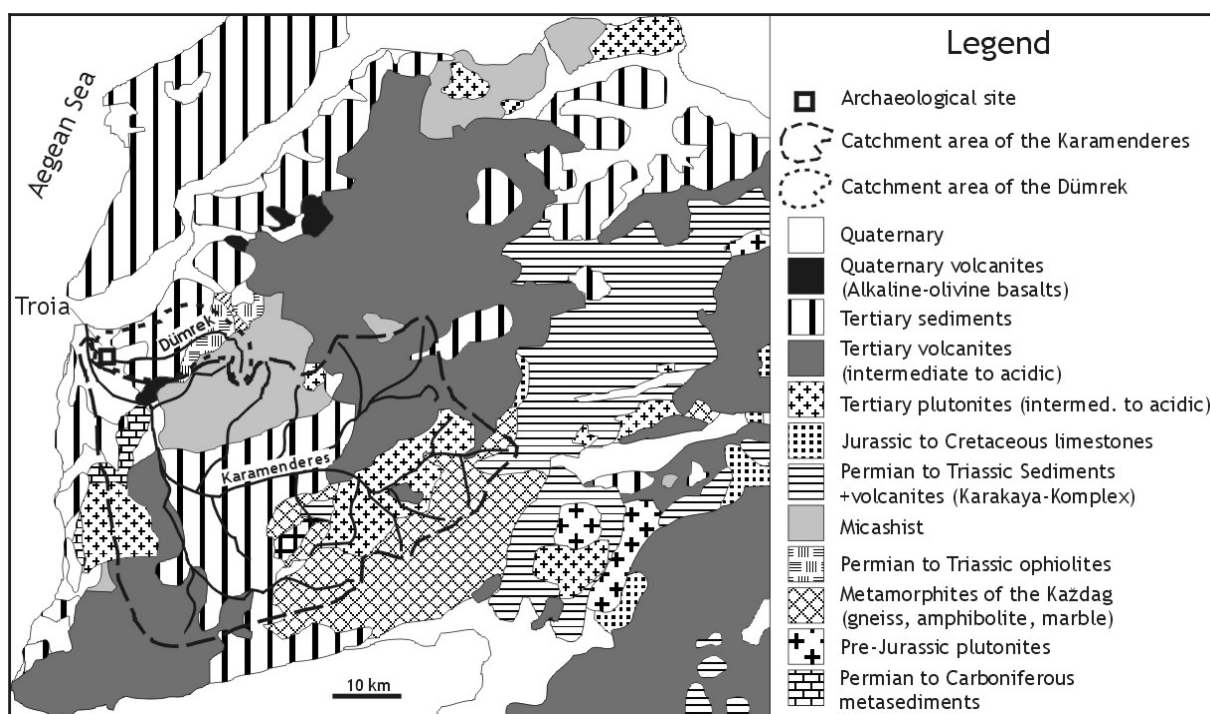


**Fig. 14 Geological map of the Troad (modified after Knacke-Loy, 1994).**

To the north lies the Ayvacik-Karabiga zone. A part of it is the large Alakeçi-Mylonite zone, situated between the metamorphites of the Kazdağ Group and the Çetmi-Ophiolite Melange and consisting mostly of gneiss and metaserpentinites. Gneiss is foliated and consists of quartz, sericite, opaque minerals, biotite and plagioclase porphyroblasts. Black amphibolites and marble bodies also appear in the gneisses. Dark green, fine-grained metaserpentinites, without any relict of ultramaphic texture, contain mostly antigorite, antophyllite, talk and diopside.

The upper Cretaceous to upper Tertiary Ophiolite Melange (Çetmi Ophiolite Melange), situated westward from the Kazdağ Massive, consists of more than 90 % basic volcanites and pyroclastics, Triassic to Cretaceous limestones and aleurites. Radiolarites and serpentinites also occur in the area. Additionally, some tectonically interbedded garnet, micashist and eclogite blocks are also present. These metamorphic overwritten basic rocks contain albite, Ti-augite, and chlorite.

The Ezine zone, situated on the north-western part of the Biga Peninsula, contains slightly metamorphosed epicontinental Carboniferous to Permian sediments (the Karadağ unit), which were overlapped by Permian to Triassic ophiolites (Denizgören Ophiolite).

The Karadağ unit is made from quartz-phyllites, quartzites, metamorphosed quartz sandstones, marble, and graywackes.

The Denizgören Ophiolite is predominantly composed of serpentinitised peridotites (harzburgite, lherzolite). Characteristic minerals are: serpentine (chrysotile, lizardite, antigorite), orthopyroxene and clinopyroxene, talc, sericite, and ore minerals (magnetite, chromite). There are also some relicts of

primer olivine minerals. The chromium and nickel content of these rocks is very high (about 3000 ppm).

The Çamlıca Micashist, situated northwards from Ezine, has a size up to 300 km<sup>2</sup>, and is made up of quartz, muscovite, carbonate, and albite as main components and chlorite, clinozoizite, and garnet as secondary components.

The Gelibolu zone relates to the Ezine zone in the northwest and spreads from the Gelibolu Peninsula to the Marmara Island (the Sea of Marmara). Lithologically it equates the Ayvacik-Karabiga zone, thus it contains serpentinites, radiolarites, red and grey pelagic limestone, spillite and dolerite (Çetmi Ophiolite Melange). Basic magmatites are partially metamorphosed (blue schist facies; high-pressure, low-temperature rocks).

The formation of the clayey, relatively unconsolidated sediments, which were used for ceramic production in Troia and in its vicinity, began on the Biga-Peninsula in the Tertiary (Knacke-Loy, 1994). The oldest Tertiary deposits are neritic chalks from the middle Eocene. They are covered by Miocene turbiditic series including andesites and andesitic tuffs.

Due to the tectonic uplift these series were eroded again mostly during the Oligocene.

During the late Oligocene calc alkaline magmatism began and continued until the middle Eocene. Many plutonite bodies with intermediate to acidic composition intruded in the Oligocene and in the early Miocene, like the Kestanbol Intrusion located 25 km southward from Troia. Petrographically these rocks are chiefly quartz-monzonites (mineralogical composition: plagioclase (40 %), orthoclase (20 %), quartz (10-15 %), green hornblende, biotite; Birkle, 1993).

Evciler Plutonite, which is also situated in the catchment area of the Karamenderes, shows similar mineralogical composition, containing some more quartz (20 %) and hornblende (Birkle, 1993).

During the early to late Miocene large areas on the Biga-Peninsula were covered by andesitic-dacitic and rhyolitic volcanites and tuffs. Based on geochemical analyses (Birkle, 1993; Birkle & Satır, 1994) these volcanites are latites and quartzlatites.

During the late Miocene fluvial to shallow marine sediments were deposited in the northern part of the Biga Peninsula. Since the Pliocene, fluvial and limnic sediments accumulated in some locations. During the Quaternary alkaline-basaltic volcanism occurred, but it spread less than the Tertiary volcanism. Alkaline-olivine basalts show iddingsited olivine crystals in a fine-grained matrix, which consist predominantly of feldspar-ridges and opaque minerals. Amygdales are filled with zeolite minerals and quartz aggregates.

### 5.3. The Avşa Island and surrounding areas

The Avşa Island is situated 12 km northwest from the Marmara Island in the Sea of Marmara. This region geologically belongs to the magmatic-metamorphic series of the Sakarya zone. The Paleozoic continental basement of the Sakarya zone consists of granitic and high-grade-amphibolite to granulite facies metamorphosed metamorphic rocks (Okay *et al.*, 1996). This Paleozoic basement is tectonically overlain by the Karakaya Complex (Okay *et al.*, 1996), which is made from several types of metamorphic rocks (metaquartzites, shists and marbles on the Marmara Island, in Manyas and near to Bandırma). Oligo-Miocene granitoids (Okay *et al.*, 1996) constitute more than 80 percent of the Avşa Island, but these acidic plutonic rocks make the most part of the surrounding islands and peninsula (Fig. 15).

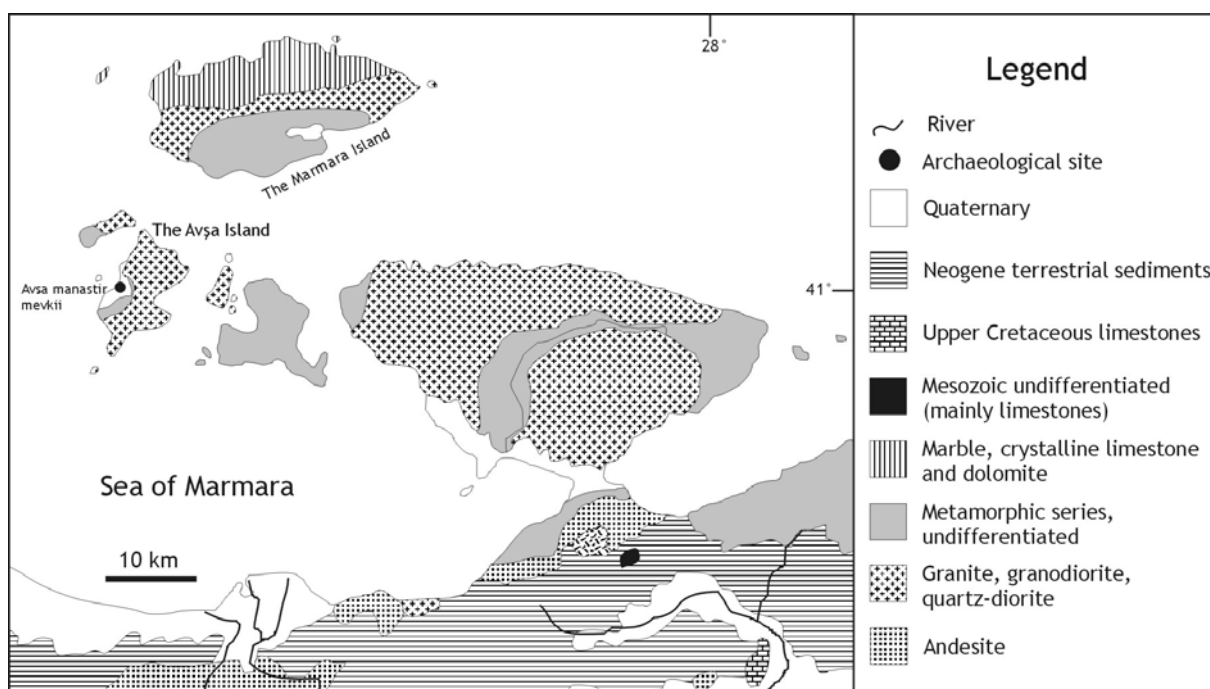
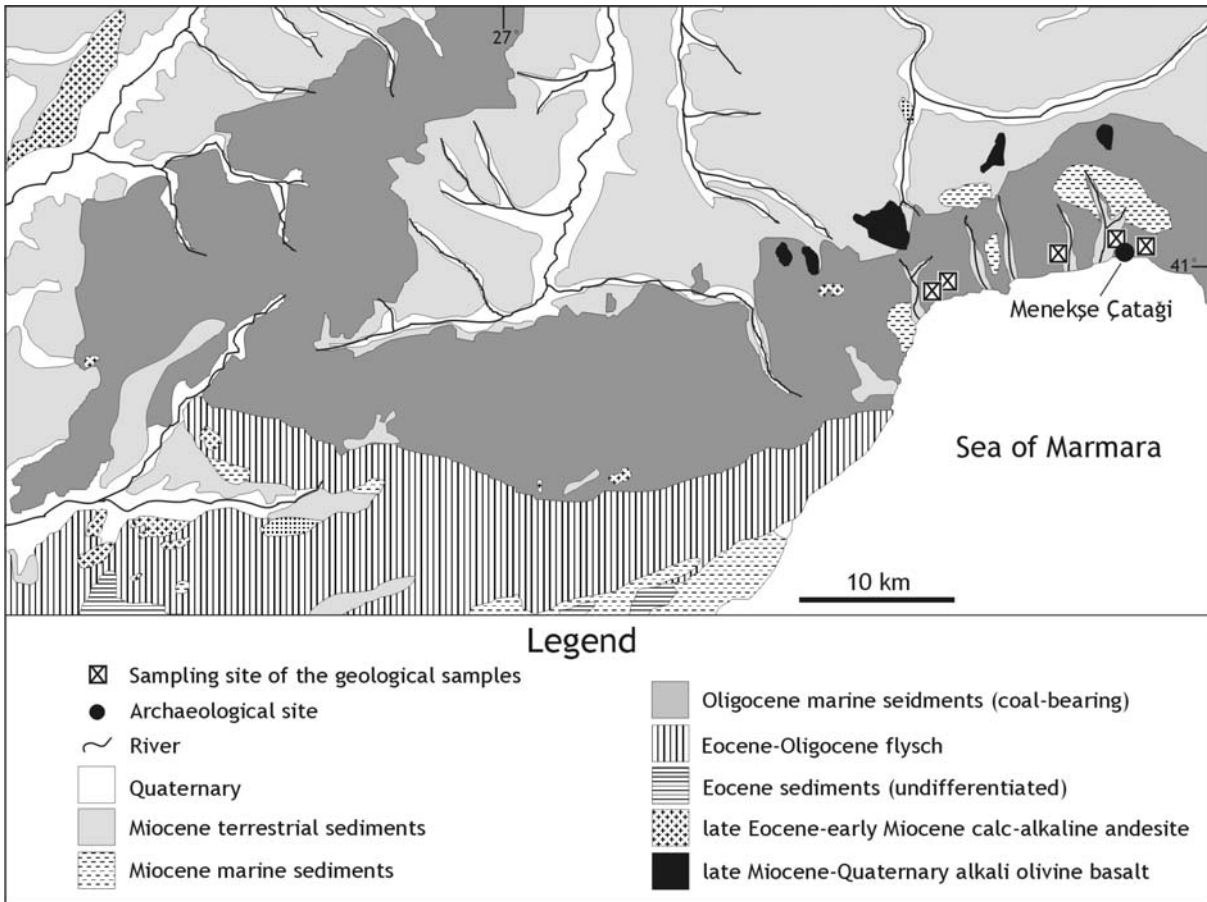


Fig. 15 Geological map of the Avşa Island and surrounding areas (after the GEOLOGICAL MAP OF TURKEY 1: 500.000, Sheet Istanbul, 1964).

### 5.4. The Thrace basin and its southern coast at the Sea of Marmara (Menekşe Çatağı)

The Thrace basin is situated between the Strandja Massive in the north and the Sea of Marmara in the south (Fig. 13 and 16). It is composed of a thick (up to 9000 m), siliciclastic sedimentary succession, which had been deposited within the basin (Kopp *et al.*, 1969). The oldest sediments were formed in a residual oceanic basin, remained after the total consumption of the Neotethyan ocean floor in the upper Cretaceous (Yılmaz *et al.*, 1995). The sediment deposition continued till the early Eocene in a

progressively shallowing sea environment. A marine transgression, which reached the Strandja Massive during the late Eocene, deposited different sediments as basal conglomerates, sandstones and limestones with a marked angular unconformity on the uplifted and elevated land (Yılmaz & Polat, 1998).



**Fig. 16 Geological map of the northern coast of the Sea of Marmara (Menekşe Çatağı; after the GEOLOGICAL MAP OF TURKEY 1: 500.000, Sheet Istanbul, 1964; Yılmaz & Polat, 1998).**

The lithology of the Oligocene is uniform; fine-grained sandstone and sandy clay of deltaic and flysch-like origin is prevalent. From the late Oligocene until the late Miocene a continental environment existed, when clastic materials from the Strandja Massive had been transported by rivers to the south part of the area. Starting with the Helvetian and until the end of the Pannonian, when the inner lake which covered the area dried up, brackish sediments (limestone, sandstone) had been deposited. In the late Pliocene Thrace was levelled and transformed into a peneplain, occurred during the Quaternary fluvial sedimentation (Kopp *et al.*, 1969). During the Cenozoic intermediate (late Eocene – early Miocene calc-alkaline andesites) to mafic (late Miocene-Quaternary basanites and alkali-olivine basalts) volcanic rocks were emplaced (Yılmaz & Polat, 1998).

The archaeological site of Menekşe Çatağı is situated 15 km northeast from Tekirdağ on the northern coast of the Sea of Marmara. Major geological features of the coastal region will be summarised

according to Jaranoff (1937). Along the seacoast between Tekirdağ and Menekşe Çatağı upper Eocene - Oligocene sedimentary sequence can be observed, containing coastal sand, green nodular clayey, coal bearing strata, and cemented clayey coarse sand. In the late Miocene cross bedded fluvial sand, partly with diorite, gneiss, and metaquartzite pebbles, indicates the source area (Strandja Massive) in the north. Discordance between upper Miocene and Levantine layers (limestone pebbles, Palaeoergine river?) signify the uplift of the coastal area. Since Quaternary only short brooks and small rivers flew into the Sea of Marmara (Fig. 16). On the basis of absolute dating basaltic volcanites northwest from Menekşe Çatağı show late Miocene – early Pliocene ages (Yılmaz & Polat, 1998).

### 5.5. The south-western Strandja Massive (north Turkish Thrace and Ovcarovo)

The geology of the Strandja (Istranca) Massive is described in several publications (Üşümezsoy, 1982; Chatalov, 1988; Çağlayan *et al.*, 1988; Savov *et al.*, 1995; Okay *et al.*, 2001). The following passage contains brief characteristics of the main geological features of the Massive, focused on the main rock types of the south-western part of the area in Turkey and the Bulgarian part near Ovcarovo.

The Strandja Massive, which belongs to the Balkan metamorphic province (containing the Serbomacedonian, Rhodope and Strandja Massives) is a mid-Mesozoic orogenic belt straddling the Turkey-Bulgaria border, built on a late-Variscian basement of gneisses, migmatites and granites unconformably overlain by a Mesozoic metasedimentary sequence (Çağlayan *et al.*, 1988; Okay *et al.*, 2001).

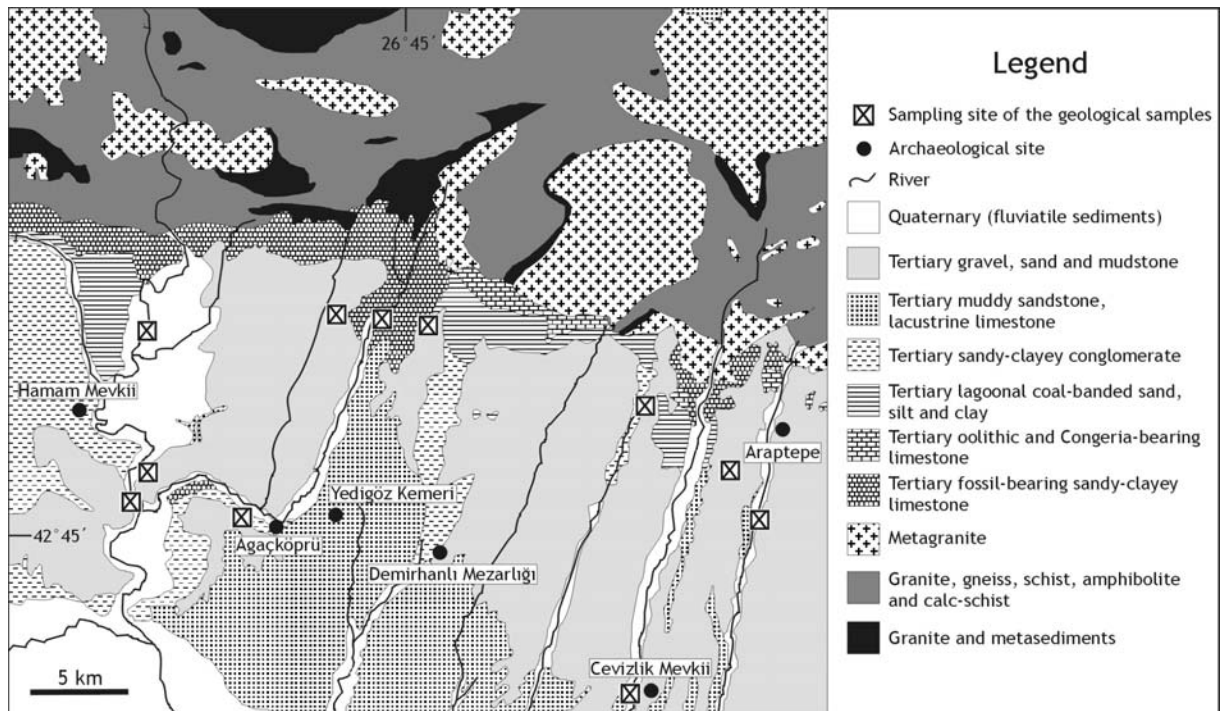
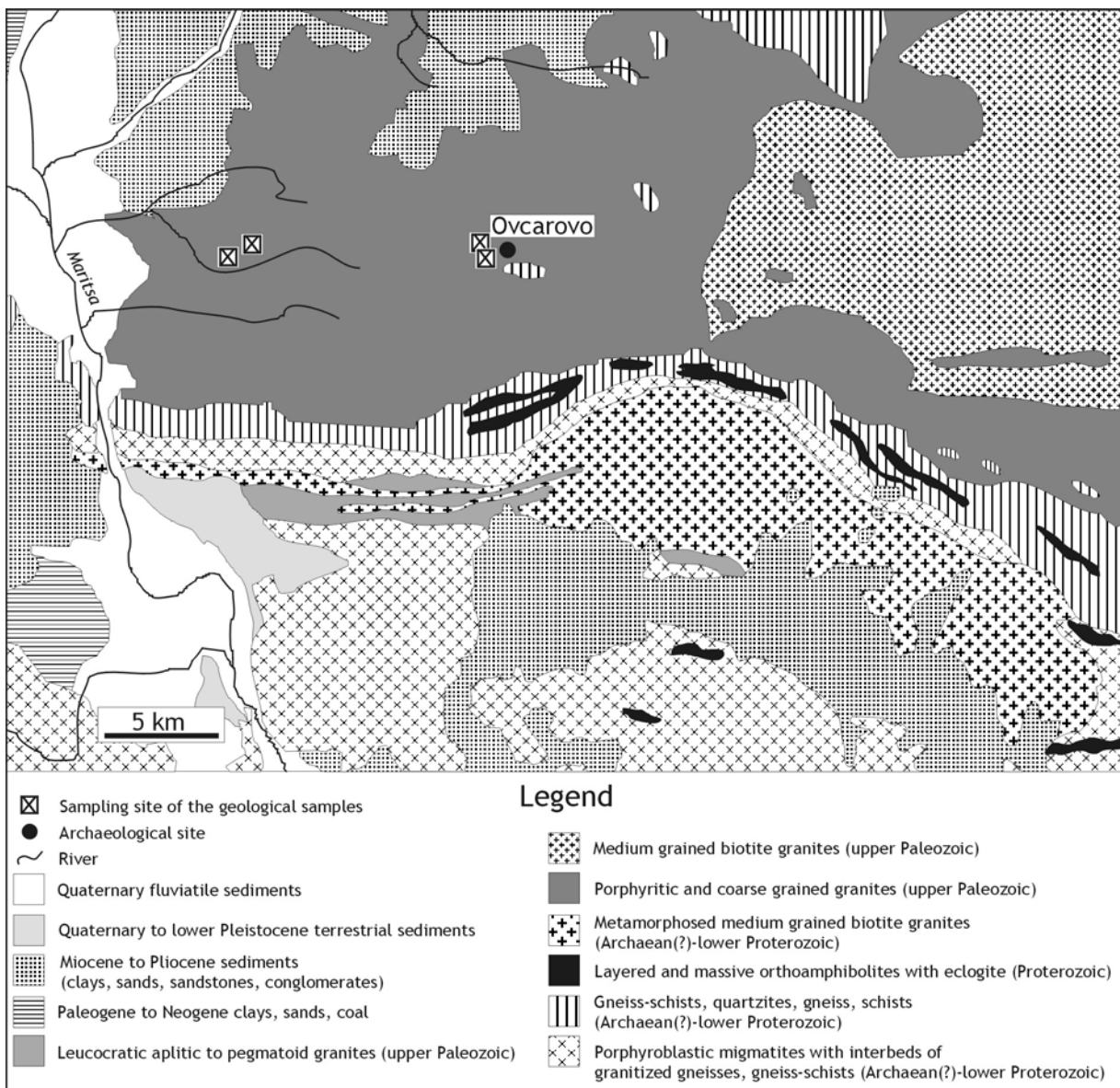


Fig. 17 Geological map of north Turkish Thrace (the Strandja Massive; after the GEOLOGICAL MAP OF TURKEY 1: 500.000, Sheet Istanbul, 1964; Yılmaz & Polat, 1998).

The oldest rocks, situated north from Edirne in the Strandja Massive, are granites (Ömeroba metagranite consists of quartz, plagioclase, microcline, muscovite, and minor biotite) and felsic gneisses, which make the bulk of the late-Variscian basement. Beside these magmatites, metamorphic rocks can also be found in the area. They are dominated by granitic gneisses with minor amounts of migmatite, amphibolite, and micashist and intruded by many granitic veins, dykes, and plutons (Okay *et al.*, 2001). These magmatites and metamorphites are unconformably overlain by a continental to shallow marine metasedimentary sequence of Triassic – middle Jurassic age, which is consisted of metaconglomerates, metasandstones, and metacarbonates (marbles; Okay *et al.*, 2001). The traces of the Tertiary sedimentary sequences can also be found in the foothill areas of the Strandja Massive.



**Fig. 18 Geological map of the westernmost Strandja Massive (Ovcarovo; after Boyanov et al., 1989; Kozhoukharov et al., 1994).**

They are mostly represented by oolitic reefal limestone, conglomerates, lacustrine limestones, sandstones, sands, clayey sands, and clays (Kopp *et al.*, 1969; Yılmaz & Polat, 1998). The area between Edirne and the Strandja Massive is now a piedmont region (north-western part of the Thrace basin), where the composition of the raw materials used for pottery production is influenced by the hinterland (magmatic-metamorphic rock association) and the Tertiary to Quaternary sediments. The products of erosion are transported by short and partly intermittent brooks and small rivers to the Thrace basin (Fig. 17).

Ovcharovo and its environs, situated on the westernmost end of the Strandja Massive (Srednogorie zone) in Bulgaria, have similar geological features to those already mentioned above. The area is mostly made from different types of late-Variscian basement granites (porphyritic, coarse grained and biotite bearing). South and north from the magmatic pluton metamorphic rock associations consisting of gneiss, orthoamphibolites, and metaquartzites are found (Kozhoukarov *et al.*, 1993; Kozhoukarov *et al.*, 1994; Okay *et al.*, 2001). The hilly area which is uplifted 2-400 meters from the surrounding river plains (Sokolica in the north and Maritsa in the west) has only short and partly intermittent small rivers (Fig. 18), which all belong to the catchment area of the Maritsa.

## **5.6. The south-eastern Rhodope Mts. (Chal)**

The Rhodope Massive which belongs to the Balkan metamorphic province in south Bulgaria and partly in north Greece is a rugged mountainous terrain made mostly from Precambrian and early Paleozoic crystalline rocks (Foose & Manheim, 1975). Its northern boundary is the Maritsa fault, to which, once belonging the Srednogorie zone situated between the Rhodope and the Balkan Mts., Archaean and Proterozoic metasedimentary rocks are common in a thickness of approximately 18000 m (Tzankov *et al.*, 1968). These metasediments attest the long-lived stability of the Rhodope crustal block during that time. During the Proterozoic the Massive was first segmented by faulting along northeast-southwest lines (Pirin, western, central, and eastern Rhodope blocks); later the segmentation was accomplished by northwest-southeast faulting in the Paleozoic and continued till the present time by recurrent movement on the faults. The intervening grabens which were situated between the stable blocks received sediments and they were also the sites of Tertiary volcanic activity (Foose & Manheim, 1975). During the Paleozoic granites were emplaced (Rila and Pirin uplifts) and along the south and northeast sides of the Rhodope early Paleozoic phyllites, chalk shists, conglomerates, and arkoses reveal that sedimentation at that time was limited to the peripheral margins. At the end of the Cretaceous and the early Paleocene the movement was renewed along the block fault system, when the Maritsa fault was locus for monzonite and diorite intrusives (Foose & Manheim, 1975). During the late Eocene – Oligocene, due to the extensive, differential vertical movement of the graben resulted in deposition of up to 2500 m of freshwater molasses, silt, clay and coal interbedded with collision

related andesite and rhyolite (Dabovski *et al.*, 1991). Neogene have resulted in up to 200-300 m of molassoid sedimentation.

The archaeological site of Chal, situated in the north-eastern part of the Rhodope Mts. near the Maritsa fault, is surrounded by several formations and rock types, which represent the complex geology of the Rhodope Mts. A short geological review of the rock formation is presented below, according to Boyanov *et al.* (1989). The oldest rocks (Pre- Rhodopian Supergroup) found in the region are gneiss-granites, porphyroblastic metamorphites, metaconglomerates, and metaserpentinities of Precambrian age. These rocks mostly make the hilly region northeast from Chal, but they are also found in smaller patches in the narrow neighbourhood of Chal.

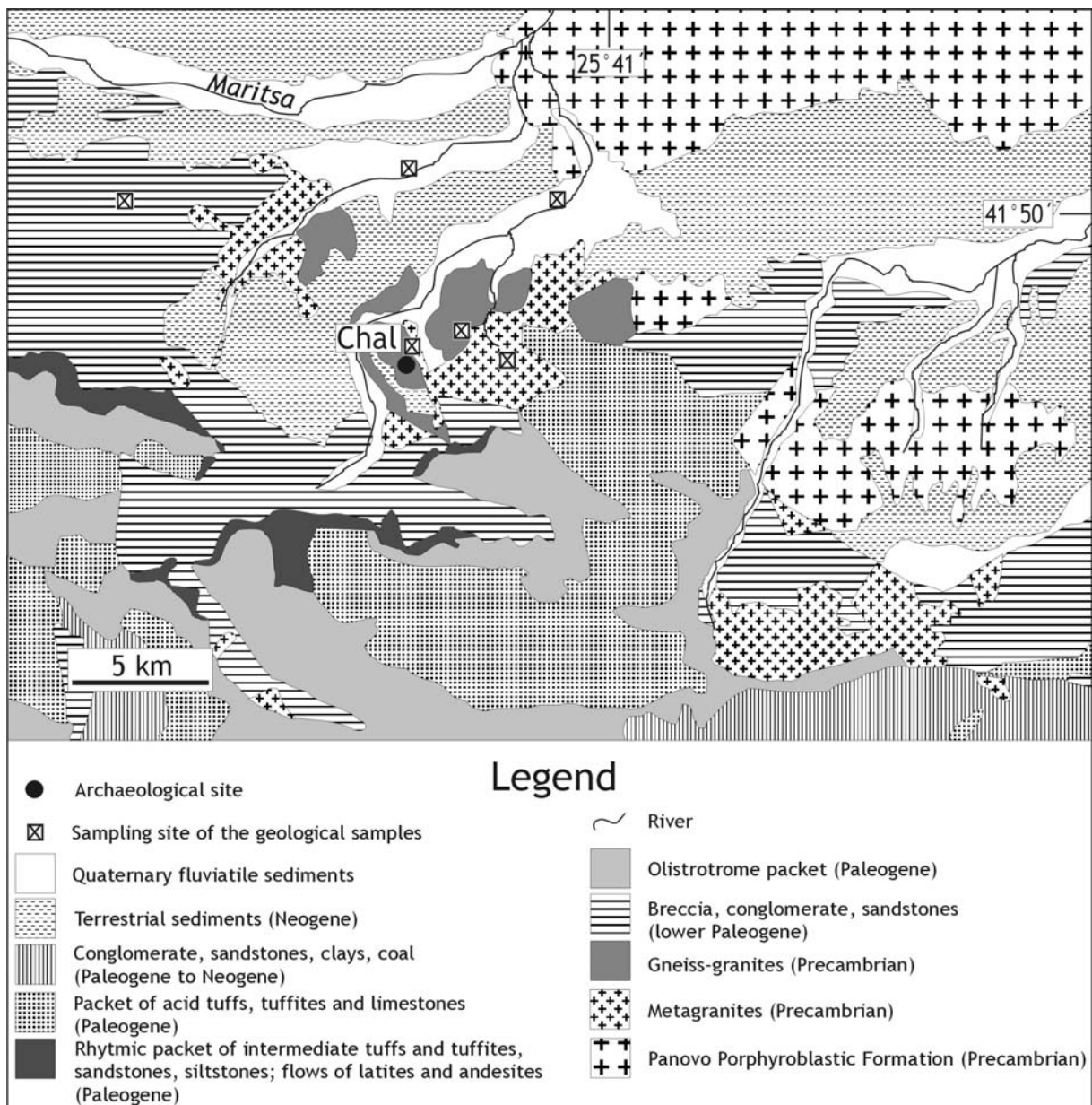


**Fig. 19** Geological map of the north-eastern Rhodope Mts. (Chal; after Boyanov et al., 1989).

Paleozoic (granodiorites, schistous-greywacke, coarse-grained, and leucocratic granites) and Triassic (metamorphosed quartz porphyres, mica, and mica-garnet schists) rocks are represented 20-30 km to the north and northeast, near the Maritsa fault. The region mostly consists of Paleogene collision-related volcanites and sediments. Products of the first intermediate volcanism (sandstones, block-breccia, conglomerates, limestone, marls as well as volcanites as latites, andesites, and their tuffs) are situated to the west, southeast, and east of the archaeological site. Formation of the first acid volcanism (packet of acid tuffs, tuffites, and organogenic limestones) can be found to the south and southeast of the settlement. Formations of the second and third intermediate as well as the second and third acidic upper Paleogene volcanism are represented by porphyric-latites, tuffs, rhyolites, trachyrhyolites, tuffs, and reef limestone in the area. Upper Paleogene to Quaternary rocks and sediments contain different clays, sands, conglomerates, acidic volcanites, and young fluvial sediments (Boyanov *et al.*, 1989; Fig. 19).

### **5.7. The southern Balkanides (Diadovo, Pshenitsevo, and Kirilovo)**

The archaeological sites Diadovo, Pshenitsevo, and Kirilovo are situated on the boundary of two main morphotectonic units: the Srednogorie and the Stara Planina zones. Both zones belong to the Balkanides, the term which also includes the Fore Balkan zone, situated between the Moesian platform and Stara Planina (Bonchev, 1971).

The Srednogorie zone is a crustal part of the old Rhodope Massive (its southern part is the Strandja Massive), which was fragmented along pre-existing faults, in Caledonian-Hercynian period. In coincidence of these tectonic events large granitic plutons (“south Bulgarian Granites”) had been emplaced. The area was a stable platform throughout most of the Mesozoic, receiving epicontinental, shelf-like sediments in areas of low elevation. Beginning in the Late Cretaceous and continued to the present, the zone was subjected to intense Alpine deformation. In this tectonic event vertical movements were dominant, accompanied by locally voluminous sedimentation, basic to acidic volcanism and north-verging gravitational nappe emplacement (Foose & Manheim, 1975).

The Stara Planina zone, defined topographically by the Balkan Mts., is made up of three major units; from west to east: Berkovitsa and Shipka anticlinorium as well as Louda Kamchiya synclinorium. In this summary only the second and third units will be presented, because all archaeological sites are situated in the area of these units. The Louda Kamchiya synclinorium, or eastern Stara Planina, associated with the Kotel strip on its northern side is the one of the deepest flysch- and molasse-filled basins in the Balkans. While the Shipka anticlinorium have well-exposed, folded, and metamorphosed Paleozoic rocks in its core, and its south limb is cut partly out by the gravitational gliding of Srednogorie granitic rocks northward on Triassic, Jurassic, upper Cretaceous, and lower Eocene rocks,

the Louda Kamchiya synclinorium has well-exposed thick upper Cretaceous and Paleogene flysch and upper Eocene molasse (Foose & Manheim, 1975).

After accumulation of the early Paleozoic sediments, metamorphosed by the Caledonian orogeny, late Paleozoic sedimentation, metamorphosed by the Hercynian orogeny, occurred in the central part of the Stara Planina. Later, 3000 m of Triassic to Middle Jurassic terrigenous and carbonatic sediments were accumulated. During the Jurassic 1000 m flysch accumulated in the Louda Kamchiya zone, which was eliminated by the middle Jurassic uplift until the Tithonian. In the early Cretaceous the Louda Kamchiya zone uplifted and during the late Cretaceous shallow water carbonates deposited in the Shipka zone and subsidence of the Louda Kamchiya zone, with simultaneous occurrence of flysch sedimentation and andesitic volcanism. At the same time folding and thrusting began (Foose & Manheim, 1975).

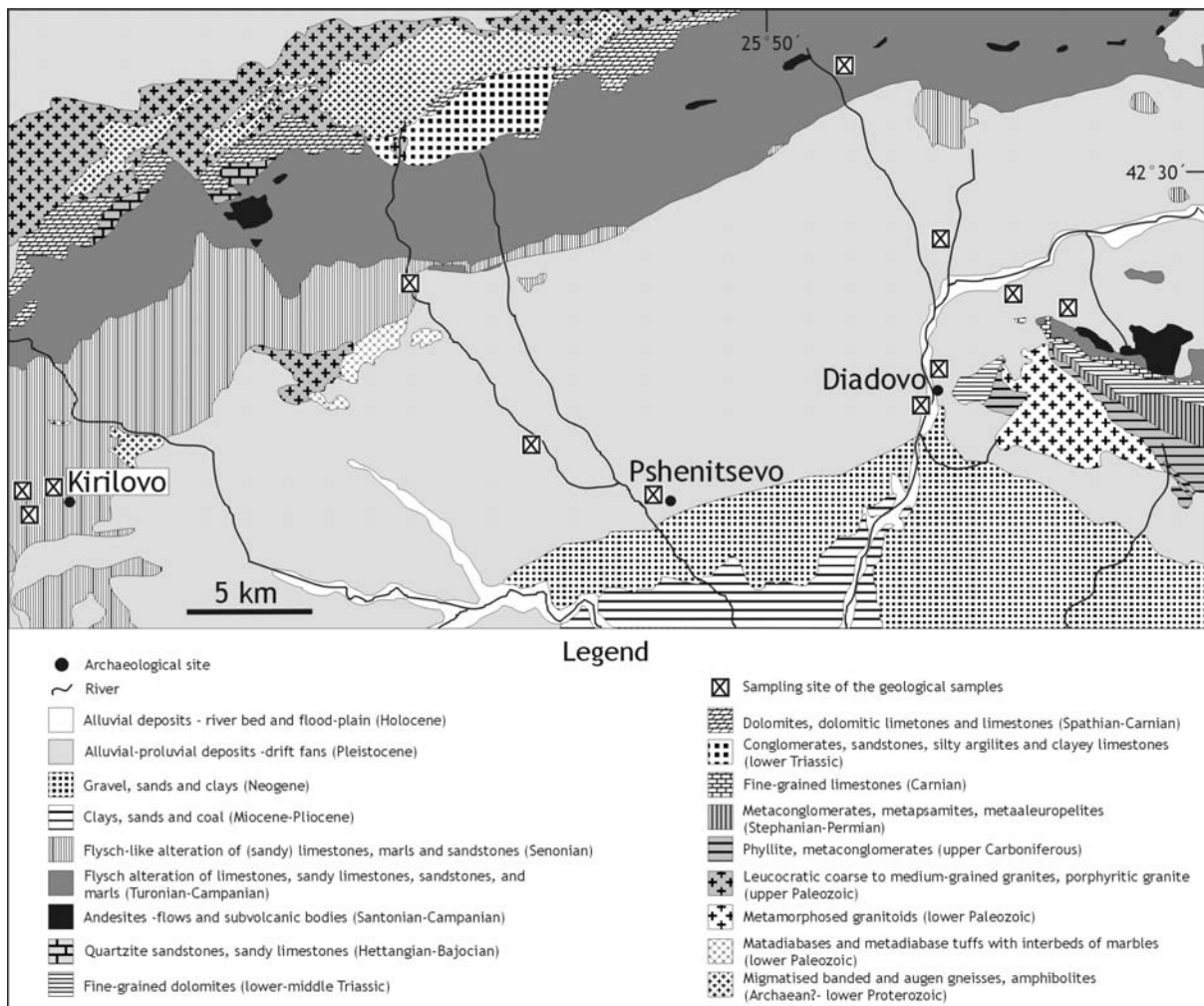


**Fig. 20 Geological map of the south-eastern Balkanides (Diadovo, Pshenitsevo, and Kirilovo; after Tzankov et al., 1992; 1995).**

Early Paleogene was marked by the deposition of thick (1500 m) terrigenous flysch in the eastern part of the Stara Planina. During the middle Eocene came the final folding and northward thrusting of the

Shipka anticlinorium with strong compression, folding and shearing accompanied by uplift in the Louda Kamchiya areas with some molasse sedimentation. From Miocene until recent time strong, vertical uplift has raised the Balkan Mts. (Foose & Manheim, 1975).

The types of sediments and their sedimentation processes of the region of Diadovo and Pshenitsevo, situated on the alluvial-fluviatile flood plain of the river Blatnica and other small brooks, which flow from the Balkan Mts, are found in the piedmont regions. The quality of sediments was influenced by different areas and rock types. The Svetiiljski Hills, situated east to the archaeological sites, belong to the Srednagorie zone, thus the oldest rocks are metamorphosed granitoids, meta-quartzporphirites and metadiabases of the Lower Paleozoic age. Carboniferous and Permian are presented by phyllites, metaconglomerates and metaquartzites. Lower-middle Triassic fine-grained dolomites, Santonian-Campanian volcanogenic formation of tuffs, sandstones marls, as well as limestone and andesitic rocks (flows and subvolcanic bodies) can be found among its Mesozoic rock types. Neogene sandy clays, sands, as well as Quaternary alluvial, talus, proluvial deposits (boulders, pebbles, sands, silts, sandy clays, and clays) origin from the hinterland and other elevated areas (the Balkan Mts.; Tzankov *et al.*, 1992; Fig. 20).

Kirilovo can be found in the southernmost range of the Stara Planina (the Balkan Mts.). The oldest rocks in the environs, near to Stara Zagora, are Precambrian magmatized, banded augengneisses and amphibolites. Paleozoic is represented by low metamorphosed schists, quartzites, and (metamorphosed) granitoids. Among Mesozoic rocks arkoses, (calcareous) sandstones, dolomites, limestone (Lower Triassic), clayey schists, and sandstones (lower-middle Jurassic) can be found. Middle-upper Cretaceous sediments and rocks play the most important role in the geology of the southern ranges of the Stara Planina. The mostly flysch and flysch-like formations of Cenomanian to Campanian contain marls, limestone, sandstones, quartzite, sandy limestone: volcanogenic sedimentary rocks made from alteration products of tuffs, sandstones and marls, deposited during Santonian to Campanian, Sredna Gora intrusions (diorites, monzo- and quartz diorites) belong to upper Cretaceous. Neogene is presented by Miocene to Pliocene clays, sands, and coal schists near Diadovo and Pshenitsevo, and basalt in the Balkan Mts., northeast from Stara Zagora. Quaternary alluvial, fluvial and talus deposit are the youngest sediments and cover the piedmont region (Tzankov *et al.*, 1995; Fig. 20).

## **5.8. The north-eastern Moesian Platform (Sborianovo)**

The Moesian platform, situated in the northern part of Bulgaria between the Fore-Balkan zone in the south and the south Carpathians (Romania) in the north, is a low relief major crustal block. It has probably been a stable crustal block since the late Proterozoic time (Foose & Manheim, 1975). Drill

holes and seismic data indicate, that its Precambrian basement is made of granitic gneiss, amphibolite, and quartzite, and is broken by faults into a mosaic of blocks similar to the Rhodope. Most of the Paleozoic, Mesozoic, and Tertiary were characterised predominantly by stable, shelf-type conditions of sedimentation. Approximately 2-4 km of shallow-water Paleozoic carbonate, carbonaceous, and deltaic sediment was accumulated on the shelf, followed by 2-3 km of Mesozoic carbonates and shales (Foose & Manheim, 1975). During the Tertiary to Quaternary mostly clayey sediments are found with unconformity on the older rocks.

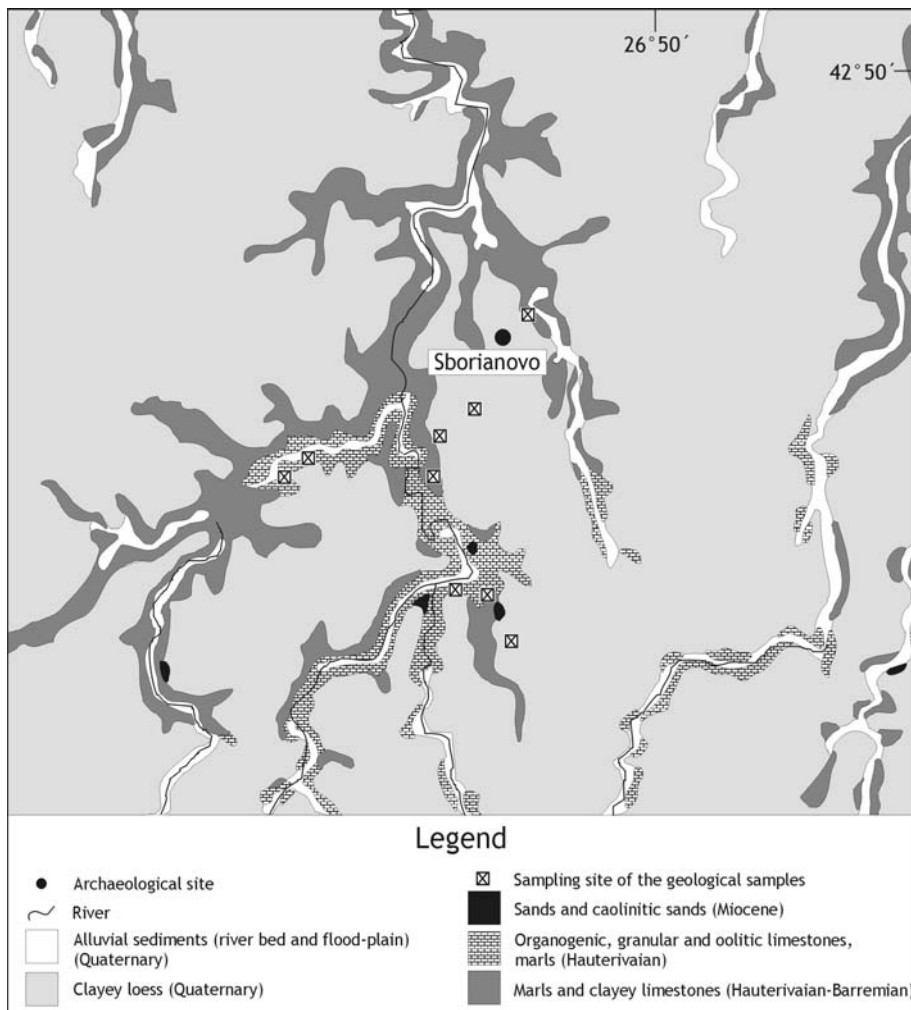


**Fig. 21 Geological map of the Moesian Platform near Sborianovo (after Filipov, 1990).**

The geology of the environs of the archaeological site of Sborianovo (between the towns Ispirih and Zavet) is quite simple. The oldest rocks are lower Cretaceous marls, clayey, and oolitic limestones. Neogene is presented in small patches southeast from the archaeological site by Miocene sands and kaolinitic sands, as well as by clayey limestone and sandy clays. With the exception of the relatively deep, but narrow river valleys, where rocks older than Neogene are exposed, the whole area is covered by Quaternary terrestrial (eolian and fluvial) sediments like loess, sandy clays, sands, gravel, and

different types of clays (Filipov, 1990). The area is cut by several small rivers, flowing into the Danube in the north (Fig. 21).

## CHAPTER 6. RESULTS

The results of the analyses will be grouped into two subchapters. In the subchapter 6.1. (Petrography, mineralogy and phase analysis) the data of microscopic petrographic observations (qualitative and quantitative) and fabric analysis will be presented. According to these data the results are completed with the cathodoluminescence (CL) observation of the sherds A-1 sherds. The phase composition of 20 selected sherds examined with X-ray diffractometry (XRD) is also presented in this part.

In the subchapter 6.2. (Geochemical analyses) the chemical data of XRF, radiogenic isotopes, NAA, and EMPA analysis will be presented. The presentation and grouping of the data below has been organised according to the archaeological localities and materials analysed in this study.

### 6.1. Petrography, mineralogy and phase analysis

#### *6.1.1. Petrographic analysis of the sherds and comparative materials*

The petrographic grouping of 91 Knobbed ware sherds including the pottery fragment *E9.158.1* analysed in a former study (Guzowska *et al.*, 2003) was based on the quality and quantity of the non-plastic inclusions.

In a first step, on the basis of the petrographic features, the petrographic groups have been formed on the site-base, i.e. sherds found in an archaeological site (e.g. group 1: Troia) and/or their narrower natural environment (e.g. group 7: Diadovo, Pshenitsevo and Kirilovo) have been regarded one main petrographic group. In many cases several subgroups have also been formed (e.g. 1B, Troian sherds with large amount of volcanic glass). Where it was necessary (e.g. the high variability of volcanic clasts in Troian sherds; 1B/1), further grouping (petrographic type) has also been carried out.

On comparative sand samples collected from riverbeds, as well as on the three locally produced, comparative sherds from Troia, from the I-V settlement phases (archaeological numbers: *K8.911.93*, *K8.911.9*, and *A5/6.502.1*) only qualitative microscopic investigation was carried out.

First the data of the comparative materials (sediments, locally produced sherds) followed by the petrographic composition (cf. Appendix 3) of the Knobbed ware sherds are presented. The results of the fabric analysis (cf. Appendix 4) of the vessel fragments are following the petrographic descriptions.

## Petrographic characteristics of mineral and rock fragments found in the sherds

### **Mineral fragments**

**Monocrystalline quartz (monoquartz):** subrounded to angular single quartz grains, mostly with slightly undulatory to undulatory (partially cloudy undulatory) or with straight extinction. On the basis of these optical properties metamorphic or plutonic origin can be assumed. Monocrystalline quartz grains are mostly in good association with quartz-bearing rock fragments found in the sherds. Polycrystalline quartz types (polyquartz, quartzite) are discussed together with the rock fragments.

**Sparite:** coarse grained (>15 µm; Folk, 1959; 1974) calcite fragments. Single rhomboidal grains may have belonged to a marble or a recrystallised limestone source rock.

**K-feldspar:** comprising term for all types of potash feldspar (orthoclase, sanidine, and microcline).

**Plagioclase:** comprising term for all types of plagioclase (albite-anorthite series).

**Pyroxene:** euhedral to subhedral, in many cases, zoned crystals.

**Amphibole (hornblende):** anhedral to subhedral greenish clasts with variable pleochroism.

**Mica:** muscovite and biotite single lamelles, or “mica packets”.

**Epidote:** anhedral clasts or crystal aggregates.

**Garnet:** subhedral crystals with isotropic optical property, partially with small inclusions.

**Olivine:** subhedral to anhedral clasts, mostly in form of pseudomorphoses.

**Opaque minerals:** comprising term for angular to subrounded clasts (e.g. hematite, spinel etc.) with non-translucent optical properties

### **Rock fragments**

**Plutonite:** comprising term for all magmatic rock fragments of plutonic origin and subhedral texture. The assumed type of plutonic rocks (intermediate to acidic composition) is given in the petrographic description.

**Volcanite:** comprising term for all magmatic rock fragments of volcanic origin and texture.

The main problem in determining volcanite clasts was the small size of the grains, which did not allow in all cases for an accurate identification of the type of the fragment. Therefore, referring to the uncertainties, in petrographic tables the terms basic-intermediate and intermediate-acidic were used.

**Recrystallised volcanite:** comprising term for volcanic rock fragments with traces of secondary recrystallisation processes (mostly silicification). Due to strongly recrystallised texture in many cases the original type of volcanite could not be exactly determined.

**Volcanic glass:** volcanite rock fragments with hyaline or hyalopilitic texture. The presumed type of volcanic glass (basic, acidic) is given in the description.

**Polycrystalline quartz (polyquartz):** in this work a comprising term for all types of quartzites of metamorphic and igneous origin, made of more than two quartz crystals. Depending on the genesis of

the rocks, grains with equate-polygonal mosaic structure, straight extinction (igneous), or with sutured to 120° triple-junctioned grain boundaries, stretched grains and (strong) undulatory extinction (metamorphic) can be observed (Götze & Zimmerle, 2000). Detailed description of polycrystalline quartz is presented together with the description of the samples.

**Microcrystalline quartz (chalcedony-chert):** fine-grained (< 5 µm) polycrystalline quartz. Comprising term for recrystallised opaline and chalcedony rocks fragments.

**Sandstone:** clastic rock of sedimentary origin. Contains mostly monocrystalline quartz, rock fragments, K-feldspar, plagioclase. Its grain size ranges from 0.06 to 2 mm.

**Phyllite:** fine-grained, foliated, low grade metamorphite. Most common mineral composition is: quartz, mica (sericite), and albite.

**Micaschist:** crystalline slate with more than 50 % mica content (mostly muscovite). Other minerals are quartz and garnet.

**Serpentine:** metamorphic rock of ultrabasic origin, which consists in more than 90 % of serpentine minerals.

**Micritic inclusion:** microcrystalline (<4 µm; Folk, 1959; 1974) calcite inclusion. Grains with micritic texture are mostly rounded to well rounded and represented as primary non-plastic inclusions (e.g. young sediments or carbonate inclusions from the soil) in the sherds. It contains partial fragments of other minerals like quartz, as well as rock fragments (e.g. chert, quartzite, volcanite, etc.).

**ARF- siltstone:** (Argillaceous rock fragment) angular to subrounded non-plastic inclusions derived from detrital sediments composed of clay, mud, and silt, which have been lithified (Whitbread, 1986).

### **Other, non-plastic or secondary inclusions**

**Clay temper:** rounded to well rounded inclusions which may conceivably have been formed within a depositional environment of the clay and are distinguishable through differences in their fabrics compared to the enclosing matrix (Whitbread, 1986).

**Secondary carbonate:** microcrystalline carbonate (micrite, grainsize <4 µm), which have been secondarily precipitated from soil solutions after the burial of the sherd and filled the pores and holes in it. The amount of secondary carbonate is only informative, it has not been compared either to the amount of non-plastic inclusions, or to the matrix.

According to Szakmány (1996) the following textural properties have been investigated with the polarising microscope (for detailed data cf. Appendix 4):

**Colour of the groundmass:** colour of the plastic groundmass (clay) using single as well as crossed nicols.

**Isotropism of the groundmass (optical activity):** the degree of isotropism of the plastic groundmass. This phenomenon is mostly affected by the fine-grained carbonate content of the clay and the firing temperature and environment (oxidative-reductive).

**Texture: hiatal** (there is a gap in the distribution of the grain size of non-plastic inclusions), or *serial* (continuous distribution of the sizes of non-plastic clasts).

**Grain-size distribution (sorting):** the amount and variation of the range of grain size in non-plastic inclusions. Well, medium, and poorly sorted types have been distinguished.

**Grain-size maximum:** the dimension of the biggest non-plastic inclusion found in the sherd.

**Roundness of the clasts:** according to Powers (1953) the classification of the clasts was described with the terms from very angular to well-rounded.

**Sphericity of the clasts:** according to Powers (1953) the classification of the clasts was described using the numbers between 1 (low sphericity) and 5 (high sphericity).

**Orientation:** orientated arrangement of the (elongated) non-plastic mineral and rock fragments.

#### 6.1.1.1. Troia

##### 6.1.1.1.1. Petrography of the comparative materials

###### Geological sample Tr-1a (medium to coarse sand), fraction: 0.5 -2 mm (Troia, Karamenderes river)

The sample shows very varied composition.

The mineral fragments are: monocrystalline quartz (mostly with undulatory extinction), plagioclase, K-feldspar (partially microcline), muscovite, amphibole and opaque grains.

The rock fragments: clasts of volcanic origin dominate. Basalt (plagioclase needles, with olivine phenocrysts, intergranular texture), obsidian and recrystallised (silicified) volcanite can be observed (Fig. 22, 24), acidic volcanites probably rhyolite (Fig. 23; glassy texture with biotite phenocrysts), and andesite or latite (plagioclase crystals in the matrix, zoned plagioclase phenocrysts, amphibole, biotite phenocrysts in porphyritic microholocrystalline texture).

Plutonite fragments probably of acidic origin (granite-granodiorite) contain quartz, partially sericitised plagioclase, K-feldspars and biotite. Gabbro fragments contain plagioclase and pyroxenes. Serpentine, prehnite-bearing metaultrabasites with pseudomorphoses after olivine were also observed. Polycrystalline quartz belongs probably to the granitic and/or granodioritic fragments. Some microcrystalline quartz (chert, chalcedony) was also found.

###### Geological sample Tr-1b (silty sand), fraction: 0.5 - 0.125 mm (Troia, Karamenderes river)

The composition of this sample is the same as the composition of the sample Tr-1a. Differences manifest themselves in the lack of acidic volcanite fragments. Furthermore, due to the smaller grain size, fraction mineral fragments (mostly monocrystalline quartz grains) and detritic, well-rounded

carbonatic clasts in their cores with quartz, quartzite, chert and magmatite fragments dominate in the material (Fig. 25).

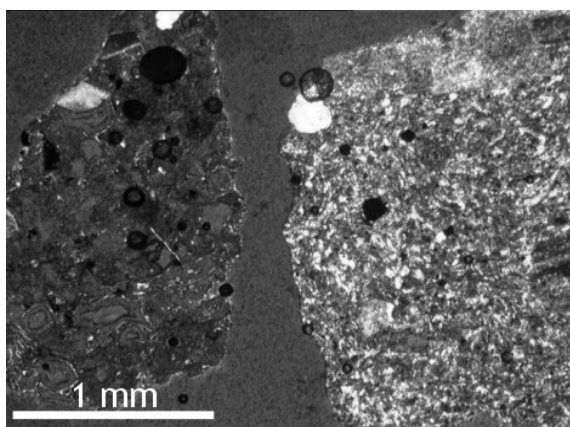


**Fig. 22** Subangular obsidian and recrystallised volcanite (sediment sample Tr-1a; +N).

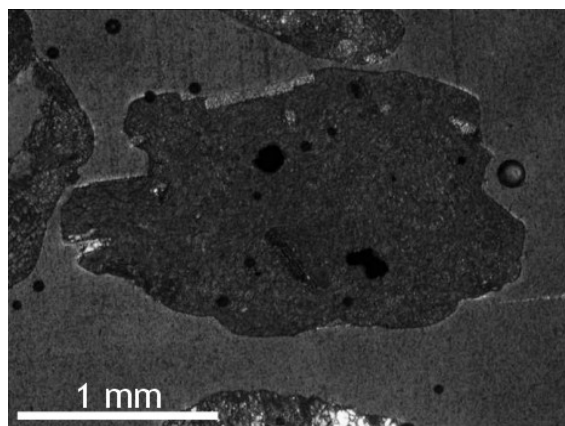


**Fig. 23** Subrounded acidic volcanic glass fragments with mica (sediment sample Tr-1a; +N).

*Geological sample Tr-2a (medium to coarse sand), fraction: 0.5 -2 mm (Troia, Dümrek river)*

Similar to the sample Tr-1a, the sand fraction has also varied composition.

The mineral fragments are: monocrystalline quartz (mostly with undulatory extinction), plagioclase, K-feldspar (microcline), biotite, muscovite, amphibole, and opaque grains.

Serpentine-bearing rock fragments dominate in the material. Further rock fragments are: basalt (plagioclase needles, with olivine phenocrysts, intergranular texture), marble fragments, ARF, siltstone, detritic, well-rounded carbonatic clasts containing lots of grains of quartz, quartzite, chert, and magmatite fragments.

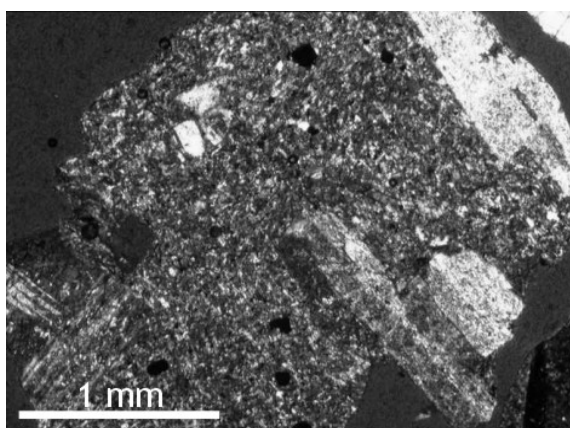


**Fig. 24** Silicified volcanite fragment with tabular K-feldspar phenocrysts (sediment sample Tr-1a; +N).

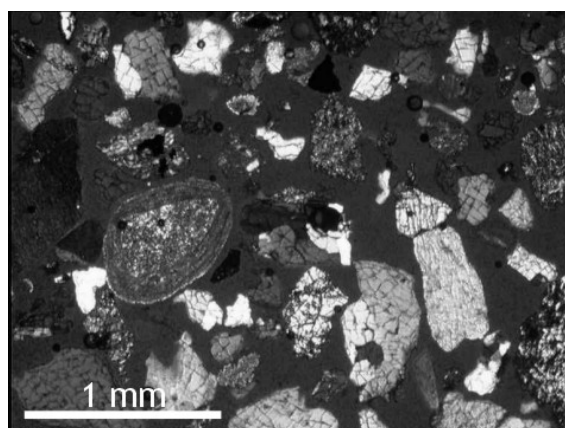


**Fig. 25** Polymict coarse sand containing mono- and polyquartz, K-feldspar and micritic carbonate inclusion (sediment sample Tr-1b; +N).

Geological sample Tr-2b (silty sand), fraction: 0.5 - 2 mm (Troia, Dümrek river)

The composition of this sample is the same as the composition of sample Tr-2a. Domination of the mineral fragments over the smaller grain size fractions can also be observed.

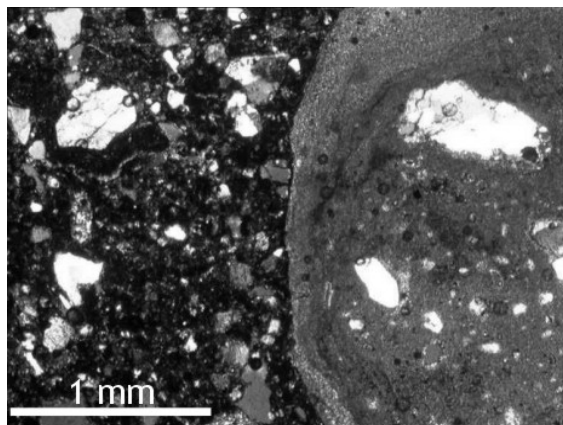


**Fig. 26 Well-rounded micritic inclusion in the Troian sherd K8.911.93 (+N).**

Comparative, locally produced ceramics from the settlement phases Troia I-V (K8.911.93, K8.911.94)

The sample *K8.911.93* contains lots of mono- and polycrystalline quartz grains, muscovite, epidote, K-feldspar, and altered plagioclase fragments. Recrystallised (silicified) volcanite fragments and well-rounded carbonate inclusions (Fig. 26), containing partially small mono- and polyquartz, K-feldspar, volcanite fragments dominate among non-plastic inclusions. Grains are subangular to well-rounded.

The sample *K8.911.94* has different composition. Beside monoquartz, plagioclase, epidote and opaque clasts amphibole can also be found. The rock fragments are represented by recrystallised volcanic fragments, acidic volcanic glass (obsidian?), and polycrystalline quartz (Fig. 27). Some plastic clay pellets were also observed. Fragments are subangular to subrounded.

Comparative, locally produced ceramics from the settlement phase Troia V (A5/6.502.1: Coarse ware)

Petrographic composition of this sample is fairly common. The mineral fragments are: monoquartz, K-feldspar, plagioclase, biotite, opaque minerals. The rock fragments are: plutonite of acidic composition (containing quartz, K-feldspar, plagioclase), polycrystalline quartz (probably as part of the plutonite), and chert or microcrystalline quartz.

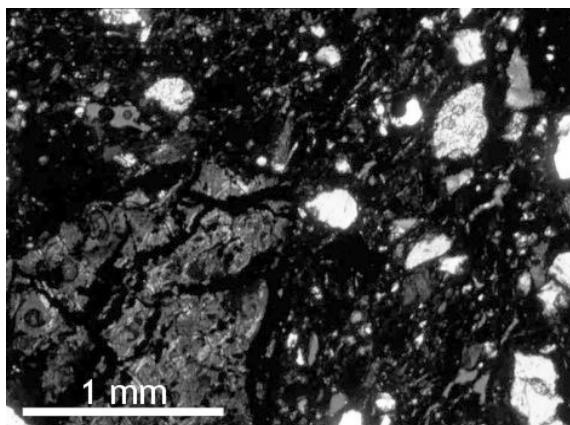


Fig. 27 Monoquartz and acidic volcanic glass fragments in the Troian sherd K8.911.94 (+N).

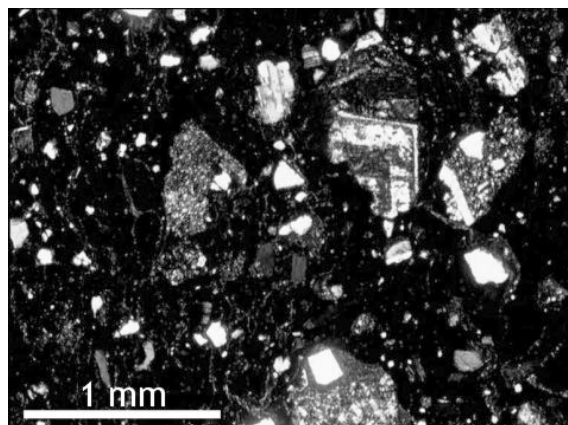


Fig. 28 Volcanic clasts containing zoned plagioclase phenocrysts in the Troian Knobbed ware sherd E9.158.1 (+N).

#### The Knobbed ware fragment E9.158.1

Matrix: 74.50 %, non-plastic inclusions: 25.50 %.

The sample contains the following minerals: subangular to subrounded monocrystalline quartz (9.70 %), partially with undulatory extinction, K-feldspar (2.30 %), plagioclase (3.30 %), biotite (1.0 %), as well as some accessories like amphibole (0.20 %), and epidote (0.20 %).

The group of rock fragments contains volcanite clasts (Fig. 28) probably of intermediate-acidic composition (60.10 %), including altered K-feldspar and plagioclase phenocrysts, biotite, amphibole, and opaque minerals in fine-grained matrix made of plagioclase needles and recrystallised volcanite (23.20 %).

The texture of the sample is hiatal, partially serial.

#### *6.1.1.1.2. Petrography of the sherds; Petrographic group 1*

Due to the complex geology of the Troad (cf. Chapter 5) many type of rock fragments belonging to the different rock associations of the region can be found in the Troian sherds (cf. also Knacke-Loy, 1994). On the basis of this observation several petrographic subgroups and types have been distinguished in Troian Knobbed ware sherds.

Petrographic grouping was carried out on the basis of the following properties:

The main components of the subgroup *1A* are: monoquartz, polyquartz, plutonite, intermediate-acidic volcanite and several accessories. Within this subgroup, type *1A/2* contains serpentinite and type *1A/3* – a large volume (64.10 %) of monoquartz.

The common feature of the subgroup *1B* is large amount of acidic volcanic glass and glassy volcanite. Within the subgroup the volume of volcanic glass in type *1B/1* is less than 50 vol %, and in type *1B/2* – more than 50 vol %.

The subgroup *IC* contains lots of recrystallised volcanite fragments. The textural properties of the sherds in this subgroup also differ from other Knobbed Ware sherds found in Troia.

Type 1A/1

(Samples: TR-1, 2, 3, 5, 13, 16, 19 and 27)

The ratio of matrix varies from 75.40 to 85.10 % and clasts from 24.60 to 14.90 %.

The samples contain varying volume of monoquartz (19.00 to 34.30 %) with undulatory extinction, partially sericitised K-feldspar (10.30 to 21.60 %), plagioclase (1.50 to 6.60 %), and amphibole (only in the sample TR-2, 1.60 %).

Among accessories, mica (muscovite 0.10 to 0.20 % and biotite 0.60 % only in the sample TR-2) and epidote (0.2 to 1.10 %) can be found. The amount of opaque minerals varies between 2.70 and 7.30 %.

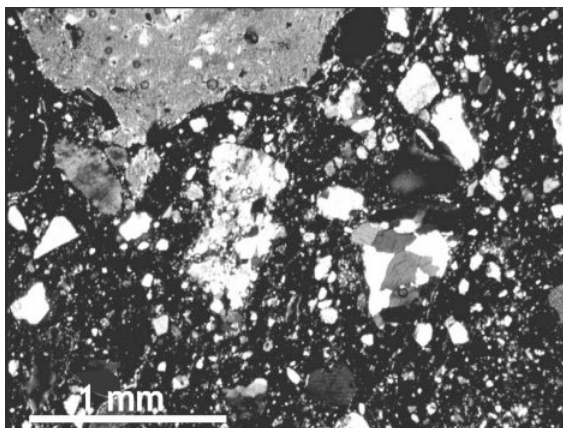


**Fig. 29 Microphotograph of the sherd TR-16 (petrographic type 1A/1, Troia). The picture shows mono- and polyquartz, plagioclase, mica and micritic carbonate inclusion (+N).**

The most prevalent rock fragment is polycrystalline quartz (3.50 to 37.70 %, Fig. 29). The grains have undulatory extinction in the texture, and their boundaries are mostly sutured, but in the sample TR-2 there were also some clasts with mosaic texture.

Plutonite fragments (2.70 to 7.30 %) contain undulatory quartz, K-feldspar, plagioclase, and some muscovite as well.

Typical clasts are volcanite fragments (except in the sample TR-16) (1.10 to 25.60 %). Some clasts are slightly silicified. There are tabular plagioclase phenocrysts and also some opaque minerals in the fine-grained matrix, which contains plagioclase needles. In the sample TR-2 there is another type of volcanite fragment. It has coarser grains (elongated plagioclase), some amphibole, and opaque minerals (subophitic texture). The above mentioned clasts belong most probably to a basic-intermediate volcanite assemblage. The second type (the sample TR-2) to be taken into consideration is most probably a subvolcanic rock (dolerite?).

Strongly recrystallised volcanite fragments, partially with recognisable texture (plagioclase phenocrysts in fine-grained matrix) have a volume of 2.70 to 24.00 % and reveal some similarities with the volcanite clast mentioned above.

There are also some subangular chert clasts in small amount (0.20 to 5.40 %). The non-plastic inclusions of the sample TR-16 also contain some (16.20 %) well rounded micritic carbonate clasts, containing angular quartz grains (Fig. 29 and 30).

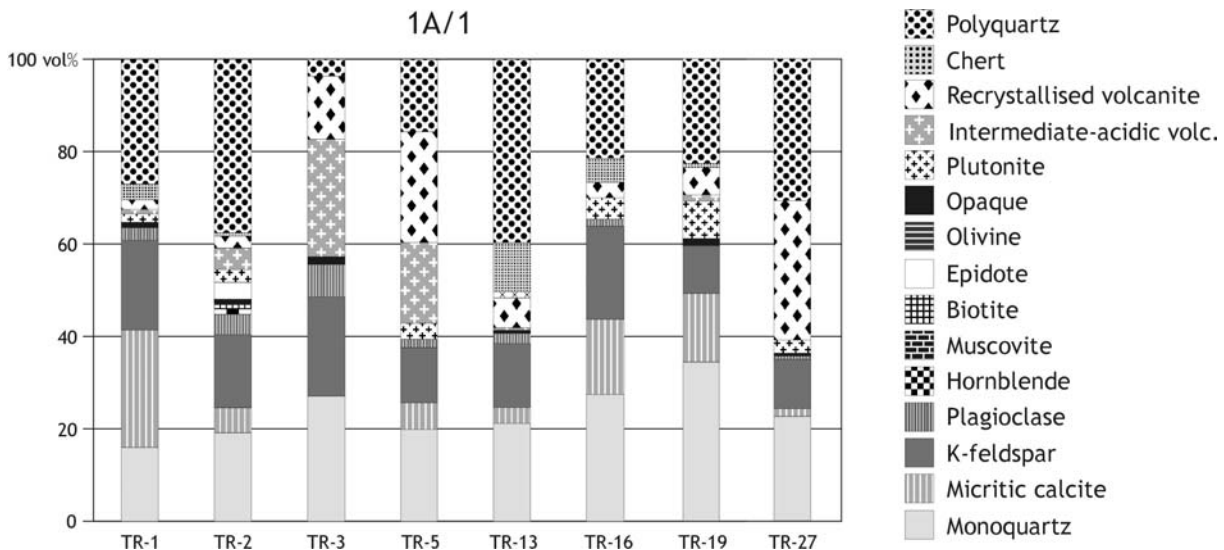


**Fig. 30 Modal composition of the sherds of the petrographic type 1A/1 (Troia).**

### Textural properties

Although these samples, based on their petrographic composition, have been grouped into the same petrologic type, they reveal different textural features especially in their colour and isotropism. The colour of the groundmass varies from orange to brown, dark brown; at the crossed polars the textures mostly show brown to dark brown colour. The isotropism of the matrix also varies from poor to complete; in most cases it is moderate or complete. With an exception of the samples TR-2 and 19 all samples have hiatal texture. The sorting of the grain size distribution varies between poor and moderate, the maximum size of the grains between 1200 and 4000  $\mu\text{m}$  (polyquartz, recrystallised volcanite). The roundness of the non-plastic inclusions varies from very angular to subrounded; in case of the sample TR-5 rounded clast have also been obtained. The sphericity of the clasts varies between the 1 and 3; in case of the sample TR-5 between 1 and 4. All samples have poor or no orientation, with an exception of the sample TR-27 which has moderate orientation. Where observed, the orientation is parallel with the rim of the sherd (cf. Appendix 4).

Type 1A/2

(Sample: TR-24)

Petrologic composition of this sample is very similar to the previous group, but the sample contains some serpentine. Because none of the Troian sherds investigated in this study so far contains this rock type, it was necessary to separate the sample into another type.

The volume of the matrix is 78.90 % and that of the non-plastic inclusions is 21.10 %. The minerals are: monoquartz (10.20 %), K-feldspar (5.90 %), and plagioclase (7.10 %), pyroxene (1.20 %), amphibole (0.40 %), epidote (0.40 %), and some (2.00 %) opaque minerals.

The rock fragments are: plutonite (3.30 %; its composition is the same as mentioned in type 1A/1 but some graphic granite fragments have also been found), polycrystalline quartz (16.30 %), and recrystallised volcanite (19.70 %). Volcanite clasts have hyalopilitic (glassy) texture with typical flow structures. Between plagioclase needles tabular K-feldspar phenocrysts can be observed (Fig. 31). These features refer most probably to (intermediate) acidic volcanites. Other type of volcanite shows well-crystallised (holocrystalline) texture where between the elongated plagioclase needles amphibole and some opaque minerals were situated. The texture may refer to dyke rock origin and probably to intermediate chemical composition.

ARF has a volume of 3.00 % and as a unique rock fragment, 1.50 % serpentinite can be observed in the sherd (Fig.32).

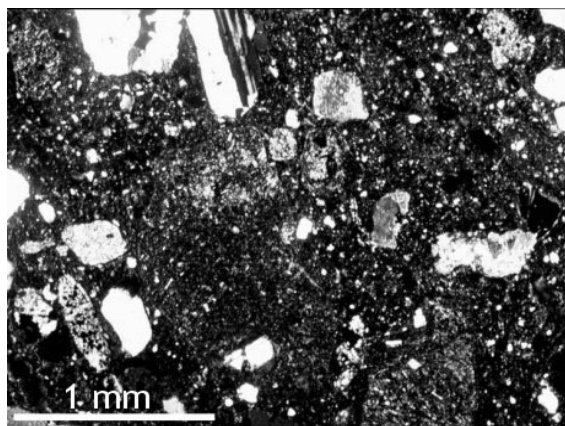


**Fig. 31** Microphotograph of the sherd TR-24 (petro graphic type 1A/2, Troia). The picture shows monoquartz, plagioclase, and recrystallised volcanite fragments (+N).

### Textural properties

The groundmass of the sample TR-24 has brown colour and good isotropism. It has hiatal texture, the largest grain found in this sherd was 3400  $\mu\text{m}$  (volcanite); the grain size distribution is poor. The roundness of the non-plastic inclusions vary from very angular to subrounded, sphericity of the clast varies between the values 1 and 4. Non-plastic inclusions have no orientated arrangement in the texture. The texture of the sample is hiatal (cf. Appendix 4).

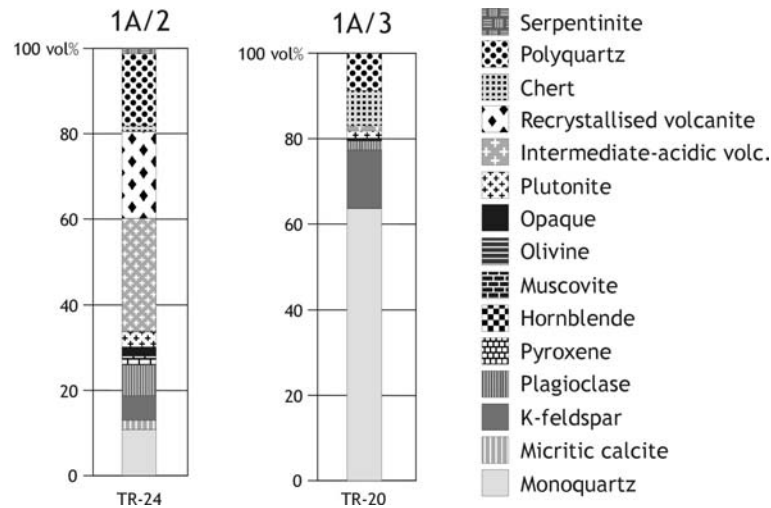


**Fig. 32 Modal composition of the sherds of the petrographic types 1A/2 (TR-24) and 1A/3 (TR-20; Troia).**

### Type 1A/3

(Sample TR-20)

The composition of the non-plastic inclusions is similar to the above mentioned types, but monoquartz grains are dominating among the clasts and the amount of rock fragments is definitely lower.

Matrix: 79.50 %, non-plastic inclusions: 20.50 %.

The volume of the monocrystalline quartz grains is 64.10 %. They are subangular to rounded, partially with straight extinction.

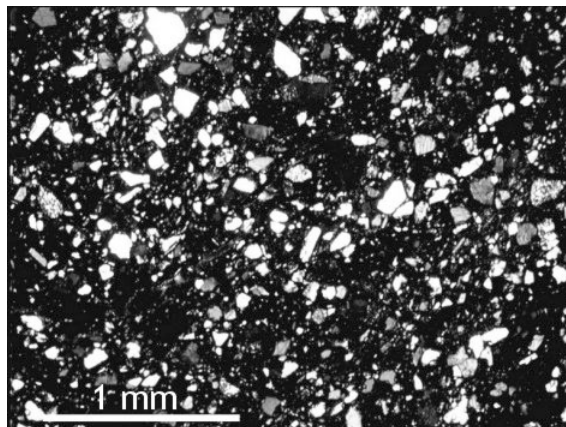


**Fig. 33 Microphotograph of the sherd TR-20 (petrographic type 1A/3, Troia). The picture shows serial distribution of the grain-size. Monoquartz and some plagioclase can be seen in the image (+N).**

Further components are: K-feldspar (13.60 %), plagioclase (2.10 %), and some accessories like amphibole (0.20 %), muscovite (0.20 %), and epidote (0.20 %).

Among rock fragments acidic plutonite (1.90 %) including quartz, altered K-feldspar, mica, and opaque minerals, few (1.00 %) volcanite fragments (due to the amount and the size of the grains

accurate identification of the clasts was not feasible), chert (8.30 %), and polycrystalline quartz (22.70 %) can be found (Fig. 32 and 33).

### Textural properties

The matrix shows brown (1 polar) and dark-brown (crossed polars) colour. Isotropism ranges from moderate to good. The type of texture is serial, sorting of the grain size distribution is moderate. The size of the largest grain in the sherd was 2000  $\mu\text{m}$  (monoquartz). Roundness of the non-plastic inclusions varies from angular to subrounded; sphericity of the clast varies between the values 1 and 4. The non-plastic inclusions show no orientated arrangement. The distribution of the non-plastic clasts in the texture shows serial property (Fig. 33; cf. Appendix 4).

### Type 1B/1

(Samples: TR-4, 11, 14, 15, 17, 21, 22, 23 and 25)

The ratio of the matrix to the non-plastic inclusions varies from 13.30 to 23.90 %. The minerals are: very angular to rounded monoquartz grains (7.30 to 30.40 %) mostly with undulatory or slightly undulatory extinction; K-feldspar (1.80 to 17.50 %), and plagioclase (1.20 to 12.80 %), in many cases altered euhedral grains, amphibole (0.10 to 1.80 %), epidote (0.10 to 2.90 %), opaque minerals (0.30 to 5.30 %), muscovite (0.10 to 0.30 %), and biotite (0.10 to 0.40 %).

Rock fragments: in this group there are generally less plutonic clasts (0.20 to 15.60 %) than in the other groups. Plutonic rock fragments consist partially of undulatory quartz grains, plagioclase and/or K-feldspar, mica, and opaque minerals. Typical hypidiomorphic texture and mineralogical composition refer to granitoid or to granodiorite parent rocks.

Volcanites (0.20 to 45.60 %) have hyalopilitic-pyrotaxitic texture. There are tabular plagioclase phenocrysts in fine-grained, partially glassy matrix. They also contain some amphibole and opaque minerals. This type can probably be related to intermediate volcanites.

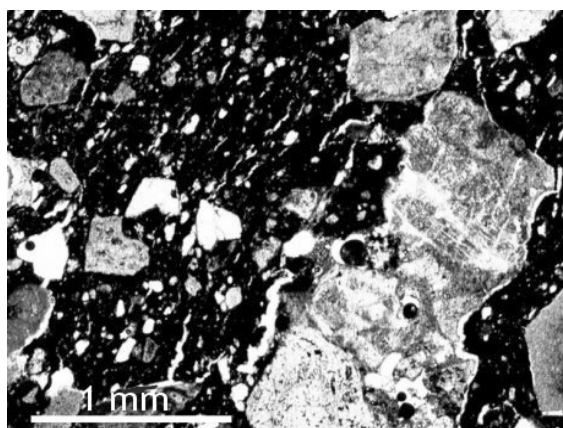


**Fig. 34** Microphotograph of the sherd TR-17 (petrographic type 1B/1, Troia). The picture shows monoquartz, recrystallised volcanite and acidic volcanic glass fragments (1N).

Another volcanite type has hyalopilitic (glassy) texture with typical flow structures. Some biotite and K-feldspar phenocrysts can also be observed (Fig. 34). These features imply most probably acidic volcanites.

Volcanic glass occurs in amount between 3.60 and 46.70 %. These rock fragments have common feature. In the hyaline matrix there are biotite needles and/or tabular plagioclase crystals, but there are also clasts where only glassy matrix can be found. On the basis of these features volcanic glass might have acidic (intermediate) origin. Recrystallised volcanites also occur in the non-plastic inclusion; they have a volume of 3.10 % to 35.70 %. Undulatory quartz grains in polycrystalline quartz (0.20 to 29.40 %) refer to metamorphic origin. Triple-junctioned and sutured grain boundaries can also be found in these clasts.

Other rock types like chert (0.20 to 3.10 %) and phyllite (1.10 % only in the sample TR-23) can only be observed in few samples (Fig. 35).

Beneath the above mentioned clasts in 7 samples (cf. Appendix 3 for details) occur well rounded micritic granules (1.60 to 29.60 %) including quartz, plagioclase, and some quartzite grains (Fig. 35).

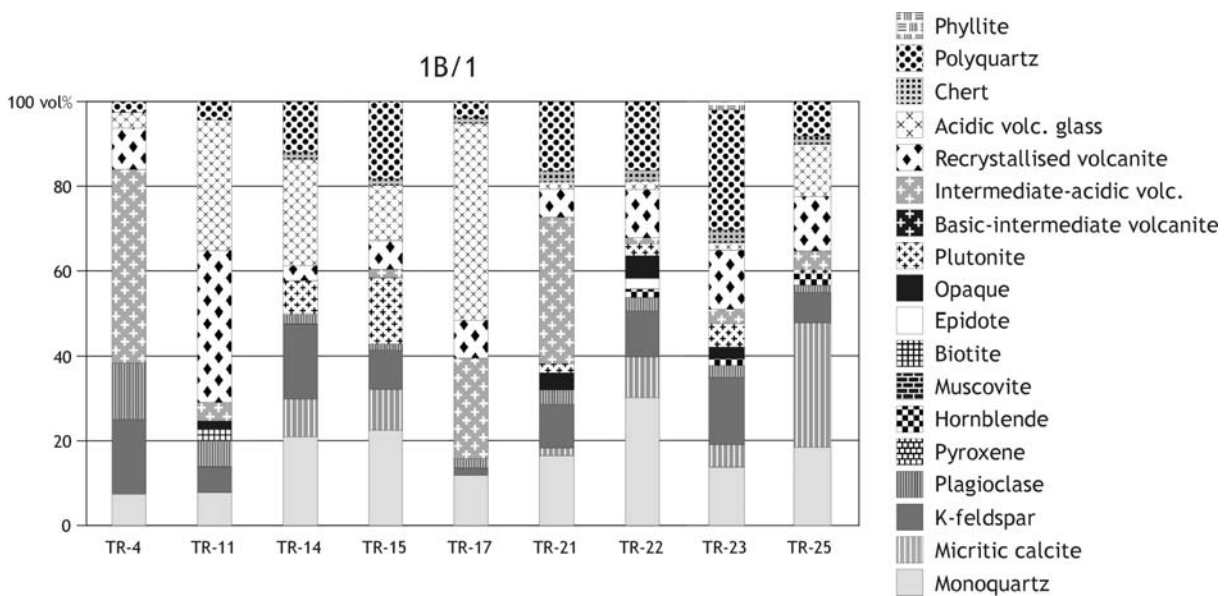


**Fig. 35 Modal composition of the sherds of the petrographic type 1B/1 (Troia).**

### Textural properties

The colour of the groundmass of these samples investigated with one Nicol is mostly brown or dark brown; with crossed polars it is dark brown. The isotropism of the matrix is mostly good or complete, with the exception of the samples TR-21, 23 and 25 where it is poor to moderate. The samples TR-4, 14, 15, 17, 21 and 23 have hiatal texture: all other samples reveal serial type of texture. Grain size distribution shows poorly sorted type. The maximum size of the grains varies between 1400 and 3800  $\mu\text{m}$ , at an average 1900-2200  $\mu\text{m}$  (volcanite, micritic carbonate). The roundness of the non-plastic inclusions varies from very angular to subrounded; in the samples TR-11 and 23 some rounded clasts

also occur. Sphericity of the clasts varies between the values 1 and 3. In the samples TR-4, 17, 22, 23 and 25 clasts with good (4) and high (5) sphericity have also been found. Non-plastic inclusions show no or poor orientation (cf. Appendix 4).

### Type 1B/2

(Samples: TR-6, 7, 9, 10, 12, 18, 26 and 28)

The percentage of the matrix varies from 75.90 to 85.20 % and that of the clasts from 24.10 to 14.80 %. The general feature of these samples is the content of more than 50 % of acidic volcanic glass.

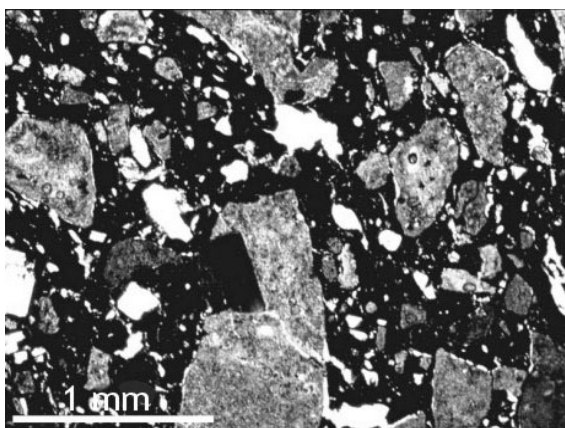


**Fig. 36 Microphotograph of the sherd TR-7 (petrographic type 1B/2, Troia). The picture shows some monoquartz and angular acidic volcanic glass fragments with biotite phenocrysts (1N).**

The non-plastic inclusions consist of monoquartz of metamorphic origin (3.90 to 19.50 %), K-feldspar (1.90 to 5.90 %), plagioclase (3.40 to 10.60 %), some amphibole (0.20 % only in the sample TR-28), mica (mostly biotite 0.10 to 1.70 %), epidote (0.20 % in the samples TR-9 and 10), and opaque minerals (0.10 to 1.30 %).

Large quantity of volcanic glass (61.60 to 87.80 %) dominated in the clasts. Texture (hyalopilitic/pylotaxitic) is the same as in the type *1B/1*. There are some plagioclase and biotite phenocrysts in glassy matrix (Fig. 36).

The other components are: recrystallised (silicified) volcanite fragments, probably of intermediate or acidic origin (1.00 to 13.80 %), and polycrystalline quartz of metamorphic origin (0.20 to 1.70 %; Fig. 37).

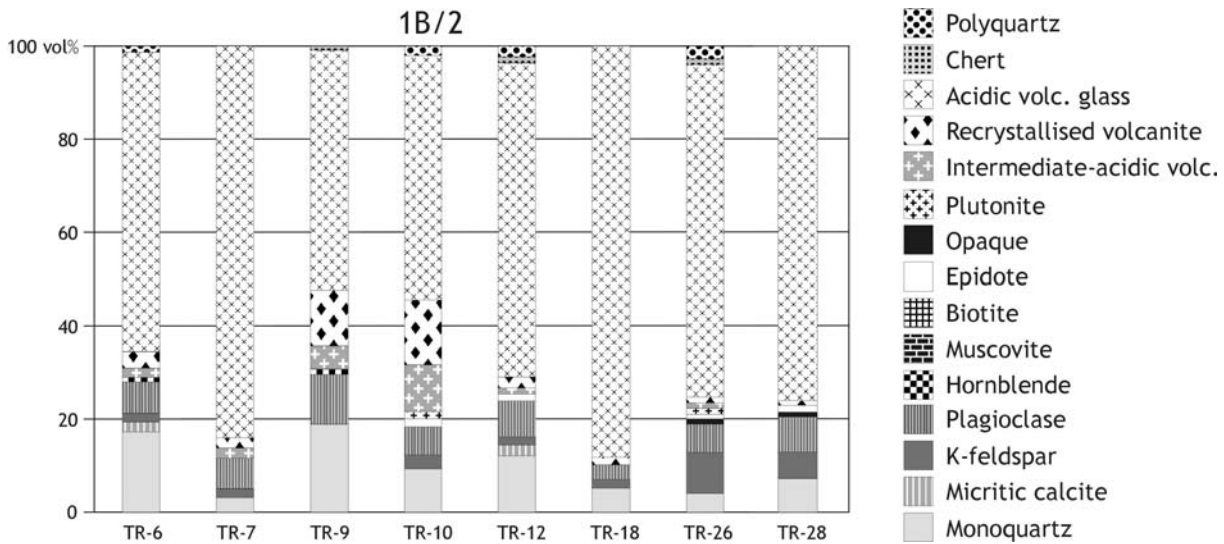


**Fig. 37 Modal composition of the sherds of the petrographic type 1B/2 (Troia).**

### Textural properties

The colour of the groundmass of these samples is uniformly brown. The isotropism of the clayey matrix is in most cases poor; in the samples TR-6, 7 and 10 it varies from moderate to complete. With the exception of the sherds TR-6, 7 and 26 all samples have hiatal texture. The maximum size of the grains ranges from 1400 to 2200  $\mu\text{m}$  (volcanite, acidic glassy volcanite); the size of the grains shows poor distribution. The roundness of the non-plastic clasts varies from very angular to subangular-subrounded; the sphericity of the clast varies between the values 1 and 3, and in case of the sample TR-28 between 1 and 5. Non-plastic inclusions show poor (TR-6, 7 and 28) or moderate (TR-9, 10, 12, 18 and 26) orientation (cf. Appendix 4).

### Subgroup 1C

(Sample TR-8)

This sample has similar mineralogical but different textural features compared to the previous types. The proportion of the matrix and the clasts are 71.80 % to 28.20 %, respectively. Undulatory monoquartz granules (8.40 %), micritic clasts (1.10 %), K-feldspar (2.30 %), plagioclase (3.10 %), some biotite (1.70 %), and opaque minerals in traces (0.10 %) constitute the mineralogical part of the non-plastic inclusions.

Recrystallised volcanite fragments (probably of intermediate or acidic origin, 83.50 %; Fig. 38) dominate among rock clasts. Due to the strong influence of recrystallisation (silification), original textural elements were problematic to identify. Chert and polyquartz appear in a volume of 2.70 % and 9.20 %, respectively (Fig. 39).

Rounded micritic clasts including quartz grains also appear in the texture (1.10 %).

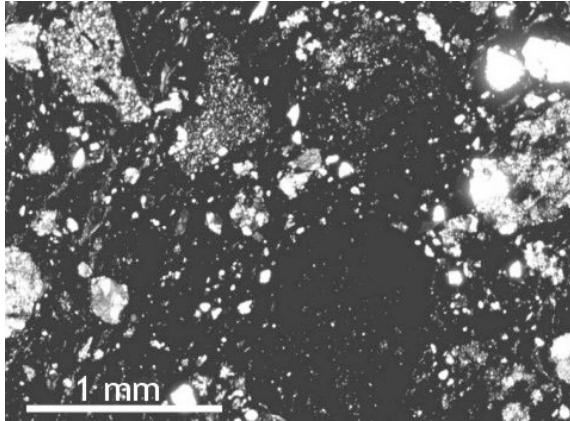


**Fig. 38** Microphotograph of the sherd TR-8 (petrographic type 1C, Troia). The picture shows dark (altered?) recrystallised volcanite fragments and some monoquartz clasts (+N).

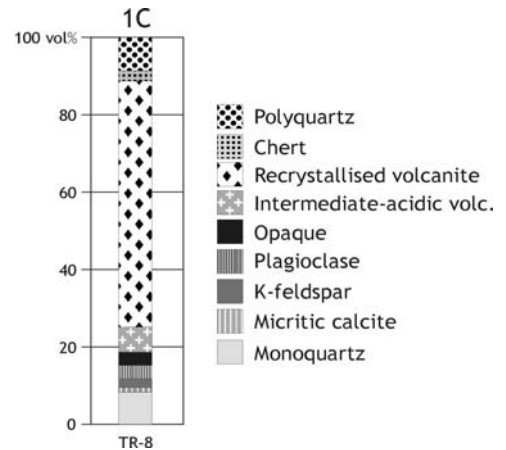


**Fig. 39** Modal composition of the sherd of the petrographic subgroup 1C (Troia).

### Textural properties

The matrix shows brown (1 Nicol), dark brown, and black (crossed polars) colour. Isotropism ranges between moderate and complete. The type of the texture is hiatal, the sorting of the grain-size distribution is poor. The maximum size of the grain found in the sherd was 7000  $\mu\text{m}$  (recrystallised volcanite). The roundness of the non-plastic inclusions varies from angular to subrounded; the sphericity of the clast varies between 2 and 4. The non-plastic inclusions show moderate orientation. The texture of the sherd is hiatal (cf. Appendix 4).

### 6.1.1.2. The Avşa Island

#### 6.1.1.2.1. Petrography of the sherd; Petrographic group 2

(Sample: A-1)

The proportion of matrix is 82.20 % and of non-plastic inclusions 17.80 %.

This sherd contains a great amount of well-crystallised or coarse-grained calcite grains and some calcite aggregates (53.90 %). The grains are angular, with typical rhomboedric form and cleavage plans (Fig. 40). Their size range extends from 100 to 1800  $\mu\text{m}$ . The features of the calcite suggest that they most probably belong to a marble and/or to a crystalline limestone source rock.

In addition to calcite, some micritic carbonate clasts (2.10 %) and angular monocrySTALLINE quartz grains (50-100  $\mu\text{m}$ ) with undulatory extinction also occur in the sherd (13.20 %). Undulatory extinction refers to metamorphic origin of the mineral. Subhedral green hornblende (1.60 %) is also a typical granule among the clasts.

The accessory minerals are: K-feldspar (0.40 %), plagioclase (0.20 %) (mostly sericitised), muscovite, biotite (0.10 %), and epidote (0.50 %).

The most common rock fragments are (meta) magmatites (28.20 %) which contain quartz (undulatory extinction), K-feldspar (partially sericitised), mica (muscovite), and green hornblende components. There are also some chert granules (0.20 %) consisting of very fine-grained quartz crystals (Fig. 41).

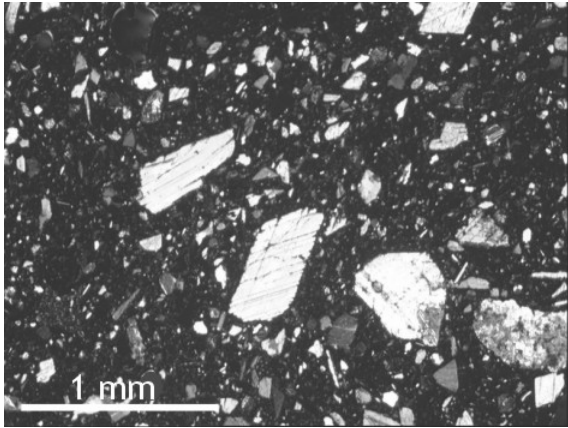


**Fig. 40** Microphotograph of the sherd A-1 (petrographic group 2, the Avşa Island). The picture shows some monoquartz, mica and rhomboidal calcite crystals (+N).

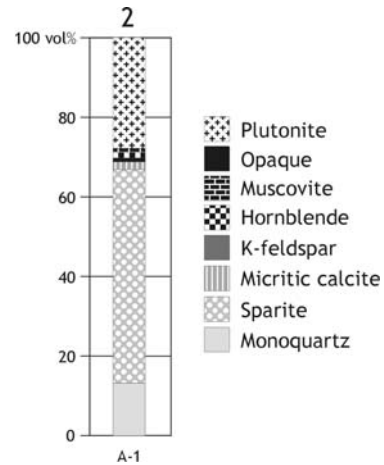


**Fig. 41** Modal composition of the sherd of the petrographic group 2 (the Avşa Island).

### Textural properties

The sample A-1 has isotrope dark brown-coloured groundmass. The type of its texture is serial, the sorting of the grain size distribution is poor. The maximum size of the grains is 1800  $\mu\text{m}$  (sparite). The roundness of the non-plastic inclusions varies from very angular (sparite) to subrounded (monoquartz); sphericity of the clast varies between 1 and 3 (cf. Appendix 4).

### 6.1.1.3. Menekşe Çatağı East (MCE) and West (MCW)

#### 6.1.1.3.1. Petrography of the sherds; Petrographic group 3

The subgroup 3A contains the following main non-plastic inclusions: monoquartz, polyquartz, plutonite, chert, and several accessories. Within this subgroup the type 3A/2 contains large amounts of polyquartz, mica, epidote, and hornblende. In addition to the non-plastic clasts mentioned above, the subgroup 3B contains lots of volcanite fragments.

Type 3A/1

(Samples: MCW-1, 3, 4, 5, MCE-2, 3, 4 and 5)

The proportions of non-plastic inclusions vary from 14.00 to 28.10 %.

Monoquartz is the most common grain (34.80 to 58.10 %) in these sherds. It has mostly undulatory extinction, but in some sherds (MCW-4, MCE-3 and 5) there are also granules with straight extinction (Fig. 42). Further components are: K-feldspar (partially sericitised; 2.40 to 13.40 %), plagioclase (0.60 to 6.10 %), and micritic primary calcite (0.20 to 1.90 %; Fig. 43).

The accessory minerals are: amphibole (0.20 to 0.40 %), muscovite (0.20 to 0.30 %), biotite (0.10 to 0.4 %), epidote (0.10 to 0.60 %), and some opaque clasts (0.30 to 0.60 %)

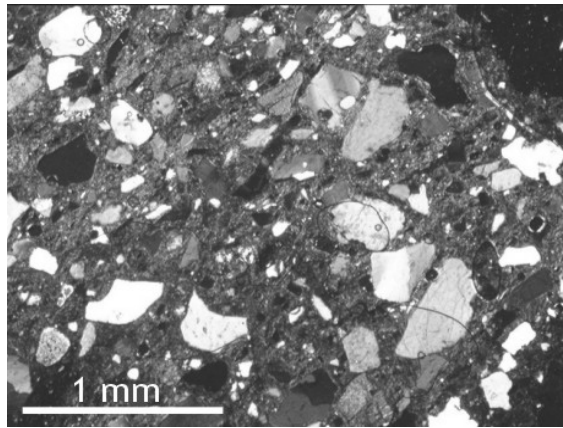


**Fig. 42 Microphotograph of the sherd MCW-1 (petrographic type 3A/1, Menekşe Çataği). The picture shows monoquartz, K-feldspar, hornblende and epidote (+N).**

There are five different types of rock fragments in this petrographic group:

- (1) Large amount of angular to subrounded polycrystalline quartz fragment (27.00 to 44.60 %). Quartz grains have in all cases undulatory extinction and sutured grain boundaries, except in the sample MCE-5, where triple-junctioned boundaries also occur. In the sample MCE-2 there are some fine-grained quartzites with mosaic texture including opaque minerals and mica (muscovite).
- (2) Angular to subangular, acidic plutonite fragments (1.90 to 15.20 %) including quartz, mostly sericitised plagioclase and some opaque minerals, have a dimension of 600 to 1600  $\mu\text{m}$ . Undulatory quartz and plagioclase grains in these fragments refer to a metamorphic event.
- (3) Microcrystalline quartz (or chalcedony) can be found in all samples (1.10 to 9.10 %). In the sherds MCE-3 and 4 some (4) phyllite grains (0.60 and 1.00 %) also occur, consisting in they deformed texture quartz and sericite. In the samples MCE-2, 4 and 5 some (1.8 to 2.5 %) recrystallised volcanites (5) can be found (Fig. 43).

Some subrounded to rounded; mostly oval clay pellets in the samples MCW-4, 5 and MCE-5 were probably situated in the clay as natural inclusions.

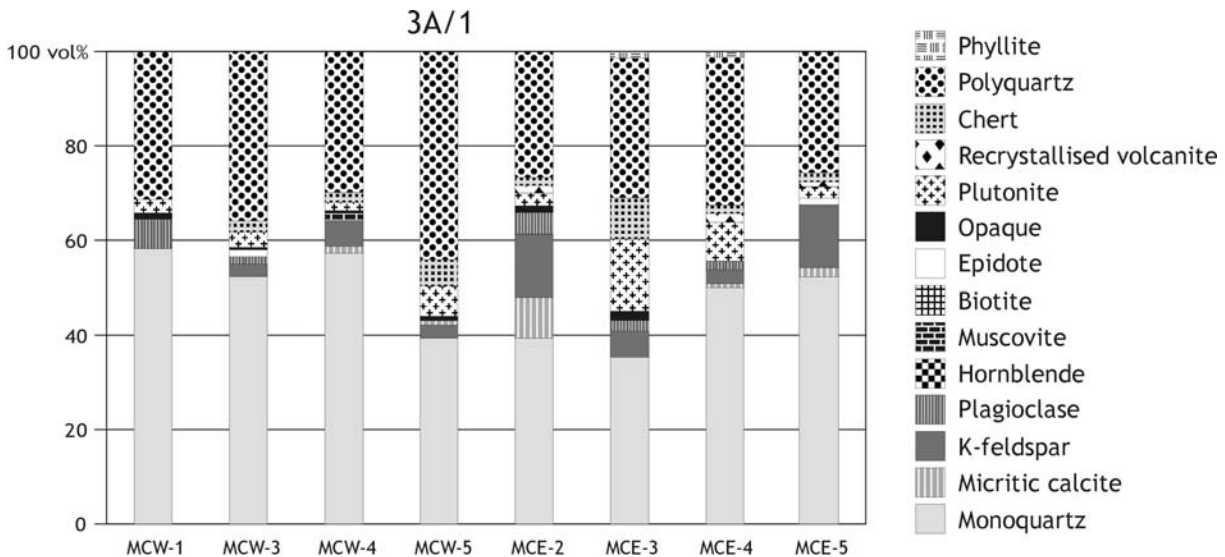


**Fig. 43 Modal composition of the sherds of the petrographic type 3A/1 (Menekşe Çatağı).**

### Textural properties

In addition to the non-plastic inclusions, the samples in this group also have common textural features. The colour of the groundmass is (dark) brown; isotropism in most cases is moderate (with the exception of the samples MCW-5 (poor) and MCE-4 (complete)). The type of the texture varies from serial (7 samples) to hiatal (MCE-4, MCW-4), the sorting of the grain size distribution varies between poor and moderate. The maximum grain size range is between 650 (MCW-3) and 2500 (MCW-4)  $\mu\text{m}$  (mostly magmatite, polyquartz and plagioclase clasts). The roundness of the non-plastic inclusions varies from very angular to subrounded; in the sample MCE-2 from angular to rounded. The sphericity of the clasts varies between 1 and 3. The non-plastic inclusions show moderate orientation in the texture (cf. Appendix 4).

### Type 3A/2

(Sample: MCW-2)

Matrix: 75.70 %, clasts: 24.30 %. Very angular and low sphericed monoquartz grains with undulatory extinction have a volume of 16.70 %.

Other main components are: green hornblende (1.10 %), muscovite (3.70 %), biotite (6.20 %), and epidote (2.20 %). Epidote grains partially form small epidosite-like knobs. Merely 0.70 % of the volume of the clasts consists of plagioclase. Some opaque minerals (0.70 %) can also be observed.

There is only one dominating rock type in the sample. Very angular to angular fragments of polyquartz showing elongated original host crystals, crenulated and sutured crystal-crystal boundaries have a volume of 68.70 %. These metamorphic rock fragments also contain great amounts of hornblende, epidote, and mica (mostly biotite; Fig. 44).

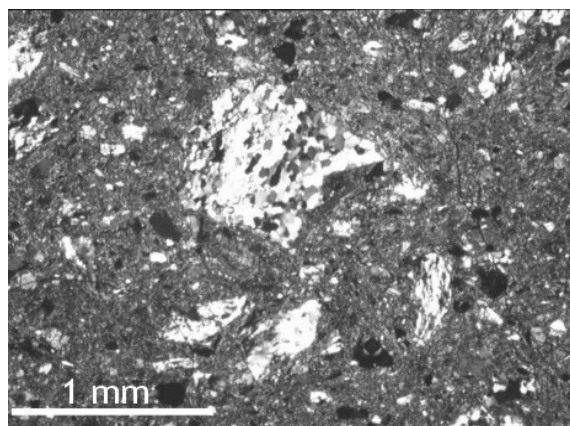


**Fig. 44** Microphotograph of the sherd MCW-2 (petrographic type 3A/2, Menekşe Çatağı). The picture shows mosaic-texture polyquartz, mica, hornblende and epidote clasts (+N).

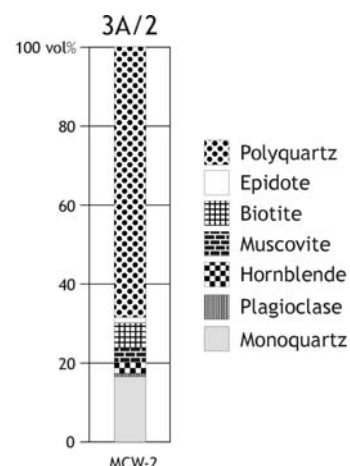


**Fig. 45** Modal composition of the sherd of the petrographic type 3A/2 (Menekşe Çatağı).

The origin of the single mineral fragments (biotite, hornblende, epidote and monoquartz fragments) can be derived from this rock association. Composition of the non-plastic inclusions seems to be homogenous and all grain types most probably belong to one rock type (Fig. 44 and 45).

### Textural properties

This sample has anisotropic, yellowish-brown coloured groundmass. The type of its texture is hiatal, the sorting of the grain size distribution is poor. The maximum size of the grains is 1800 µm (polycrystalline quartz). The roundness of the non-plastic inclusions varies from very angular to subangular, sphericity of the clast varies between the values 1 and 2. The non-plastic inclusions have moderate orientation in the texture (cf. Appendix 4).

### Subgroup 3B

(Sample: MCE-1)

Composition of the non-plastic inclusions in this sample is similar to the composition of the type 2A, with the sample MCE-1 containing lots of volcanic and recrystallised volcanic rock fragments being the main difference.

The proportion of the matrix and the clasts is 74.20 to 25.80 %, respectively.

Subangular to subrounded monocrystalline quartz grains with undulatory extinction have a volume of 12.10 %.

Lots of subhedral K-feldspar (13.70 %) and plagioclase (5.50 %) granules, partially altered (sericitised and carbonatised), and some anhedral epidote (0.30 %) and opaque (2.10 %) minerals also occur in non-plastic inclusions.

Among rock fragments the main component (52.70 %) is volcanite grains. There are two types of volcanites. Accurate identification of the texture was hardly feasible, due to the small size of grains.

One type of volcanites has well-crystallised (intergranular) texture, where few quartz and some opaque minerals were situated between elongated plagioclase and hornblende (Fig. 46). The texture may reflect dyke rock origin and an intermediate or acidic chemical composition. The other type of volcanites has porphyric-pyrotaxitic texture. These fragments are also slightly recrystallised. This type contains euhedral tabular plagioclase phenocrysts, some hornblende and opaque minerals in the matrix made of small plagioclase needles. Mineralogical composition and texture may refer to intermediate (andesitic?) composition.

There are also some (7.10 %) recrystallised volcanite fragments, but the samples are so hard silicified, that no accurate identification was possible.

Angular polyquartz granules of metamorphic origin, with undulatory extinction and triple-junctioned boundaries have a volume of 6.00 % (Fig. 47). Beneath rock clasts there are also some (2.10 %) clay temper fragments in the matrix.

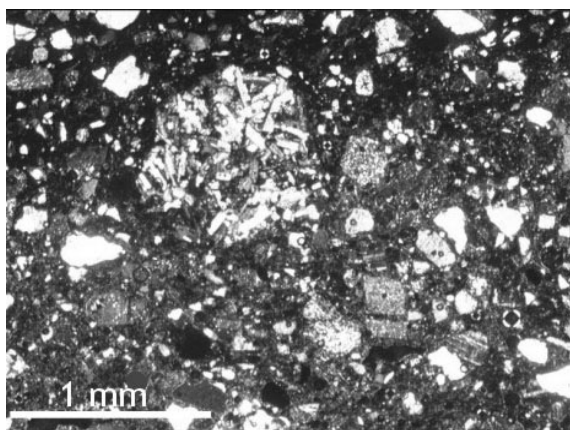


**Fig. 46** Microphotograph of the sherd MCE-1 (petrographic subgroup 3B, Menekşe Çatağı). The picture 3B shows monoquartz, altered plagioclase and a slightly silicified (sub)volcanic clasts with tabular K-feldspars and/or plagioclase (+N).

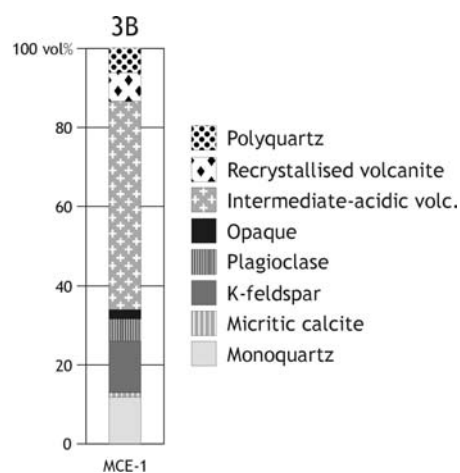


**Fig. 47** Modal composition of the sherd of the petrographic subgroup (Menekşe Çatağı).

### Textural properties

The groundmass of the sherd is isotrope and dark brown in colour. The type of texture is hiatal, the sorting of the grain size distribution is poor. The maximum size of the grains is 3400  $\mu\text{m}$  (volcanite) Roundness of the non-plastic inclusions varies from very angular to subrounded, sphericity of the clast has a range from 1 to 4. The non-plastic inclusions do not show orientation (cf. Appendix 4).

#### 6.1.1.4. North Turkish Thrace

##### 6.1.1.4.1. Petrography of the comparative material

###### Geological sample Ntt-2, fraction: 0.125 - 2 mm (Yeniköy, north Turkish Thrace)

In this sand fraction dominate plutonic and metamorphic rock fragments.

The minerals are: monocrystalline quartz (mostly with undulatory extinction), plagioclase, K-feldspar, biotite, muscovite, amphibole, and opaque grains.

The rock fragments: (meta) plutonite fragments probably of acidic origin (granite-granodiorite) containing quartz, partially sericitised plagioclase, K-feldspars, and biotite, polycrystalline quartz, belonging probably to the granitic and/or granodioritic fragments or to quartzite of metamorphic origin. Microcrystalline quartz (chert, chalcedony), amphibolite, phyllite, ARF, and other type of magmatic rock fragments containing plagioclase and epidote were also found.

##### 6.1.1.4.2. Petrography of the sherds; Petrographic group 4.

The petrographic type *4A/1* which includes most samples from this region contains lots of metamorphic and magmatic rock and mineral fragments. Type *4A/2* differs only by of its high mica and micashist content. Type *4B* differs completely from the types mentioned above, because it contains volcanite fragments and minerals of volcanitic origin.

###### Type 4A/1

(Agaçköprü, Araptepe, Cevizlik Mevkii, Demirlihanlı Mezarlığı, Yedigöz Kemeri; samples: AK-1, 2, AT-1, CM-1, 2, 3, 4, DH-1, 2, 3, YK-1, 2, 3, 4 and 5)

The amount of the non-plastic inclusions varies from 31.90 to 16.70 %.

The most common clast is monocrystalline quartz (32.20 to 63.10 %). It is generally angular to subrounded, mostly with undulatory extinction (in the sample AT-1 40-50 % of the quartz clasts have straight extinciton).

Other typical clasts are: partially sericitised plagioclase (0.20 to 27.50 %) and K-feldspar (0.10 to 10.40 %). Granules are mainly subhedral, and have angular to subrounded shape.

Minerals in lesser volume are: hornblende (0.10 to 0.70 %), muscovite (0.10 to 0.40 %), biotite (0.10 to 0.40 %), epidote (0.10 to 1.90 %), and some opaque clasts (0.1 to 0.80 %). Among rock fragments polycrystalline quartz can be found in the largest volume (10.10 to 47.20 %). These quartzite grains always have undulatory extinction. Grain boundaries mostly have sutured and/or triple-junctioned contact. As accessories, only some muscovite and opaque mineral grains can be observed.

Plutonic fragments (1.20 to 25.50 %) usually contain quartz (partially undulatory extinction), partially altered K-feldspar and/or plagioclase, and further accessories (muscovite, opaque grains). Plutonic rock granules are angular and they have a dimension of 600 to 2500  $\mu\text{m}$ . In the sample AK-1 there is also another type of magmatite. It has hipidiomorphic texture and merely contains anhedral quartz and plagioclase grains which have triple junctioned boundaries (Fig. 48). This rock type had most probably formed during equilibrium crystallisation and probably belonged to a migmatitic granite parent rock.

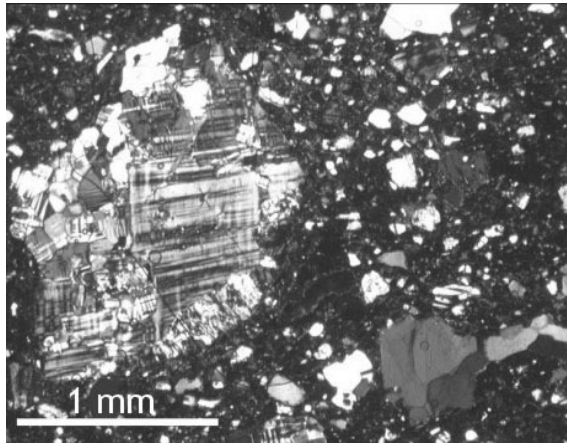


**Fig. 48 Microphotograph of the sherd AK-2 (petrographic type 4A/1, north Turkish Thrace). The picture shows mono- and polyquartz, plagioclase and plutonic rock fragments containing microcline and some monoquartz (+N).**

The volcanite fragment (3.50 %) in the sample AK-1 is slightly silicified, but the original texture (porphyritic, pilotaxitic) and minerals (plagioclase needles in the matrix and hornblende, plagioclase phenocrysts) are still identifiable. Based on texture and mineralogical composition volcanite clasts probably have intermediate or acidic composition.

On the basis of microscopic investigation the identification of recrystallised volcanite fragments in the samples DH-1 and 3 (0.60 to 1.00 %) was complicated because of the disorderly textural images and the size of the clasts. The original texture could not be identified; fine-grained quartz crystals permeated the whole clasts, but in some parts relicts of elongated K-feldspars were observable.

Few samples contain variable volume of phyllite (1.00 %, the sample AK-1), argillaceous rock fragments (0.10 to 1.90 %) and some - clay pellets (0.20 to 4.30 %; Fig. 49).

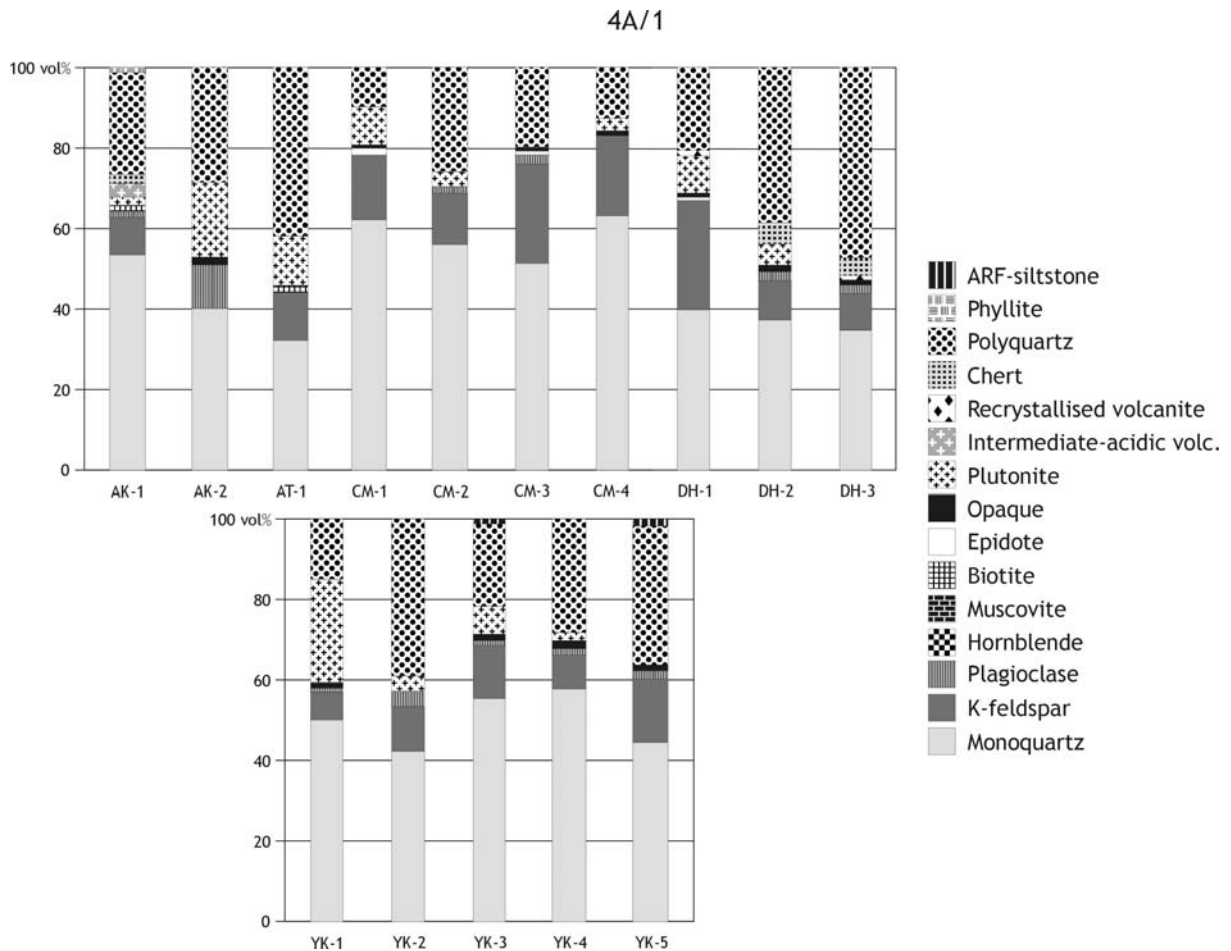


**Fig. 49 Modal composition of the sherds of the petrographic type 4A/1 (north Turkish Thrace).**

### Textural properties

The colour of the groundmass of these samples, investigated with one Nicol, is brown; with crossed polars it is dark brown with the exception of the sample AT-1, where yellowish brown paste has been observed. The sorting of the grain size distribution ranges between poor and moderate. The isotropism of the clayey matrix varies from poor to complete; mostly it is moderate or good. The samples AT-1, CM-1, 2, 3, 4, DH-2, 3, YK-2, 4, and 5 have serial type of texture, the samples AK-1, 2, DH-1, YK-1, and 3 - hiatal.

The roundness of the non-plastic inclusions varies from very angular to subrounded, sphericity of the clast varies between the values 1 and 3, and in case of the sample AK-1 – between 1 and 4. Non-plastic inclusions have poor, and in case of the samples AT-1 and YK-5 – moderate orientation (cf. Appendix 4).

### Type 4A/2

(Hamam Mevkii, sample HM)

Volume of the matrix is 74.10 % and of the clasts is 25.90 %. The sample contains undulatory, subangular monoquartz grains (48.20 %), partially altered K-feldspar (10.20 %), plagioclase (3.40 %)

clasts, muscovite (6.40 %), biotite (2.80 %), and subhedral garnet (1.70 %). To accessory minerals belongs hornblende (0.20 %).

Angular to subangular plutonite (12.40 %) and polyquartz (11.50 %) fragments have the same textural feature as that in the samples in type 4A/1. Only in this sample appear garnet-bearing micashist (2.90 %; Fig 50). The matrix of this metamorphic rock fragment consists of muscovite and some opaque minerals (Fig. 51).

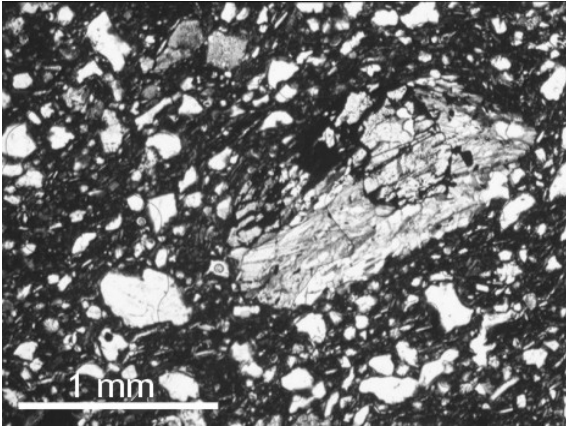


**Fig. 50** Microphotograph of the sherd HM (petrographic type 4A/2, north Turkish Thrace). The picture shows monocrystalline quartz, plagioclase and garnet-bearing micashist fragment (1N).

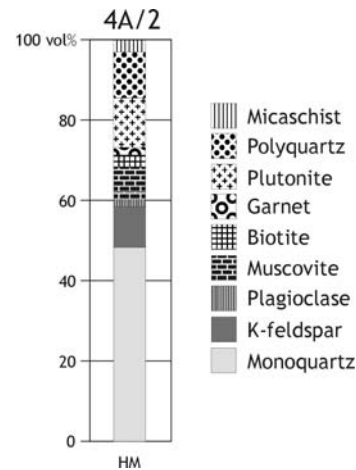


**Fig. 51** Modal composition of the sherd of the petrographic type 4A/2 (north Turkish Thrace).

### Textural properties

The sample HM has moderately anisotrope, brown-coloured groundmass. The type of its texture is hiatal, the sorting of the grain size distribution is poor. The maximum size of the grains is 3600  $\mu\text{m}$  (micashist). The roundness of the non-plastic inclusions varies from very angular to subrounded; sphericity of the clast is low to moderate (1-3). Non-plastic inclusions show moderate orientation in the texture. The sample has hiatal texture (cf. Appendix 4).

### Subgroup 4B

(Araptepe, sample AT-2)

The composition of the non-plastic inclusions differs significantly from other samples belonging to the group 4A. Volcanic rock fragments and pyroxene granules are dominating in the material.

The ratio of the matrix and clasts is 76.70 % and 23.30 %, respectively. There are few (8.60 %) partially undulatory monoquartz granules and some (1.70 %) K-feldspar fragments.

Euhedral to anhedral partially rounded and zoned clinopyroxene (30.30 %) are dominating among the minerals (Fig. 52).

The most dominant rock fragments are the above mentioned volcanite granules (53.10 %). They have vitrophanic texture and in case of some fragments traces of secondary alteration, devitrification or metasomatism can be observed. Plagioclase and clinopyroxene phenocrysts were observed in the matrix, which consist of small plagioclase needles and some opaque minerals. There were also some dark green-brown and yellowish coloured volcanic glass fragments (0.50 %) probably of basic origin. One fragment probably contains pseudomorphoses after olivine, but due to the small size the safe identification of these minerals was not unambiguous. Another type of volcanite is made of coarse-grained tabular plagioclases (intergranular texture) and it was probably part of a dyke or subvolcanic rock.

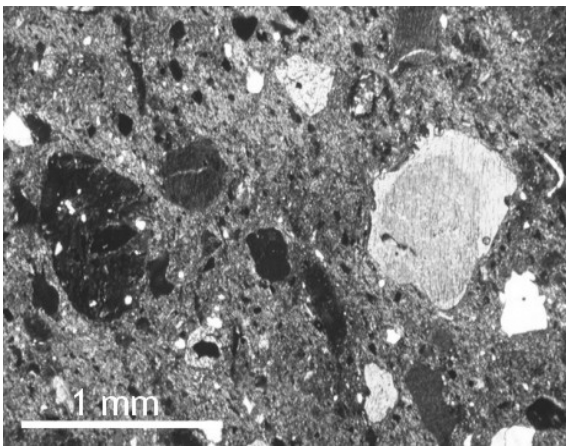


**Fig. 52** Microphotograph of the sherd AT-2 (petrographic subgroup 4B, north Turkish Thrace). The picture shows some monoquartz, altered volcanite fragments, rounded ARF, basic volcanic glass, and subhedral zoned pyroxene (+N).

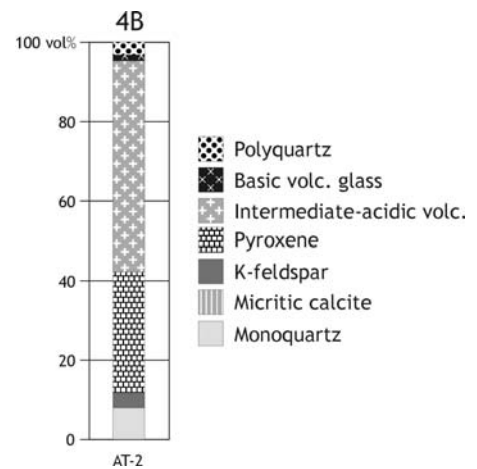


**Fig. 53** Modal composition of the sherd of the petrographic subgroup 4B (north Turkish Thrace).

Beneath volcanite fragments some (3.80 %) polycrystalline quartz of metamorphic origin as well as sparitic carbonate fragment (1.90 %) can also be observed (Fig. 53). The sample also contains large amounts of sub- to well-rounded clay pellets.

#### Textural properties

This sample has anisotropic, yellowish-brown coloured groundmass and serial texture. The sorting of the grain size distribution is moderate. The maximum size of the grains is 1800  $\mu\text{m}$  (volcanite). The roundness of the non-plastic inclusions varies from angular to rounded; sphericity of the clast variegates between the values 1 and 4. Non-plastic clasts show no orientation (cf. Appendix 4).

### 6.1.1.5. Ovcárovo

#### 6.1.1.5.1. Petrography of the sherds; Petrographic group 5

The sherds from Ovcárovo can be grouped into two totally different subgroups. Samples belonging to the *subgroup 5A* contain mineral and rock fragments which were derived from a magmatic rock association. The sherds of the subgroup *5B* contain very few non-plastic mineral inclusions and they do not contain any rock fragments.

#### Subgroup 5A (samples OVC-1, 2 and 3)

The composition of the non-plastic inclusions in this group is very similar to that observed in the group 4 (with the main difference being presence of some fragments of volcanitic origin in the group 4), but the sherds were found at different location, therefore they have been arranged into another petrographic subgroup.

The ratio of non-plastic inclusions varies from 23.50 to 18.60 %. Mineral composition is: angular to subangular monoquartz (23.30 to 37.20 %) grains with straight (partially undulatory) extinction, sericitised K-feldspar (20.40 to 29.90 %), and plagioclase (0.70 to 2.30 %).

Minerals in lesser volume are: muscovite (0.20 to 1.70 %), biotite (0.20 to 0.50 %), epidote (0.20 to 0.40 %), and some opaque clasts (0.40 to 0.60 %).

Rock fragments are: intermediate to acidic plutonite containing quartz, K-feldspar and mica (6.30 to 33.30 %; Fig. 54), polycrystalline quartz of metamorphic origin with sutured grain boundaries and undulatory extinction (11.40 to 23.80 %). There are some ARF fragments (10.70 %) in the sample OVC-2 (Fig. 55).

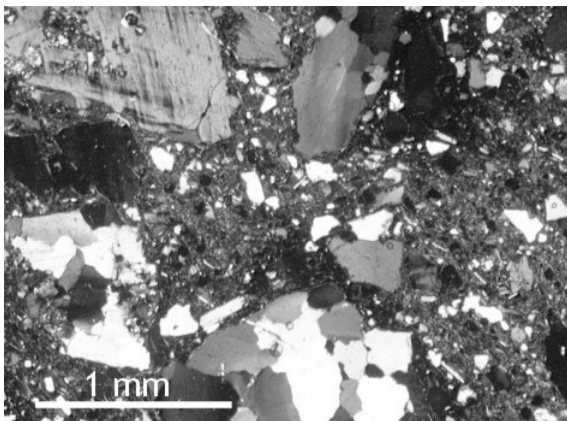


**Fig. 54** Microphotograph of the sherd OVC-1 (petrographic subgroup 5A, Ovcárovo). The picture shows mono- and polyquartz, K-feldspar, plagioclase, muscovite, and slightly metamorphosed granitic rock fragments (+N).

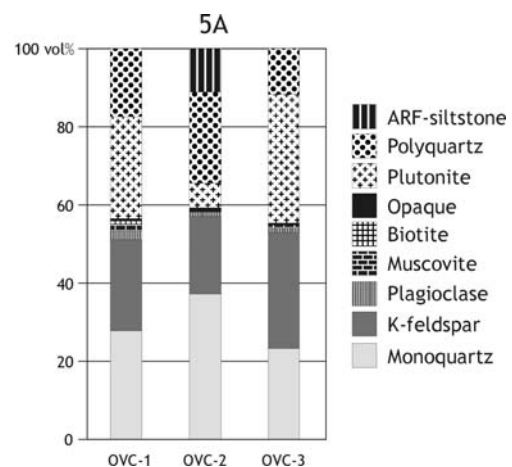


**Fig. 55** Modal composition of the sherds of the petrographic subgroup 5A (Ovcárovo).

### Textural properties

The groundmass of the samples OVC-1 and 3 is uniformly brown; the OVC-2 is yellow in colour. The isotropism is poor to moderate, all samples have hiatal texture. The extent of the largest grains found in these sherds ranges between 2700 and 3600  $\mu\text{m}$  (polyquartz, plutonite), the size of the grains show poor distribution. The roundness of the non-plastic clasts varies from very angular to subangular-subrounded, sphericity of the clast varies between the values 1 and 3. Non-plastic clasts, show no orientated arrangement in the texture with the exception of the sample OVC-3, which has good orientation (cf. Appendix 4).

### Subgroup 5B (samples OVC-4, 5 and 6)

This petrographic type is very different from the other types mentioned so far. The amount of non-plastic inclusions is lower than in the samples from other groups and types, and the samples contain large amounts of rounded clay pellets (18.60 to 63.70 %) and no rock fragments.

The ratio of matrix and non-plastic clasts varies from 86.90 to 96.20 % and 3.80 to 13.10 %.

Monoquartz fragments with straight to slightly undulatory extinction (48.80 to 84.60 %), (sub)rounded micrite clasts (10.40 to 36.90 %) which were probably part of solid soil inclusions, some muscovite (2.10 to 3.70 %), biotite in traces (0.50 to 0,80 %), and opaque clasts (2.10 to 10.10 %) are dominant components of the non-plastic inclusions (Fig. 56 and 57).

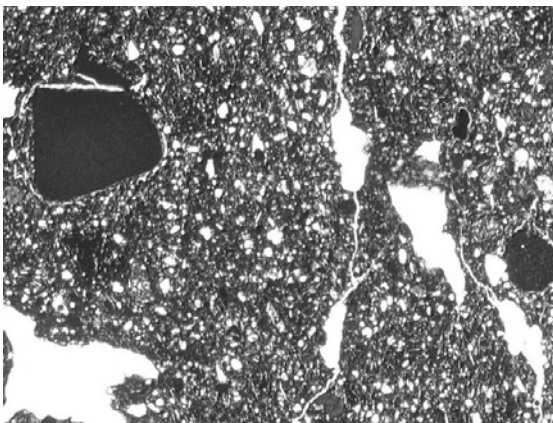


**Fig. 56** Microphotograph of the sherd OVC-4 (petrographic subgroup 5B, Ovcarovo). The picture shows monoquartz, and opaque clasts (1N).

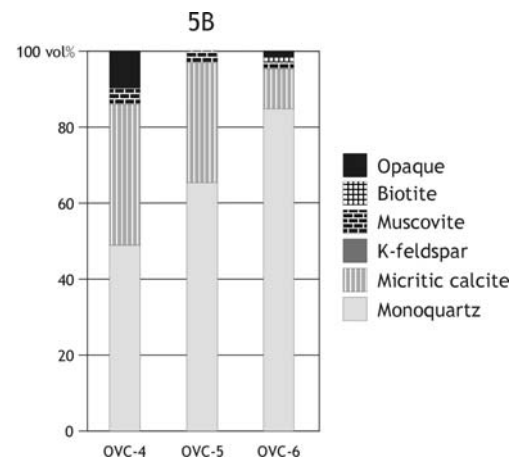


**Fig. 57** Modal composition of the sherds of the petrographic subgroup 5B (Ovcarovo).

### Textural properties

The colour of the clayey paste of these samples is uniformly brown. The isotropism of the clayey matrix varies between moderate and complete. The sample OVC-5 has (partially) hiatal texture; all other samples have serial texture. The maximum size of the grains ranges between 700 and 2500  $\mu\text{m}$  (monoquartz, micritic calcite), the size of the grains shows poor to good distribution. Non-plastic clasts are in average subrounded or rounded, some smaller quartz inclusions with angular sphericity of

the clast vary between the values 1 and 5 (mostly between 2 and 4). This petrographic subgroup contains no sample with orientated texture (cf. Appendix 4).

### 6.1.1.6. Chal

#### 6.1.1.6.1. Petrography of the comparative material

##### Geological sample Ch-5, fraction: 0.5 -2 mm (Koren-Elhovo, near Chal, south Bulgaria)

Minerals: monocrystalline quartz, K-feldspar, microcline, plagioclase, biotite, muscovite, amphibole, epidote, opaque minerals.

Rock fragments: quartzite of metamorphic origin (partially sutured, mostly triple-junctioned grains with undulatory extinction), intermediate or basic (?) volcanite with rests of pseudomorphoses after olivine or pyroxene, few acidic and/or intermediate volcanite, acidic plutonite (quartz, K-feldspar, altered plagioclase, biotite, muscovite), fragments of graphic granite, phyllite, ARF-siltstone. Polyquartz and plutonites dominate in the sample.

#### 6.1.1.6.2. Petrography of the sherds (samples CH-1, 2, 3, 4, 5 and 6, petrographic group 6)

The ratio of matrix vary between 23.20 and 16.60 %,

The most common minerals are: (sub) angular monoquartz grains (35.20 to 54.50 %) with undulatory extinction, partially altered K-feldspar (7.50 to 27.20 %) and plagioclase crystals (2.60 to 5.80 %). Some minerals in smaller amounts can also be found in these samples: green hornblende (0.20 % in the sample CH-4), muscovite (0.20 to 2.90 %), biotite (0.20 to 1.30 %), epidote (0.10 to 1.40 %), and some opaque clasts (1.20 to 1.40 %). In the sample CH-4 there is a relative large amount (7.00 %) of olivine or pseudomorphoses after olivine.

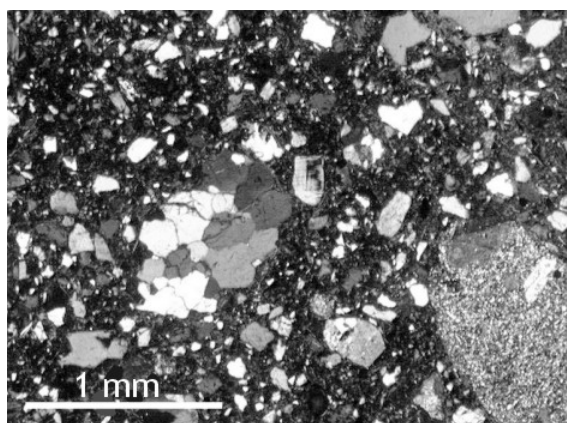


**Fig. 58** Microphotograph of the sherd CH-1 (petrographic group 6, Chal). The picture shows mono- and polyquartz, K-feldspar, plagioclase, and slightly recrystallised volcanite fragments (+N).

Rock fragments are: slightly metamorphosed plutonite (1.40 to 13.70 %) containing quartz, K-feldspar and/or plagioclase, some mica (muscovite and few biotite), and other accessory minerals like zircon and apatite. Polycrystalline quartz, with sutured grain boundaries and undulatory extinction appears in amount of 8.90 to 27.30 %.

In the sample CH-1 intermediate and/or acidic volcanite fragments are found (7.30 %; Fig. 58). In cryptocrystalline, partially hyalin texture potash feldspar phenocrysts, amphibole and opaque minerals are observed. Other rock fragments are: chert in the sample CH-1 (0.30 %), phyllite in the sample CH-1 (1.90 %), and ARF (2.90 to 5.50 %) in the samples CH-3, 4, and 6 (Fig. 59).

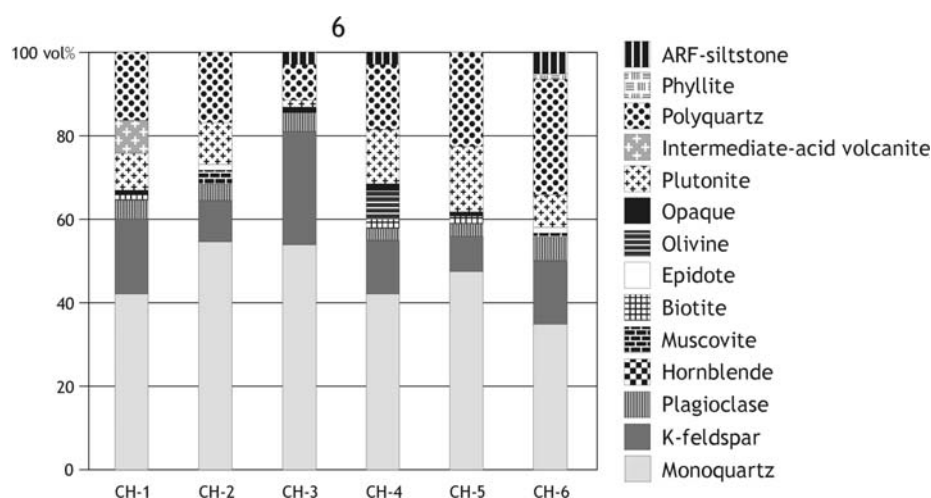


**Fig. 59 Modal composition of the sherds of the petrographic group 6 (Chal).**

### Textural properties

The colour of the groundmass of these samples varies from yellowish-brown to brown. The isotropism of the clayey matrix ranges between moderate and complete, in the samples CH-3 and 4 it is poor. The sherds CH-1, 3 and 6 have serial, all others - hialat texture. The maximum size of the grains ranges between 1400 and 2000  $\mu\text{m}$  (polyquartz, plutonite, K-feldspar), the size of the grains show poor to moderate distribution. The roundness of the non-plastic clasts varies from very angular to subangular; in the sample CH-3 the clasts are very angular or angular. Sphericity of the clast varies between 1 and 3; in case of the samples CH-3 and 4 – between 1 and 4. Non-plastic inclusions show poor (CH-4 and 6), moderate (CH-1, 2 and 5), and good (CH-3) orientation (cf. Appendix 4).

### 6.1.1.7. Diadovo, Pshentisevo, and Kirilovo

#### 6.1.1.7.1. Petrography of the comparative materials

##### Geological sample Dia-14, fraction: 0.125 -2 mm (Diadovo, central Bulgaria)

Minerals: monocrystalline quartz, K-feldspar, microcline, plagioclase, biotite, muscovite, opaque minerals.

Rock fragments: two types of polycrystalline quartz (1. sutured grain boundaries with undulatory extinction; 2. triple-junctioned grains with straight extinction), recrystallised volcanite, acidic plutonite (quartz, K-feldspar, altered plagioclase, biotite, muscovite), sub arkose-arkose type fine-grained sandstone fragments partially with dark brown limonitic veins containing quartz clasts, some K-feldspars, and mica (muscovite and biotite), as well as metamorphic (polyquartz, phyllite), and magmatic rock fragments (Fig. 60). Further rock clasts are: few volcanites probably of intermediate origin (plagioclase phenocrysts in cryptocrystalline matrix, amphibole and opaque minerals), phyllite, and ARF-siltstone.

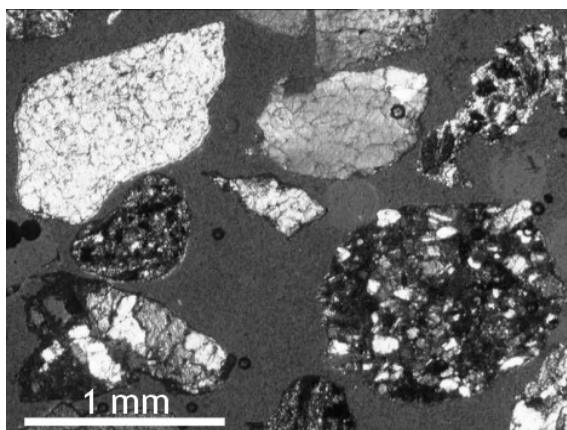


Fig. 60 Quartzite and sandstone fragments in the sediment sample Dia-14, (+N).

#### 6.1.1.7.2. Petrography of the sherds, Petrographic group 7

Grouping of these sherds was based on common petrographic features and the relatively small distances between the different archaeological localities (cf. Fig. 20).

The type 7A/1 contains lots of plutonite fragments, polycrystalline quartz of metamorphic origin, and K-feldspars. The type 7A/2 differs a little from 7A/1, as it also contains clasts of sandstone and volcanite in different amount beside the above mentioned clasts.

Type 7A/1

(Kirilovo, Pshenitshevo, Diadovo, the samples: KIR-1, 2, 3, PSH-1, 2, 3, DIA-1, 2, 5, 7, 8, 10 and 11)

The ratio of the matrix varies from 71.60 % to 88.60 % and the ratio of the temper – from 28.40 % to 11.40 %.

Similarly to the petrographic subgroups 4A and 5A the composition of the non-plastic inclusions in this group is also relatively simple. Most components belong probably to a magmatic-metamorphic rock association.

Monocrystalline quartz grains (7.80 to 39.80 %) have undulatory extinction, only in the samples DIA-2 and 3 there are some clasts with straight extinction. Subhedral K-feldspar (7.10 to 38.20 %) and plagioclase (0.10 to 6.80 %) are in most cases altered (sericitised).

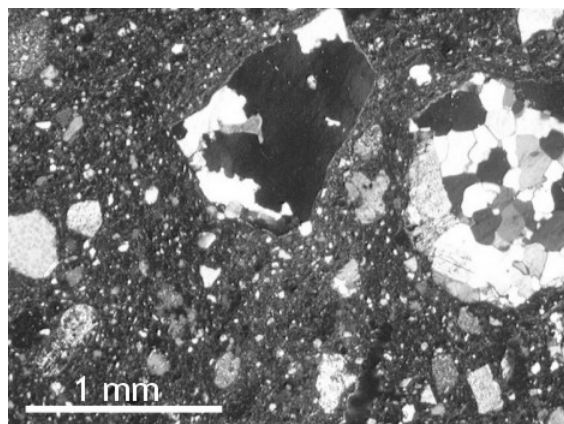


**Fig. 61** Microphotograph of the sherd DIA-11 (petrographic type 7A/1, Diadovo-Pshenitsevo-Kirilovo). The picture shows mono- and polyquartz, K-feldspar, plagioclase, opaque minerals, and granitic rock fragments (+N).

Most common rock fragments are: partially metamorphosed plutonite (17.30 to 62.60 %) containing undulatory quartz, K-feldspar and/or plagioclase, mica, some accessories like zircon, and apatite (Fig. 61).

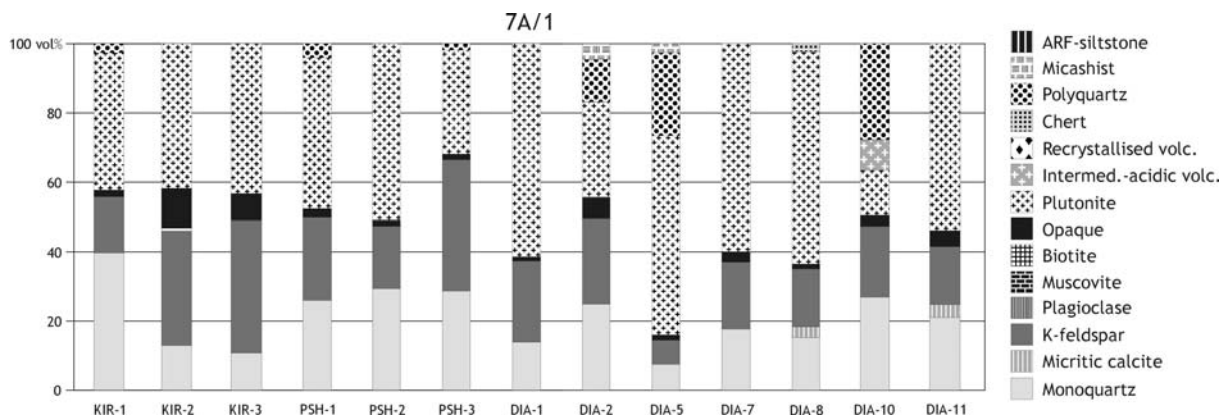


**Fig. 62** Modal composition of the sherds of the petrographic type 7A/1 (Diadovo-Pshenitsevo-Kirilovo).

Further common rock type is polycrystalline quartz of metamorphic origin (2.20 to 30.60 % in the samples KIR-1, DIA-2, 5 and 10). In the samples DIA-2 and 5 there is also some (4.20 and 2.30 %) well-foliated micashist (Fig. 62).

### Textural properties

This petrographic group contains samples with different textural properties. Most samples have, unlike other sherds, pale groundmass (yellow-pale brown), only the samples DIA-10 and PSH-1 have darker (brown to dark-brown) paste. In addition to these optical phenomena isotropism of the matrix is also poor, with the exception of the two samples mentioned above, which have moderate and good isotropical properties. The samples KIR-1, PSH-1, 2, 3, DIA-1, 2, 5, 7, 8, and 11 possess hiatal, and the samples KIR-2, 3, and DIA-10 - serial texture.

The maximum size of the non-plastic grains found in the sherds ranges between 1000 and 3800  $\mu\text{m}$  (plutonite, polycrystalline quartz), in average 1800-2200  $\mu\text{m}$ . The size of the grains shows poorly distribution. The roundness of the non-plastic clasts varies from very angular to subangular-subrounded, sphericity of the clast varies between the values 1 and 3, and in case of some samples (cf. Appendix 4) between 1 and 4. Non-plastic inclusions have poor orientation; partially they are situated unorientated in the texture.

### Type 7A/2

(Diadovo, samples: DIA-3, 4, 6, 9, 12 and 13)

In these samples the amount of the matrix varies from 68.10 % to 86.20 % and of the non-plastic clasts – from 31.90 % to 13.80 %.

The main mineral components are: monoquartz (8.80 to 61.30 %) mostly with undulatory extinction, K-feldspar (2.70 to 18.60 %), and plagioclase (0.10 to 2.80 %) grains.

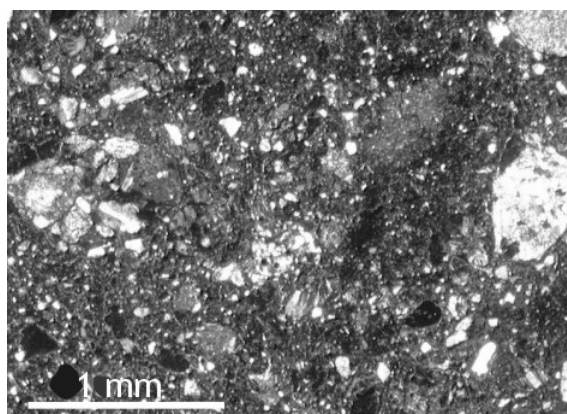


**Fig. 63** Microphotograph of the sherd DIA-12 (petrographic type 7A/2, Diadovo). The picture shows mono- and polyquartz, K-feldspar, plagioclase, ARF, and sand-stone fragments (+N).

In the samples DIA-3, 6, and 12 some micritic calcite fragments (1.00 to 10.20 %), also occur. Accessories are: hornblende (in the samples DIA-6 and 12, 0.10 and 0.30 %, respectively, in DIA-4 - 2.90 %), muscovite (0.10 to 0.70 %), epidote (0.10 to 0.30 %) and opaque minerals (0.10 to 0.50 %, in DIA-4 - 1.40 %). Similar to further groups plutonite (mostly with subhedral texture) is the most common rock fragment (4.30 to 76.70 %). In the samples DIA-3, 6, and 12 variable amount (1.50 to 14.60 %) of volcanites can be observed. The texture of these clasts is slightly recrystallised, which obscures their exact identification. There are K-feldspar, plagioclase phenocrysts, and some opaque minerals in the completely crystallised matrix. Other minerals could not be identified. Due to the high variability of the texture and minerals volcanic fragments have probability intermediate origin. The samples DIA-3 and 6 contain polycrystalline quartz of metamorphic origin (sutured grain boundaries, undulatory extinction of the grains; 6.30 and 22.70 %). As a unique rock type, which can be merely found in this petrographic type, fine-grained sandstone (3.10 to 45.60 %) appears amongst the non-plastic inclusions. Two types of fine-grained sandstone can be distinguished: (1) in all samples occur sub arkose containing aside from quartz clasts some, K-feldspars, and mica (muscovite and biotite), and (2) arkose in the sample DIA-12 (Fig. 63) made mostly up of metamorphic (polyquartz, phyllite), magmatic fragments, K-feldspar and mica (mostly biotite) partially with iron-rich, limonitic (?) veins.

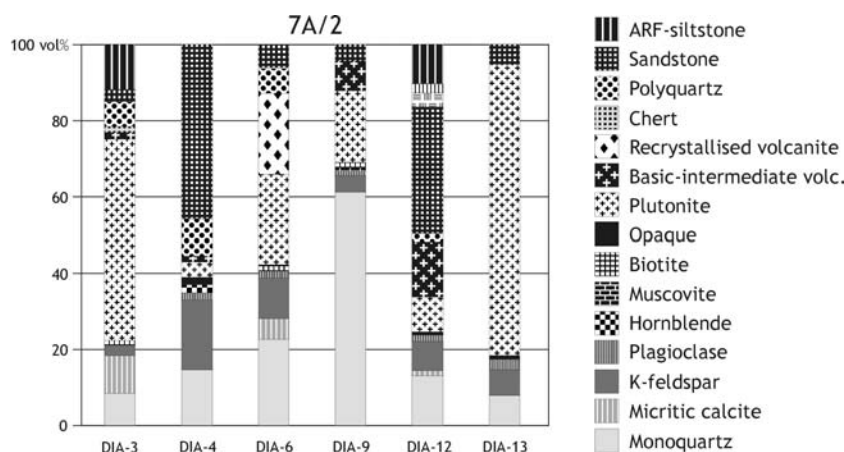


**Fig. 64 Modal composition of the sherds of the petrographic type 7A/2 (Diadovo).**

Some other rock fragments of metamorphic origin were also: in the sherd DIA-3 ARF (11.30 %), in the sample DIA-12 ARF (10.30 %), and micashist (1.70 %). Due to the dark brown-black colour the ARF fragments they are probably iron-rich rock fragments (Fig. 64).

### Textural properties

The colour of the groundmass is very similar (yellow to brown) to the samples described in the previous type. The isotropism varies between poor and complete, it is mostly good. The sherds DIA-3, 6 and 13 have hiatal and the sherds DIA-4, 9 and 12 have serial textural properties. The maximum size of the grains ranges between 1700 and 4600  $\mu\text{m}$  (polyquartz, sandstone), the size of the grains shows

poorly distribution. The roundness of the non-plastic inclusions varies from very angular to subangular-subrounded, in the sample DIA-12 some rounded clasts have also been observed; sphericity of the clast varies between the values 1 and 4. Non-plastic inclusions show no, and in case of the sample DIA-3 - moderate orientation (cf. Appendix 4).

### 6.1.1.8. Sborianovo

#### 6.1.1.8.1. Petrography of the sherds; Petrographic group 8

##### (Samples: SBO-1, 2 and 3)

This group is very different from the other types mentioned so far, but it reveals lots of similarities with the petrographic subgroup 5B (Ovcarovo). The amount of non-plastic inclusions is lower than in the samples from other groups and the group contains large amounts of rounded clay pellets (20.30 to 76.60%).

The ratio of non-plastic clasts varies from 3.40 to 24.30 %.

Monoquartz fragments with straight to slightly undulatory extinction (17.90 to 38.70 %), subangular to (sub)rounded micrite clasts (35.30 to 78.20 %), which were probably part of solid soil inclusions, some K-feldspar (1.30 to 1.60 % in the samples SBO-1 and 2), muscovite (0.90 to 1.90 %), and opaque clasts (2.50 to 24.10 %) are dominant components of the non-plastic inclusions (Fig. 65). The sherds do not contain any rock fragments (Fig. 66).

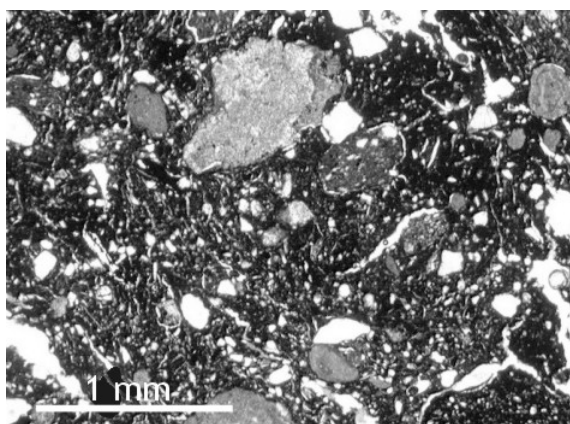


**Fig. 65** Microphotograph of the sherd SBO-1 (petrographic group 8, Sborianovo). The picture shows monoquartz, clay pellets and micritic inclusions (1N).

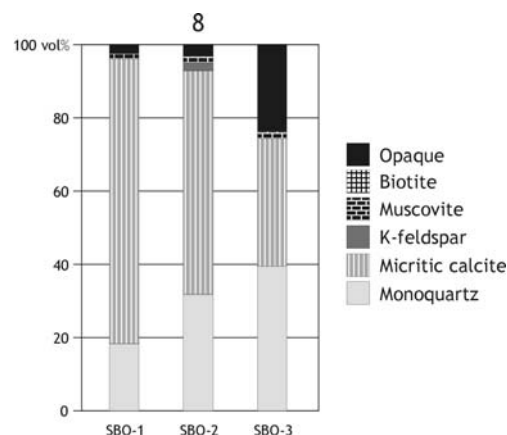


**Fig. 66** Modal composition of the sherds of the petrographic group 8 (Sborianovo).

#### Textural properties

The colour of the clayey paste of these samples is uniformly brown, only the sample SBO-2 has orange-brownish colour. The isotropism of the clayey matrix varies between moderate and complete. The sample SBO-1 has (partially) hiatal texture; all other samples have serial texture. The maximum

size of the grains ranges between 700 and 2500  $\mu\text{m}$  (monoquartz, micritic calcite), the size of the grains shows poor to good distribution. Non-plastic clasts are in average subrounded or rounded, some smaller quartz inclusions with angular sphericity of the clast vary between the values 1 and 5 (mostly between 2 and 4). This petrographic group contains no sample with orientated texture (cf. Appendix 4).

### 6.1.2. Cathodoluminescence investigation

The petrographic analysis has shown that the sample A-1 (the Avşa Island) contains large amounts of euhedral calcite fragments, which could have originally belonged to a marble or crystalline limestone parent rock. Because the cathodoluminescence properties of white marbles in the eastern Mediterranean and west Anatolian regions have been extensively discussed in other publications (e.g. Zöldföldi and Satır, 2003), it seemed to be useful to investigate the CL image of the calcite fragments found in this sherd and compare the data to the information published in the literature.

The CL investigation was carried out on different areas of the polished thin section. Generally it can be established that most calcite fragments have either very slightly orange or no luminescence. Most fragments were completely black. In some cases bright orange luminescence, mostly on tiny fragments, or between bigger clasts in veins was also observed (Fig. 67).

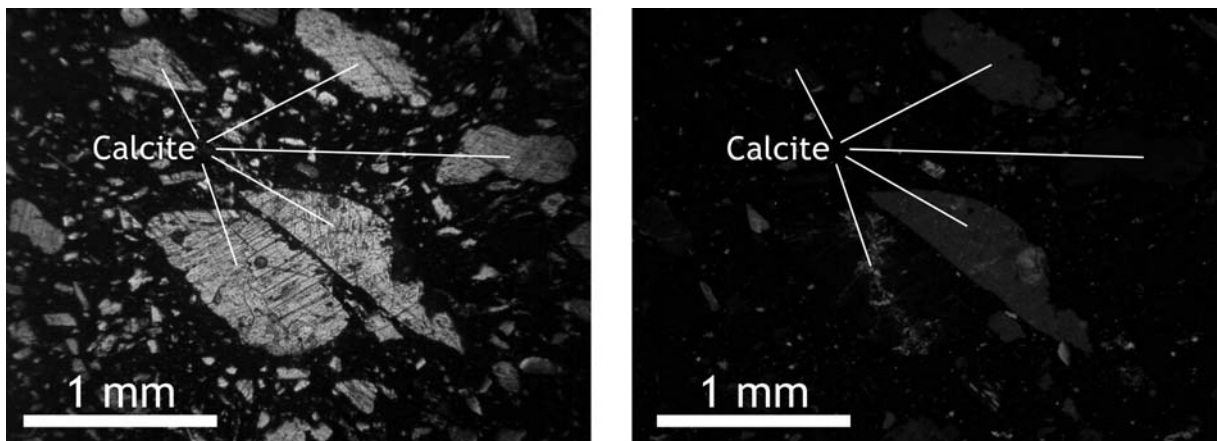


**Fig. 67** Microphotograph (left, 1 Nicol) and CL image (right) of the same area of the sherd A-1 (petrographic group 2, the Avşa Island). The lack (or the very low intensity) of the luminescence of the calcite crystals is obvious.

### 6.1.3. X-ray diffractometry (XRD)

Considering the macroscopic features, the microscopic grouping, and the petrographic composition of the archaeological samples, 20 sherds were selected for the XRD analysis from each archaeological site discussed in this study.

Due to the importance of the phyllosilicates in determination of the maximum firing temperatures of the ceramics in this study, in the following short description of the two main phyllosilicate types, observed in the samples, will be briefly presented below.

Chlorite: its structure is composed of the regular alternation of two different types of layer lattice (talc- and brucite-type layers). According to Nemezc (1973) and Thorez (1975) its 001 peak ( $I=65$ ) can be found between  $d=13.9$  and  $14.3\text{\AA}$ . The peak 002 ( $I=100$ ) is situated between  $d=7.15$  and  $7.05\text{\AA}$ .

On the basis of the form of the 001 peak of the chlorite between  $13.9$  and  $14.1\text{\AA}$ , in case of the samples TR-19 and PSH-2, the presence of swelling clay minerals (montmorillonite, vermiculite) was not unambiguously excluded. Therefore, according to the modern clay mineralogical diagnostic (Thorez, 1975; Brindley & Brown, 1980), these samples have been treated with ethylenglycol and analysed with XRD. If a sample contains swelling clay minerals, the treatment with ethylenglycol must generate  $1$  to  $3\text{\AA}$  swelling in the layer lattice. This phenomenon is well observable on the diffractogram by the shift of the 001 peak. Because after the ethylenglycol treatment no shift was observed on the diffractograms, the samples do not contain swelling clay minerals and the peaks at  $14\text{\AA}$  indicated the mineral chlorite.

10 Å phyllosilicate: a summarised term for the phyllosilicate types with  $10\text{\AA}$  lattice plain distance. Two different minerals belong to this group:

- 1) sericite-muscovite,
- 2) illite (its structure always contains interbedded swelling layers).

On the basis of the form of the 001 peak, the type of the  $10\text{\AA}$  phyllosilicate is determinable. If the peak is narrow and sharp, the sample contains sericite-muscovite; if it is broad and diffuse, the questionable phase is illite. In some cases both phases can be found in a sample. In this case the form of the 001 peak is different: the lower part is broad and diffuse, its top is sharp and narrow (Thorez, 1975; Brindley & Brown, 1980).

The terms K-feldspar, plagioclase, amphibole, and pyroxene are used as general terms for these mineral groups. The amount of the powder samples and the presence of many phases did not allow the exact identification of these minerals.

In the description of the diffractograms, only the main identification peaks of the phases will be presented. The volume of the different phases was given by the estimation of the ratios of the peaks relative to the peak with the largest intensity (mostly the 101 peak ( $I=100$ ) of quartz).

### 6.1.3.1. Sherds from Troia (TR-7, 12, 19, and 25)

Following crystalline phases were determined in the samples TR-7, 12, 19, and 25:

10Å phyllosilicate, which in the sample TR-7 is sericite-muscovite, in all other samples is illite. Quartz, K-feldspar, and plagioclase are the main phases in each sample. The amount of K-feldspar and plagioclase is very similar (there is more plagioclase than K-feldspar).

The sample TR-19 contains chlorite in traces (peak 001,  $d = 13.90 \text{ \AA}$ ) and lots of (20-30 vol %) calcite. The sherds TR-12 and 25 also contain some calcite, but its amount is much lower, than in the sample TR-19.

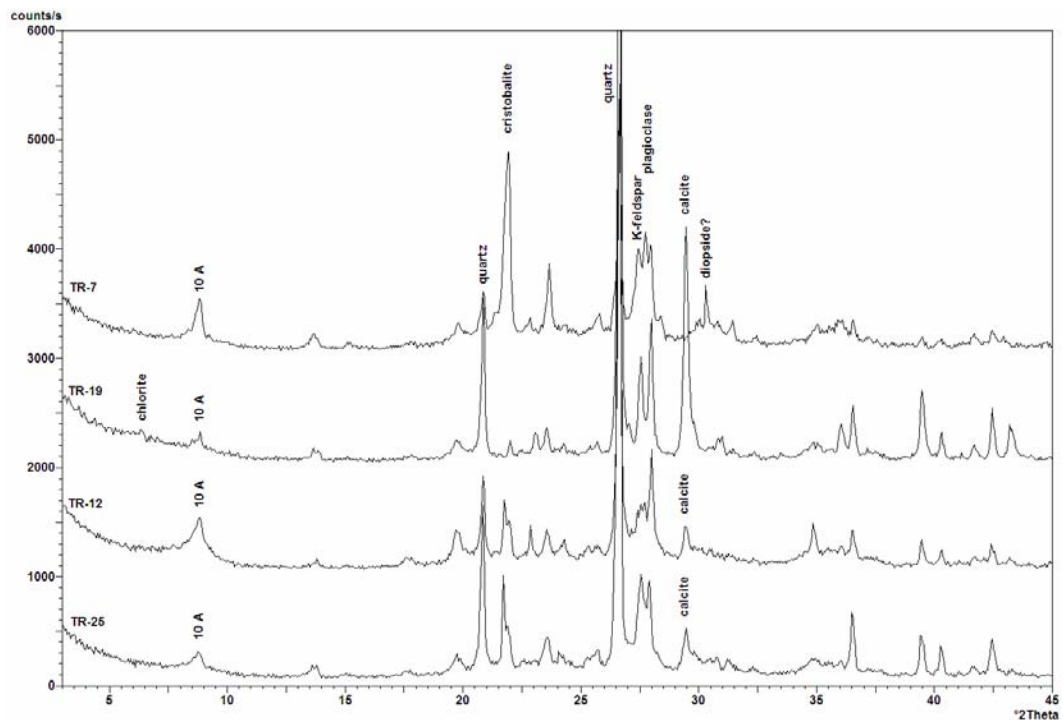


Fig. 68 X-ray diffractogram of the sherds TR-7, 12, 19 and 25 (Troia).

In the sample TR-7 a unique mineral phase was determined. Cristobalite has an amount of approximately 15-20 vol % (Fig. 68). The sharp peak at  $d = 2.94 \text{ \AA}$  ( $30.5^\circ 2\theta$ ) probably belongs to the mineral phase diopside, although petrographic observations do not confirm this supposition. Other peaks with large intensity which can determine the exact type of the phase in question are overlapped by the peaks of other phases (e.g. plagioclase, quartz) of larger intensity (Fig. 68).

### 6.1.3.2. Sherds from the Avşa Island and Menekşe Çatağı (A-1, MCW-6, and MCE-1)

The main phases are: quartz in the samples MCE-1 and MCW-2, calcite in the sample A-1 (the sherd MCW-2 also contains calcite in small amount), K-feldspar, and plagioclase.

Each sample contains 10Å phyllosilicates (A-1 and MCW-5 sericite-muscovite, MCE-1 illite); furthermore, MCW-5 and A-1 also contain chlorite minerals, where the peak 002 is also observable. A difference can be observed in the amount of the chlorite in the two samples. The intensity of the 001 (at  $6.35^\circ 2\theta$ ;  $d = 14.02 \text{ \AA}$ ) peak is smaller than the intensity of the peak 002 (at  $12.5^\circ 2\theta$ ;  $d = 7.07 \text{ \AA}$ ) of chlorite in the sample A-1. The ratios of the intensity of the chlorite peaks in the sample MCW-5 is the opposite of the intensity measured in the other sherd. Furthermore, due to the form (Fig. 69) of the 001 chlorite peak, the mineral phase smectite also appears on the diffractogram.

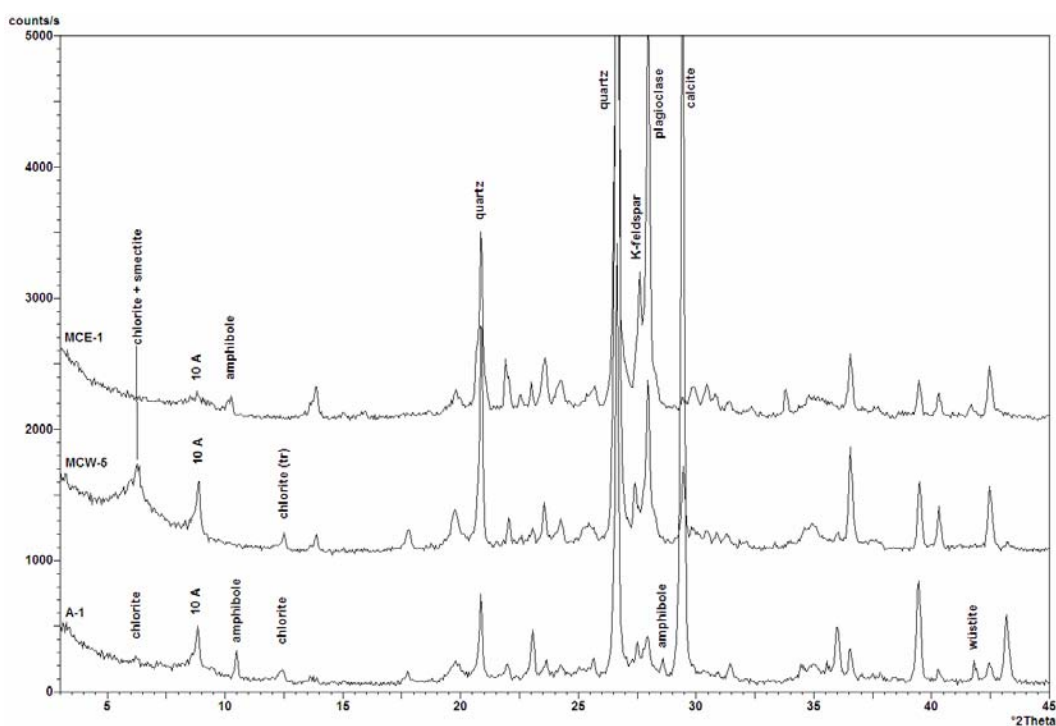


Fig. 69 X-ray diffractogram of the sherds A-1, MCW-5 and MCE-1 (the Avşa Island, Menekşe Çatağı).

The small peaks at  $10.25^\circ 2\theta$  ( $d = 8.60 \text{ \AA}$ ) as well as  $28.60^\circ 2\theta$  ( $d = 3.12 \text{ \AA}$ ) in the samples MCE-1 and A-1 refer to the amphibole content. The peak at  $2.15 \text{ \AA}$  in the sample A-1 refers probably to the presence of the mineral wüstite. This peak could also belong to the mineral plagioclase, but the low amount of this mineral in this sample does not explain the relatively high intensity of the peak at  $2.15 \text{ \AA}$ . (Fig. 69).

### 6.1.3.3. Sherds from north Turkish Thrace (AT-2, DH-2, HM, and YK-3)

The composition of these samples, determined by an X-ray diffraction, is very similar; major differences can only be observed in the relative amount of the different phases. As in most sherds, also

in these samples quartz is the dominating phase. According to the diffractogram the sample AT-2 contains only K-feldspar, the sherd HM only plagioclase, the samples DH-2 and YK-3 contain both of them. Due to the sharp form of the 10 Å peak, this phyllosilicate in all samples refers to muscovite (sericite). Chlorite can be found in small amount in the sample DH-2 and in the sample HM, the peak 002 was also detectable. The sample HM also contains amphibole (hornblende), the sample AT-2 pyroxene (29.80° 2θ; d = 2.99 Å) and iron oxide, probably magnetite and/or maghemite (35.70° 2θ; d = 2.51 Å) in detectable amount (Fig. 70).

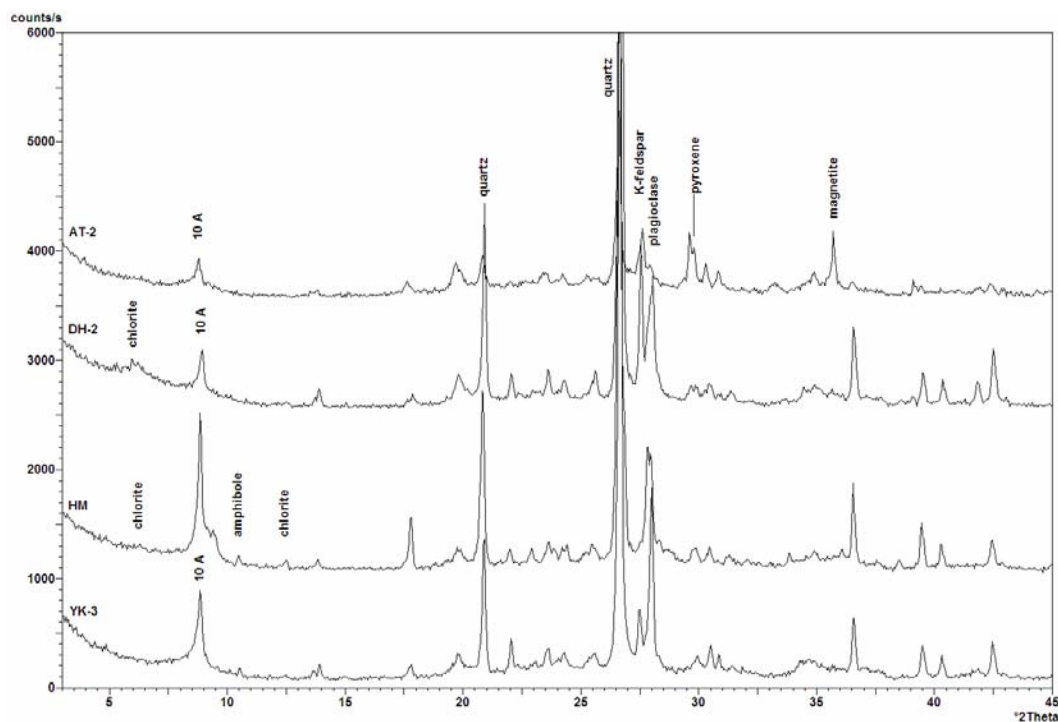


Fig. 70 X-ray diffractogram of the sherds AT-2, DH-2, HM, and YK-3 (north Turkish Thrace).

#### 6.1.3.4. Sherds from Chal (CH-1 and 3)

The phase composition and the ratios of the minerals are almost identical in both samples. Four different minerals were distinguished. The main phases are: quartz, K-feldspar and plagioclase.

On the basis of the form and the position of its 001 peak, the fourth phase is illite; in the sample CH-1 some sericite-muscovite can also be found. The ratio of K-feldspar and plagioclase is almost the same, with some more plagioclase in the samples (Fig. 71).

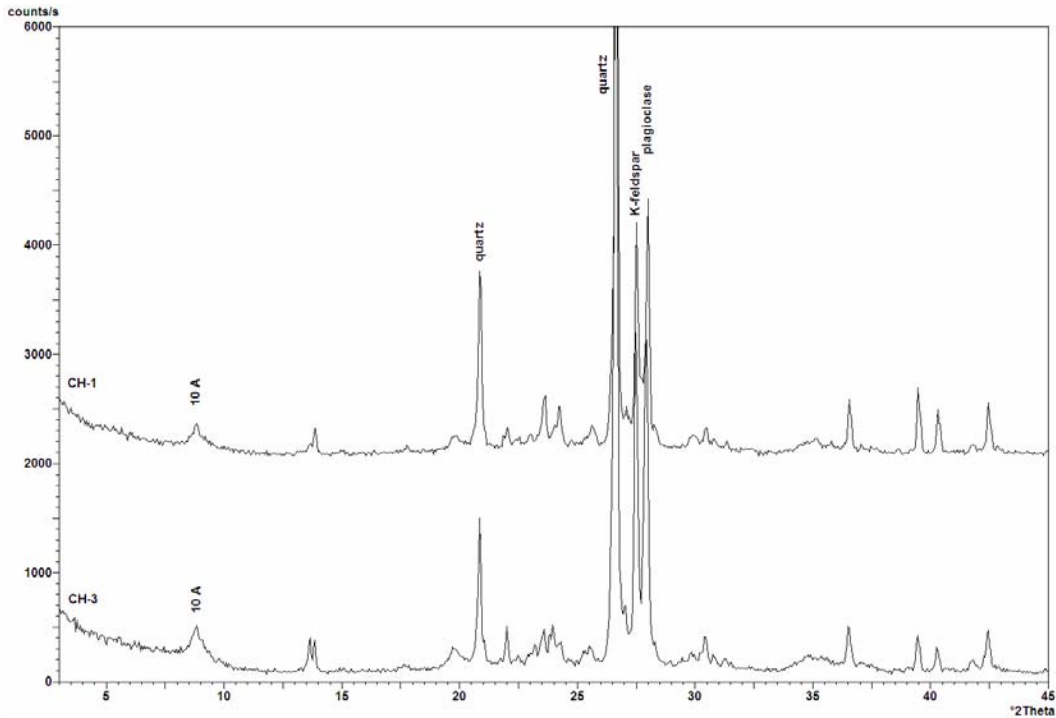


Fig. 71 X-ray diffractogram of the sherds CH-1 and 3 (Chal).

#### 6.1.3.5. Sherds from Ovcarovo and Sborianovo (OVC-1 and 4, SBO-3)

As in other samples, also here the dominating mineral is quartz. In the sherd OVC-1 great amount of K-feldspar (10-15 vol %) and even more plagioclase (20-25 vol %) are found. The samples OVC-4 and SBO-3 contain small amount of plagioclase and K-feldspar in traces.

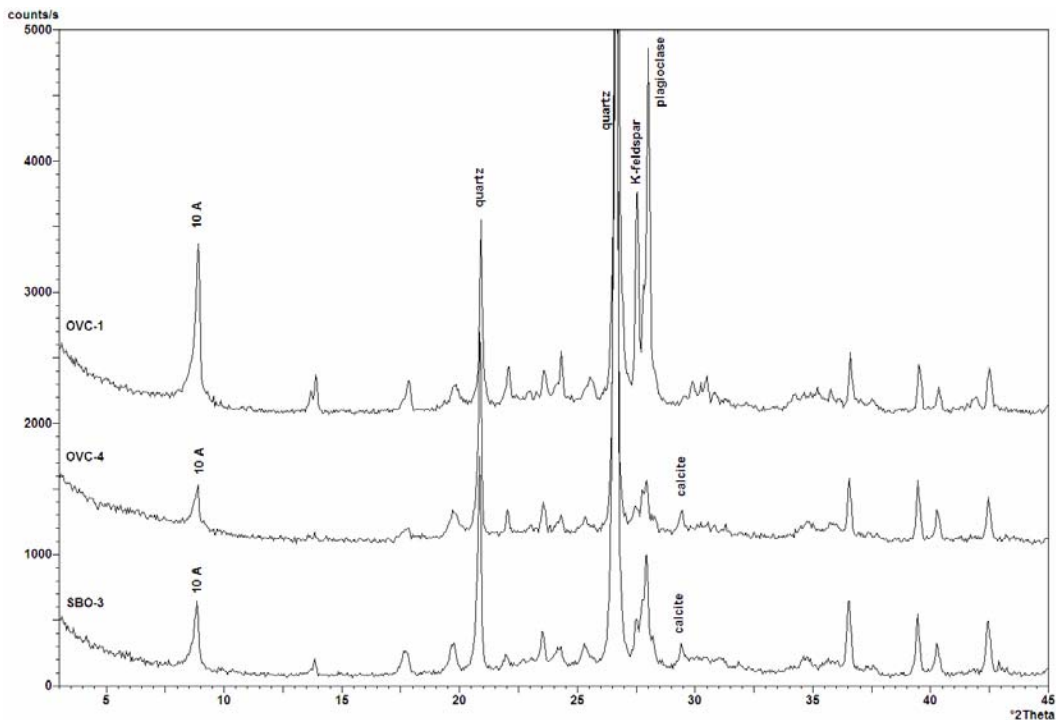
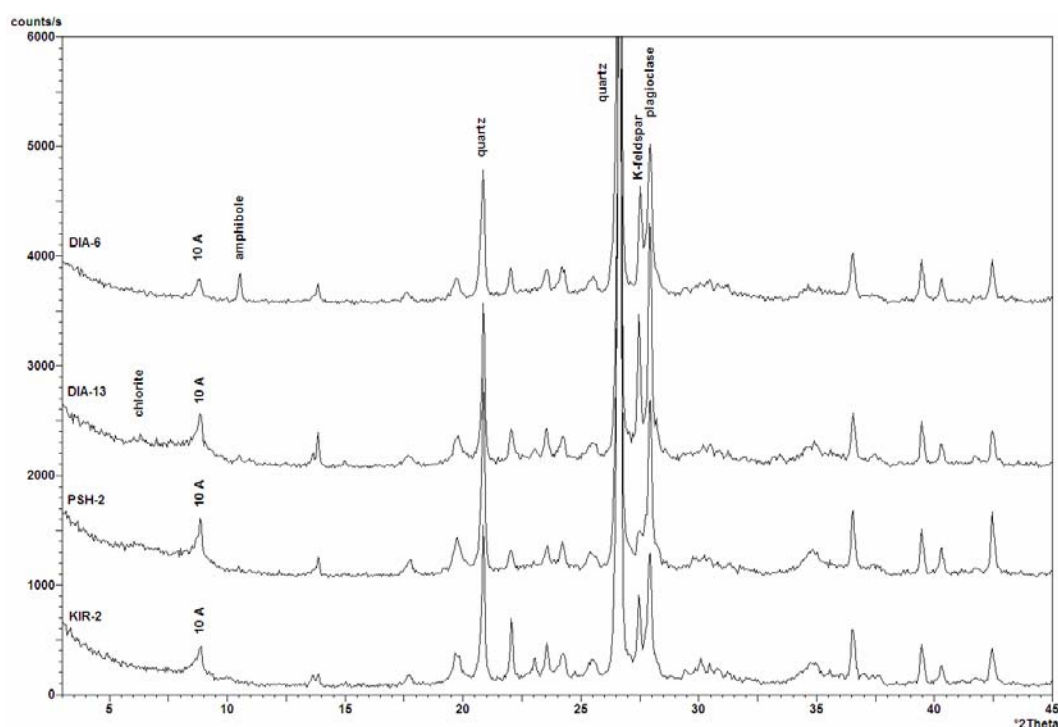


Fig. 72. X-ray diffractogram of the sherds OVC-1, 4, and SBO-3 (Ovcarovo, Sborianovo).

In the sherds OVC-4 and SBO-3 the phase calcite was detected, however only in small amount. The 001 peaks of the 10Å phyllosilicate is characterised by a sharp form, thus they are sericite-muscovite. However, in the sample OVC-4 the flared bottom refers to the presence of some illite. The high intensity of the 9.93Å peak in the sample OVC-1 refers to the presence of well-crystallised mica (Fig. 72).

#### 6.1.3.6. Sherds from Diadovo, Pshenitsevo and Kirilovo (DIA-6, 13, PSH-2 and KIR-2)

These four sherds have also similar and common features in their phase composition (Fig. 73).



**Fig. 73 X-ray diffractogram of the sherds DIA-6, 13, PSH-2, and KIR-2 (Diadovo, Pshenitsevo, and Kirilovo).**

The main phases are: quartz, K-feldspar (in the sample PSH-2 in traces), and plagioclase, which is presented in each sample in larger amount, than K-feldspar. The sample DIA-6 contains illite, the other samples mostly sericite-muscovite phases with some illite. The archaeological samples DIA-13 and PSH-2 contain some chlorite in traces (only the peak 001 was detectable). The 8.38 Å peak (at 10.27° 2θ) in the samples DIA-6 and DIA-13 refers to the presence of the mineral amphibole; in the sherd DIA-13 only in traces (Fig. 73).

## 6.2. Geochemical analyses

In this subchapter the data of chemical and geochemical analyses (XRF, radiogenic isotopes, NAA, EMPA) are presented. The data have been organised according to the archaeological localities: first the major and trace element composition (XRF measurements) of all sediments will be presented followed by the results of the analyses of the sherds (except of the sherd A-1). As in some cases the petrographic and chemical (XRF) data did not provide sufficient results on the origin of the sherds, several samples have been chosen for the radiogenic isotope analysis in order to get more detailed information about their geochemical properties and thus about their origin. Further 3 sherds and a geological rock sample have been chosen for the electron microprobe analysis and neutron activation analysis. Because in the whole chapter the presentation of the geological samples and the sherds was based on the the results of the petrographic and XRF analyses, the data of the radiogenic isotopes, EMPA, and NAA analyses of the selected sherds are presented below in a separate section.

### 6.2.1. *Geochemical composition of comparative sediments and the sherds*

Using optical microscopic investigation all sherds have been grouped on the basis of their petrographic composition. This method proved very useful in classification and distinguishing of the archaeological material. As it has been described in Chapter 5, there exist many similarities in the similar geological assembly of the different areas, where the archaeological material have been collected. With the exception of Troia (according to Knacke-Loy, 1994; Knacke-Loy *et al.*, 1995); the geochemical data of the sediments of the Troad are well known and have also been used as comparative database in this work) and the Avşa Island, 69 sediment samples (cf. Appendices 2 and 6) have been collected from the surrounding of the archaeological sites and survey areas investigated in this work. In order to elaborate petrographic grouping and to define the chemical patterns of the geological samples (clays, silts, sands, etc.) and sherds, as well as the similarities between sherds and local sediments, multi-element X-ray fluorescence analysis has been carried out. Data are found in the the Appendices 6 and 7.

The chemical data will be discussed in two parts. As a first step the chemical properties of the sediments will be presented, followed by the discussion on the chemical patterns of the shreds as compared to the sediments.

The XRF-analysis provides lots of information about the elementary composition of the sediments of the different areas. In the first step several bivariate plots have been produced in order to find characteristic trends and differences between the investigated geological samples. After running all possible bivariate plots in order to distinguish areas characterised by their sediments, it has been established that the element pairs of the bivariate diagrams did not allow separating clearly different

sediments. In many cases the variation was bigger within an area characterised by their elementary composition, than between two different groups. Also overlaps in elementary composition made the identification of the different sedimentary groups and the chemical characterisation of the localities impossible.

To give an example of this phenomenon  $\text{SiO}_2$  vs.  $\text{Al}_2\text{O}_3$  plot is presented (Fig. 74). It is clearly visible that the  $\text{SiO}_2$  content of the, mostly fluviatile, sediments (Neogene to recent) in the Troad varies between 41.2 and 75.5 % (Knacke-Loy, 1994).

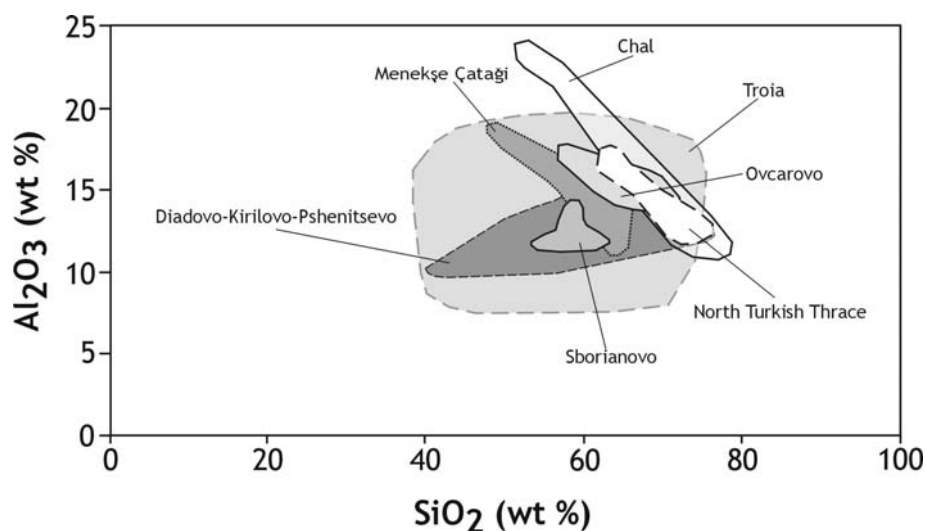


**Fig. 74  $\text{SiO}_2$  vs.  $\text{Al}_2\text{O}_3$  plot of sediment samples analysed in this study (Troian data after Knacke-Loy, 1994).**

In case of  $\text{Al}_2\text{O}_3$  these values are between 6.3 and 17.5 %. All other samples from Turkish Thrace and Bulgaria overlap with these values. This phenomenon is related to the type of samples. Because most samples are “mixed” fluviatile sediments (silty clays, sandy clays, etc.), silicon and alumina content of these materials are similar and differences within a group are caused by the poor grain size sorting (higher proportion of quartz/coarse fractions causes higher  $\text{SiO}_2$  values, clays with good grain size distribution have higher volume of alumina).

The only elements which provide more information about the chemical properties of the sediments and also show bigger differences between the single groups, are magnesium and chromium (proportion of mafic and/or ultramafic components in the material), although this type of classification also did not provide in all cases satisfactory results.

Because the bivariate plots did not prove to be a convenient tool to distinguish the samples, normalised multi-element diagrams have been used in order to find differences and characteristic properties between the localities and the samples.

In the following passage the chemical patterns of all areas will be presented in detail, with the exception of the Avşa Island, from where there was no possibility to collect geological samples. In a

first step MgO vs. Cr plots (the amount of mafic components in the samples; Fig. 75), followed by PAAS-normalised multi-element diagrams will be discussed.

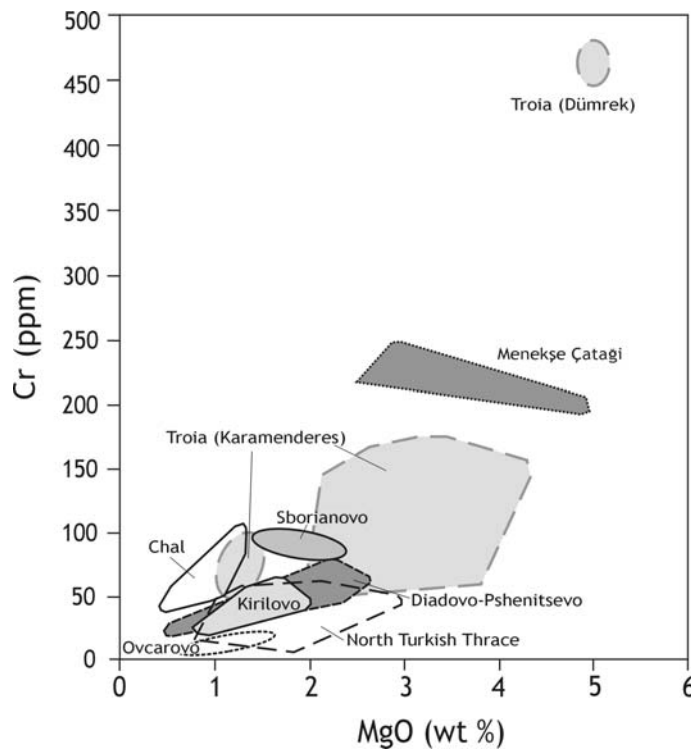


**Fig. 75 MgO vs. Cr plot of sediment samples analysed in this study. For detailed information cf. the description of the MgO vs. Cr plots of sediments (Troian data after Knacke-Loy, 1994).**

For a better distinction the PAAS-normalised multi-element diagrams of the sherds will be discussed in relation to the petrographic grouping. The first step is the discussion on main properties of the distribution of the elements in the groups, followed by the chemical features of all groups compared to the local sediment pattern (on the multi-element diagrams numbers (e.g. 4A/1) signify the petrographic (sub) groups or types of the sherds).

#### **6.2.1.1. Comparative sediments and the sherds from Troia**

##### *MgO vs. Cr diagrams of sediments*

As it has already been mentioned in the Chapter 5, the sediments of the Troad originated from two main rivers (Karamenderes and Dümrek) and from their drainage basins. Sandy sediments from Karamenderes flood plain show in their MgO concentration a variation between 0.9 and 1.6 %, and they range in their Cr values between 50 and 100 ppm. Fine-grained (clayey) sediments show higher MgO (from 1.9 to 4.2 %) and Cr (from 60 to 200 ppm) values. In contrast to relatively low magnesium and chromium content of the Karamenderes sediments, clayey deposits of the Dümrek show much higher MgO (4.8 to 4.9 %) as well as Cr (450 to 480 ppm) content (Fig. 77).

### *Multi-element diagrams of sediments*

According to Knacke-Loy (1994) chemical data of 16 samples have been chosen from the Karamenderes flood plain and from different layers of several boreholes near Troia. Based on geomorphologic studies (shallow drilling; Kayan, 1991, 1997) the sediment layers obtained were near to or on the surface in the Early Iron Age, thus they probably reflect the chemical composition of the fluvial sediments, which had lain on the surface at that time and were probably used as raw material for the locally produced Knobbed Ware and other ceramics. Furthermore the values of three clayey samples near the Dümrek have also been plotted (Fig. 76).

Different sediments from the Karamenderes flood plain and the boreholes show similar chemical behaviour (Fig. 76). The PAAS-normalised values of the incompatible and mobile elements in the different samples range in the following way: K, Rb, have slightly decreased values, Ba has averaged composition, Sr shows some positive anomaly. Elements from Nb to the compatible V show negative or slightly negative anomalous values. Thirteen from sixteen sediments have positive or slightly negative anomalies in their compatible elements Cr and Ni. Three sandy samples (K2, 4, and 6; cf. Appendix 2 and Knacke-Loy, 1994) show in their Cr and Ni composition values less than the standard mean.

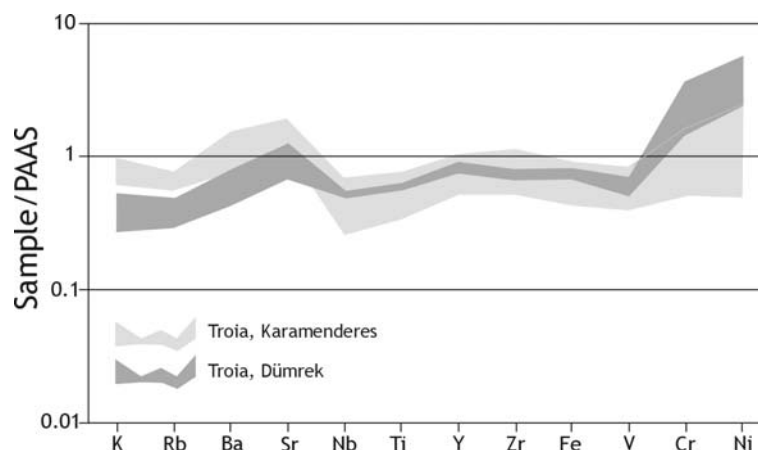


**Fig. 76 PAAS-normalised multi-element diagram of the Karamenderes and Dümrek sediments, Troia (data after Knacke-Loy, 1994).**

Together with these data chromium and nickel range between slight decreased and enriched Sediments from the Dümrek flood plain (Fig. 76) are similar in their chemical composition to the sediments of the Karamenderes, with the exception of the compatible immobile Cr and Ni. Mobile and incompatible elements like K, Rb, Ba, and Sr show some more negative anomalies than the sediments of the Karamenderes. Elements between Nb and Y have slightly increasing trend. Following elements (Zr, Fe, and V) are characterised with values near to the mean of the PAAS.

### *MgO vs. Cr diagrams of the sherds*

All Troian sherds, with the exception of five samples, have similar magnesium and chromium content to the sandy and clayey sediments of the river Karamenderes (Knacke-Loy, 1994). 10 samples (MgO: 1.0 to 1.5 %, Cr: 47 to 95 ppm) fall into the plot of sandy sediments, 4 (MgO: 2.6 to 2.8 %, Cr: 78 to 158 ppm) into the signal of the clays, and further 8 samples (MgO: 1.4 to 1.9 %, Cr: 65 to 132 ppm) show a bulk composition characteristic for the mixture between sandy and clayey sediments. The sherds Tr-2, 4, 20, 21, and 22 have also similar MgO (1.6 to 3.6 %) but significantly different chromium content (Tr-2: 308 ppm, Tr-4: 262 ppm, Tr-20: 256 ppm, Tr-21: 196 ppm and Tr-22: 471 ppm). Although the samples Tr-2, 4, 20, and 21 show no overlap, their chemical MgO vs. Cr composition are most similar to the composition of the sediments near Menekşe Çatağı (Fig. 75 and 77).

The MgO content of the sample Tr-22 is 1.5 % lower than the average composition of the Dümrek sediments, but their chromium composition is identical (Fig. 77).

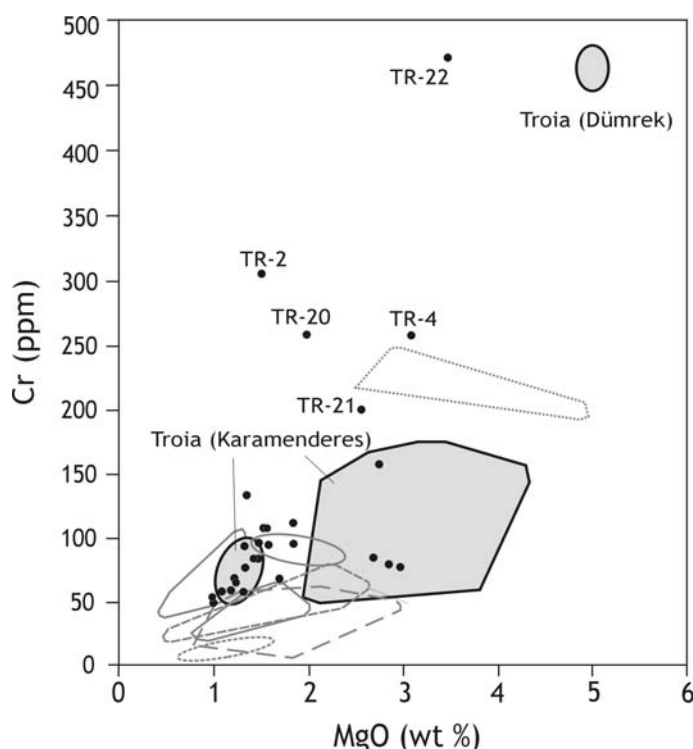


**Fig. 77 MgO vs. Cr plot of Troian sherds (black dots) and sediments (grey fields; Troian sediment data after Knacke-Loy, 1994).**

### *Multi-element diagrams of the sherds*

1A/1 (samples: Tr-1, 2, 3, 5, 13, 16, 19 and 27), 1A/2 (sample: Tr-24), 1A/3 (sample: Tr-20)

The PAAS-normalised major and trace elements show very similar distribution and progression in each sample (Fig. 78 and 79). With the exception of the elements Ba and Sr, which show some positive anomalies, negative or slightly negative trends can be obtained in case of all elements. The

samples Tr-2, 3, and 20 have also similar element patterns to the other sherds, but they show clear differences in their compatible element composition. Comparing the data to the Karamenderes signal (Fig. 78), with the exception of Rb and Ba in some sherds, good overlap and parallel progression can be seen between sediments and sherds found in Troia. Although the anomaly of the compatible element Cr is also reflected on the multi-element diagrams of the sherds TR-2 (Fig. 78) and 20 (Fig. 80), most elements have good progression with the local Karamenderes sediment signal.

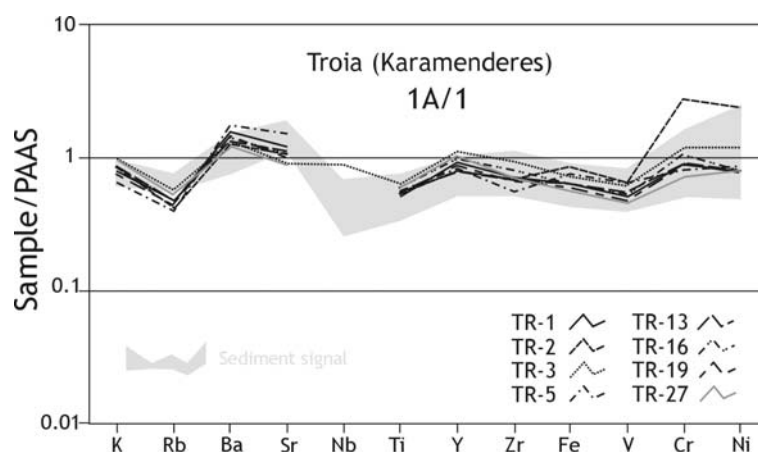


Fig. 78 PAAS-normalised values of the sherds of the petrographic type 1A/1 compared to the multi-element diagram of the Karamenderes sediments, Troia (sediment data after Knacke-Loy, 1994).

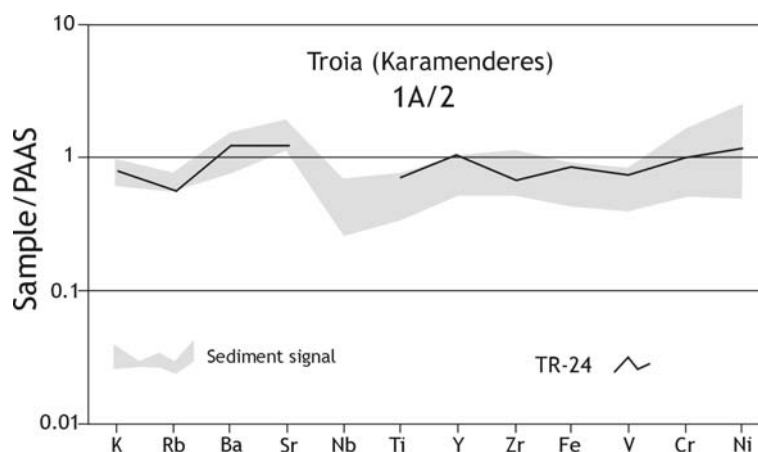
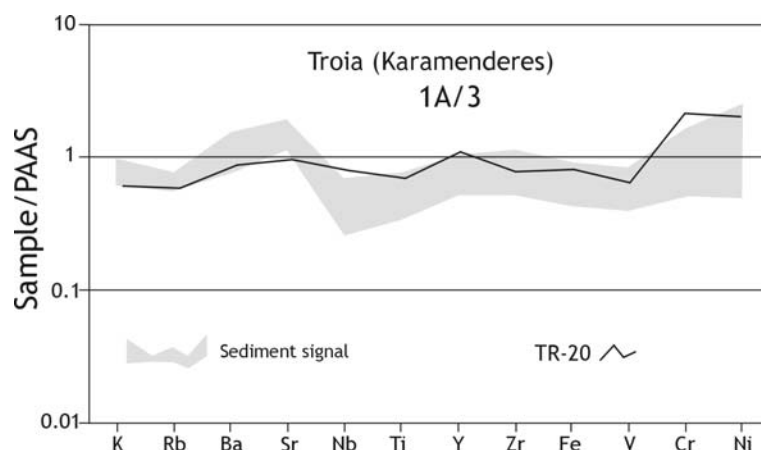


Fig. 79 PAAS-normalised values of the sherd of the petrographic type 1A/2 compared to the multi-element diagram of the Karamenderes sediments, Troia (sediment data after Knacke-Loy, 1994).



**Fig. 80** PAAS-normalised values of the sherd TR-20 (petrographic type 1A/3) compared to the multi-element diagram of the Karamenderes sediments, Troia (sediment data after Knacke-Loy, 1994).

1B/1 (samples: Tr-4, 11, 14, 15, 17, 21, 22, 23 and 25)

On the basis of the geochemical data two different types of archaeological material in this group have been distinguished. One (Tr-11, 14, 15, 17, 23, and 25) can be characterised by the values of the elements Fe, V, Cr, and Ni lower than the average, while the other one (Tr-4, 21, and 22) by positive anomalies in the elements iron, vanadium, chromium, and nickel, (Fig. 81) which is in good accordance with the differences obtained in their MgO and Cr content (cf. Fig. 77).

Other PAAS-normalised major and trace elements show similar distribution in each sample. Similar to the groups 1A/1 and 3 with the exception of the elements Ba and Sr, which show positive or no anomalies, negative anomalies or values similar to the average values can be obtained in the following elements: K, Rb, Nb, Ti, Y, and Zr.

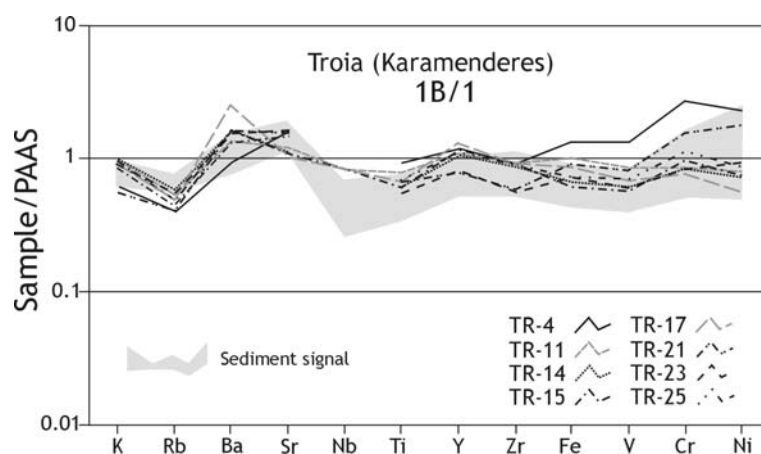


**Fig. 81** PAAS-normalised values of the sherds of the petrographic type 1B/1 compared to the multi-element diagram of the Karamenderes sediments, Troia (sediment data after Knacke-Loy, 1994).

Aside from the K and Rb data of some samples, the higher values of the Nb in all samples with lower Fe, V, Cr, and Ni values show good overlap with the Karamenderes signal (Fig. 81). The sample Tr-4 has clearly higher content of Fe, V, and Cr (Fig. 81). Due to the high Cr and Ni content the Tr-22 seem to derive from the Dümrek sediments (Fig. 82).

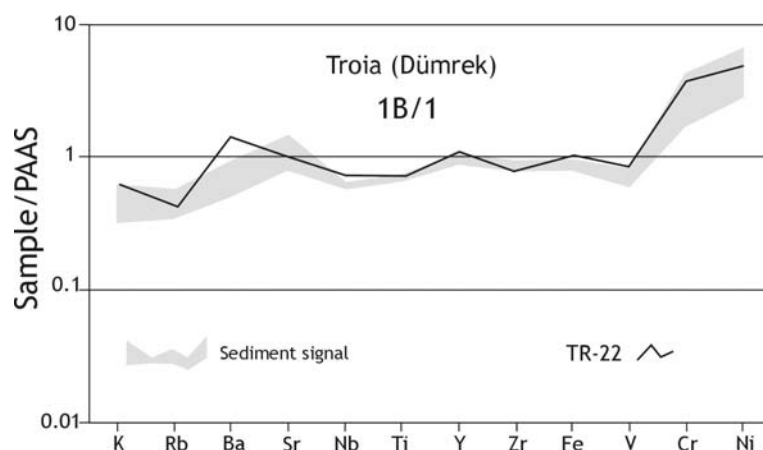


Fig. 82 PAAS-normalised values of the sherd TR-22 (petrographic type 1B/1) compared to the multi-element diagram of the Dümrek sediments, Troia (sediment data after Knacke-Loy, 1994).

1B/2 (samples: Tr-6, 7, 7a, 9, 10, 12, 18, 26 and 28)

Samples belonging to this group, with the exception of Tr-12, show very similar and typical chemical features (Fig. 83). The sample Tr-12 has lower Ba and Zr as well as clearly higher Fe, V, Cr, and Ni content, which can chemically clearly separate this sample from the others in the group. Although in case of most elements there is an overlap between the samples and the Karamenderes signal (Fig. 83), due to higher Nb, Y, and especially lower Cr and Ni values, only the samples Tr-9 and 26 show clear affinity to local raw materials. Multi-element diagram of the sample Tr-12 fits well to the Karamenderes signal in case of its all values. Comparing the values of the sherd TR-7 to the sample TR-7a (non-plastic inclusions separated from the same sample) it can be seen, that in case of most elements there is no or only infinitesimal difference.

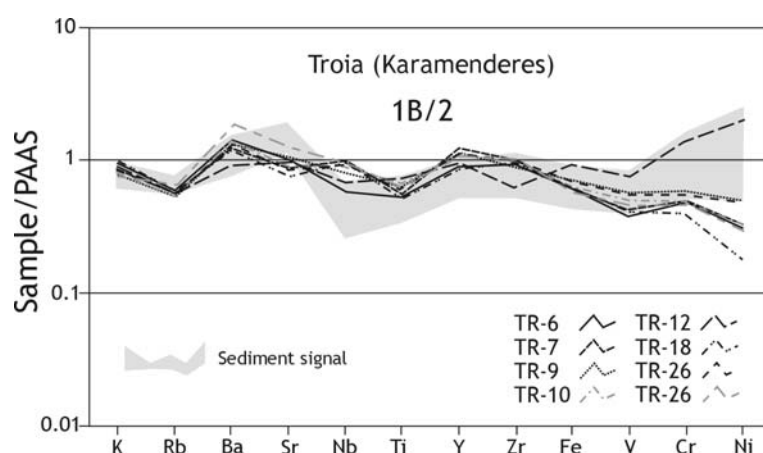
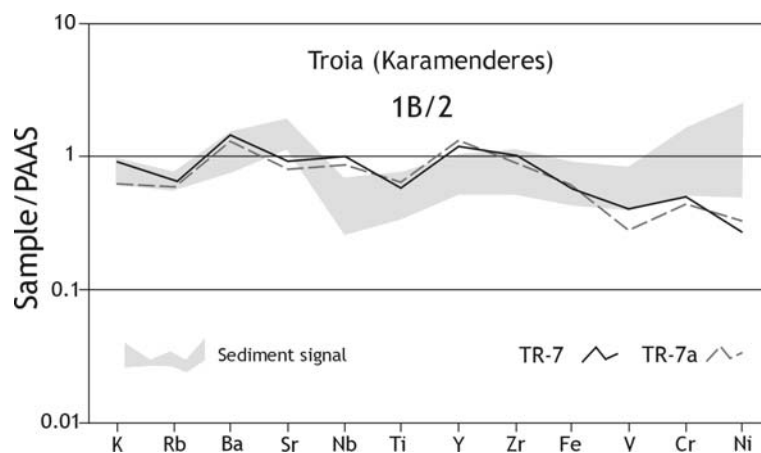


Fig. 83 PAAS-normalised values of the sherds of the petrographic type 1B/2 compared to the multi-element diagram of the Karamenderes sediments, Troia (sediment data after Knacke-Loy, 1994).

Observable differences are only in the following elements (in brackets first the values of the sample Tr-7, followed by TR-7a): K (0.9, 0.7), Sr (0.9, 0.8), Nb (1.0, 0.9), V (0.5, 0.3) and Ni (0.3, 0.4). In the

incompatible elements (K, Sr, and Nb) and in V slight decrease, in case of the compatible Ni slight increase can be observed (Fig. 84).



**Fig. 84** PAAS-normalised values of the sherds TR-7 and 7a (petrographic type 1B/2) compared to the multi-element diagram of the Karamenderes sediments, Troia (sediment data after Knacke-Loy, 1994).

#### 1C (sample: TR-8)

The sample TR-8 has similar PAAS-normalised data to the average values. The following elements have data similar to the standard: K, Sr, Nb, Y, Fe, and V. Rubidium, titanium, chromium, and nickel show lower, barium higher values than average. Considering the distribution of normalised elements, the sample seems to be in accordance with the Karamenderes signal; however Nb has higher value, than the local sediments (Fig. 85).

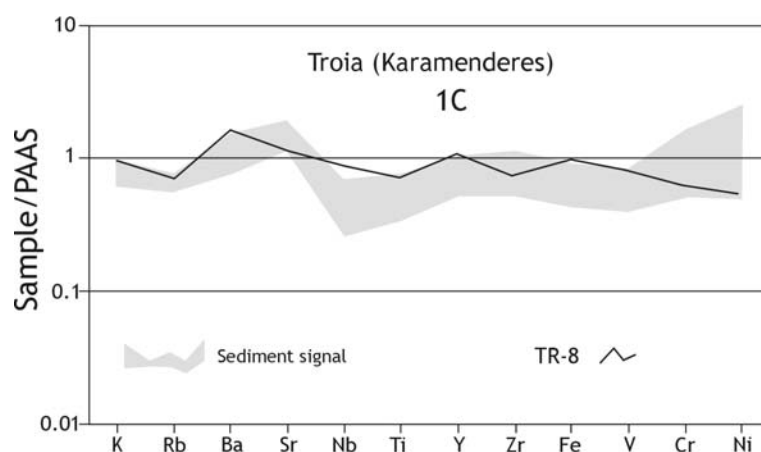


**Fig. 85** PAAS-normalised values of the sherd of the petrographic subgroup 1C compared to the multi-element diagram of the Karamenderes sediments, Troia (sediment data after Knacke-Loy, 1994).

### 6.2.1.2. Comparative sediments and the sherds from Menekşe Çatağı

#### *MgO vs. Cr diagrams of sediments*

Quaternary fluvial sediments near the archaeological site Menekşe Çatağı show higher magnesium and chromium (Fig. 75 and 87) content than the sediments of the river Karamenderes, but they contain lower amount of these elements than the Dümrek sediments. Values (Fig. 87) vary between 2.5 and 4.9 % (MgO) and 210 to 260 ppm (Cr).

#### *Multi-element diagrams of sediments*

Elements from K to Ti show slightly increased values in the clay samples from Menekşe Çatağı and its environment. Yttrium slightly enriches in all samples, but values are near to the average. Zirconium slightly depletes in all samples, but values are near to the average. Iron and vanadium range between slightly depleted and enriched values. Compatible Cr and Ni show enrichment in their data relative to the standard mean (Fig. 86).

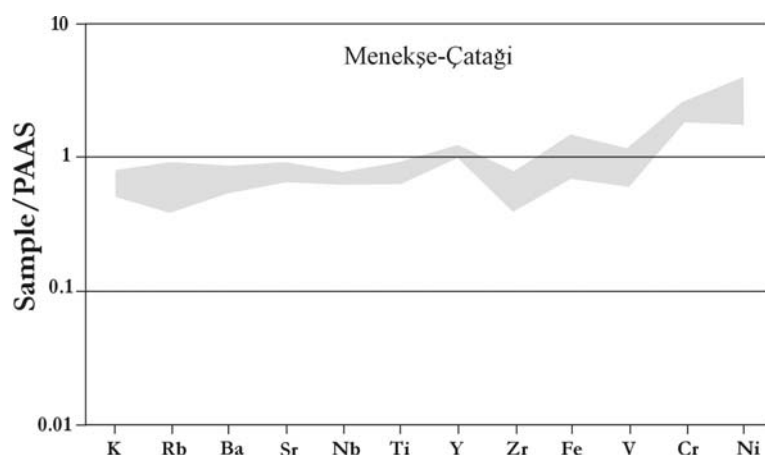


**Fig. 86 PAAS-normalised multi-element diagram of clayey sediments from Menekşe Çatağı.**

Further elements, like Zr, have slightly decreased values, iron and vanadium range between slightly depleted and enriched values. Compatible Cr and Ni show enrichment in their data relative to the standard mean (Fig. 86).

#### *MgO vs. Cr diagrams of the sherds*

Ceramics from Menekşe Çatağı can be grouped into two significantly different groups on the basis of their MgO and Cr content. The samples MCE-2, 3, 4, and 5 as well as the MCW-1, 3, 4, and 5 are signified with higher MgO (1.1 to 2.6 %) and Cr (178 to 298 ppm) content, while the other group (the samples MCE-1, MCW-1, and 2) shows similar magnesium values (0.9 to 1.9 %) but much lower chromium content (9 to 64 ppm; Fig. 87).

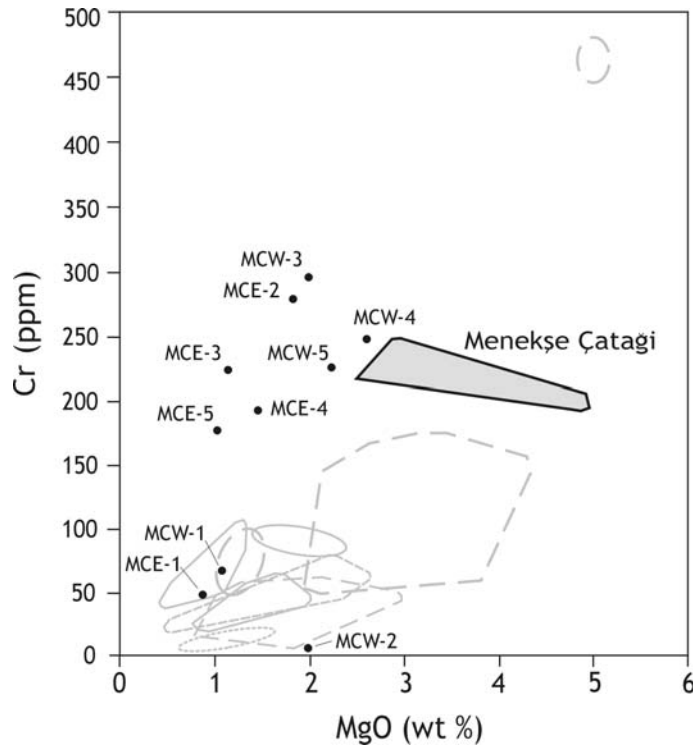


**Fig. 87 MgO vs. Cr plot of sherds (black dots) and sediments (grey field) from Menekşe Çatağı.**

Although there is no clear overlap between the sherds signified with higher Cr values and the sediments from Menekşe Çatağı, it is obvious that the chemical composition of these seven samples is very similar to the local raw materials. But as demonstrated above, four Troian Knobbed ware sherds also show very similar composition in the MgO vs. Cr plot. The samples MCE-1 and MCW-1 fall into the area of the sediments of Chal. The sherd MCW-2 shows clear similarity with the sediments from north Turkish Thrace (Fig. 87).

#### *Multi-element diagrams of the sherds*

3A/1 (samples: MCE-2, 3, 4, 5, MCW-1, 3, 4, and 5), 3A/2 (sample: MCW-2), 3B (sample: MCE-1)

Chemical data signify two different types of material among the sherds found in Menekşe Çatağı. One of them (MCE-2, 3, 4, 5, MCW-3, 4, and 5; Fig. 88) is characterised by high concentration of chromium and nickel, the other one (MCW-1, 2, and MCE-1; Fig. 88, 89, and 90) by the negative anomalies of these elements.

Other PAAS-normalised elements show similar distribution in each sample, with the exception of some smaller anomalies in the mobile trace elements. K and Rb show lower values than the average, Ba has values similar to the standard, Sr is presented in each sample, belonging to the group characterised by high Cr and Ni, under the average, but in case of the samples MCW-1, 2, and MCE-1 it is higher than the mean value. The values of Nb, Ti, Zr, Fe, and V are under the mean or they

approximate it. Yttrium is also signified by values near to the mean, but its values scatter less than by other elements (Fig. 88, 89, and 90).

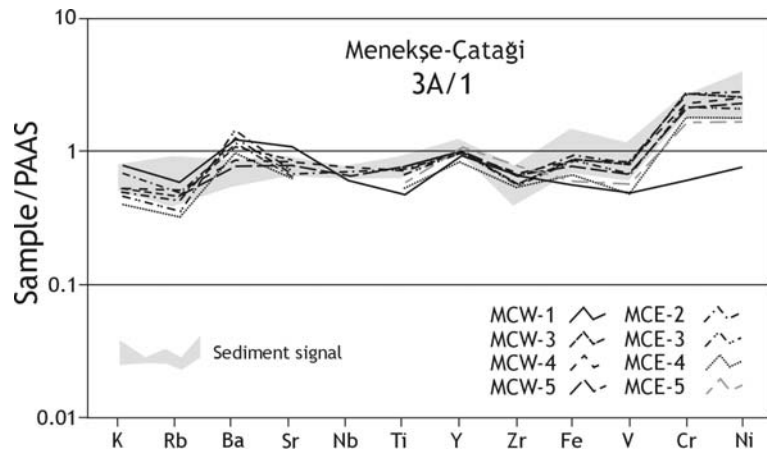


Fig. 88 PAAS-normalised values of the sherds of the petrographic type 3A/1 compared to the multi-element diagram of the sediment samples from Menekşe Çatağı.

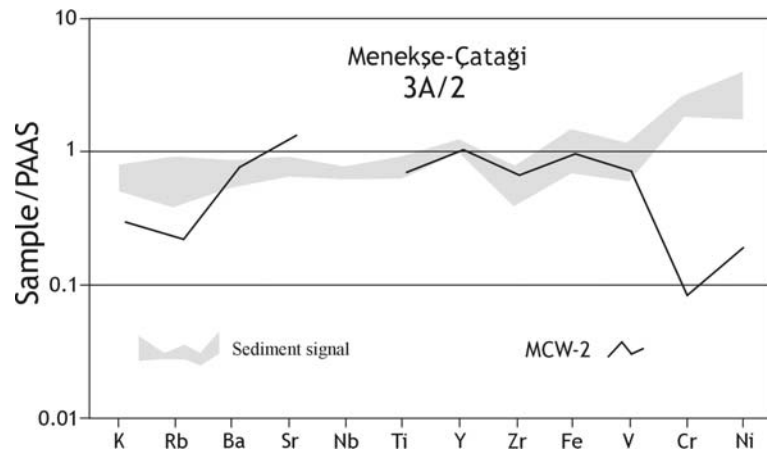


Fig. 89 PAAS-normalised values of the sherd of the petrographic type 3A/2 compared to the multi-element diagram of the sediment samples from Menekşe Çatağı.

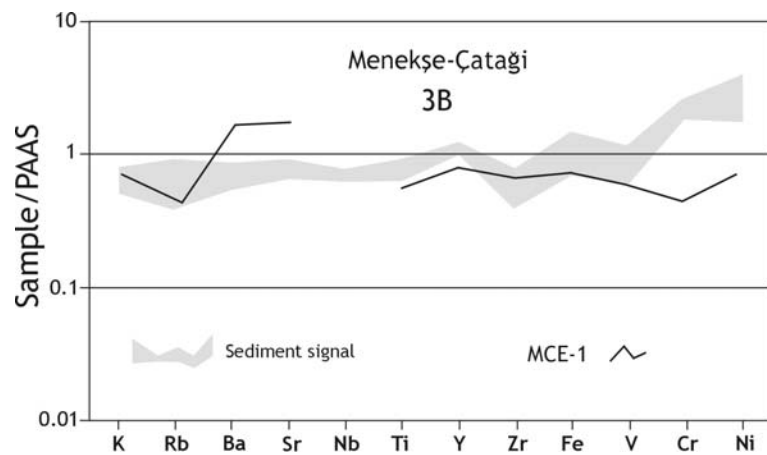


Fig. 90 PAAS-normalised values of the sherd of the petrographic subgroup 3B compared to the multi-element diagram of the sediment samples from Menekşe Çatağı.

The progression of the samples, characterised by high Cr and Ni values, shows good overlap with the local sediments of Menekşe Çatağı, although some samples have lower or higher values in their mobile elements like K, Rb, Ba, and Sr, and most samples have lower values of Ti, Fe, and V. The samples MCW-1, 2, and MCE-1 (Fig. 88, 89 and 90) show in their elementary composition (especially Cr and Ni) clear differences, which do not show affinity with the signal of the local sediments.

### 6.2.1.3. Comparative sediments and the sherds from north Turkish Thrace

#### *MgO vs. Cr diagrams of sediments*

The geological samples from the north-western part of Turkey (Turkish Thrace) show following values: MgO varies between 0.8 and 3 %, and chromium between 8 and 67 ppm (Fig. 75 and 92).

#### *Multi-element diagrams of sediments*

The PAAS-normalised multi-element diagram of the fluvial sediments (Fig. 91), collected from the piedmont region of north Turkish Thrace are the following: an increasing trend can be obtained in the values of the incompatible elements K, Rb, Ba, and Sr. Nb, Y, and Zr range between the depleted and slightly increased values; Ti shows slight decrease in all samples. More compatible (Fe, V, Cr, Ni) elements indicate clearly decrease in their values.

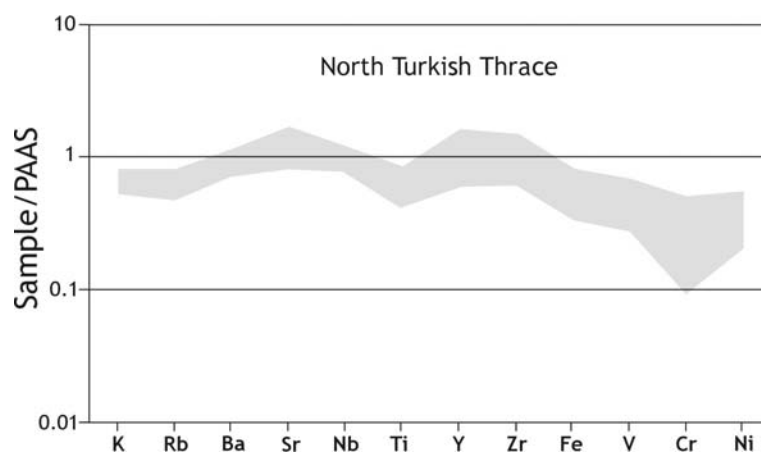


**Fig. 91 PAAS-normalised multi-element diagram of the sediment samples from north Turkish Thrace.**

#### *MgO vs. Cr diagrams of the sherds*

With the exception of the sample AT-2, all sherds from north Turkish Thrace show good overlap with the local sediments. MgO values vary between 0.8 and 1.6 %, Cr between 9 and 56 ppm. Most sherds also overlap with the chemical composition of other areas like Ovcarovo, Diadovo-Kirilovo. The sample AT-2 has significantly different MgO (4.3 %) and Cr (316 ppm) composition, which is not comparable with the composition of other samples found in this area (Fig. 92).

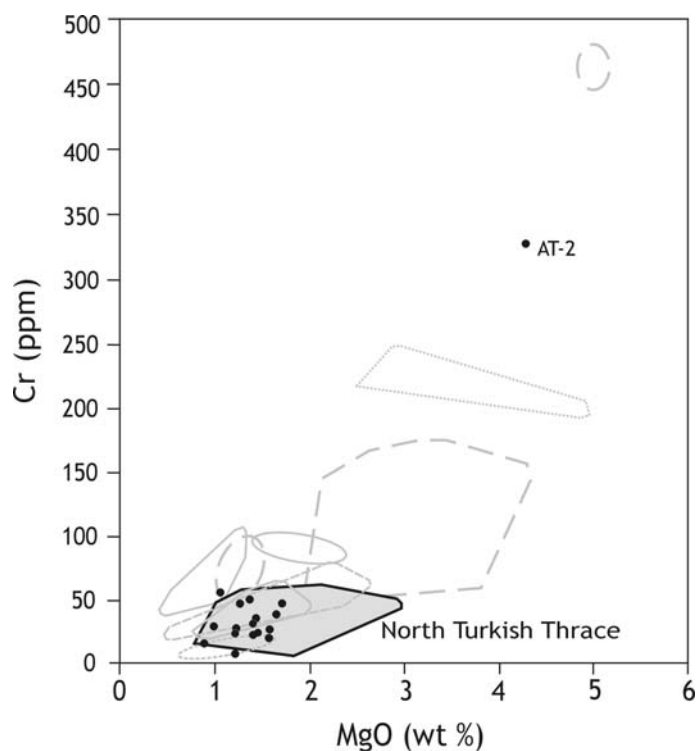


Fig. 92 MgO vs. Cr plot of sherds (black dots) and sediments (grey field) from north Turkish Thrace.

*Multi-element diagrams of the sherds*

4A/1 (samples: AK-1, 2, AT-1, CM-1, 2, 3, 4, DH-1, 2, 3, YK-1, 2, 3, 4, and 5), 4A/2 (sample: HM), 4B (sample: AT-2)

Although archaeological the samples from north Turkish Thrace have been classified into three petrographic groups, the types 4A/1 and 4A/2 seem to be chemically identical (Fig. 93 and 94).

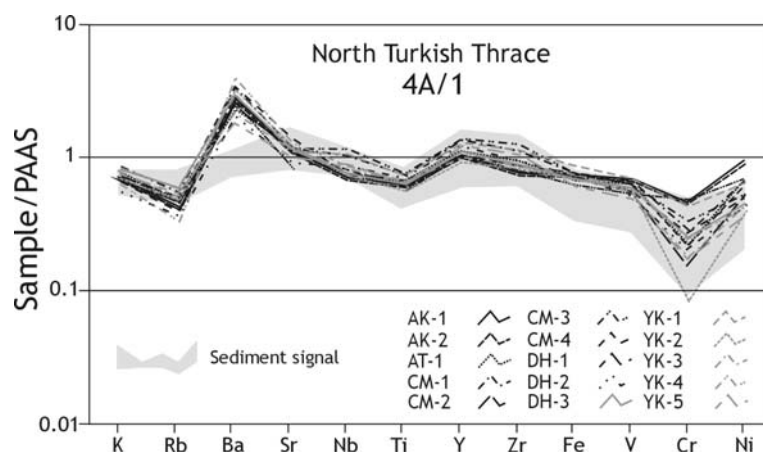
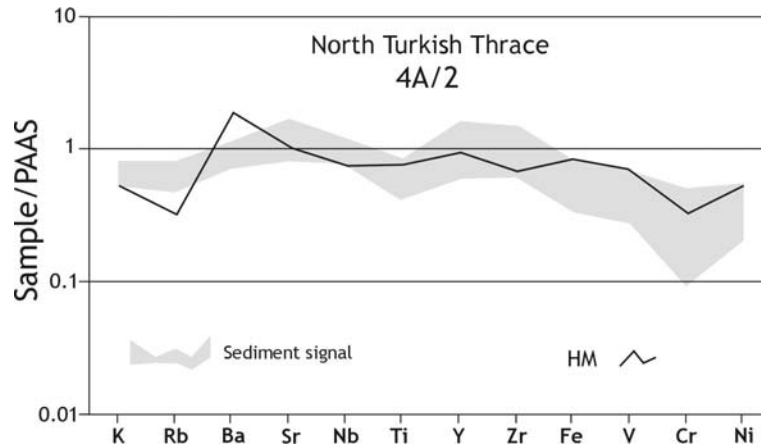


Fig.93 PAAS-normalised values of the sherds of the petrographic type 4A/1 compared to the multi-element diagram of the sediment samples from north Turkish Thrace.

The sample AT-2 shows petrographically as well as chemically totally different properties (Fig. 95). The main differences between the type 4A/1-2 and 4B are reflected in the compatible element content

of samples. While the samples in the types 4A/1 and 2 have low concentrations of compatible elements (Fe, V, Cr, Ni), the sample AT-2 has high concentrations of them. Apart from high positive Ba anomalies, the distribution and the progression of the elements in each sample in the types 4A/1 and 2 clearly overlap with the chemical patterns of the north Turkish Thracian sediments.



**Fig. 94** PAAS-normalised values of the sherd of the petrographic type 4A/2 compared to the multi-element diagram of the sediment samples from north Turkish Thrace.

Due to the high quantity of incompatible elements and the different progression of the chemical signal, the sample AT-2 does not overlap with the local sediment pattern, and shows no affinity with it (Fig. 95).

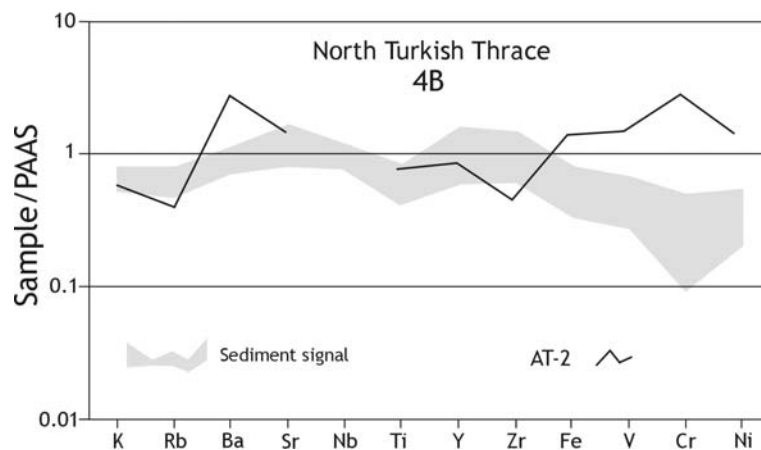


**Fig. 95** PAAS-normalised values of the sherd of the petrographic subgroup 4B compared to the multi-element diagram of the sediment samples from north Turkish Thrace.

#### 6.2.1.4. Comparative sediments and the sherds from Ovcarovo

##### *MgO vs. Cr diagrams of sediments*

Ovcarovo and its environment also belong to the north-western part of the Strandja Massive. Therefore it is not surprising, that magnesium and chromium values of this area are very similar to the results from north Turkish Thrace. Although MgO (0.7 to 1.5 %) and Cr (7 to 17 ppm) data are lower than values from the Turkish area of the Strandja Massive, significant overlap can be observed (Fig. 75 and 97).

##### *Multi-element diagrams of sediments*

Due to the very similar geological backgrounds, the chemical signals of the sediments from Ovcarovo (Fig. 96) are very similar to the main chemical properties of the materials from north Turkish Thrace (K, Rb, Ba, Sr, and Nb).

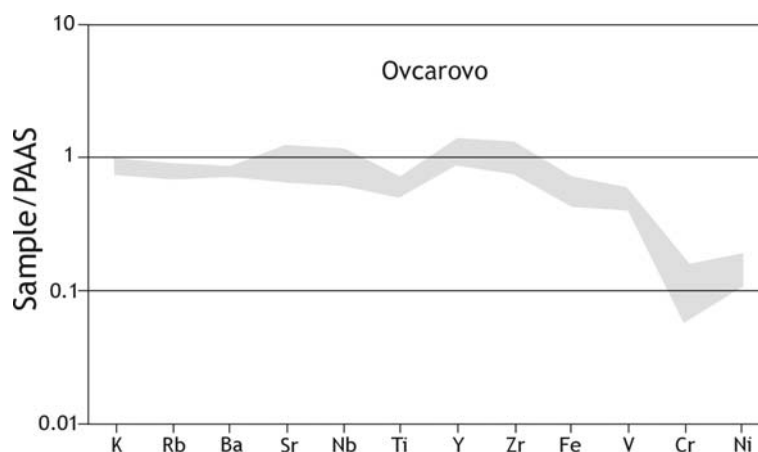


**Fig. 96 PAAS-normalised multi-element diagram of the sediment samples from Ovcarovo.**

Ti also indicates slightly negative anomaly like the samples from the Edirne (north Turkish Thrace) region. Yttrium and zirconium have average or higher than average values. The serial Fe, V, Cr, and Ni shows decreasing trend and the two most compatible elements also have lower values than samples from the Edirne region.

##### *MgO vs. Cr diagrams of the sherds*

Potteries from Ovcarovo can also be classified as two groups. The samples OVC-1, 2, and 3 have lower MgO (0.6 to 1.3 %) and Cr (13 to 28 ppm), others are signified with higher values (MgO: 0.9 to 1.57, Cr: 94 to 98 ppm).

The sherd OVC-1 fell into the area of the MgO and Cr composition characteristic for the local sediments, the samples OVC-2 and 3 overlap with the chemical data from central Bulgaria and north

Turkish Thrace. The sample OVC-5 fell into the Sborianovo (north Bulgaria) plot, the OVC-3 and 4 show similarities with the sediments from Chal (Fig. 97).

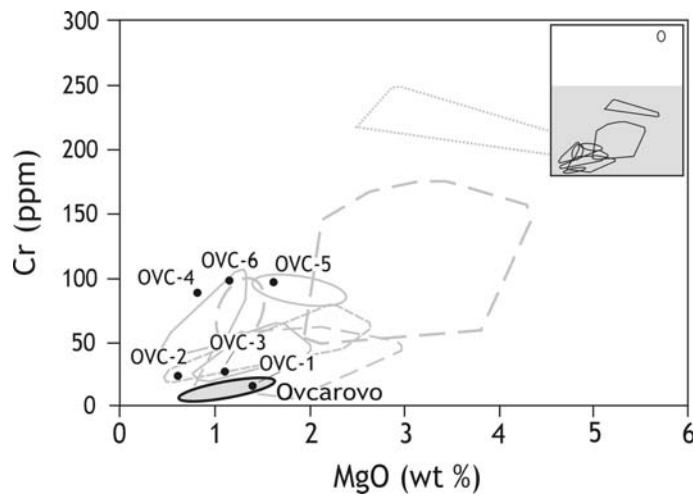


Fig. 97 MgO vs. Cr plot of the sherds (black dots) and sediments (grey field) from Ovcárovo.

### *Multi-element diagrams of the sherds*

#### 5A (Samples OVC-1, 2, and 3)

These three sherds, belonging to the petrographic subgroup 5A, have very similar chemical features. Each sample is characterised by values near to the mean, or slightly under it, positive Ba anomaly, and decreasing content of compatible elements with significant negative Cr anomaly. Although the values of Rb and Zr are slightly lower, Cr and Ni content is slightly higher than in the local sediments and there is a significant Ba anomaly in each sherd, the progression of the samples and the good overlap in most elements refer to affinity with the local raw materials and sediments (Fig. 98).

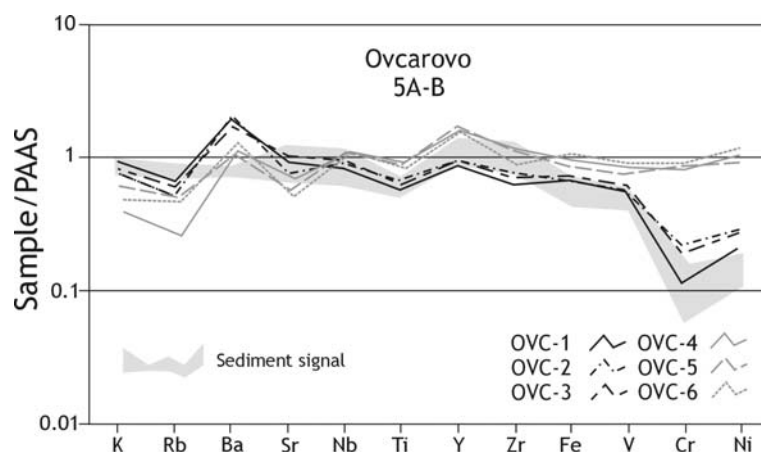


Fig. 98 PAAS-normalised values of the sherds of the petrographic subgroups 5A and B compared to the multi-element diagram of the sediment samples from Ovcárovo.

### 5B (Samples OVC-4, 5, and 6)

These 3 sherds, belonging to the petrographic subgroup 5B, have very different chemical features from the previous group containing the samples OVC-1, 2, and 3. Most elements do not fit the local sediment signal. Although Nb, Y, and Zr have similar values to that of the sediments, the lower content of the mobile (K, Rb, Sr) elements, the positive Ba anomaly and the clearly higher content of the compatible element series Fe, V, Cr, and Ni do not confirm the affinity between the chemical composition of the sherds and the possible local raw materials (Fig. 98).

#### 6.2.1.5. Comparative sediments and the sherds from Chal

##### *MgO vs. Cr diagrams of sediments*

The MgO content of the geological samples vary between 0.5 and 1.4 % and chromium ranges from 47 to 108 ppm. Although these values are not as high as the data from Troia or Menekşe Çatağı, they clearly show higher values than the data from the Strandja Massive (Fig. 75 and 100).

##### *Multi-element diagrams of sediments*

Chemical patterns of the sediments from Chal (Fig. 99) and its environment are similar to the chemical patterns of Ovcarovo, most elements, however, differ in wider range.

K, Rb, and Ba show values near to the average, most samples have in their Sr content slightly negative anomaly. Nb, Y, and Zr indicate average or increased values; titanium has in most samples negative anomaly. Fe, V, and Cr have similar but ranging under the mean values, Ni shows clearly negative anomaly.

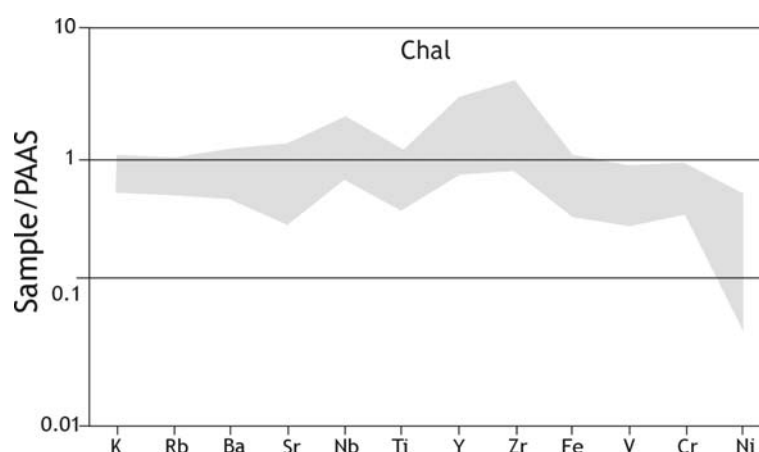


**Fig. 99 PAAS-normalised multi-element diagram of the sediment samples from Chal.**

##### *MgO vs. Cr diagrams of the sherds*

Five ceramics from the total of six show clear similarities with the sediments collected near the settlement (Fig. 100). They values vary between 0.8 and 1.2 % (MgO) and between 52 and 90 ppm

(Cr). The sherd CH-2 has higher magnesium (1.8 %) and chromium (92 ppm) content, thus it overlaps with the sediments of Sborianovo.

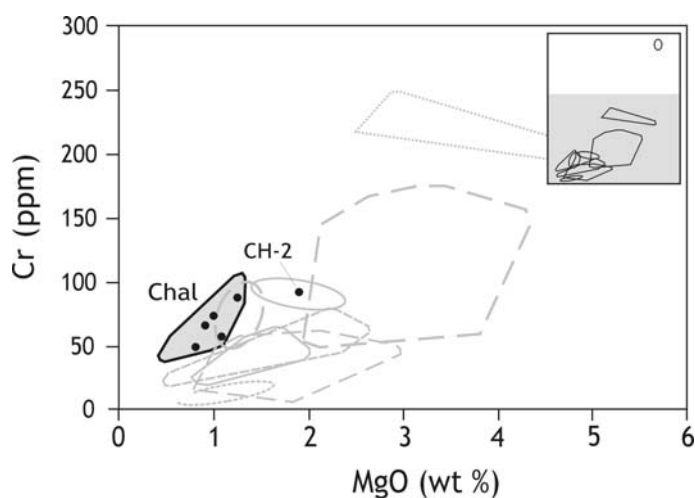


Fig. 100 MgO vs. Cr plot of sherds (black dots) and sediments (grey field) from Chal.

### *Multi-element diagrams of the sherds*

#### *Petrographic group 6; samples: CH-1, 2, 3, 4, 5, and 6)*

On the basis of the chemical composition, two different types of pottery can be distinguished in Chal. One of them (represented by the samples CH-1, 3, 4, 5, and 6) is characterised by the values of the elements K, Rb, Nb, Ti, Y, Zr, Fe, V, Cr, and Ni and the mobile elements, like Ba and Sr, which show values near to the average or slightly above on it.

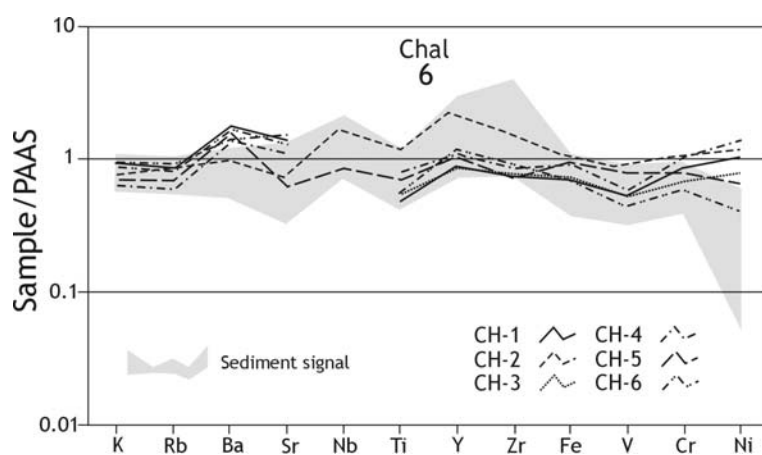


Fig. 101 PAAS-normalised values of the sherds of the petrographic group 6 compared to the multi-element diagram of the sediment samples from Chal.

The other group, including one sherd (CH-2), shows in the elements K, Rb, Ba, Sr, V, and Cr slightly negative anomalies, while other elements, like Nb, Ti, Y, Zr, and Fe show a distribution near to the mean or increase relative to the PAAS. Comparing the data from the archaeological material to the local sediments it can be clearly seen, that the progression of the chemistry of the sherds follows well

the chemistry of the local sediments and in any case they overlap with it. In the samples CH-1, 3, 4, 5, and 6 barium has higher values than in the sediments (Fig. 101).

### 6.2.1.6. Comparative sediments and the sherds from Diadovo-Pshenitsevo, and Kirilovo

#### *MgO vs. Cr diagrams of sediments*

Although Kirilovo lays about 25 km from Diadovo and Pshenitsevo, its MgO/Cr ratio is very similar to theirs. MgO ranges between 0.6 and 2.7 % (Diadovo-Pshenitsevo) and from 0.9 to 2.0 % (Kirilovo). Chromium content varies in case of sediments from Diadovo and Pshenitsevo between 25 and 76 ppm and in case of fluvial sediments from Kirilovo between 24 and 61 ppm (Fig. 75 and 103).

#### *Multi-element diagrams of sediments*

Multi-element diagrams from Diadovo-Pshenitsevo and Kirilovo are very similar, due to the fact that all three archaeological sites are situated near to each other, and the geological settings are also similar or the same, which had influenced the chemical composition of the sediments. Both diagrams show negative K, Rb, Nb, and Ti, positive Sr anomalies, as well as decreasing trend in the serial Y, Zr, Fe, V, Cr, and Ni (Fig. 102).

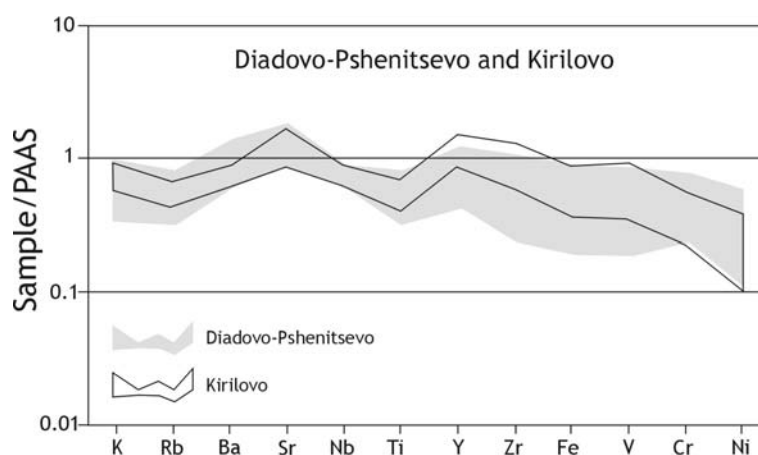


**Fig. 102 PAAS-normalised multi-element diagram of the sediment samples from Diadovo-Pshenitsevo and Kirilovo.**

#### *MgO vs. Cr diagrams of the sherds*

Sherds from these archaeological sites are discussed here because of the similar geological hinterland and petrographic similarities. The samples from Diadovo scatter between the values 0.8 and 2.8 % (MgO) and 1 and 2 ppm (Cr), thus only three sherds (DIA-8, 9, 10 and 11) fall into the area of local sediments from central Bulgaria. Other samples from Diadovo have on average higher values in MgO and overlap with the fields of other sediments from Bulgaria and Troia (Fig. 75 and 103).

The sherds from Pshenitsevo and Kirilovo clearly overlap with the local sediments. Their values are: Pshenitsevo: 1.2 to 1.5 % (MgO) and 26 and 36 ppm (Cr) and Kirilovo: 1.2 to 1.3 % (MgO) and 32 and 46 ppm (Cr; Fig. 103).

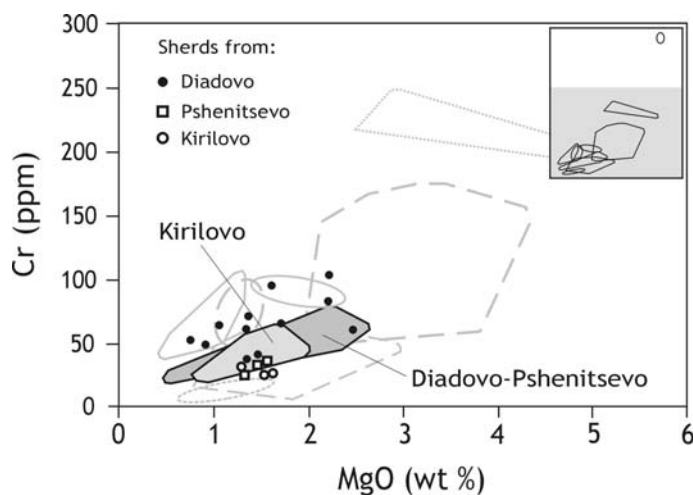


Fig. 103 MgO vs. Cr plot of the sherds and sediments from Diadovo-Pshenitsevo (dark grey field) and Kirilovo (grey field).

#### *Multi-element diagrams of the sherds*

7A/1 (samples: KIR-1, 2, 3, PSH-1, 2, 3, DIA, 1, 2, 5, 7, 8, 10, and 11), 7A/2 (samples: DIA-3, 4, 6, 9, 12, 13)

Although the samples from Kirilovo belong to the petrographic type 7A/1, due to the differences in their chemical features they are discussed separately from other samples in the group. The samples KIR-1 and 2 have almost identical chemical composition. In the samples KIR-1 and 2 the elements Rb, Zr, Cr, and Ni indicate negative anomalies, K, Ti, Ba, and Y are similar to the mean Sr, Fe, and V show some positive anomalies. The progression of the elements in KIR-3 is similar to the two other sherds, but it has in some elements higher, in others lower values.

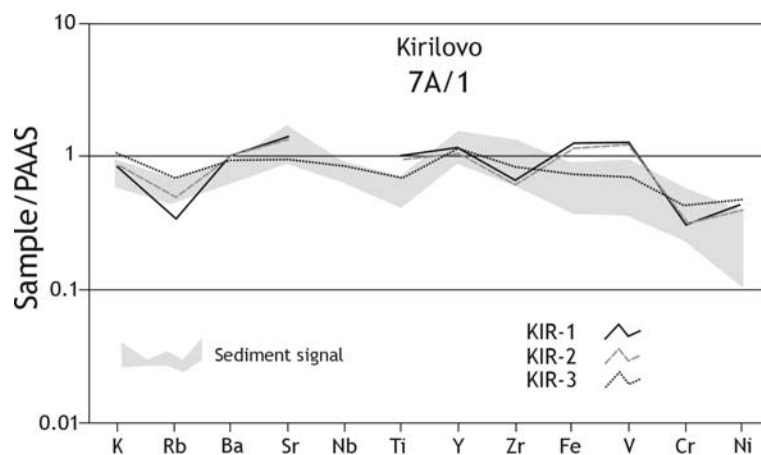


Fig. 104 PAAS-normalised values of the sherds from Kirilovo (petrographic type 7A/1) compared to the multi-element diagram of the sediment samples from Kirilovo.

The sample KIR-3 fits well into the local sediment pattern of Kirilovo, and the distribution of the elements also follows the pattern. The samples KIR-1 and 2 also show similarities with the local sediments, although in case of Ti, Fe, and V they have higher values, than observed in the sediments (Fig. 104).

Sherds found in Pshenitsevo and Diadovo can be also divided into two types on the basis of their chemical properties. Although samples equal or are similar in most elements, positive Ba and Sr as well as prominent negative chromium anomaly distinguish the samples from Pshenitsevo from the others (Fig. 105).

Other samples (DIA, 1, 2, 5, 7, 8, 10, and 11) have also very similar values to each other, characterised by slightly decreasing values from Y to Ni and more prominent negative anomalies of rubidium and titanium.

Comparing the data with the local sediments from Diadovo and Pshenitsevo a good overlap can be seen, even though in few samples Ba and Sr have more positive or negative values (Fig. 105).

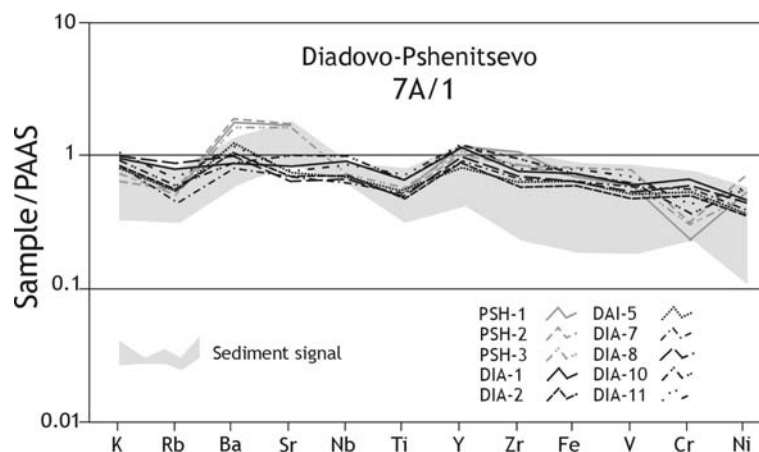


**Fig. 105** PAAS-normalised values of the sherds from Diadovo and Pshenitsevo (petrographic type 7A/1) compared to the multi-element diagram of the sediment samples from Diadovo-Pshenitsevo.

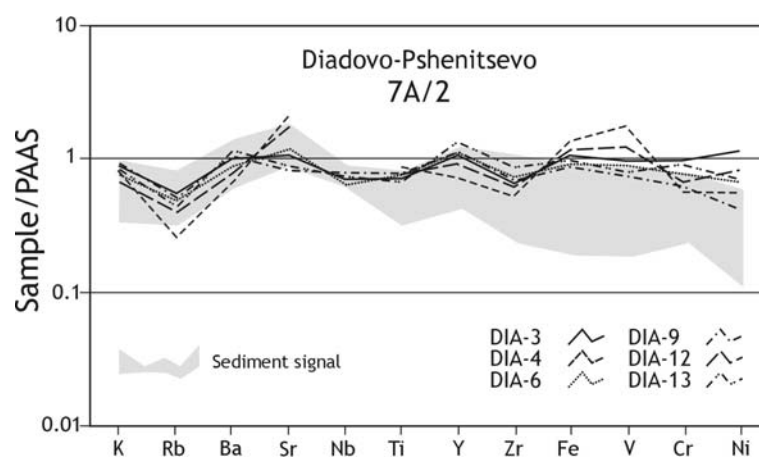


**Fig. 106** PAAS-normalised values of the sherds from Diadovo (petrographic type 7A/2) compared to the multi-element diagram of the sediment samples from Diadovo-Pshenitsevo.

In the petrographic type 7A/2 two different signals can also be distinguished (Fig. 106). The samples DIA-4 and 12 form the one, DIA-3, 6, 9, and 13 – the other signal. DIA- 4 and 12 can be characterised by low amount of Rb, Zr, Cr and Ni and higher amount of Sr, Fe, and V. Other elements are little under the values of the standard: K, Ba, Ti, and Y. The remaining samples have negative Rb anomalies, other elements scatter at the mean. Although there is an overlap between the chemical signal of the local sediments and the chemical pattern of the archaeological samples, higher Fe and V in the samples DIA-4 and 12 as well as higher Cr and Ni values in the samples DIA-3 and 13 do not fit completely the local reference materials (Fig.106).

### 6.2.1.7. Comparative sediments and the sherds from Sborianovo

#### *MgO vs. Cr diagrams of sediments*

Fine-grained (mostly clayey) sediments from Sborianovo show relatively higher MgO (1.4 to 2.2 %) and Cr (85 to 100 ppm) content than other Bulgarian samples (Fig. 75, 108).

#### *Multi-element diagrams of sediments*

Clayey river sediments and samples from terrestrial clay deposits show a unique pattern in northeast Bulgaria (Fig. 107).

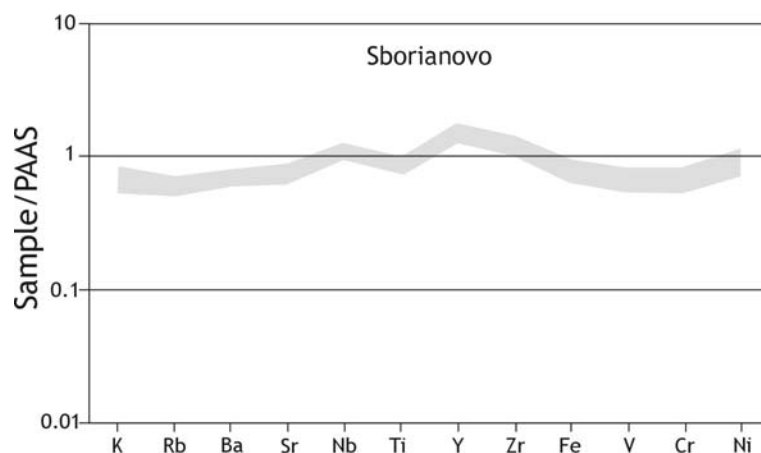


**Fig. 107 PAAS-normalised multi-element diagram of the sediment samples from Sborianovo.**

It has already been mentioned that this group is the most homogenous of all areas studied in this work. Incompatible and mobile elements (K, Rb, Ba, and Sr) indicate similar values and low variation. Niobium has average, Ti slightly negative, Zr and Y – (slightly) positive values. Compatible elements like Fe, V, Cr, and Ni show slight decrease relative to the average values in their amount.

#### *MgO vs. Cr diagrams of the sherds*

Pottery fragments found in Sborianovo show in their chromium values (79 to 91 ppm) similarities to the local sediments, but Mg content has larger variability (0.7 to 1.6 %). Therefore only the sample

SBO-3 overlaps clearly with the chemical patterns of the local sediments. The samples SBO-1 and 2 do not fit in this field (Fig. 108).

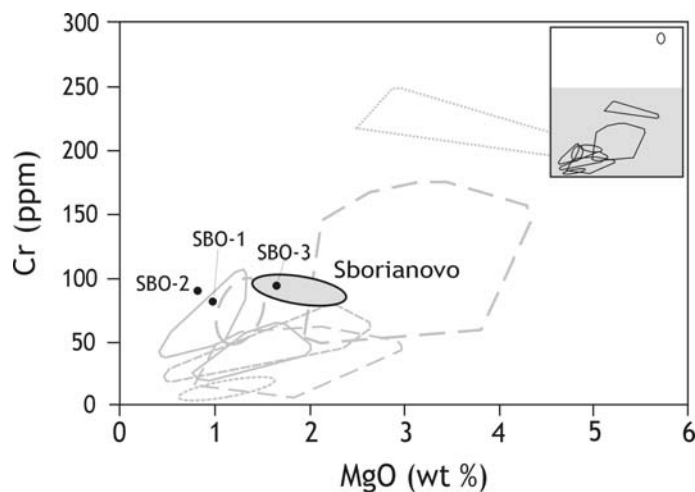


**Fig.108 MgO vs. Cr plot of sherds (black dots) and sediments (grey field) from Sborianovo.**

*Multi-element diagrams of the sherds*

*8 (samples: SBO-1, 2, and 3)*

The common chemical features are: clearly negative K and slightly negative Sr anomalies, positive Y anomalies, and values near to the main of the other elements. Comparing all these data to the local sediment signals of Sborianovo, good similarity can be found between the sherds and clayey sediments. There is some difference in the mobile elements of some samples, but the well fitting elements refer to the affinities with the raw materials (Fig. 109).

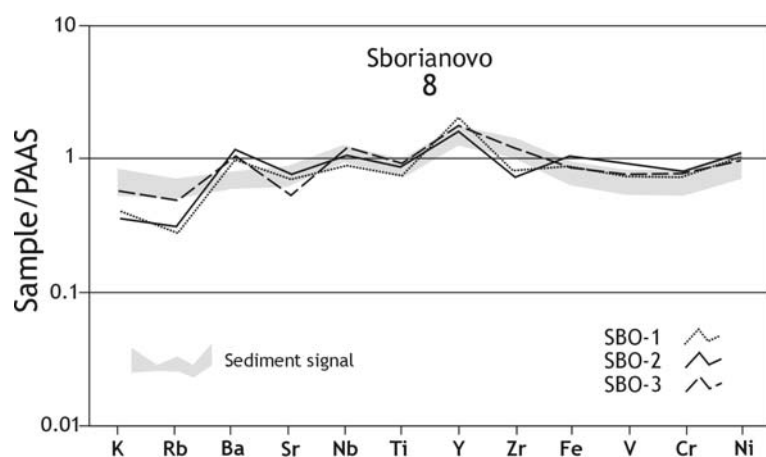


**Fig. 109 PAAS-normalised values of the sherds (petrographic group 8) compared to the multi-element diagram of the sediment samples from Sborianovo.**

### 6.2.2. Radiogenic isotopes

The combined use of petrographic and chemical analyses has demonstrated that most pottery groups can be distinguished. However, in several cases, overlaps were found in the petrographic and chemical composition of the archaeological materials found in different areas. The use of radiogenic isotopes of Sr and Nd as tracers proved to be a powerful method in the separation and classification of fine wares and different clayey materials (Knacke-Loy, 1994).

The aim of the radiogenic isotope analysis was to characterise the Thracian, south, central, and northeast Bulgarian clayey sediments and ceramics, and to compare their values to the Troian signal, in order to determine the isotopic composition of sherds whose origin was not unambiguously clear on the basis of their petrographic and XRF analyses. Furthermore I wanted to get more information about the phenomenon and the influence of the so-called tempering effect (cf. Chapter 7).

To determine the radiogenic isotope signal of an area clayey-silty sediments and locally produced sherds were chosen. The criterion in the assortment of the sediments was the average chemical composition within the place of find. This was determined on the basis of the XRF-analyses and the PAAS-normalised classification.

In several cases, already the combined use of petrographic and chemical analyses allowed deciding, whether the sherd in question is locally produced, or not. In that case, the sherd which was likely or certainly locally produced, together with the local sediments, used for determining the isotopic signal of the area.

To investigate the role of the non-plastic inclusions in influencing the isotopic composition, a sherd (*E9.153.1*) from Troia was chosen; its radiogenic isotope composition has already been investigated in a former study (Guzowska *et al.*, 2001).

Considering the above mentioned factors, 7 geological (clays, silty-clays) and 13 archaeological samples were measured. The data are presented in the Appendix 8.

#### 6.2.2.1. Troia

The radiogenic isotope composition of the Troian sediments (clays, and silty clays of the Karamenderes river and its deposits) were well prepared in the Knacke-Loy's study (1994). Sediments vary between 0.708236 and 0.70925 ( $^{87}\text{Sr}/^{86}\text{Sr}$ ) and 0.512359 to 0.512446 ( $^{143}\text{Nd}/^{144}\text{Nd}$ ). The isotopic composition of two sherds was measured. Due to the ambiguous petrographic results the sherds TR-8 and 20 were analysed. The results ( $^{87}\text{Sr}/^{86}\text{Sr}$ : 0.708733,  $^{143}\text{Nd}/^{144}\text{Nd}$ : 0.51236) show that the sample TR-8 fits well into the Troian isotopic signal. The sherd TR-20 has the following isotopic composition: 0.710325 ( $^{87}\text{Sr}/^{86}\text{Sr}$ ) and 0.512319 ( $^{143}\text{Nd}/^{144}\text{Nd}$ ). These data put the sample between the isotopic fields of Troia and Menekşe Çataği, furthermore it overlaps with the isotopic field of the materials from Chal (Fig. 110).

On the basis of the NAA and radiogenic isotope investigations of the Knobbed ware sherd *E9.153.1* in the study of Guzowska *et al.* (2003), the sample was described as an import. After the microscopic analysis (cf. 6.1.1.1.1.) of the sample, which contained plenty of volcanic rock fragments, it has been suggested, that the isotopic composition of the raw material (clay, clayey sediment) was influenced by the non-plastic inclusions. Therefore volcanic clasts were separated under a binocular microscope (cf. Chapter 4) and only the fine-grained matrix was measured. Further analyses (Guzowska *et al.*, 2003) established the following isotopic composition: 0.707928 ( $^{87}\text{Sr}/^{86}\text{Sr}$ ), 0.512515 ( $^{143}\text{Nd}/^{144}\text{Nd}$ ). My data show lower values in  $^{87}\text{Sr}/^{86}\text{Sr}$  (0.707823) and also lower values in  $^{143}\text{Nd}/^{144}\text{Nd}$  (0.512478). However, after separating the volcanic clast from the clayey matrix, no unambiguous overlap occurred with the Troian sediments, the isotopic composition of the sherd shows more similarity with the local raw materials.

After plotting the data onto the  $\epsilon_{\text{Nd}}$  vs  $^{87}\text{Sr}/^{86}\text{Sr}$  diagram it can be clearly demonstrated, that all data situate between the  $\epsilon_{\text{Nd}}$  values -2 and -5.8 (Fig. 110).

#### 6.2.2.2. Menekşe Çatağı

Two clayey sediment samples and 4 sherds were investigated from Menekşe Çatağı. The sediment samples Mc-1 and 5 and the sherd MCE-4 show the locally sediment pattern. The values range from 0.710605 to 0.712515 ( $^{87}\text{Sr}/^{86}\text{Sr}$ ) and from 0.512359 to 0.512250 ( $^{143}\text{Nd}/^{144}\text{Nd}$ ).  $\epsilon_{\text{Nd}}$  values vary between -7 and -8. The sherd MCW-1 has similar values: 0.710775 ( $^{87}\text{Sr}/^{86}\text{Sr}$ ) and 0.512223 ( $^{143}\text{Nd}/^{144}\text{Nd}$ ). Two other sherds show different values. The MCE-1 has similar  $^{143}\text{Nd}/^{144}\text{Nd}$  ratio to the local materials (0.512232), but much lower  $^{87}\text{Sr}/^{86}\text{Sr}$  (0.707333) values. The sample MCW-2 is characterised by the lowest  $^{87}\text{Sr}/^{86}\text{Sr}$  (0.706485), and the highest  $^{143}\text{Nd}/^{144}\text{Nd}$  (0.512656) values ( $\epsilon_{\text{Nd}} = +0.4$ ), which clearly refers to the different source of the raw material (Fig. 110).

#### 6.2.2.3. North Turkish Thrace

Due to the very similar petrographic and bulk chemical properties of the geological and archaeological samples collected near Edirne, one sediment sample (Ntt-7) and one sherd (CM-2) were analysed. The values of the two materials are very similar to each other ( $^{87}\text{Sr}/^{86}\text{Sr}_{\text{sediment}} = 0.711782$ ,  $^{87}\text{Sr}/^{86}\text{Sr}_{\text{sherd}} = 0.711962$  and  $^{143}\text{Nd}/^{144}\text{Nd}_{\text{sediment}} = 0.512238$ ,  $^{143}\text{Nd}/^{144}\text{Nd}_{\text{sherd}} = 0.51221$ ).  $\epsilon_{\text{Nd}}$  values are found around -8 (Fig. 110).

#### 6.2.2.4. Chal

One silty sediment sample and three sherds (CH-2, 3, and 5) were investigated from the south Bulgaria. Although on the basis of the petrographic and XRF data the sherds seemed to be, with high probability, locally produced, in their isotopic composition relatively big range can be obtained. The

pottery fragments CH-2 and 3 have the lowest  $^{87}\text{Sr}/^{86}\text{Sr}$  values within the group (0.709014 and 0.708605, respectively;  $^{143}\text{Nd}/^{144}\text{Nd}$  values are: 0.51227 and 0.512327, respectively). The sediment sample Ch-4 and the sherd CH-5 have the following values:  $^{87}\text{Sr}/^{86}\text{Sr}_{\text{sediment}} = 0.71063$ ,  $^{143}\text{Nd}/^{144}\text{Nd}_{\text{sediment}} = 0.512317$  and  $^{87}\text{Sr}/^{86}\text{Sr}_{\text{sherd}} = 0.711878$ ,  $^{143}\text{Nd}/^{144}\text{Nd}_{\text{sherd}} = 0.512252$ .  $\epsilon_{\text{Nd}}$  values range between -6 and -8 (Fig. 110).

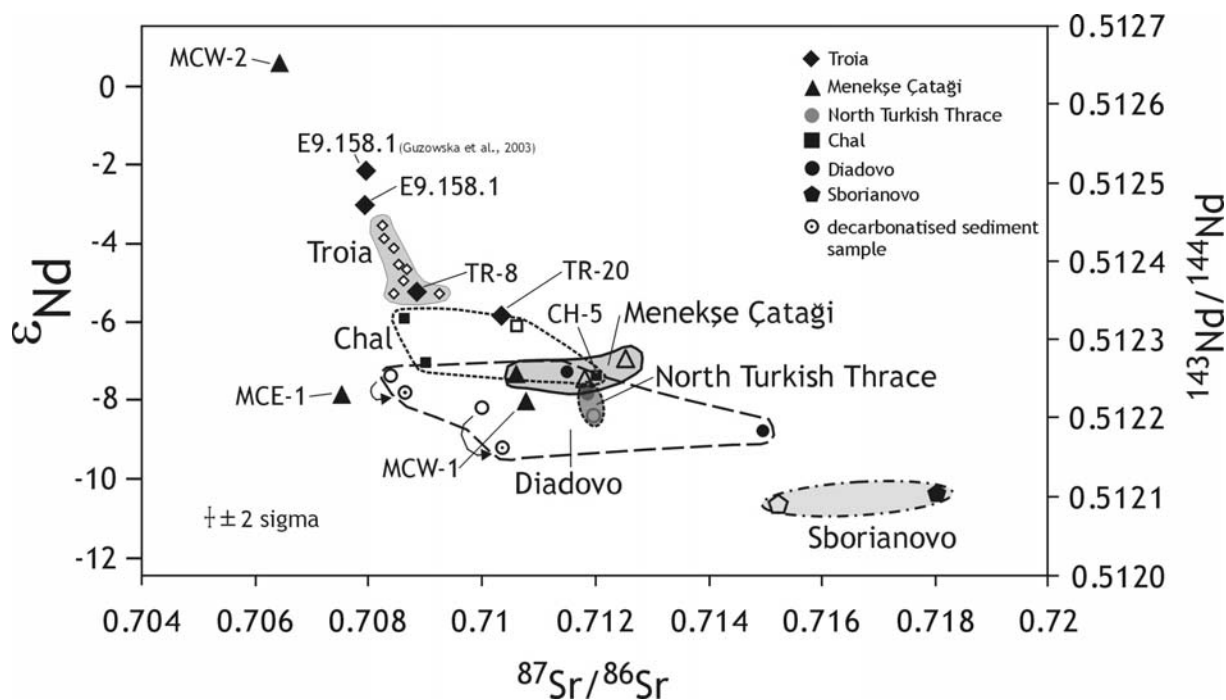


Fig. 110  $^{87}\text{Sr}/^{86}\text{Sr}$  vs.  $^{143}\text{Nd}/^{144}\text{Nd}$  ( $\epsilon_{\text{Nd}}$ ) plot of sediments (empty symbols) and sherds (full symbols; sediment data after Knacke-Loy, 1994).

### 6.2.2.5. Diadovo-Pshenitsevo

The sediments collected near Diadovo and Pshenitsevo show the following isotopic values:  $^{87}\text{Sr}/^{86}\text{Sr} = 0.708422$  and  $0.709995$  and  $^{143}\text{Nd}/^{144}\text{Nd} = 0.512255$  and  $0.512212$ . The isotopic composition of the pottery fragments DIA-1 and 9 are:  $^{87}\text{Sr}/^{86}\text{Sr} = 0.714891$  and  $0.711475$ , respectively, as well as  $^{143}\text{Nd}/^{144}\text{Nd} = 0.512183$  and  $0.512261$ , respectively.  $\epsilon_{\text{Nd}}$  values vary between -9.5 and -7.5. The question whether the big difference in the  $^{87}\text{Sr}/^{86}\text{Sr}$  ratios of the geological and archaeological samples has been influenced by the presence of secondary  $\text{CaCO}_3$  in the clayey sediments, which could influence the low  $^{87}\text{Sr}/^{86}\text{Sr}$  ratios in the sediments, was also analysed in the following way: First the carbonate content of the sediment samples has been measured, which was 15-20 wt %, respectively. After decarbonatisation of the samples (the sherds were carbonate free) new isotopic measurement was carried out. The data show ( $^{87}\text{Sr}/^{86}\text{Sr} = 0.708642$ ,  $0.710333$ , respectively, and  $^{143}\text{Nd}/^{144}\text{Nd} = 0.512232$ ,  $0.512161$ , respectively; Fig. 110), that secondary carbonate did not influence strongly the ratios of the Sr isotopes (cf. arrows in Fig. 110), moreover the Nd isotopic composition of the samples changed more significantly (Fig. 110).

### 6.2.2.6. Sborianovo

The sherd SBO-3 and a clay sample Sbo-6 were investigated from Sborianovo. The values are:  $^{87}\text{Sr}/^{86}\text{Sr}_{\text{sediment}} = 0.715209$ ,  $^{143}\text{Nd}/^{144}\text{Nd}_{\text{sediment}} = 0.512098$  and  $^{87}\text{Sr}/^{86}\text{Sr}_{\text{sherd}} = 0.718055$ ,  $^{143}\text{Nd}/^{144}\text{Nd}_{\text{sherd}} = 0.512103$ . The Nd isotopic composition is very similar, but in the values of the  $^{87}\text{Sr}/^{86}\text{Sr}$  values wider range can be seen.  $\epsilon_{\text{Nd}}$  value is around -10.5 (Fig. 110).

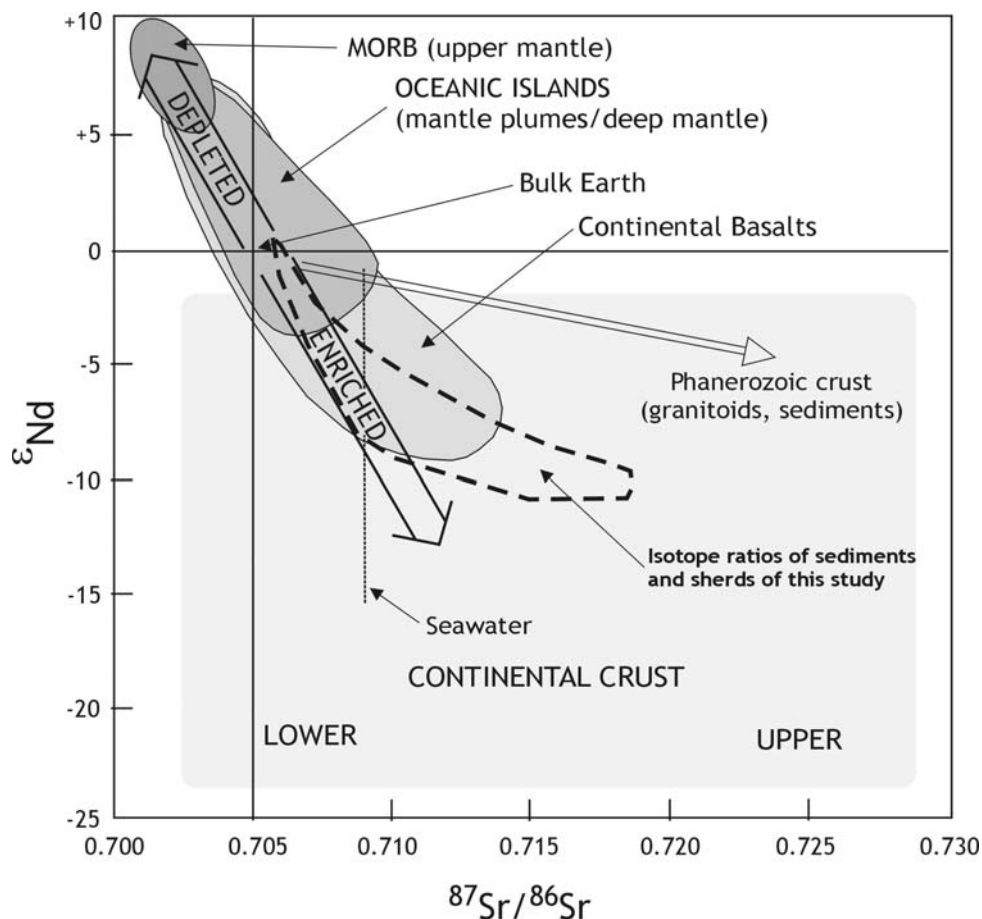


**Fig. 111 Sr isotope ratios and  $\epsilon_{\text{Nd}}$  values in major geochemical reservoirs with the isotope ratios of sediments and the sherds of this study (after White, 2001).**

The radiogenic isotope ratios ( $^{87}\text{Sr}/^{86}\text{Sr}$  and  $^{143}\text{Nd}/^{144}\text{Nd}$ ) of all sherds and sediments studied in this work fall into the immobile element enriched field on the  $^{87}\text{Sr}/^{86}\text{Sr}$  vs.  $\epsilon_{\text{Nd}}$  plot (Fig. 111). However, on the basis of the data, most sediments and sherds are related to the average values of the upper crust (sediments and granitoid rocks), a trend can be also obtained in the results, which is in good accordance with the local geological settings (cf. Chapter 7).

This trend shows a distribution from  $^{143}\text{Nd}/^{144}\text{Nd}$  relatively enriched (positive  $\epsilon_{\text{Nd}}$  values) and  $^{87}\text{Sr}/^{86}\text{Sr}$  relatively depleted results to the  $^{143}\text{Nd}/^{144}\text{Nd}$  relatively depleted (negative  $\epsilon_{\text{Nd}}$  values) and  $^{87}\text{Sr}/^{86}\text{Sr}$  relatively enriched materials (Fig. 110 and 111).

### 6.2.3. Electron microprobe analysis (EMPA)

On the basis of the petrographic, chemical, and isotope-geochemical investigations two sherds with uncertain origin have been chosen for an electron microprobe analysis. Although all the analytical methods used by far suggested, that these two sherds were probably not produced from local raw materials, no more accurate information could be obtained about their possible origin. In order to get more information the chemical composition of some non-plastic inclusions of these sherds were investigated. Analyses were focused on the volcanic inclusions and minerals of volcanic origin. With the help of the data I have tried to find a match between the type of the volcanites and their possible plate tectonic setting. Comparing the data to the information from geological literature, the possible source area of the clasts and that of the origin of the material used for potting can be limited or determined. Results of the electron microprobe analyses and the calculated parameters are presented in the Appendix 9.

#### 6.2.3.1. Sample MCE-1 (Menekşe Çatağı)

This sherd contains lots of volcanic rock fragments. The aim of the electron microprobe analysis was to investigate the composition of the K-feldspar and plagioclase crystals in order to determine the type of the volcanite fragments.

Based on the petrographic investigation, four rock fragments were chosen for the EMP analysis.

##### *Fragment A*

The volcanite fragment is mostly composed of tabular albite crystals ( $Ab_{98-99} - An_{1-0.1}$ , Fig. 116) with K-feldspar ( $Ab_{3-4} - Or_{96-97}$ ) on their margins (Fig. 112 and 116).

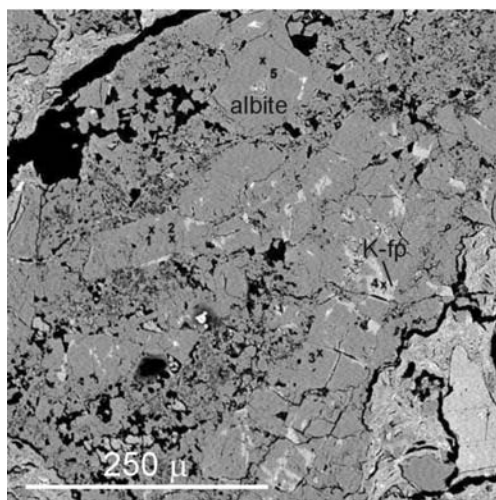


**Fig. 112** Backscattered electron image (BEI) of albite and K-feldspar in the volcanite fragment “A” (sherd MCE-1).

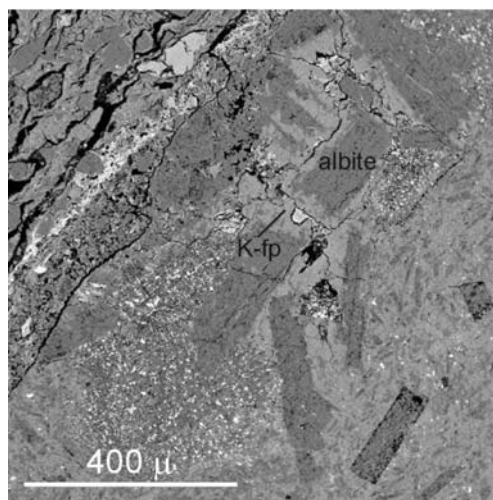


**Fig. 113** BEI of albite and K-feldspar in the volcanite fragment “B” (sherd MCE-1).

*Fragment B*

Three mineral fragments were measured in the sample. One of them was quartz ( $\text{SiO}_2 = 99.25 \text{ wt } \%$ ), the other one was K-feldspar ( $\text{Ab}_5 - \text{Or}_{94}$ ), and the third one was a large albite ( $\text{Ab}_{98} - \text{An}_2$ , Fig. 113 and 116) phenocryst. The marks of recrystallisation have already been well observed in the polarising microscope, thus it is likely that quartz grains are products of secondary silicification.

*Fragment C*

This small volcanite is made of albite crystals ( $\text{Ab}_{98.99} - \text{An}_{0.2-2}$ ). The large phenocryst situated on the margin of the volcanite grain was measured (Fig. 114 and 116).

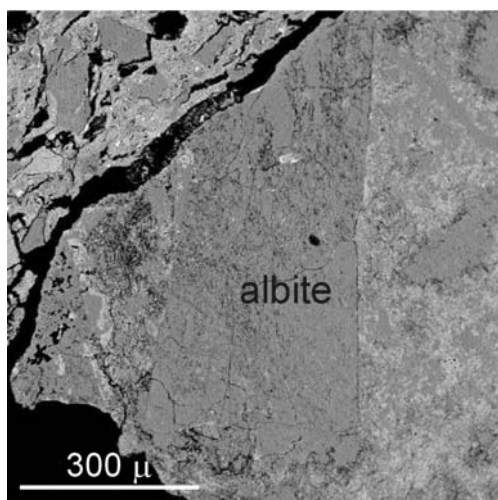


**Fig. 114** BEI of albite and K-feldspar in the volcanite fragment “C” (sherd MCE-1).

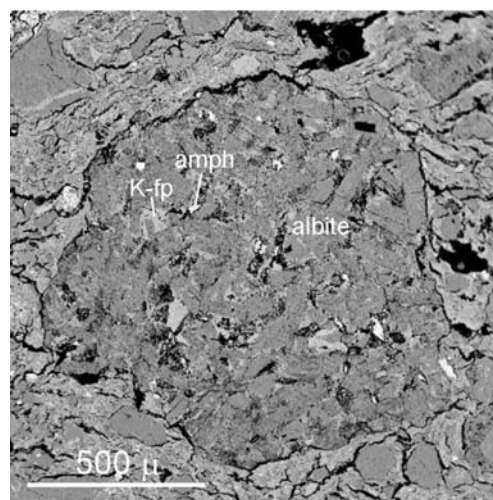


**Fig. 115** BEI of albite, K-feldspar and amphibole in the volcanite fragment “D” (sherd MCE-1).

*Fragment D*

This volcanite differs in its texture from the other ones found in the sherd. Tabular plagioclases form intergranular texture, interstitial space is filled with fine-grained matrix, amphibole, and opaque minerals (Fig. 115). Three tabular, four anhedral plagioclase and K-feldspar, and a third phase, probably an amphibole, were measured. On the basis of the EMP analysis five of the seven plagioclases seemed to be albite ( $\text{Ab}_{98.99} - \text{An}_{1-2}$ ), the two other grains are K-feldspar ( $\text{Ab}_{1-2} - \text{Or}_{97-98}$ ; Fig. 116). The third measured phase is an amphibole; according to the classification of Leake (1978) it is a calcic amphibole, magnesio hornblende.

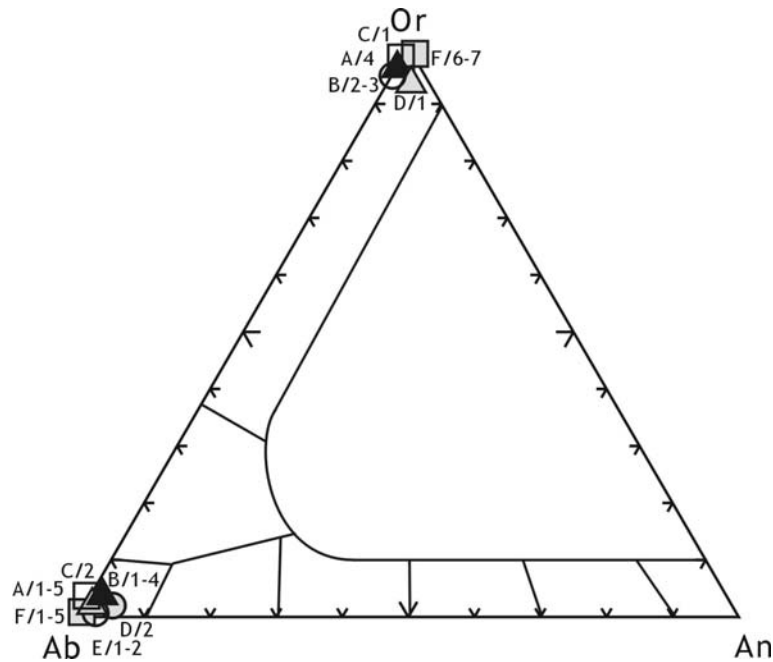


Fig. 116 Composition of K-feldspars in the Ab-Or-An triangle (sherd MCE-1; letters show measuringpoints in the fragments; cf. Appendix 9).

### 6.2.3.2. Sample AT-2 (north Turkish Thrace)

The non-plastic inclusions of the sherd from Araptepe (north Turkish Thrace) contain mainly volcanic rock fragments and minerals of volcanic origin. Investigations were focused on the following fragments:

- clinopyroxene,
- plagioclase, K-feldspar
- volcanic rock fragments,
- altered volcanic glass, containing Cr-spinel.

#### *Clinopyroxene*

Pyroxenes are important rock-forming minerals. Based on the chemical composition, type of the pyroxenes (Morimoto *et al.*, 1988) and the presumable tectonic setting (Laterrier *et al.*, 1982) can be given.

Five clinopyroxene crystals (measurements 1 to 12: separate crystals in the clayey matrix) were chosen in order to determine their chemical composition (data: cf. Appendix 9). Each clast was measured in two points (central part and near to the rim; Fig. 117), with the exception of a zoned crystal, where four measurements were carried out (Fig.117).

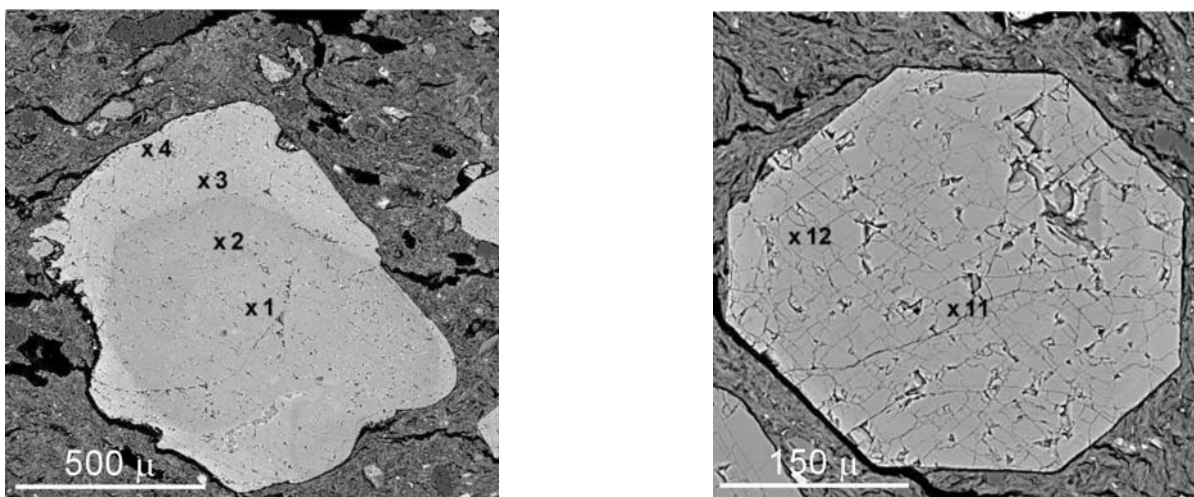


Fig. 117 BEI of anhedral zoned (left) and euhedral (right) diopside crystals in the matrix of the sherd AT-2 (numbers show measuring points; cf. also Appendix 9).

Using the En-Wo-Fs diagram (Morimoto *et al.*, 1988) each sample has diopside ((Ca, Mg, Fe<sup>2+</sup>, Mn<sup>2+</sup>, Fe<sup>3+</sup>, Cr<sup>3+</sup>)[Si<sub>2</sub>O<sub>6</sub>]) composition (Fig. 118).

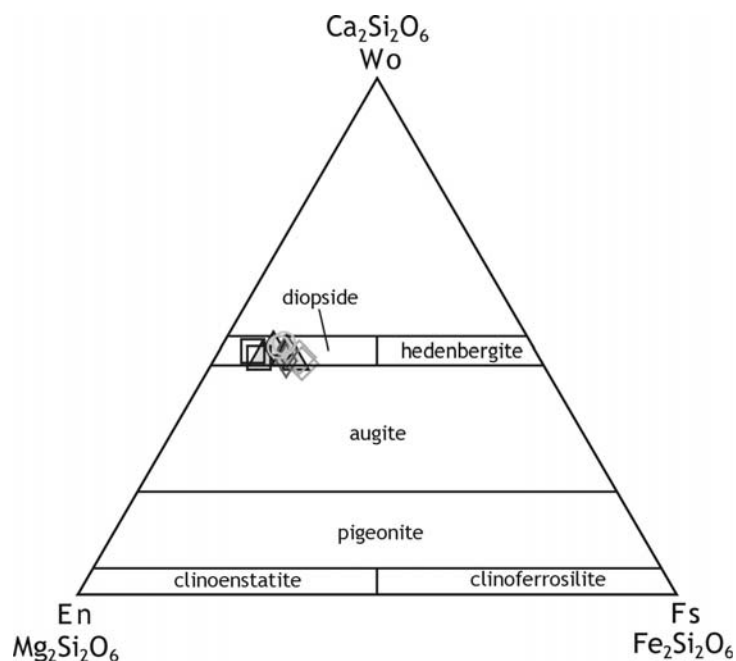
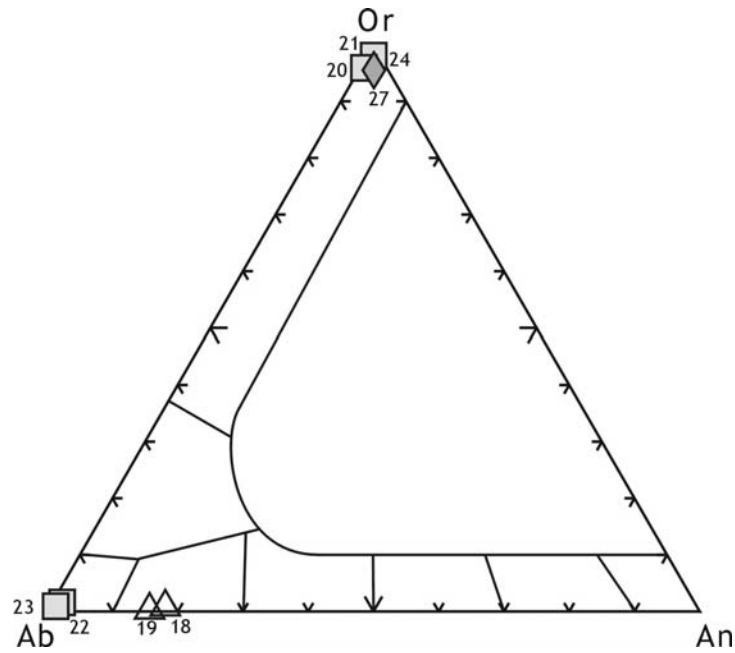


Fig. 118 Chemical composition of pyroxenes in the En-Wo-Fs diagram (Morimoto *et al.*, 1988).

#### *Plagioclase (Na[AlSi<sub>3</sub>O<sub>8</sub>]-Ca[Al<sub>2</sub>Si<sub>2</sub>O<sub>8</sub>])*

Only two small plagioclase fragments were found in the whole thin-section. Furthermore, they were separate crystals in the matrix, and not parts of a rock fragment.

The high albite (Na[AlSi<sub>3</sub>O<sub>8</sub>]) and low anortite (Ca[Al<sub>2</sub>Si<sub>2</sub>O<sub>8</sub>]) components (Ab<sub>82-84</sub> – An<sub>16-18</sub>) suggest acidic plagioclase (oligoclase) composition (Fig. 119).



**Fig. 119** Composition of K-feldspars and plagioclases in the Ab-Or-An triangle (sherd AT-2; numbers show measuring points; cf. Appendix 9)

#### *Volcanic rock fragments*

The matrix of a volcanic rock fragment has also been investigated. The data are plotted into the Ab-Or-An triangle (Fig. 119). The two measured phases are almost clear K-feldspar ( $K[AlSi_3O_8]$ ;  $Ab_{2-3} - Or_{96-98}$ ) and albite ( $Ab_{97-99} - Or_{0.5-2}$ ). The BE image (Fig. 120) may suggest that K-feldspar fragments, which enclose the smaller albite crystals, are products of secondary processes (e.g. K-metasomatism); it is also in good accordance with the microscopic observations.

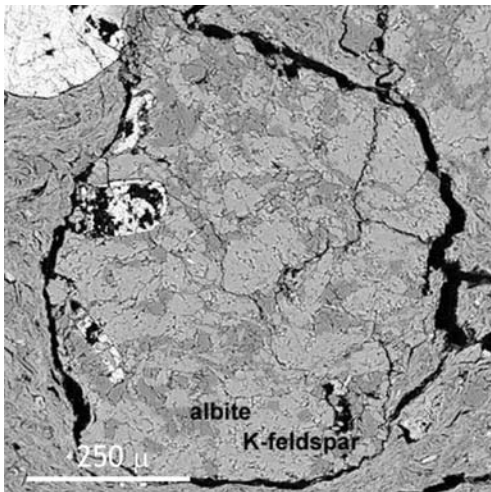


**Fig. 120** BEI of albite and K-feldspar in a volcanic rock fragment (sherd AT-2).

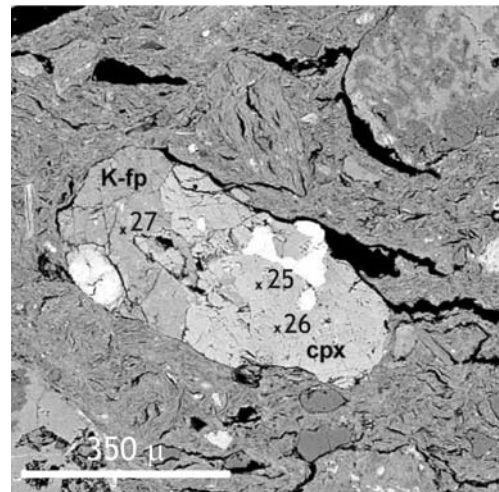


**Fig. 121** BEI of a volcanic rock fragment containing K-feldspar and clinopyroxene (sherd AT-2).

Another magmatite fragment (Fig. 121) has been measured where the intergrowth of K-feldspar ( $Ab_{2.4} - Or_{97.6}$ ; Fig. 117) and clinopyroxene (measurements 25 and 26) can be observed. Also in this case the clinopyroxene shows diopsidic composition (Fig. 118).

*Cr-spinel*  $((Mg, Fe^{2+})(Cr, Al, Fe^{3+}, Ti)O_4)$

Cr-spinel is a common accessory mineral in basaltoid rocks and in peridotites. According to Arai (1992) and Kamenetsky *et al.* (2001) its chemical composition is widely regarded as a sensitive indicator of the petrogenesis of its parent rocks. Due to the variations in Al,  $Fe^{2+}/Fe^{3+}$ , Mg, Ti, and Cr, which reflect the nature of fractional crystallisation of the resulting magmas, it can be used to determine the plate tectonic setting of the parent rocks.

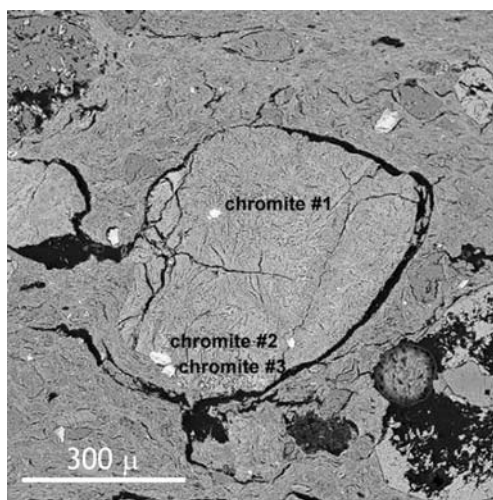


**Fig. 122** BEI of an altered glassy clast containing chromite crystals (sherd AT-2).

Three Cr-spinel fragments were found and measured (measurements 13 to 17) in a yellowish-orange altered and well-rounded rock fragment (probably volcanic glass of basic composition) (Fig. 122).

As a first step, calculated values were plotted onto the  $TiO_2$  vs.  $FeO/Fe_2O_3$  diagram (Lenaz *et al.*, 2003), which is used for the separation of the two most important sources of the Cr-spinels: mantle peridotites and mantle-derived magmatic rocks.

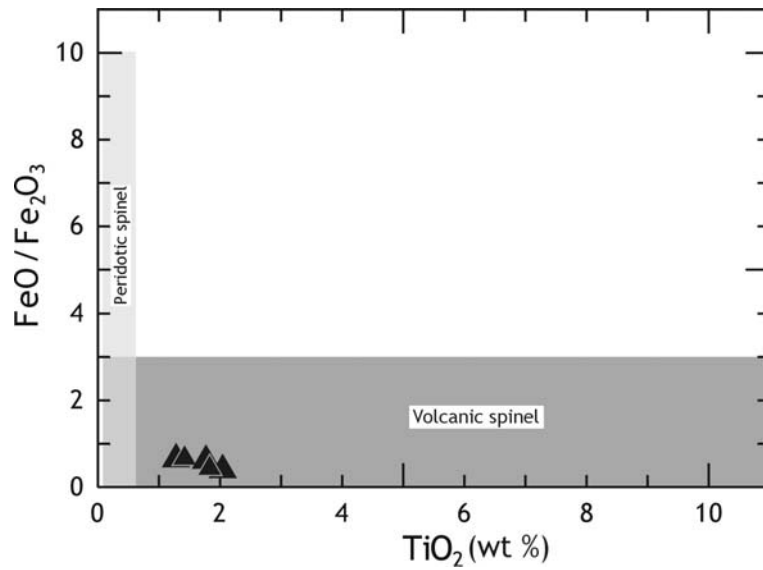


Fig. 123 Chromite data in the  $\text{TiO}_2$  vs.  $\text{FeO}/\text{Fe}_2\text{O}_3$  diagram (Lenaz *et al.*, 2003).

Each sample fulfills the criteria of Lenaz *et al.* (2003) and Kamenetsky *et al.* (2001), having all high  $\text{TiO}_2$  (around 2 wt %) contents and  $\text{FeO}/\text{Fe}_2\text{O}_3 < 4$  values. Thus all Cr-spinel fragments have volcanic origin (Fig. 123).

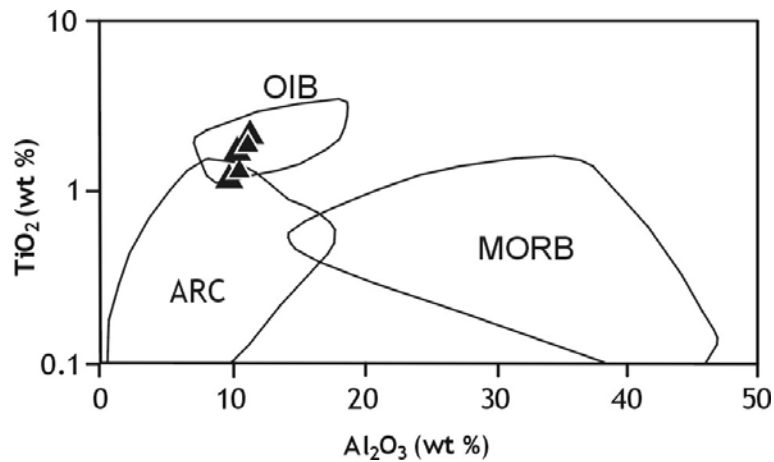


Fig. 124 Chromite data in the  $\text{Al}_2\text{O}_3$  vs.  $\text{TiO}_2$  diagram (Kamenetsky *et al.*, 2001; Lenaz *et al.*, 2003).

Using the  $\text{Al}_2\text{O}_3$  vs  $\text{TiO}_2$  bivariate plot (Kamenetsky *et al.*, 2001; Lenaz *et al.*, 2003), further classification of the spinels can be carried out. The spinels range in  $\text{TiO}_2$  from 1.28 to 2.04 wt %. They are probably derived from a basaltic source formed at an island arc or in intraplate basalt setting as suggested by the  $\text{Al}_2\text{O}_3$  vs.  $\text{TiO}_2$  diagram (Fig. 124).

#### **6.2.4. Neutron activation analysis (NAA)**

Multi-element XRF-analysis can provide valuable information about the bulk composition of these materials, but it needs a relatively big volume of a material (1-2 g) for investigation and the detection of several elements (like REE) is not amenable, or due to the high detection limit, not reliable. This fact limits the adaptability of the method in cases when only small amount of the material (small pieces of sherds, temper) is available. In order to bridge these gaps of the XRF, rare earth element composition of some samples has been analysed using the neutron activation analysis. The aim of the NAA was to characterise potteries, which on the basis of their petrographic and bulk chemical composition show no significant similarities or differences, and materials which are available only in small amount. The data are presented in the Appendix 10.

Considering these criteria two types of materials have been chosen for this investigation.

(1) A sherd from Troia (TR-20), of uncertain origin, containing mostly common non-plastic inclusions (e.g. quartz, K-feldspars, polyquartz, micrite, etc.), which are not characteristic for the place of production, furthermore (2) non-plastic inclusions (rock fragments) separated from sherds, were selected for the analyses. The benefit of such investigations is that the chemical composition of the mineral and rock fragments, similar to the EMPA, can be directly compared to the chemical composition of identical or similar rock types situated in the environs of the supposed place of origin. Basing on previous analyses (Gherdán, 1999) volcanic rock fragments from the sherd MCE-1 (Menekşe Çataği) and a basanite rock sample found near Menekşe Çataği have been chosen and analysed. Data are normalised to CI-chondrite (Taylor & McLennan, 1985).

##### **6.2.4.1. The sherd from Troia (Tr-20)**

The following rare earth elements were plotted: La (134.8), Ce (115.7), Nd (52.5), Sm (41.5), Eu (25.2), Tb (20.6), Yb (17.7), Lu (14.8). The sample is characterised by the LREE enriched patterns and flat HREE coupled with very slight Eu anomaly.

Comparing these data to the REE patterns of the locally produced Troian VI sherds (Grey Minyan Ware; Knacke-Loy, 1994), good overlap and similar properties in the distribution of the elements can be obtained: La (122.9 to 148.9), Ce (95.8 to 116.1), Nd (53.7 to 77.2), Sm (38.5 to 41.5), Eu (22.8 to 25.2), Tb (16.0 to 20.2), Yb (13.3 to 13.9), Lu (13.5 to 14.8). The REE pattern of the locally produced sherds also characterised by the LREE enriched and flat HREE patterns coupled with the minor Eu anomaly (Fig. 125).

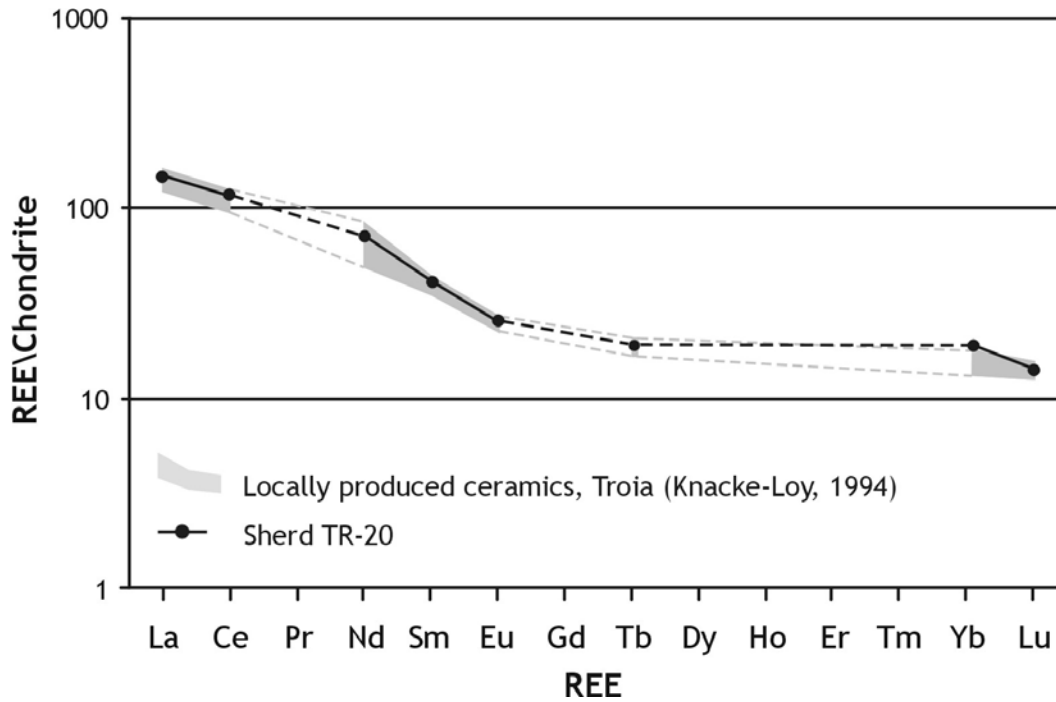
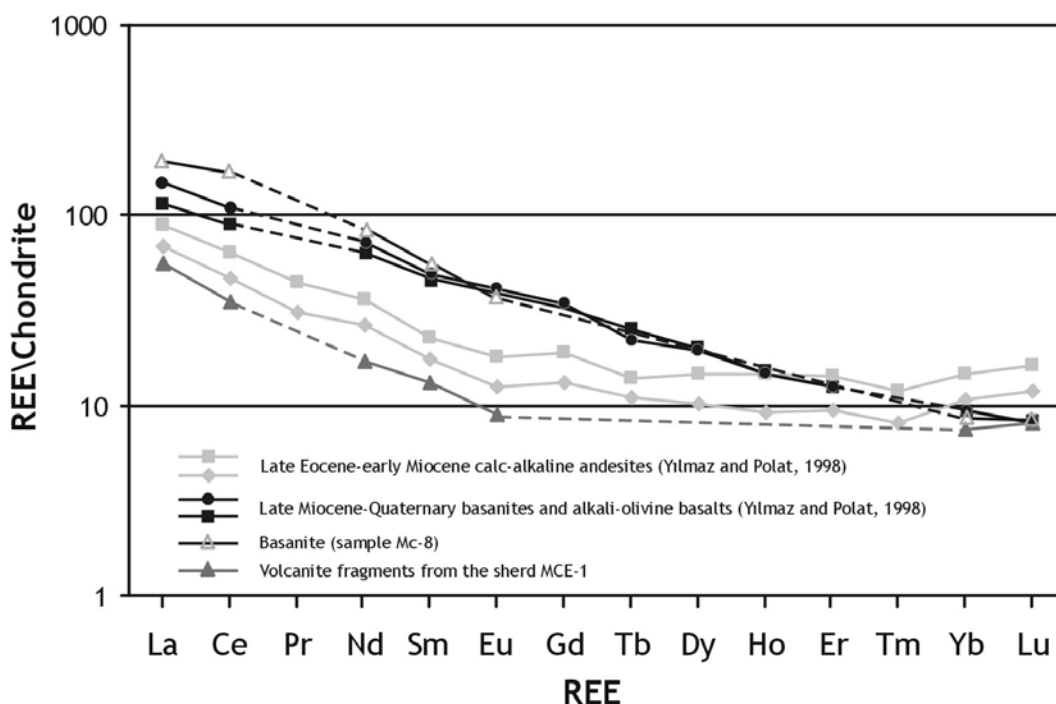


Fig. 125 REE pattern of the sherd TR-20 as well as Troian locally produced ceramics (Knacke-Loy, 1994).

#### 6.2.4.2. Intermediate volcanite fragments from the sherd MCE-1 and the rock sample Mc-8 (Menekşe Çatağı)

Chondrite-normalised REE diagram of the intermediate volcanite fragments separated from the sherd MCE-1 is characterised by the LREE enriched patterns ( $La/Sm = 4.2$ ) and flat HREE; there is also probably a little Eu anomaly, which cannot be unambiguously seen, due to the lack of Gd. The data are: La (55.5), Ce (35.1), Nd (17.1), Sm (13.1), Eu (8.9), Yb (7.5), Lu (8.0). Comparing our measurements to the REE patterns of calc-alkaline andesites from the Thrace basin (Yılmaz & Polat, 1998), clear similarity can be obtained in the main features of the patterns of the volcanites and the fragments found in the sherd. However, values of the sample MCE-1 are somewhat lower than in the local volcanites. Andesites are also characterised by the LREE enriched patterns (10 to 20 times chondrite) and flat HREE ( $La/Sm = 3.4 - 4.1$  and  $Gd/Yb = 1.2 - 1.3$ ), coupled with minor Eu anomalies (ICP-MS data, Yılmaz & Polat, 1998).

The basanite (based on microscopic analysis) sample collected near Menekşe Çatağı has different REE patterns (La (230.9), Ce (178.6), Nd (63.5), Sm (48.9), Eu (30.7), Yb (9.4), Lu (9.2)), which are similar to the Miocene-Quaternary basanites and alkali olivine basalts (Fig. 126).



**Fig. 126** REE patterns of the volcanic rock fragments from the sherd MCE-1, the basanite pebble (Mc-8), as well as andesites and basalts from the Thrace Basin (Yılmaz & Polat, 1998).

The basanite sample shows, however, higher La and Ce values. These rock types are characterised by smoothly enriched REE patterns ( $La/Sm = 2.6 - 3.1$ ,  $Gd/Yb = 3.2 - 3.8$ ; Yılmaz & Polat, 1998); the sample Mc-8 has  $La/Sm = 4.6$ . On the basis of their REE patterns significant differences between young basalts/basanites and Tertiary andesites can be demonstrated (Fig. 126).

## **CHAPTER 7. Summary and interpretation of the results**

Due to the amount and the complexity of the data from analyses, in this chapter I summarise and discuss them according to the geological build-up and informations of the different areas. On the basis of the comparative evaluation of the data I answer the two basic questions of my dissertation.

To answer the first question of this study, concerning the origin of the Knobbed ware, the following criteria have been considered.

During the evaluation of the results it has become clear that the use of a single method (e.g. petrography or XRF only) in most cases cannot provide adequate and reliable information about the origin of the sherds. This fact is related to several factors which correspond to each other. The most important factor is the geological setting of the study areas. In several places, especially between the central Bulgaria and the north Turkish Thrace, the main features of the geological build-ups are very similar (cf. Chapter 5). Therefore the main rock types in these regions, the alteration products of these materials, and thus the possible raw materials for the ceramics production can also be very similar in their petrographic as well as chemical compositions. This phenomenon makes the provenance analysis more difficult and partially uncertain. With the combined use of petrographic, chemical, and isotope geochemical investigations have I tried to find such properties or fingerprints, which are typical for a ceramic group collected from an archaeological place and give information about the place of origin of the ceramics.

For an effective provenance analysis two phenomena must be distinguished: (1) are the vessels similar in their material qualities because they were produced in the same locality, or (2) do similarities refer to the similar geological backgrounds of the different areas?

In order to distinguish between these two phenomena, I have summarised, interpreted, and presented the results of the different analytical methods together. In a first step the results of microscopic observations and grouping, as well as the CL analysis are explained, comparing the data to the geology of the localities and local materials (locally produced sherds, geological samples). As a second step the results of the bulk chemistry (XRF data) of local sediments and sherds are presented. In the explanation of the chemical data, the results of the petrographic investigations as well as the knowledge of the geology of the areas play an important role. This part is followed by the results of radiogenic isotope, electron microprobe and neutron activation analyses, presented in order to complete our knowledge with more information about the natural composition and properties of the sherds.

In the second part (7.2.) the results of X-ray diffractometry and the data of the fabric analysis will be compared and interpreted in order to answer the questions related to the technology of production of the Knobbed ware.

## 7.1. The origin of Knobbed ware

### 7.1.1. Summary and interpretation of the petrographic and cathodoluminescence results

Petrographic (sub)group/type	Samples
1A/1	TR-1, 2, 3, 5, 13, 16, 19, 27
1A/2	TR-24
1A/3	TR-20
1B/1	TR-4, 11, 14, 15, 17, 21, 22, 23, 25
1B/2	TR-6, 7, 9, 10, 12, 18, 26, 28
1C	TR-8
2	A-1
3A/1	MCW-1, 3, 4, 5, MCE-2, 3, 4, 5
3A/2	MCW-2
3B	MCE-1
4A/1	AK-1, 2, AT-1, CM-1, 2, 3, 4, DH-1, 2, 3, YK-1, 2, 3, 4, 5
4A/2	HM
4B	AT-2
5A	OVC-1, 2, 3
5B	OVC-4, 5, 6
6	CH-1, 2, 3, 4, 5, 6
7A/1	KIR-1, 2, 3, PSH-1, 2, 3, DIA-1, 2, 5, 7, 8, 10, 11
7A/2	DIA-3, 4, 6, 9, 12, 13
8	SBO-1, 2, 3

**Table 2 Petrographic grouping of the Knobbed ware sherds analysed in this study.**

#### 7.1.1.1. Troia

Twenty-eight sherds from Troia were grouped into 3 subgroups and 5 different petrographic types (Table 2). The main characteristic of the Troian sherds is that all of them contain different volcanic rock fragments in various (3 to 80 vol %), but relatively high amounts (mostly over 15-20 vol %). Although the sherds were grouped into different petrographic types, two main characteristic groups can be differentiated. The sherds belonging to subgroup *1A* have various amounts of fragments of recrystallised and intermediate-acidic volcanites. The samples belonging to type *1B* are characterised by the presence of acidic volcanic glass. The fact that every sample contains at least some percent of rock fragments of volcanic origin refers to the presence of extensive volcanic areas in the vicinity of the production site(s). Further important rock fragments are plutonic clasts. They have probably

granitic-granodioritic composition, on the basis of their mineral composition. Polycrystalline quartz (quartzite) fragments belong either to this plutonic association (crystals with straight, or slightly undulatory extinction), or to a metamorphic (metaquartzite, metagranite?) rock association (crystals with undulatory extinction). Single mineral fragments like monoquartz, K-feldspar, plagioclase, micas, amphibole, epidote are well-related to the volcanic-plutonic-metamorphic rock fragments. Moderate to well rounded, primer (not pore-filling) micritic clasts containing mostly quartz, quartzite, partially volcanite fragments (Fig. 127) are also characteristic inclusions in several Knobbed ware sherds.

One sherd (TR-24) contains clasts which refer to parent rocks of ultrabasic origin. Pseudomorphose after pyroxene and/or olivine as well as serpentinite fragments refer to the presence of ophiolitic rocks in the environs of the place of origin of its raw material.

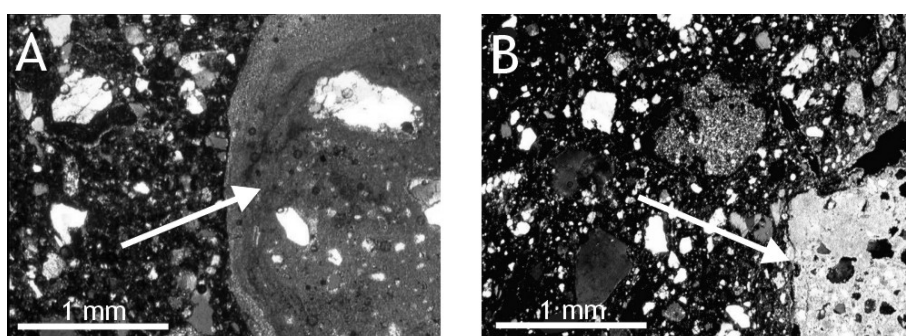


**Fig. 127** Comparative microphotographs of carbonate inclusions (arrows) in a locally produced Troian sherd, K8.911.93 (A) and the sample TR-15 (B), Troia (+N).

The mineralogical-petrographic composition of sandy fluviatile sediments (the samples Tr-1a and b, Tr-2a and b; cf. 6.1.1.1.1), collected from the flood plains of the Karamenderes and Dümrek, presents a good geological cross-section of the main geological units, belonging to the catchment areas of the rivers. Thus granitic-granodioritic fragments, andesitic-latitic volcanites, some fragments of acidic volcanites and acidic volcanic glass, recrystallised volcanites (Fig. 128), serpentinite, polycrystalline quartz, as well as rounded to well-rounded micritic fragments with detrital mineral and rock clasts present the geological diversity of the Troad.

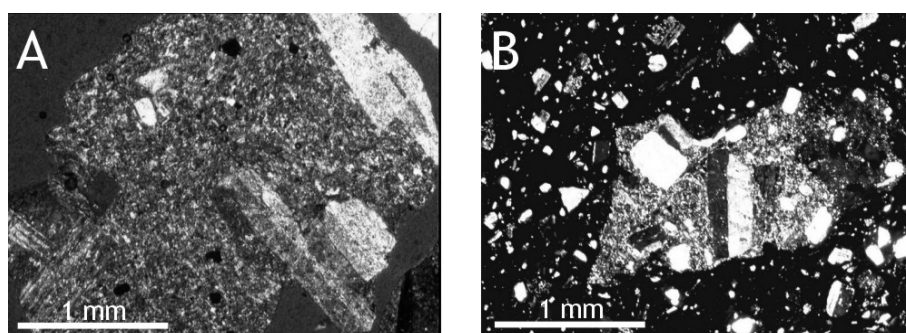


**Fig. 128** Comparative microphotographs of recrystallised volcanite fragments in the Troian sediment sample Tr-1a (A) and the sample TR-4 (B), Troia (+N).

Comparing the petrographic composition of the Knobbed ware sherds to the non-plastic inclusions found in the local sediment samples and locally produced sherds from the settlement phases Troia I-V lots of similarities can be revealed. Common rock and mineral fragments, like mono- and polyquartz, plagioclase, etc. cannot be effectively used petrographically for provenance analyses, but clasts like micritic clasts with quartzite, chert inclusions (Fig. 127), recrystallised volcanites, and acidic volcanic glass fragments (Fig. 128 and 129), found in these sherds and local sediments, are texturally very similar to those found in the Knobbed ware fragments investigated in this study.

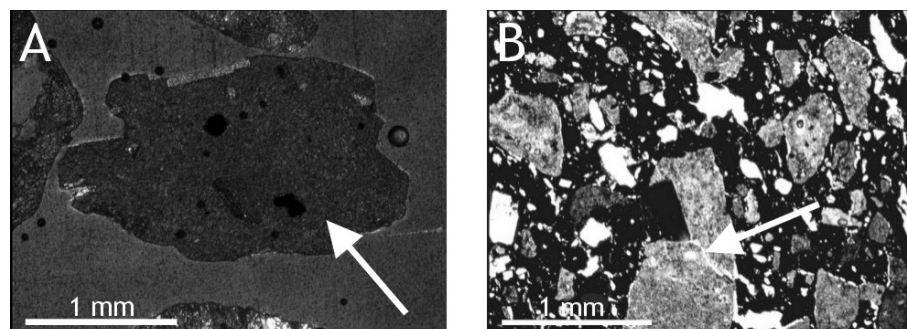


**Fig. 129 Comparative microphotographs of acidic volcanic glass (arrows) in the Troian sediment sample Tr-1a (A) and the sample TR-7 (B), Troia (+N).**

The results are partially in good accordance with Knacke-Loy's investigations (1994), although he described several, mainly metamorphic, local rock types (e.g. micaschist, chalkschist, gneiss, ironschist, etc.), which are not presented in the Troian material of this study. On the basis of the petrographic analyses, carried out on two Knobbed ware fragments from Troia, he reported similar petrographic composition (domination of volcanite clasts; Knacke-Loy, 1994), as those described in this work.

Summarising the knowledge of the petrographic-mineral composition of the Troian Knobbed ware sherds and local materials, one can establish that the source area of these inclusions has a complex build-up, where mostly volcanic (basaltic-andesitic-rhyolitic), plutonic (granite-granodiorite), metamorphic (metaquartzite), ultrabasic (serpentinite) rocks, and mineral associations belonging to them are found. This picture is in good accordance with the main geological features of the Troad (cf. Chapter 5) and suggests an affinity of the sherds to local raw materials. Because of the small grain size, alteration, etc. of the single non-plastic inclusions, it was not possible to characterise all rock types unambiguously, but one can attempt to put in order the most important and characteristic rock fragments found in the potteries to the main geological units of the Troad.

Therefore volcanic clasts of intermediate (probably andesitic), acidic (probably rhyolitic-rhyodacitic) composition, as well as recrystallised (silicified) volcanites could originate from the Tertiary volcanite complexes (Okay *et al.*, 1991), situated south- and eastward from Troia.

Acidic volcanic glass (either rhyolite or obsidian) could belong to the small obsidian outcrop situated to the southeast from the archaeological site, or to the acidic volcano complexes. Intermediate to acidic plutonite fragments can belong to the early Miocene Kestanbole-intrusion southwest from Troia, however, the main rock type found in this area is quartz-monzonite and monzo-granite (Birkle, 1993; Birkle & Satır, 1994). The Evciler-pluton situated to the east of Troia, which also belongs to the catchment area of the Karamenderes, is made up of similar plutonites (Birkle, 1993; Birkle & Satır, 1994). Serpentine fragments and pseudomorphoses after olivine and/or pyroxene from the sherd TR-24 may originate from the ophiolite complex of the Ezine-Zone, situated to the east-southeast from Troia.

With the exception of the samples TR-8 (dominating presence of hard recrystallised volcanites of unknown type) and TR-20 (lots of quartz, quartzites, very few rock fragments), each sherd collected in Troia unambiguously bears in different dimensions the main characteristics of the geology of the Troad, especially the volcanite clasts. There was no sherd found, which was contained minerals and/or rock fragments untypical for the region.

#### **7.1.1.2. The Avşa Island**

The unique mineral composition of the sherd A-1 (great amount of euhedral calcite fragments) refers to the vicinity of this raw material source, or to the use of marble/crystalline limestone temper (rhombohedral calcite → crushing?). Other metamorphic (metaquartzite) and (meta) plutonic rock fragments suggest correlation with local undifferentiated series of metamorphites and magmatites (Oligo-Miocene granitoids; Okay *et al.*, 1996) found on the island and in its environs.

Although on the island there is no marble, the Marmara Island, situated approximately 12 km to the northeast from Avşa, is a well-known marble source (Zöldföldi & Satır, 2003). Further marble occurrences to the south and southeast from Avşa are: Manyas, Mustafa Kemalpaşa, and Bandırma on the mainland (Zöldföldi & Satır, 2003). Although the possibility that marble fragments belong to another source, situated somewhere in western Anatolia and the vessel was thus produced there, is very low, on any account I wanted to emphasize the similarities between the calcite fragments found in the pottery and the local marbles.

The results of the CL investigation (no luminescence, most fragments were completely black) correspond well with the CL properties of local marble occurrences (Zöldföldi & Satır, 2003). Because all of the marble sources of the Marmara Island (the Sea of Marmara), Manyas, and Mustafa Kemalpaşa (the southern coast of the Sea of Marmara) belong to the Sakarya Zone and their genesis also similar, CL properties are also similar, and thus marbles near Avşa do not show luminescence either. Other marble occurrences in east and southwest Anatolia have characteristically different (red, orange) CL images, which allow for distinguishing my material from other formations in the Marmara region (Zöldföldi & Satır, 2003). The theory of the origin of the calcite fragments and thus the raw

material from the Marmara Island can also be supported by the archaeological fact that there is no known Early Iron Age archaeological site along the southern coast of the Sea of Marmara (Mehmet Özdoğan, personal communication).

### 7.1.1.3. Menekşe Çatağı

The non-plastic inclusions observed in the sherds (petrographic type *3A/1*; Table 2) from Menekşe Çatağı, imply the magmatic-metamorphic parent rocks and source area of the grains. The sample MCW-2 (type *3A/2*) contains mineral and rock fragments which seem to belong to one rock type, probably a hornblende-, biotite- and epidote-bearing metaquartzite or metagranite. Strongly sutured grain boundaries refer to the metamorphic event. Epidote probably formed during low grade metamorphism.

The sherd MCE-1 (subgroup *3B*) with different petrographic composition (great amount of intermediate volcanic and silicified volcanic fragments) refers to another geological background from where the raw material for the pottery production originated.

The supposed geological setting of the areas, from where non-plastic clasts could originate, contains magmatic and (probably) low-grade metamorphosed rocks (types *3A/1* and *2*) as well as in a different area volcanic and magmatic rock associations (subgroup *3B*). Studying the geology of the northern coastline of the Sea of Marmara one can see, that none of these rock types exist in the closer region of the archaeological site (cf. Chapter 5).

According to Jaranoff (1937) and Yılmaz & Polat (1998) it is known, that late Miocene cross-bedded fluvial sand, partially with exotic granite, gneiss, and metaquartzite pebbles indicates that the sedimentation in that time occurred from the North to the South, thus the material of the Strandja Massive, transported by rivers, is found in the sedimentary sequence of the coastline of the Sea of Marmara. Naturally, this is not a sufficient argument to prove the local production of these sherds, but it shows clearly that in order to understand the possible presence of “exotic” inclusions, geological backgrounds must be well known.

In contrast, the sample MCE-1 with great amount of intermediate to acidic rock fragments, does not fit this theory, because of the lack of volcanites in the Strandja Massive. Neogene to Quaternary alkali olivine basalts and basanites north-northwest from the archaeological site Menekşe Çatağı have different texture and mineral composition (Yılmaz & Polat, 1998). The nearest possible source of the volcanite fragments can be the late Eocene-early Miocene calc-alkaline andesites 30-70 km west-southwest from the excavation site.

#### 7.1.1.4. North Turkish Thrace

The petrographic image of the samples from the north Turkish Thrace belonging to the petrographic type *4A/1* (Table 2) suggests a source area which is mainly made up of granitic-granodioritic and (slightly) metamorphosed rocks, (metaquartzite with epidote minerals, phyllite, etc.).

The sample HM (type *4A/2*) shows similar petrographic composition to the samples belonging to the previous petrographic type, although the amount of metamorphic minerals and rock fragments, especially of garnet-bearing muscovite micaschist, is dominant. This petrographic image also suggests a magmatic-metamorphic area in the catchment area of the river(s) providing the raw materials for the studied vessel fragment.

Comparing the mineral components of the sherds to the composition of the local sediment samples, most rock fragments (cf. 6.1.1.4.1.) with similar texture and proportions are also found in them.

Confronting the results to the local geological and sediment patterns, one can see that the presumed magmatic-metamorphic source areas of the non-plastic inclusions found in the sherds match quite well the granitic-granodioritic and metamorphic rock (e.g. quartzite, micaschist, etc.) associations of the southern part of the Strandja Massive (Okay *et al.*, 2001; cf. Chapter 5), yet the source of the recrystallised volcanite and a volcanite clast in the samples DH-1, 3, and AK-1 is certainly not found in the vicinity of the southern part of the Strandja Massive. The rock fragments could be transported e.g. from the eastern Rhodopian region (cf. Chapter 5) by the Maritsa river with its tributary. The small amount of rounded clasts also refers to the fact that they were probably transported from larger distances.

The domination of volcanites, pyroxene, basic volcanic glass, some recrystallised volcanites as well as few quartz and quartzite in the sample AT-2 (subgroup *4B*) suggests that the vessel has been produced in a region with different geological patterns. On the basis of these observations the origin of the raw material from the southern Strandja can be certainly excluded.

#### 7.1.1.5. Ovcarovo

The samples from Ovcarovo, belonging to the petrographic subgroup *5A*, contain great amount of granitic rock fragments, minerals of magmatic (granitoid) origin and polyquartz. They refer to the presence of plutonic rocks in the source area of the raw material of these sherds. The archaeological site of Ovcarovo is found in the north-western end of the Strandja Massive, where in extensive areas Archaean (?) to upper Paleozoic granitic rocks are situated (Okay *et al.*, 2001). These petrographic data suggest the affinity with local, plutonic rock types (cf. Chapter 5), however, due to the almost same geological setting, many similarities are also found with the north Turkish Thracian region.

The mineral composition, the lack of rock fragments, and the small amount of non-plastic clasts signify clearly the differences between the subgroups of the sherds from Ovcarovo. All these data refer

to the fact that the vessels were produced in an area with a totally different geological build-up. Although the texture of the samples is unique, they show clear similarities with the geological samples of the petrographic group 8 (Sborianovo).

#### **7.1.1.6. Chal**

The dominating presence of acidic plutonites (granite), polyquartz, K-feldspar, plagioclase, mica, amphibole epidote, monoquartz, some phyllite, chert and ARF in the samples of the petrographic group 6 also refers to an area dominated mainly by magmatic rocks. Partially undulatory extinction of the plutonic rocks indicates that they probably underwent different metamorphic event(s). Although intermediate or acidic volcanic rock fragments and pseudomorphoses after olivine in two samples indicate the presence of effusive rocks within the catchment area of the river(s) providing the raw materials for ceramic production, their amount is quite insignificant relatively to the other rock and mineral clasts. Due to the instability of the pseudomorphoses after olivine during the fluvial transport, the presence of these clasts implies that their source area was relatively near to the deposition region.

Optical microscopic investigation of the comparative sediment samples are manifested also by mineral and rock fragments similar and partially identical to those found in the sherds from Chal, although the amount of volcanic clasts in the sediment samples were, in comparison with the sherds, definitely larger.

Comparing the microscopic results to the geological patterns (Precambrian granitoids, Paleogene volcanites; Foose & Manheim, 1975; Boyanov *et al.*, 1989) of the environment of the archaeological site Chal, several similarities can be found in the presence of plutonic, volcanic, and metamorphic fragments and minerals, although the relatively low amount of volcanites is obvious.

#### **7.1.1.7. Diadovo-Pshenitsevo, Kirilovo**

These central Bulgarian sherds were classified into two petrographic types (Table 2). Most sherds belong to the type 7A/1, characterised by granitic clasts and minerals belonging also to this rock type. Some polyquartz, partially probably as part of the granite, as well as micaschist refer to metamorphic rocks in the source area.

Archaeological material belonging to the type 7A/2 (Table 2) has more varied composition. Aside from the rock fragments mentioned in the previous type, sandstone fragments, basic and/or intermediate volcanites, ARF, phyllite and, micaschist can also be found. Comparing the results to the composition of the comparative sediment sample, I have found several similarities. Most obvious is the presence of texturally quite similar fine-grained sandstone clasts in the geological sample Dia-14

(Fig. 130). Other fragments (e.g. volcanites, ARF, phyllite, polyquartz, plutonites, etc.) found in the sherds are also present in the local river sediments.

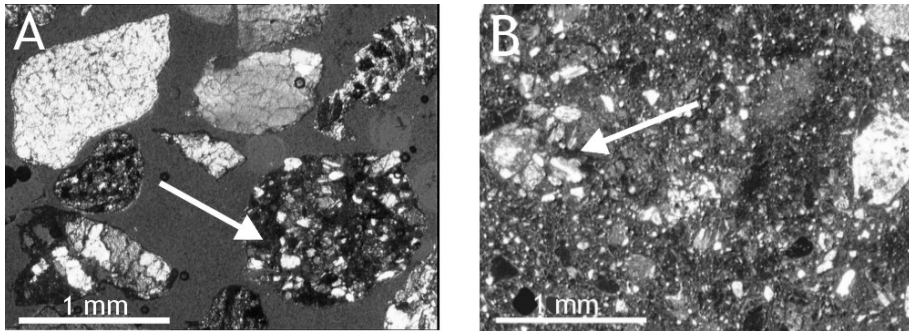


**Fig. 130** Comparative microphotographs of fine-grained sandstone fragments (arrows) in the sediment sample Dia-14 (A) and the sherd DIA-14 (B), Diadovo (+N).

The diverse geological setting of the southern Central Balkanides (cf. Fig. 20 and Chapter 5) is also reflected in this fluvial sediment sample. There are several similarities between the geological material and the sherds, especially small fine-grained sandstone clasts suggest the affinity to local raw materials, thus the local production of the vessels. The non-plastic rock fragments found in the archaeological material might be connected to the lower Proterozoic – upper Paleozoic granitic, Cretaceous volcanic and flysch and flysch-like sediments (Foose & Manheim, 1975; Tzankov *et al.*, 1992; 1995).

#### 7.1.1.8. Sborianovo

Although the distance between the archaeological sites of Sborianovo (north Bulgaria) and Ovcarovo (south-central Bulgaria) is at least 200 km, the very similar texture of the samples SBO-1, 2, 3, as well as OVC-4, 5, and 6 (Fig. 131) suggests the common origin of these pottery fragments.

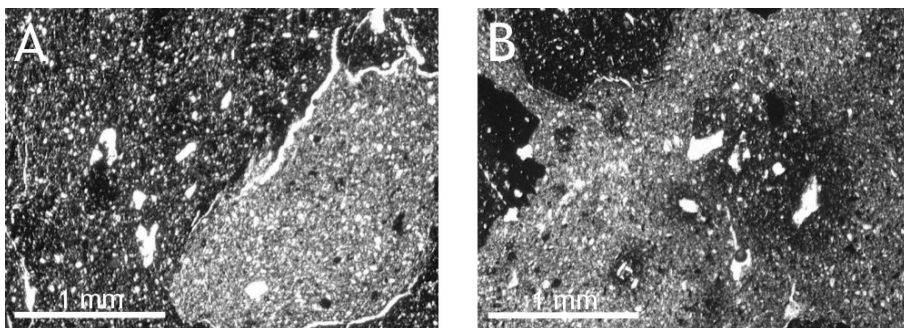


**Fig. 131** Comparative microphotographs of the sherds from Ovcarovo (OVC-1; A) and Sborianovo (SBO-1; B; 1N).

The mineral composition, the lack of rock fragments, and the amount of non-plastic clasts are also unique. Plastic, partially rounded clay pellets, with texture similar to the matrix of the sherds refer to the fact that they were originally part of the clayey raw material. Textural image, mineral composition, the lack of rock fragments make these sherds a well-distinguished petrographic group from other archaeological materials analysed in this study.

Comparing the petrographic results to the geological build-up of northeast Bulgaria, the possibility of the local production is supported. This part of the Moesian Platform is covered by different terrestrial sediments; furthermore a Cretaceous marine limestone is also on the surface in patches (Foosse & Manheim, 1975). Catchment areas of short rivers flowing into the north belong solely to the Moesian Platform, thus they cannot transport materials from areas with more complicated geological settings (e.g. the Balkanides in the South). This is clearly reflected in the mineral composition of the sherds, which also suggests the local production of the samples SBO-1, 2, and 3.

### ***7.1.2. Summary and interpretation of the chemical data of comparative sediments and the sherds***

#### **7.1.2.1. Troia**

According to the geology of the Troad, the lower Mg and Cr values of the sandy and silty-clayey material of the Karamenderes refer to the presence and the alteration products of intermediate to acidic plutonites, neutral and acidic volcanites and different metamorphic series (Kazdağ Massive) belonging to the catchment area of the river. The chromium enrichment in the finer grain size range (clays) of the Karamenderes sediments corresponds to the behaviour of the element (Wedepohl, 1970). Definitely higher MgO and Cr content of the Dümrek sediments is caused by incised metamorphosed ultrabasic rock associations (Knacke-Loy, 1994; Knacke-Loy *et al.*, 1995).

The presence of the (partially) different rock types which belong to the catchment areas of the two rivers in the Troad is also reflected in their multi-element signals. The chemical signal of the Karamenderes also shows more variability especially in Cr and Ni (cf. Fig. 76), which can be ascribed to the presence of ophiolitic to acidic volcanic materials, magmatites, metamorphites, etc. The increase of compatible elements, like Cr and Ni, in some sediment samples of the Karamenderes suggest the influence of intermediate to basic volcanites of the Troad, as well as the effect, in which Cr and Ni, due to their chemical behaviour, are enriched in sediments in finer grain size fraction (Wedepohl *et al.*, 1970).

Positive anomalies in the compatible elements chromium and nickel clearly show the influence of the ultrabasic rocks, which left their chemical fingerprint in the sediments of the Dümrek signal (cf. Fig. 76). Lower K and Rb in the Dümrek sediments and some higher signals of the same elements on the Karamenderes plot refer also to the same processes. Ba is higher in the Karamenders signal than in

that of Dümrek; slightly positive anomalies in Sr may refer to the presence of plagioclase and/or carbonatic material in the samples. The negative anomaly in niobium may refer to the lack of Nb-bearing minerals in the clays or to the diluting effect of quartz (sand fraction). The fact that the elements from Y to V have similar values to PAAS is probably related to the grain size distribution of the sediments.

The MgO and Cr content of most Troian sherds are analogous to the sediment patterns of the river Karamenderes, and clearly overlap with them (cf. Fig. 77). The sample TR-22 with the highest MgO and Cr values suggests affinities with the Dümrek signal (Fig. 132). This statement can be assisted by the presence of olivine and pyroxene fragments found in the sherd (cf. 6.1.1.1.2.), which may have derived from ophiolitic parent rocks found in the vicinity of Troia. The sample TR-24 which contains serpentinite, derived most probably also from ophiolitic parent rocks. It shows, against the expectations, low Cr content and does not match the Dümrek signal neither (Fig. 132). This phenomenon can be either explained by the theory of the mixed (fluvatile) raw material, or with the mixing of different sediments, although the Karamenderes (lower MgO and Cr values) also crosses the Denizgören-Ophiolite zone, thus serpentinite in small amount, may have also preserved in the river sediments. This phenomenon is also confirmed by the petrographic analysis of some Karamenderes sediment samples (cf. 6.1.1.1.1.), where several magmatic mineral and rock fragments of basic-ultrabasic origin have been obtained.

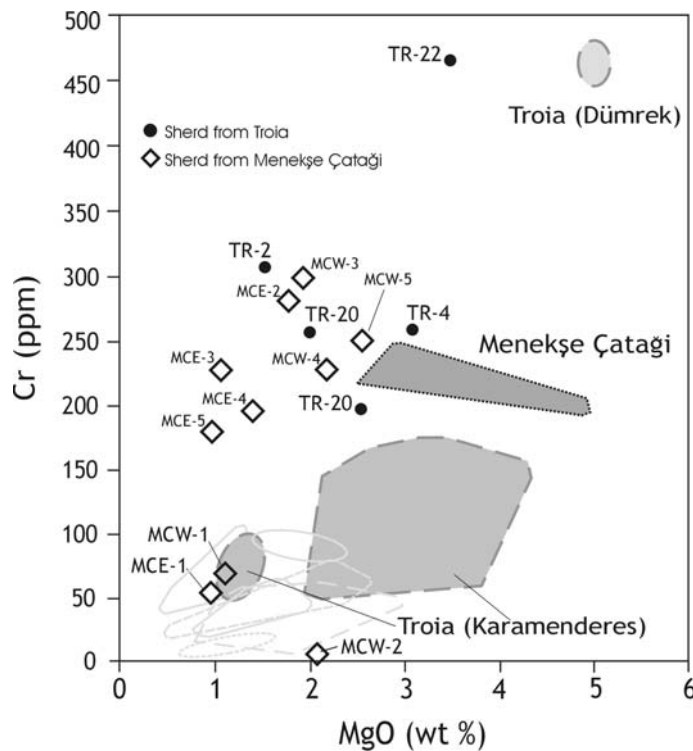


**Fig. 132 Comparative MgO vs. Cr plot of sediments and the sherds from Troia and Menekşe Çatağı (Troian sediment data after Knacke-Loy, 1994).**

The samples TR-2, 4, 20, and 21 match neither the Karamenders nor the Dümrek signals and they overlap with the values of some potteries from Menekşe Çatağı (Fig. 132). To distinguish between the south Turkish Thracian (Menekşe Çatağı) and Troian potteries intermingled due to their Cr content the petrographic data can be used. The samples TR-2 (type *IA/I*), 4 (type *IB/I*), and 21 (type *IB/I*) contain lots of clasts of volcanic origin as well as volcanic glass. These are typical for the geology of the Troad, but atypical for the environment of Menekşe Çatağı. Thus the results suggest the affinity of these 4 sherds to Troian raw materials. The source of the higher chromium content in the sherds must be searched in the clayey matrix, because the non-plastic composition of the potteries does not explain these anomalies. Furthermore, one can establish that there is no connection between the chemical composition and the petrographic grouping of these sherds.

The multi-element data of most Troian sherds also support the petrographic results suggesting the local origin of the samples. Sherds belonging to the petrographic type *IA/I*, and 2 (Table 2) match well the Karamenderes multi-element signal, although most sherds have slightly positive Ba anomaly. According to the data of the microscopic observations, this phenomenon can probably be explained either by the chemical properties of this element (cf. 4.2.3.), or by the presence of Ba-bearing K-feldspars (cf. Chapter 6). It has to also be mentioned that in these sherds Nb has some higher values than the average Karamenderes signal. This may refer to the dominating presence of Nb-rich non-plastic inclusions (e.g. volcanic rock fragments). As we have already seen on the MgO vs. Cr plot, the higher Cr (and Ni) content of the sherd TR-2 also appears in the multi-element plot (cf. Fig.78). Because this phenomenon cannot be explained on the basis of the petrographic data, I assume the mixing of different materials (e.g. Karamenderes and Dümrek sediments) as a possible explanation for this effect.

Although the sample TR-20 (type *IA/3*) also matches the Karamenderes signal, comparing its magnesia, chromium content and its multi-elementary distribution to those of the chemical signals of some samples from Menekşe Çatağı (Fig.132 and 133), no unambiguous differences can be found. Furthermore, its untypical mineral composition does not confirm unambiguously its Troian origin, but does not contradict it either.

In the samples belonging to the petrographic type *IB/I* and 2, as well as *IC* (Table 2), the above described properties can also be observed. Most samples match well the local Karamenderes sediments and follow their pattern.

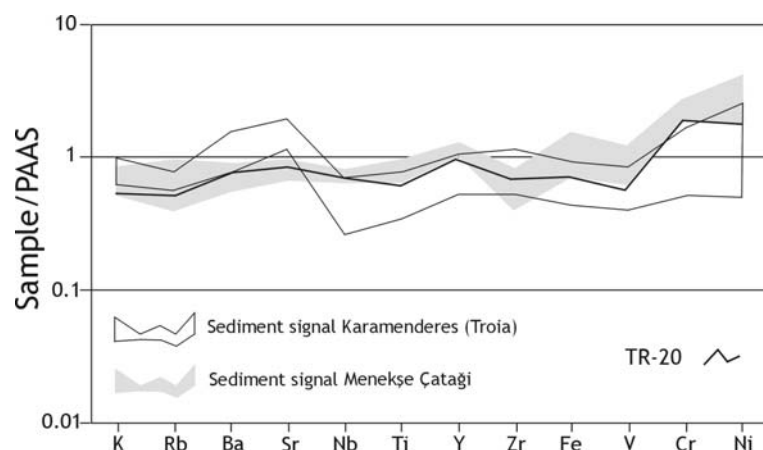


**Fig. 133 PAAS-normalised comparative diagram of the sherd TR-20 and the sediment signals from Menekşe Çatağı and Troia.**

As suggested by the petrographic data and the result of the MgO vs. Cr plot, the sherd TR-22 (type *IB/1*) was directly compared to the multi-element signal of Dümrek sediments. With the exception of barium, there is a very good overlap between the patterns of the sediment signal and the archaeological material.

Two other samples (TR-4 and 21, petrographic type *IB/1*) show higher Fe, V, Cr, and Ni data (cf. also Fig. 81), which cannot be unambiguously explained by the tempering effect or the influence of non-plastic inclusions. Although the sample TR-21 contains almost 4 vol % of opaque minerals, I think that higher Fe and V content are not caused by these Fe-bearing clasts. The theory of mixing different raw materials (clays with higher Fe, V, Cr, and Ni content) is more probable.

The sherds of the petrographic type *IB/2* (Table 2) show similar element distribution to the other samples found in the same group, but they show in their Cr and especially in Ni content negative anomalies, thus they do not unambiguously overlap with the local sediment signal. Considering the non-plastic inclusion content of these sherds, the dominating amount (over 50 vol %) of acidic volcanic glass can be observed. These fragments could cause the dilution of the elementary composition of these compatible elements, although after separating volcanic glass from the paste of the sample TR-7, its chemical composition have shown (Fig. 134) minimal differences between the bulk chemistry and the chemistry of the temper-free material of the sample.

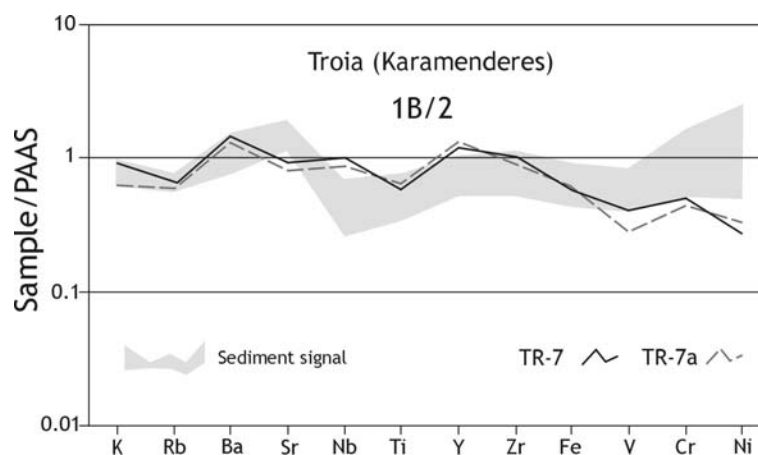


**Fig. 134** PAAS-normalised values of the sherds TR-7 and 7a (petrographic type 1B/2) compared to the multi-element diagram of the Karamenderes sediments, Troia (sediment data after Knacke-Loy, 1994).

Although several studies (e.g. Marro, 1978; Di Pierro, 2003; etc.) have demonstrated the role of tempering in changing the chemical composition, in this case I explain this phenomenon in the following way: paste and tempering material (non-plastic clasts) chemically must have the same or very similar source. This means that the clay used for the ceramic production must be related to the acidic volcanic material (rock formation and/or alteration products). Furthermore, one can also figure out that the vessel of the sherd TR-7 was produced from a raw material situated probably much nearer to the parent rocks (volcanites), and not from the mixed sediments of the Karamenderes plain (polymict grain distribution). In case of the sample TR-7 the very homogenous composition of the non-plastic fragments (volcanic glass, few monoquartz and K-feldspar) and the differences in the chemical patterns also support this suggestion.

#### 7.1.2.2. Menekşe Çatağı

The clayey fine sediments from Menekşe Çatağı indicate higher MgO and Cr content than other sediments from north Turkish Thrace and the Balkans. Cr values between 200 and 250 ppm may refer to the presence of basic volcanites (Yılmaz & Polat, 1998) and their alteration products near to the archaeological site, and/or signify accumulation of this element in the clayey fraction (Wedepohl, 1970; 1972); the latter is, considering the type of geological samples analysed in this study (cf. Appendix 2), more possible explanation.

The high Cr, Ni, Y, Fe, and partially V, as well as low Zr values of the multi-element plot of clayey sediments from Menekşe Çatağı are also typical for the fine-grained (clayey) sediments. Elements from K to Ti do not show big anomalies, they have slightly lower values than the average values of PAAS. Lower Sr values refer probably to non-carbonatic materials.

Comparing the values of the MgO vs. Cr plot of the sherds MCE-2, 3, 4, 5, and MCW- 3, 4, and 5 to the local materials, clear similarities can be found in their MgO vs. Cr content. However, due mostly to the lower MgO content, none of the sherds from Menekşe Çatağı overlap with the local sediment pattern. The difference in the MgO content of the sherds and sediments can either be explained with the high variability of the sediments or by the relatively few sediment samples collected.

The 3 Troian sherds (TR-2, 4, and 20) mentioned above (cf. Fig. 132), which have similar MgO and Cr content to the archaeological samples from Menekşe Çatağı can be distinguished on the basis of their petrographic composition.

The samples MCE-1 and MCW-2 have clearly lower values in chromium, thus the non-local origin suggested by the petrographic analyses is also supported by the magnesia and chromium data. Although the sample MCW-1 was also grouped with other samples into the petrographic type *3A/1*, its chromium value is definitely lower, thus against the petrographic theory it is probably not locally produced.

Observing the multi-element plots one can see that the archaeological material belonging to the petrographic type *3A/1* matches very well the local sediments; furthermore, the distribution of the elements also follows the local sediment pattern. Slightly positive Ba anomaly may refer to the presence of Ba-bearing minerals like different feldspars and mica; however, 3.20 to 17.40 vol % of K-feldspar and plagioclase does not unambiguously explain higher Ba content. In case of this element the role of post burial alteration in the sherds is unclear.

Notwithstanding the good overlap of most samples with the multi-element plots of local sediments, the samples MCW-1 (type *3A/1*), MCW-2 (type *3A/2*), and MCE-1 (type *3B*) show different chemical properties, especially in their compatible elements, which are probably caused by the not local raw materials, thus indicating non-local origin of the vessels. This supposition has already been suggested partially by the petrographic data (cf. 6.1.1.3.1.) and the MgO vs. Cr plots (Fig. 132).

### **7.1.2.3. North Turkish Thrace**

The low MgO and Cr values and the low content of compatible elements (Fe, V, Cr, and Ni) of sediments of the regions of north Turkish Thrace are caused by the geological features of the Strandja region (cf. Chapter 5), because intermediate to acidic plutonites, metamorphites, from which they were derived, have characteristic low content of magnesia and chromium (Wedepohl, 1970; 1972). Slightly positive anomalies (but also some variability) in the elements Sr, Y, and Zr refer to the nature of the parent rocks (mostly acidic magmatites, metamorphites) and also to the diversity of the samples (fine-grained to coarse sediments). Potassium, rubidium, and niobium have values similar to the PAAS-values, or lower. Negative titanium anomaly may also refer to the geological setting of the parent rocks.

Furthermore, the data from this region also overlap, or are very similar to those from Ovcárovo and Diadovo-Pshenitsevo-Kirilovo. This fact can also be explained by the geological setting of the different areas (cf. Chapter 5). On the basis of MgO vs. Cr plot, the sediments of these areas cannot be further distinguished. The above mentioned similarities are also found in the multi-element signal of the sediments of the central Bulgarian and north Turkish Thracian regions; although the signals of the sediments from Diadovo-Pshenitsevo-Kirilovo have more various patterns, and thus they are useful for distinguishing them from the north Turkish Thracian signal.

The multi-element sediment pattern (Fig. 135) also shows clear similarities with that of Ovcárovo, due to the almost same geological build-up of these study areas (the south-western Strandja Massive).

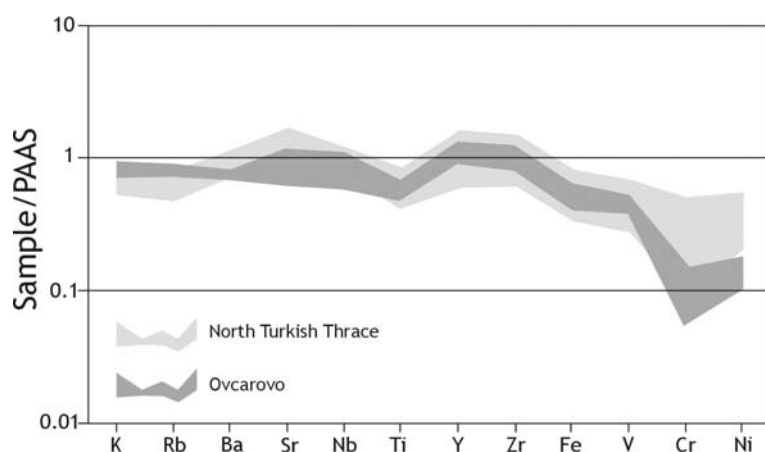


**Fig. 135 Comparative plot of PAAS-normalised multi-element sediment patterns from north Turkish Thrace and Ovcárovo.**

More variability obtained in the north Turkish Thracian sediments is probably due to more complex geology of the region and larger amount of samples collected there (cf. Appendix 2).

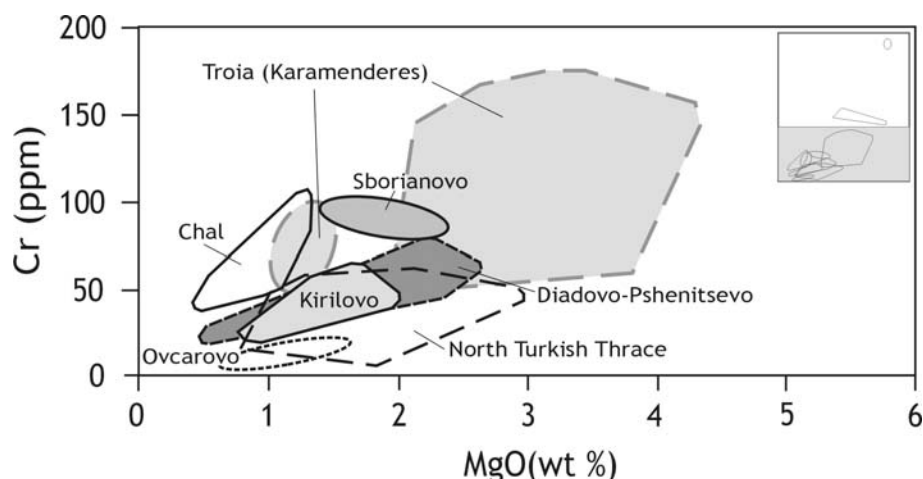


**Fig. 136 Overlaps of the MgO vs. Cr sediment signals from central Bulgaria, north Turkish Thrace and Troia (Troian sediment data after Knacke-Loy, 1994).**

The chemical data (MgO vs. Cr plot) of the sherds from north Turkish Thrace (with the exception of the sherd AT-2), overlap well with the local sediments, but also with other sediment patterns

(Ovcarovo, Diadovo-Kirilovo-Pshenitsevo; Fig. 136) and with the sherds from different areas (Troia, Ovcarovo, Diadovo-Kirilovo-Pshenitsevo).

Notwithstanding the above mentioned good overlaps between the sherds and local sediments, on the basis of their MgO vs. Cr plots, the differentiation of the sherds from north Turkish Thrace and the archaeological materials from Ovcarovo (the samples OVC-1, 2, and 3), Diadovo, Kirilovo, and Pshenitsevo is not possible. The common origin with the Troian sherds of similar MgO and Cr content can be excluded, due to the great amount of volcanic rock fragments and volcanic glass (cf. 7.1.1.1.), which is typical for the Troad, but atypical for the Strandja Massive.

The low Cr content of the archaeological materials from north Turkish Thrace, Ovcarovo, and Diadovo-Kirilovo-Pshenitsevo indicates the dominating presence of mono- and polyquartz, granitic rock fragments and the parent rocks of the clayey alteration products (cf. Chapter 5). These chemical results are also in accordance with the microscopic observations.

The multi-element pattern of the sherds collected in north Turkish Thrace (the petrographic type *4A/1*) has very similar chemical properties, which generally match well the local sediment pattern, although every sherd has clearly positive Ba anomaly. This phenomenon is either caused by the mobile chemical property of the element or by the presence of the Ba-bearing minerals (alteration products) of the sediments. Cr and Ni values range in wider scale, but the negative chromium and nickel anomaly with slightly nickel increase is a typical property of each sherd. Low values in the elements iron, vanadium, chromium and nickel are in good accordance with the petrographic features of the sherds and the dominating presence of minerals and rock fragments related to magmatic-metamorphic source rocks of intermediate-acidic origin.

The distribution of the elementary composition of the pottery fragment HM, ranked into the petrographic type *4A/2*, is very similar to other sherds found in north Turkish Thrace and thus it refers also to the affinity with local raw materials.

Contrary to this, the sample AT-2 (petrographic type *4B*), as already suggested by its optical microscopic and its very high magnesia and chromium content, shows totally different chemical patterns, which appear in clearly negative Zr and positive Fe, V, Cr and Ni anomalies, which also confirm the non-local production of the vessels.

#### **7.1.2.4. Ovcarovo**

As it has been mentioned above, the overlap on the magnesia vs. chromium plot with sediments from north Turkish Thrace is caused by the almost the same geology of these study areas and thus by the similar chemical properties of the sediment samples.

In Ovcarovo on the multi-element plot the serial Fe, V, Cr, and Ni show decreasing trend and the two most compatible elements also have lower values than in samples from the north Turkish Thracian

region. This phenomenon can also partially be explained by the coarser grain size of the samples (fine sands to sandy clays).

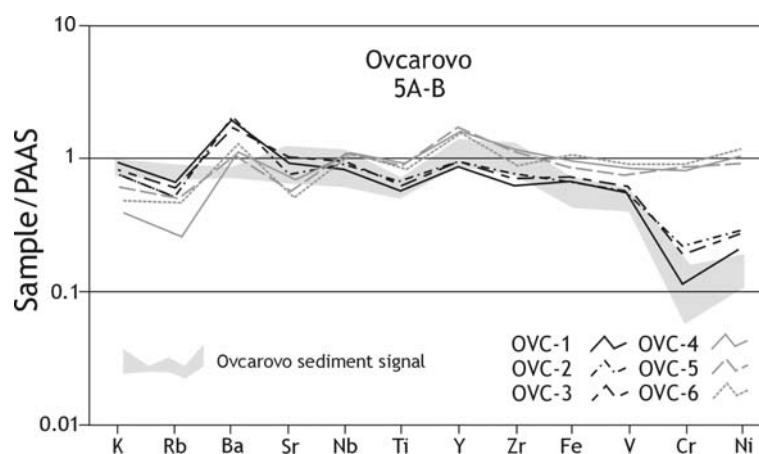


**Fig. 137 Comparative plot of the PAAS-normalised multi-element sediment pattern of Ovcarovo and the sherds OVC-1, 2, 3, 4, 5, and 6 (petrographic subgroups 5A and B).**

Although the sherds from Ovcarovo (petrographic subgroup 5A, the samples OVC-1, 2, and 3) match well the local sediments, due to the similarities in the geology of the south- and north-western part of the Strandja Massive, they have very similar chemical patterns to the archaeological material from north Turkish Thrace. The same positive Ba anomaly can also be observed, but Y, Zr, Fe, and V content is slightly lower than the average values of the sherds from NTT. This difference is, however, not sufficient for clear differentiation. Comparing the chemical data of the sherds OVC-4, 5, 6 (petrographic subgroup 5B) to the local sediment pattern clear differences can be observed. Almost all elements have different values, as those of the local sediments (Fig. 137). The data of the microscopic observations support the supposition that the vessels from which these sherds originated were not produced in their place of find.

#### 7.1.2.5. Chal

The MgO vs. Cr content of the sediments from Chal is also similar to other central Bulgarian samples, although some higher Cr and Mg values distinguish its chemical pattern from them. The multi-element patterns range between wider values (cf. Fig. 99), which is probably caused by the grain size distribution of the sediment sample Ch-2 (high values in Y, Zr, low in Fe, V, Cr, and Ni). All sediment samples reflect approximately the main geological features of the region (cf. Chapter 5). To this refer low Ti, Fe, V, Cr and Ni data, high Y, Zr and Nb. The averaged or slightly lower values of K, Rb, Ba, and Sr can be in accordance with leaching and/or adsorption effects.

The magnesia and chromium content of the sherds overlaps with the local sediment patterns, thus suggesting local origin of the raw materials.

Multi-element plots of the sherds have geochemical similarity to the local sediments, but mobile elements, like Ba and Sr have higher values, and Ni does not show negative anomaly; it rather slightly increased relative to Cr. The sample CH-2 has clearly higher values in most of its elements, but the distribution of Nb, Ti, Y, Zr, and Fe match well the local geological materials. Higher Nb, Y, and Zr may refer to the presence of material derived from acidic plutonic or volcanic material; however, the distribution of the elements is not exactly clear, especially the lack of the negative Ni anomaly and the lower amount of Ba and Sr relative to the other sherds. Although on the basis of the MgO vs. Cr plot the sherd CH-2 clearly overlaps with the sediment pattern of Sborianovo, due to its petrographic features (cf. 6.1.1.8.1.) and due to the good match of the multi-element data its origin from Sborianovo can be excluded.

#### **7.1.2.6. Diadovo-Pshentitsevo, Kirilovo**

As it has already been mentioned, the magnesia and chromium content of the geological samples from Diadovo-Pshentitsevo and Kirilovo overlap with each other and also with other sediment signals from the southern Bulgarian and Strandja region. This is due to the similar geological build-ups of the different study areas (cf. Chapter 5) which have left their geochemical fingerprints on the analysed sediments.

Multi-element data of sediments show more variable patterns; therefore they can be regarded as a tool for distinguishing local geological materials from other sediments (north Turkish Thrace, Ovcarovo).

The signals from Diadovo-Pshentitsevo and Kirilovo are similar, with the main difference that the sediments from Diadovo-Pshentitsevo range more (also more have been collected samples from there; cf. Appendix 2) in the values lower than average. Slightly negative Ti and positive Y and Sr anomaly, and decreasing values from Fe to Ni may refer to the geology of the parent rocks of the sediments (cf. Chapter 5), although it is not clear whether Sr originated from carbonates, or from the weathering of Ca (Sr)-bearing minerals like plagioclase.

As it was mentioned above, because of the overlaps, only the MgO and Cr composition of the central Bulgarian sherds does not provide sufficient information for distinguishing these samples from other sherds from other localities with similar magnesia and chromium content.

Using the multi-element patterns of sediments (Fig. 138) and the sherds from Diadovo-Pshentitsevo and Kirilovo one can see, that they form three element distribution patterns (cf. Fig. 104, 105, and 106).

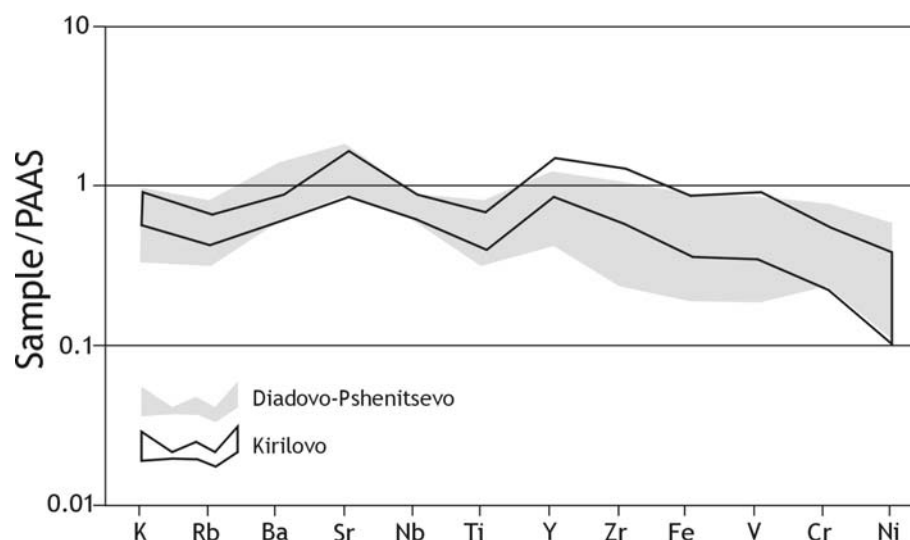


**Fig. 138 Comparative plot of the PAAS-normalised multi-element sediment patterns from Diadovo-Pshenitsevo and Kirilovo.**

The differences which can be observed between the distribution of the elements of the sherds PSH-1, 2, and 3 (type 7A/1) and DIA-1, 2, 5, 7, 8, 10, and 11 (type 7A/1) are probably related to the different clayey materials and not to the influence or diluting effect of the magmatic, quartz-bearing temper, because all sherds mentioned above belong to the same petrographic group (Table 2) and the amount of non-plastic inclusions are also approximately similar.

The pottery fragment KIR-3 (Kirilovo, type 7A/1) follows accurately the local sediment patterns. The samples KIR-1 and 2 (type 7A/1) which are, due to the almost same chemical pattern, possibly two fragments of the same vessel, have lower Rb and higher Fe, Cr content. These phenomena cannot be explained by the tempering effect, because the non-plastic composition of the sherds (quartz, magmatic of acidic origin, low content of Fe rich minerals e.g. opaque clasts, etc.) does not support this interpretation. Higher Fe and V content must probably be the specialty of another clay source, about which I have no information.

The sherds DIA-3, 4, 6, 9, 12, and 13 (petrographic type 7A/2) have different chemical patterns, which are mainly reflected in the amount of compatible elements like Fe, V, Cr, and Ni.

Elements from K to Zr (Fe) match well the local material patterns and they also follow their distribution, but the partially slightly anomalous Fe, V and Ni values do not necessary mean non-local production but the presence of the natural variation of the raw materials.

#### **7.1.2.7. Sborianovo**

The values in magnesia and chromium of the geological material from Sborianovo can probably be ascribed to the grain size of the samples, but the averaged Cr content of terrestrial sediments (Wedepohl, 1970; 1972) also corresponds with my data.

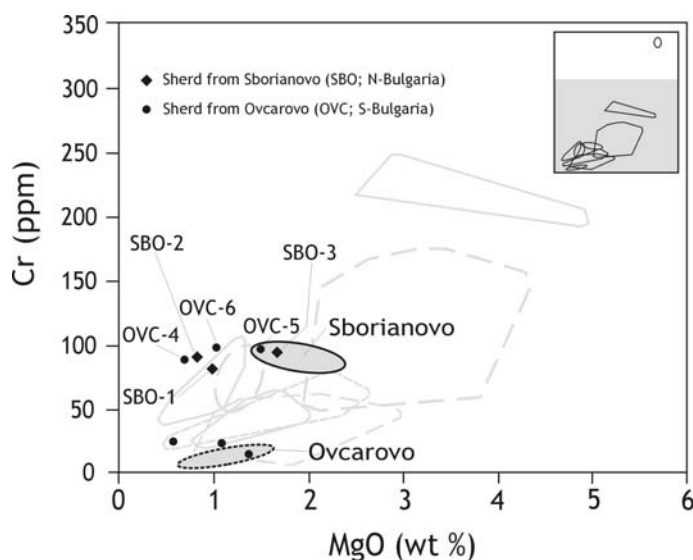


**Fig. 139 Comparative MgO vs. Cr plot of sediments and the sherds from Ovcarovo and Sborianovo.**

Very small range in the multi-element data of Sborianovo has been reflected in the homogenous samples and geological setting, and in the fact that no fluvial contamination occurred between the local sediments and other materials transported from other areas with different geological settings. Slightly positive Nb and Y, as well as negative Ti anomalies may also refer to the presence of fine-grained materials and terrestrial sediments (Wedepohl, 1972; 1974)

The sherds SBO-1, 2, 3, as well as OVC-4, 5, and 6 have higher Cr values than other samples from the Balkans analysed in this study, and although only two samples overlap clearly with the local sediments from Northeast Bulgaria, they are similar in their main chemical features. Similarly to the petrographic data, these results also suggest the affinity of these six pottery fragments to the raw materials from Sborianovo (Fig. 139).

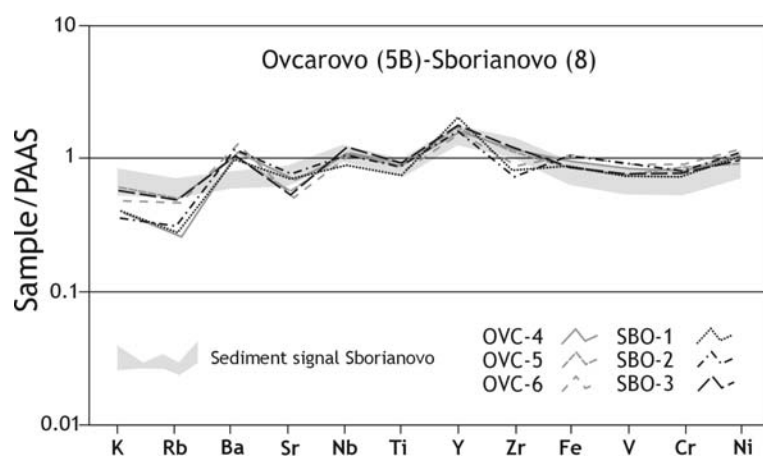


**Fig. 140 Comparative plot of the PAAS-normalised multi-element sediment pattern of Sborianovo and the sherds OVC-4, 5, and 6 (petrographic subgroup 5B), and SBO-1, 2, and 3 (petrographic group 8).**

The chemical data of multi-element plots also support this theory. Comparing the chemical patterns of the sherds (SBO-1, 2, and 3, as well as OVC-4, 5, and 6) very good match can be obtained with the

sediment patterns from Sborianovo. The only differences are: elements K, Rb, Sr, and Zr show lower values in the samples OVC-1, SBO-1, and 2 (Fig. 140) but most elements and the average chemical patterns refer also to the affinity to the local sediments. Slight differences in the K and Rb content may refer to post burial (leaching, etc.) processes, although the presence of this effect is not proved.

### ***7.1.3. Summary and interpretation of the radiogenic isotope results***

The trend which was observed in the isotopic composition of the samples analysed in this study can be interpreted in the following way from  $^{143}\text{Nd}/^{144}\text{Nd}$  relatively enriched and  $^{87}\text{Sr}/^{86}\text{Sr}$  relatively depleted to the  $^{143}\text{Nd}/^{144}\text{Nd}$  relatively depleted and  $^{87}\text{Sr}/^{86}\text{Sr}$  relatively enriched materials:

Troian sediments (Knacke-Loy, 1994) seem to be the most depleted in the more incompatible Sr and enriched in the more compatible Nd. These results are in accordance with the geology of the Troad: namely various rock types and eminent domination of different volcanites and plutonites (from ultrabasic to intermediate-acidic types). These features are released in the higher  $^{143}\text{Nd}/^{144}\text{Nd}$  and lower  $^{87}\text{Sr}/^{86}\text{Sr}$  ratios of the clayey-silty sediments taken from fluvial sediments.

By means of the radiogenic isotope ratios, the sherd TR-8 shows clear affinity with Troian local raw materials, due to the clear overlap with the local sediment signal of the area (cf. Fig. 110).

The sherd TR-20 of uncertain origin falls on the diagram between the plots of the local Troian materials and the locally produced sherds (Knacke-Loy, 1994) and local sediments of Menekşe Çatağı; it also overlaps with the material from Chal (Fig. 140). The origin of the vessel fragment TR-20 from Chal can be excluded, due to the chemical and petrographic differences of the sherds and sediments. The isotopic results confirmed unambiguously neither the origin from Troia nor from Menekşe Çatağı. This means that either the isotopic variability of one or both areas is larger than the data indicate (from Menekşe Çatağı only four local sediment samples and sherds have been measured), or the mixing of different Troian raw materials (cf. MgO vs. Cr plot; Fig. 132) occurred. Because of the relatively fine-grained texture of the sherd (cf. Fig. 33), the influence of temper on the bulk isotopic composition can be excluded.

The third Knobbed ware sherd (*E9.158.1*; cf. Guzowska *et al.*, 2003), which was analysed after separating its volcanic inclusions, shows clearly a shift towards the lower Nd ratios (in the Sr isotopic data no remarkable changes occurred). I think, this phenomenon can be predicated on the lack of the separated volcanic clasts, which have influenced the composition of the whole clayey material with their relatively higher  $^{143}\text{Nd}$  isotope content. Although after separating these clasts no clear overlap has been obtained, the values, the shift of the data, and the petrographic composition suggest the affinity to the local materials, and thus the local production (Fig. 141).

Following the isotopic trend, suggested by the samples from different areas, the sherds and sediments from Chal (southwest Bulgaria) with lower  $^{143}\text{Nd}/^{144}\text{Nd}$  and higher  $^{87}\text{Sr}/^{86}\text{Sr}$  ratios may refer to the presence of granitic and volcanic material in the vicinity of the study area. Although Nd isotopic data

range relatively little, bigger differences can be observed between the Sr values of the sherds and sediment samples. One can also obtain this effect in other samples (e.g. Diadovo), where similar Nd isotopic values but clearly higher  $^{87}\text{Sr}/^{86}\text{Sr}$  ratios were measured in the sherds than in sediments (Fig. 141).

This can be either explained by the non-local production of the sherds (although, in order to constrain the local isotopic fields, on the basis of petrographic and chemical analyses, sherds of local origin have been chosen) or, and this is more probable explanation, the presence of temper has influenced the final isotopic composition of the archaeological material. It is also possible that the variation within the local sediments is larger.

The sherd CH-5 (Chal) has very similar values to the sediments from Menekşe Çatağı. The possible place of origin from the coast of the Sea of Marmara can be excluded due to the different chemical properties of the sherd. Higher  $^{87}\text{Sr}/^{86}\text{Sr}$  ratio could be caused by the presence of biotite in the material (Fig. 141).

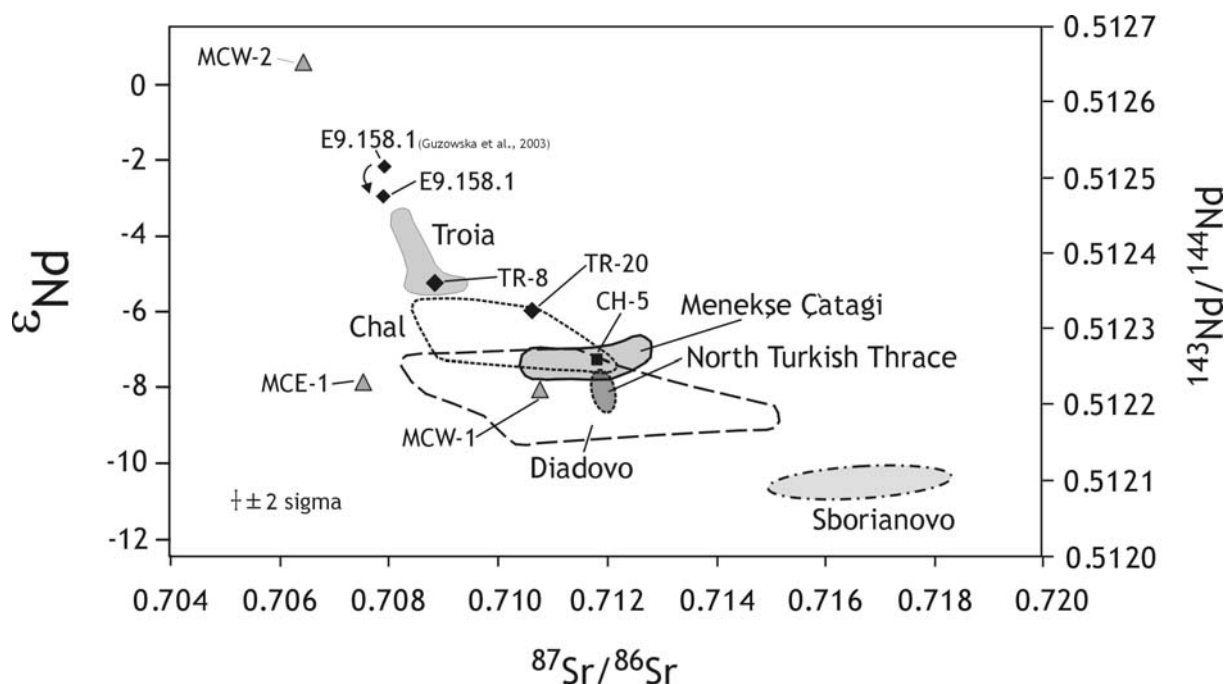


**Fig. 141** Isotope ratios of the “study areas” determined by geological samples and locally produced sherds as well as the sherds (triangles, diamonds, and quadrangle) of uncertain origin (Troian sediment values after Knacke-Loy, 1994).

Unfortunately, the regions with similar geological build-ups show also similar isotopic data, thus they strongly overlap and more accurate distinction is not possible. These samples and areas are: Diadovo, Menekşe Çatağı, and north Turkish Thrace. The samples with low  $^{143}\text{Nd}/^{144}\text{Nd}$  and higher  $^{87}\text{Sr}/^{86}\text{Sr}$  ratios imply the presence of crustal (granitic) materials in the environment. The data of the samples from Menekşe Çatağı suggest that clayey material is probably not related to the alteration products of the basaltic materials in the environs. Thus high Cr and Ni values of the sediments (XRF data)

probably refer to the finer grain size of the sediments. The variation of the values of sediments and sherds, which suggested local origin is small, thus the isotope signal of Menekşe Çatağı is relatively well-determined.

The isotopic data of the pottery fragment MCW-1 (Menekşe Çatağı) which did not suggest the local origin on the basis of its chemical signal, refer either to the affinity to local materials, or maybe to the north Turkish Thrace region (Fig. 141). This latter hypothesis would also be supported by the low Cr and Ni content.

The origin of the raw material of the sherds MCE-1 and MCW-2 (Menekşe Çatağı) from different regions is also supported by radiogenic isotope investigation. Comparing to local materials the lower  $^{87}\text{Sr}/^{86}\text{Sr}$  ratios (MCE-1) as well as lower Sr and higher Nd isotopic data of the sherd MCW-2 refer to this phenomenon (Fig. 141). Although the isotopic results of the latter sherd show big difference, petrographic composition of the material does not explain this difference. Lots of biotite found in the sherd MCW-2 (high amount of  $^{87}\text{Rb}$  which decays to  $^{87}\text{Sr}$ ) would rather effect higher  $^{87}\text{Sr}/^{86}\text{Sr}$  ratios. Although the positive  $\epsilon_{\text{Nd}}$  value of the sample suggests the presence and/or the influence of mantle-derived (e.g. basaltic) materials in the raw material, this supposition is not supported by the petrographic data either. On the basis of the data the supposed place of origin is still unknown.

The small variation of the geological and archaeological samples from the north Turkish Thrace forms a well-determined signal and confirms the results of petrographic and other chemical results. The overlap of the north Turkish Thrace signal with other materials can be explained with the geological similarities again.

Similarly to the material from Chal, the pottery and clayey geological samples from Diadovo show more variability in the  $^{87}\text{Sr}/^{86}\text{Sr}$  ratios. Although the  $\epsilon_{\text{Nd}}$  values are similar, local sediments have clearly lower  $^{87}\text{Sr}/^{86}\text{Sr}$  ratios than the sherds (Fig. 141).

After leaching the calcite content of these carbonate-bearing clays, I have estimated some increase in the  $^{143}\text{Nd}/^{144}\text{Nd}$  ratios. In the Sr values no appreciable changes occur. The phenomenon of the secondary carbonate in the clayey material not influencing strongly its  $^{87}\text{Sr}/^{86}\text{Sr}$  ratio is in good accordance with the results of other studies (Carter *et al.*, 2004). There are two possible explanations for the differences in  $^{87}\text{Sr}/^{86}\text{Sr}$  values between local sediments and locally produced ceramics. One of them is the “tempering effect”. The presence of granitic temper (high amount of the  $^{87}\text{Sr}$  isotope) in the sherds might influence the bulk composition of the materials and/or the presence of seawater related sediments (e.g. flysch sediments and rocks in the Southern Balkanides; cf. Chapter 5) which may imply lower  $^{87}\text{Sr}/^{86}\text{Sr}$  ratio; this phenomenon is reflected in the geological materials investigated in this study.

The clearly lower  $^{143}\text{Nd}/^{144}\text{Nd}$  as well as higher  $^{87}\text{Sr}/^{86}\text{Sr}$  ratio of the sherd and clay taken from Sborianovo implies the terrestrial origin of these samples (Rollinson, 1993).

By means of the isotopic results, the South, North Bulgarian, and Troian regions, and locally produced sherds are distinguishable. Unfortunately, the data do not allow for the more accurate separation of the north Turkish Thracian and Central Bulgarian regions, which can be explained by the similar chemical properties of the materials, caused again by the similar geological setting.

Isotopic data provide only complementary data in this study; based on these results Troian local sediments and sherds are distinguishable from other areas. **Furthermore, the new isotopic data on ceramics proved the importance of the simultaneous use of geochemical and microscopic results and the role of “tempering effect” in the provenance analysis.**

#### ***7.1.4. Summary and interpretation of the EMPA results***

##### *Sherd MCE-1 (Menekşe Çatağı)*

Unfortunately, the chemical composition of the volcanic fragments found in this sherd did not supply sufficient information about the accurate composition of the minerals nor about the exact type of the rocks. Although the petrographic data and the texture of the volcanic clasts suggest intermediate (maybe andesitic) composition of the rock fragments, only K-feldspar, albite, and amphibole were determined in them. Lots of albite and lack of intermediate plagioclase suggest that during or after the petrogenesis of the volcanic rocks albitisation took place. Recrystallised texture of most volcanites also suggests that alteration, recrystallisation, silicification (secondary quartz in fragment B) has changed the textural and probably also the chemical properties of the original parent rocks.

Giacomini (2003) reports that in ceramics albites with potash feldspar-rich rim can be developed as a result of a mutual exchange of K and Na between albite and clay minerals at temperature exceeding 850 °C. Very similar K-feldspar-rich zoned albites were also found in the sample MCE-1 (cf. Fig. 112), although they were situated in a volcanic fragment, thus I have excluded the theory of mutual exchange between the albite and clay. Furthermore, based on the XRD analysis (cf. 7.2.3.), the supposed firing temperature in most cases probably did not reach 850°C. This phenomenon may either refer to secondary alkali metasomatism or to the exsolution of albite and K-feldspar during the cooling phase of the volcanic rock (Gábor Dobosi, personal communication).

On the basis of these results, this supposition did not sufficiently converge to the solution of the origin of the volcanite fragments in the sample. I suppose that these fragments have most probably had intermediate composition. As we have seen, in the southern part of the Balkans many areas are made up of intermediate volcanites. In the south western part of the Thrace basin late Eocene-early Miocene high-K calc alkaline andesites are found (Yılmaz & Polat, 1998). This is the nearest place to Menekşe

Çataği, where andesite is situated. The EMPA data do not unambiguously refer to these rocks, but they can be considered as potential parent rocks (cf. also NAA data).

*Sherd AT-2 (north Turkish Thrace)*

The composition of clinopyroxenes measured in the sherd and in volcanic fragments can imply different magmatites as parent rocks. According to Deer *et al.* (1978) diopside is mainly characteristic for magmatites of basic and ultrabasic origin, although in that case the presence of relatively high amount of chromium would refer to these parent rocks. Furthermore, K-feldspar and a rock fragment, where diopside occurs together with K-feldspar, do not support this suggestion. Other important rock types where diopside can occur are: skarn rocks (due to the non-plastic fragment composition of the sherd its presence can be excluded) and alkaline rocks. Acidic magmatic rocks mostly contain hedenbergite (Deer *et al.*, 1978). Although diopside-bearing intermediate (andesite), maybe more acidic (dacite) rocks are not very common, they can be found in some geological environments (Gábor Dobosi, personal communication). Furthermore, potash feldspars in diopside-bearing volcanite fragments and the fragment containing clinopyroxene and K-feldspar phenocrysts may refer to the intermediate composition of the volcanite. However, I did not find any plagioclase with intermediate composition in the phenocrysts of the volcanic clasts. The two plagioclase crystals, situated in the clayey material with low anorthite component ( $Ab_{82-84} - An_{16-18}$ ), rather imply an acidic parent rocks. Furthermore, the presence of albite was probably at least partially caused by a primary albitisation process of the plagioclase.

Considering the relatively few measurements, the small size of inclusions, and the uncertainties in the possible interpretation, I suppose, that the parent rock of the clinopyroxene was either andesite or dacite. In the latter case the presence of acidic plagioclase could also be explained.

On the basis of their chemical composition, Cr-spinels found in a glassy volcanic clast are probably derived from a basaltic source rock formed at an island arc or in intraplate basalt setting, as suggested by the  $Al_2O_3$  wt % -  $TiO_2$  wt % diagram (cf. Fig. 124).

Because of the domination of these two materials in the sherd, the results suggest that in the place of origin, or near to, it intermediate (andesite?) or more acidic (dacite?) and basalt volcanoes are found. Intermediate to acidic volcanoes are widely spread in the eastern part of the Rhodope Mts. Near to the present Greek-Bulgarian border island-arc and intraplate basalts also occur (Dabovski *et al.*, 1989). These rock formations can be followed until the south-eastern spur of the Rhodope Mts. in Greece. More detailed data can be found in the works of Nedialkov & Pe-Piper, (1998), Yanev (1998), and Yanev *et al.* (1998).

Without the detailed review of the geology of these volcanic areas, I have used the data from Nedialkov & Pe-Piper's (1998) report. They investigated volcanites of different (rhyolite, dacite, andesite, latite and basalt) composition in the Tintyava-Ustern extensional zone (East-Rhodope, Bulgaria). They reported about K-feldspars found in the dacites with  $Ab_{22-38}-Or_{77-58}$  composition. The clinopyroxenes found in basalts and andesites have an average composition of  $Wo_{3-4}En_{66-67}Fs_{29-30}$ . Yanev (1998) presented data from the same area mostly on rhyolitic volcanites. He analysed rocks from the Hissar volcano (trachydacite) and found that the composition of the clinopyroxene is  $Wo_{44}En_{38}Fs_{18}$  and that of K-feldspar is  $Or_{43}Ab_{48}$ . Based on my and other authors' data, this area (and the southernmost Maritsa valley in Greece) seems to be the best candidate for the possible place of origin of the sherd AT-2. But also comparing our EMPA data to those of other authors, several differences can be observed in the composition of clinopyroxenes, plagioclases, and K-feldspars. Furthermore no data were found referring to the supposed albitisation process.

### ***7.1.5. Summary and interpretation of the NAA results***

The distribution of REE, the enrichment of LREE in the sherd TR-20 similar to locally produced Grey Minyan wares from Troia (Knacke-Loy, 1994) suggest the affinity to Troian local materials. Notwithstanding the similarities of the REE pattern between the sample TR-20 and locally produced vessels, there is no data available about the locally produced sherds from Menekşe Çatağı. Therefore doubtful results of petrographic investigation, XRF, and isotopic analyses, and the lack of the REE pattern of sherds from Menekşe Çatağı have to be observed by the final provenance.

The REE pattern of the volcanite fragments of the sample MCE-1 does not show affinity to the LREE more enriched (Yılmaz & Polat, 1998) Miocene-Quaternary basanites and alkali olivine basalts nor to the basaltic rock fragment (Mc-8) found in the archaeological site, but the data refer to the affinity to a LREE more depleted volcanic parent rock. As the data (Yılmaz & Polat, 1998) have shown, one of the best candidates for these parent rocks are calc-alkaline andesites situated westward and larger distance (20-60 km) from the archaeological site of Menekşe Çatağı, although on the basis of the EMPA results unambiguous affinity cannot be observed.

### ***7.1.6. Grouping of the sherds on the basis of their origin***

On the basis of the results, the sherds can be grouped into 4 groups concerning their origin:

- (1) The complex petrographic-chemical analyses carried out in this study revealed that the following sherds show clear similarities to local materials (sediments, rock samples, locally produced sherds), and they are also well distinguishable from other sherds; thus they were produced locally (43 samples):
  - all sherds from Troia (with the exception of the sample TR-20);
  - all sherds from Menekşe Çataği (with the exception of the samples MCE-1, MCW-1, and 2);
  - the sherds from Diadovo belonging to the petrographic type 7A/2;
  - the sherds from Sborianovo.
- (2) The following vessels were with high probability locally produced or the place of production can be connected with the environs of their place of find (39 samples):
  - the sample A-1 (the Avşa or the Marmara Island);
  - all sherds from north Turkish Thrace (with the exception of the sample AT-2) and from Ovcarovo (with the exception of the samples OVC-4, 5, 6);
  - all sherds from Chal, and from central Bulgaria (Kirilovo, Pshenitsevo, Diadovo; belonging to the petrographic type 7A/1).
- (3) One sherd, and consequently the vessel, turned out to be of uncertain origin:
  - Troia: the sample TR-20.
- (4) Some analysed sherds show that the vessels they originated from were certainly not produced locally in the place of find (7 samples):
  - Menekşe Çataği: MCE-1 (supposedly originating from the volcanic region of the south-western Thrace basin?), MCW-1, 2 (supposedly originating from the Strandja region?);
  - North Turkish Thrace: AT-2 (supposedly originating from the southern Rhodope?);
  - Ovcarovo: OVC-4, 5, 6 (supposedly originating from Sborianovo or its environs).

## 7. 2. The production technology of the Knobbed ware

In the subchapter 7.2. I will summarise and interpret the results of the fabric and phase analyses concerning the second question of my dissertation: under what circumstances (raw-materials, firing temperature, and atmosphere) was the Knobbed ware produced.

### 7.2.1. Possible raw materials used for the pottery production

I have used the results of the fabric analysis (colour and isotropism (optical activity) of the groundmass, type of texture, sorting of grain size distribution, maximum grain size, roundness and sphericity of the clasts; cf. Appendix 4) in order to detect the types of the raw materials used for pottery production as well as the technology of ceramics producing.

Among the 90 studied sherds, 35 have anisotropic or partially anisotropic texture (yellow-orange colour), the rest have isotropic textural properties (brown-dark brown colour; cf. Appendix 4; Fig. 142).

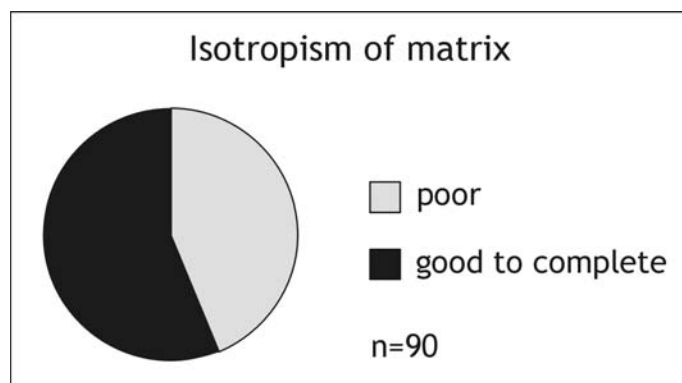


**Fig. 142 Isotropism of matrix of all Knobbed ware sherds analysed in this study.**

Isotropic textures (61 %), as we will also see it in the interpretation of the XRD data, signify non-calcareous paste (clays) and not high firing temperatures, where carbonate does not exist anymore. Primary and/or artificially added calcite temper (carbonatic inclusions, marble fragments, etc.) have not been regarded in the isotropism of the sherds.

Mostly hiatal texture and coarse clasts in the sherds (Fig. 143) refer directly to artificial tempering, but potential raw materials and sedimentary environments must also be considered in the interpretation of the textural properties of ceramics. In loams in the vicinity of piedmont areas, due to the short distance of transport, angular clasts can be found (Maggetti, 1994).

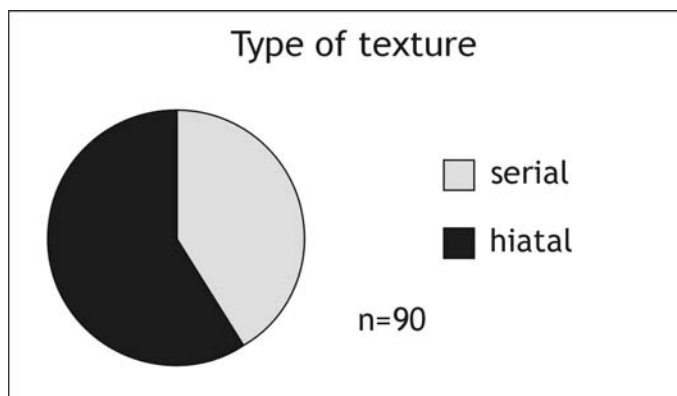


**Fig. 143 Type of texture of all Knobbed ware sherds analysed in this study.**

Sands derived from sedimentary environments, like fluvial or shoreline systems, different fragments of different roundness, depending on the hardness of the clasts, could also be added as artificial temper to the paste (Szakmány, 1998). The variable (polymict) mineral composition and rock fragments of a sherd may also suggest the fluvial origin of the material (lower course of the river or different rock associations in the catchment area). Especially when the distribution of the grain size is serial, the material is unsorted, and the roundness of the clasts generally varies from subangular to (sub) rounded, fluvial material (mud, silty clay, etc.) had probably been used for pottery production.

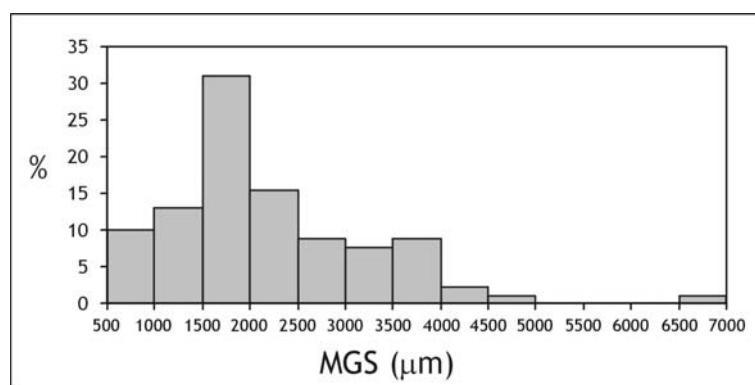


**Fig. 144 Distribution of the maximum grain size (MGS = largest non-plastic inclusion found in the sherds) of all Knobbed ware sherds analysed in this study.**

The histogram (Fig. 144) of the maximum grain size (MGS) of the non-plastic inclusions shows that in most sherds the largest grains belong to the grain size range 1500-2000  $\mu\text{m}$  (very coarse sand) and several samples contain grains over 2 mm. Comparing these data with the type of texture (serial, hiatal; cf. Appendix 4; Fig. 143) the following preparatory techniques for sediments and raw material can be differentiated and assumed:

- (a) sediments with (very) fine-grained texture and serial distribution of the grain size containing partially some larger, well rounded, carbonatic clasts belonging originally to the clay or plastic clay pellets (e.g. OVC-6, SBO-1; 6 samples; Fig. 145a);

- (b) sherds with serial texture, subangular to rounded clasts, MGS 600 to 1000  $\mu\text{m}$  refer to fluvial sediments (sandy clay, sandy mud, etc.). These materials were not artificially tempered (e.g. TR-20, DH-3; 6 samples; Fig. 145b);
- (c) sherds with hiatal (partially serial) texture, angular to subrounded clasts, MGS 1000 to 4000  $\mu\text{m}$  (very coarse sand to granules) refer to silty clays or fluvial fine-grained sediments, probably tempered with sand, or granules originated also from the fluvial systems (e.g. TR-14, YK-2; 67 samples; Fig. 145c);
- (d) sherds with hiatal texture, very angular to subrounded clasts, MGS 4000 to 7000  $\mu\text{m}$  (granules to pebbles), which were artificially added to the paste. The sediments used for pottery making have also fluvial origin similar to the non-plastic inclusions, used for tempering in case of these vessels. The crushing of large sized rocks (Maggetti, 1994) using as temper can be excluded, due to the partially rounded clasts (e.g. DIA-5, DIA-13; 9 samples; Fig. 145d).

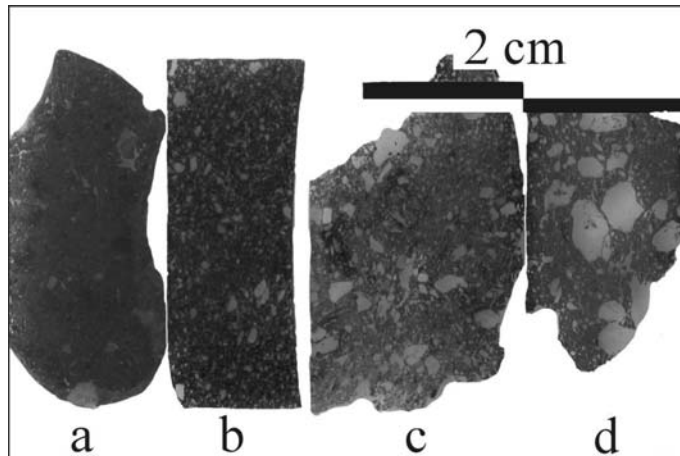


Fig. 145 Types of typical macroscopic textural images of Knobbed ware sherds (cf. text for details).

### 7.2.2 Firing atmosphere of the sherds

On the basis of colour and different layers and cores, which refer to the firing conditions, 6 different types of sherds can be distinguished. These are:

- (a) completely black, dark grey or brown sherds (46 samples);
- (b) sherds with black core, outer and inner sides are reddish (6 samples);
- (c) sherds with reddish core and black outer and inner sides (15 samples);
- (d) sherds with black core and very thin black outer and inner layers, between them reddish layers (sandwich structure, 15 samples);
- (e) sherds with black outer and reddish inner side and (4 samples);
- (f) sherds with reddish-yellowish body (4 samples).

According to Picon (1973) and Clive *et al.* (1993) the colour of the cores suggests the following firing atmospheres and firing techniques: the sherds (a) with completely black or dark grey colour suggest the type B firing in reducing firing and cooling atmosphere. The samples with black core and outer and inner sides in red colour (b) can signify that the vessel was fired under reduced conditions and cooled in oxidising atmosphere (type A firing process). Diffuse black core suggests the presence of organic material; sharp boundaries between black and red layers refer to rapid cooling (Orton *et al.*, 1993).

The sherds with red core (c) also refer to firing and cooling under reducing circumstances, although the firing process begun under oxidising circumstances, where the red core refers to this procedure. However it must be mentioned that most probably every firing procedure begun with the use of oxidising atmosphere, and afterwards, probably when the required temperature was reached, reducing firing (and cooling) took place.

The sherds belonging to the type (d) with „sandwich structure“ suggest also reduced firing and cooling process (type B), where during cooling, oxidising processes also took place (red layers - probably the door of the kiln was open), afterwards the sherds were again exposed to the reduced atmosphere. Sharp core margins refer to rapid cooling (Orton *et al.*, 1993).

In case of sherds where half of the body (inner side) is red and the other (outer) part is black (e) probably the following procedure took place. The sherd was first fired under oxidising, than in reducing atmosphere, and cooled also under the reducing condition. This is clearly shown by the outer black colour. The inner oxidising circumstances could have taken place when there was another vessel situated inside the first one. In case of good position it was possible, that reducing circumstances did not take place in the inner side of the ceramic, thus it remained red, while the outer side became black. Sherds with red and reddish body (f) were fired, soaked and cooled under oxidising circumstances.

### ***7.2.3. Maximum firing temperatures of the sherds***

First it can be established, that the results of X-ray diffractometry are in good accordance with the petrographic data (cf. Appendix 3), although only the main phases (quartz, calcite, K-feldspar, plagioclase, 10Å phyllosilicates, chlorite, amphibole, and pyroxene) are presented on the diffractograms. Wüstite (Fe<sup>II</sup>O) in the sample A-1, which can form under reducing circumstances, refers probably to the firing atmosphere of the former vessel, which is also proved by the colour of the sherd. The presence of the mineral cristobalite in the sample TR-7 is probably related to the large amount of acidic volcanic glass in the non-plastic inclusions.

As a second step, it must be decided whether temperature indicator phases (e.g. calcite, clay minerals, etc.) are primary (i.e. the clay contained them originally or they were artificially added to the paste) or they have secondary character (post-burial phases resulted by soil solutions, weathering, etc.).

Based on petrographic data calcite detected by XRD has at least partially primary origin (soil inclusions, marble fragments, etc.) in every analysed sherd. In the sample MCW-5 fine-grained carbonate is situated in the paste (anisotropic texture, calcareous clay); the sherds TR-12 and 19 contain, beside primary carbonatic inclusions, also secondary calcite in form of pore-filling carbonate. Although pores, holes filled with fine-grained clayey material, or traces of alteration and forming of secondary clay minerals were not observed in the investigated samples, the smectite content in the sherd MCW-5 can be regarded as a secondary (post-burial) mineral in the sample (Mária Tóth, personal communication). Smectite loses its interstitial water until 300 °C, but until 700 °C it can adsorb water. However, due to the chlorite content of the same sherd (cf. later), its maximum firing temperature probably did not reach 700 °C; the primary origin of the smectite is hard to prove. It is more probably, that its origin is secondary and it is situated in the paste in form of very fine-grained clay. Considering this theory, the smectite was not taken into consideration by the evaluation of the maximum firing temperature.

I can establish that all temperature indicator phases are, at least partially, primary in the analysed sherds and they can be used for estimating the approximate maximum firing temperatures.

Based on these minerals the sherds can be divided into three groups:

- 1) the samples with chlorite and 10Å phyllosilicates content (TR-19, A-1, MCW-5, DH-2, DIA-13);
- 2) the sherds with 10Å phyllosilicate and calcite (TR-12, 25, OVC-4, SBO-3, KIR-2);
- 3) the samples with 10Å phyllosilicate content (TR-7, MCE-1, AT-2, HM, YK-3, OVC-1, CH-1, 3, DIA-6, PSH-2).

According to the investigations of Thorez (1975), Brindley & Brown (1980), Rye (1981), Maggetti (1982, 1994), and Cultrone *et al.* (2001) the following maximum firing temperatures can be estimated: The samples belonging to the group (1) contain chlorite, signified by its 14 Å reflection (001), which means, that the firing temperature did not reach, or was at the maximum 650 °C (the samples TR-19, DIA-13). The phase chlorite also has its 7 Å reflection (002, I=100) in the sherds A-1 and MCW-5 (in traces). This suggests that the firing temperature was lower and the decomposition of chlorite is signified by the growth of intensity of its 001 peak (I=30-65) at approximately 550 °C. After approximately 600 °C only the 14 Å reflection (001) exists. Therefore the estimated maximum temperature for these two sherds should be between 550-600 °C.

The sherds (2) containing 10Å phyllosilicate and primary calcite refers to the fact that the firing temperature was not higher than approximately 700-750 °C because of the decomposition temperature of calcite, and/or the firing/soaking time was relatively short. However, this later assumption must be excluded, because of the structure and firing mode (use of kilns and reduced atmosphere) of the pottery.

The samples (3) which contain only 10Å phyllosilicate as temperature indicator phase, theoretically could reach the temperatures of 850-900 °C. However, I think that the maximum firing temperature was probably lower. I have based this supposition on two observations:

- (a) the physical properties (hardness, micro cracks, etc.) of all sherds, independent from their firing temperatures, refer to the relatively low firing temperature. The Knobbed ware sherds from Troia were macroscopically compared to other, high-temperature fired Troian vessel fragments (e.g. Grey Minyan ware). The sherds fired in high temperatures (over 900 °C) have higher hardness and resistance against alteration and other secondary processes;
- (b) there is no correlation between the possible highest firing temperatures and the place of origin of the sherds. That means that there are no producing areas, which are exactly determined by using of higher or lower firing techniques. Furthermore, within the kiln under specific circumstances, 100 to 200 °C temperature difference can occur (e.g. nearer to the wall of the kiln, or in the middle of it).

By determining the possible temperature reached during the firing of the vessel, the limits of XRD analyses can be seen.

Firstly, one does not know the composition of the clay or clayey paste which was used in the production of the vessel. That means that e.g. clay containing illite and chlorite, and fired in 700 °C, has the same phases as the paste containing only illite and fired in 600 or even in 800 °C. Thus, based on these data one cannot give the exact range of firing temperature of Knobbed ware, only the possible highest firing temperatures. There is another possibility to determine the firing temperature of the sherd, refiring of the sample (Klenk, 1987; Maggetti, 1994). After refiring in predefined temperatures, XRD analyses are made, and they will be compared to the diffractogram of the same sample, which have been made before the refiring process. Due to the small amount of the material this method could not be applied in this study.

## CHAPTER 8. Conclusion and Discussion

### 8.1. General conclusions

The aim of this study was to determine the origin of Knobbed ware (Buckelkeramik), a hand-made ceramic type from the Early Iron Age found in the Troian settlement phase VIIb2 (ca. 1100-1000 B.C.) as well as in the Balkans from the same period. My investigation focussed on the questions of similarities and differences of the Knobbed ware found in Troia and in Thrace (the Balkans), as well as on the production techniques of the pottery.

In order to answer these questions sampling of 90 pottery fragments, 69 comparative geological samples (clayey, silty, sandy sediments, rock fragments, etc.) and 3 locally produced vessel fragments from the most important archaeological sites and survey areas (Troia, the Avşa Island, Menekşe Cataği, north Turkish Thrace (near Edirne) in Turkey and Chal, Ovcarovo, Diadovo, Pshenitsevo, Kirilovo, and Sborianovo in Bulgaria) have been collected.

The complex geoarchaeological procedure used in the study included the following analytical techniques: optical microscopy (petrographic modal analysis), cathodoluminescence observation, chemical (XRF, radiogenic isotopes of  $^{87}\text{Sr}/^{86}\text{Sr}$  and  $^{143}\text{Nd}/^{144}\text{Nd}$ , NAA, EMPA) and XRD analyses.

On the basis of petrographic grouping and chemical analyses (XRF) most sherds found in the different archaeological sites could be distinguished. Samples, which could not be differentiated unambiguously with microscopic and bulk chemical data, were analysed with radiogenic isotopes, NAA, and EMPA.

Additionally, I have used XRD and microscopic fabric analysis in order to determine the possible firing temperature of the Knobbed ware vessels and the type of the raw material used for the production of the pottery.

The following conclusions can be drawn from the results:

- on the basis of petrographic grouping and chemical (XRF) data most sherd seem to show affinity to possible local raw materials;
- similarities in the petrographic (e.g. domination of granitic and polyquartz inclusions) and chemical results between the different study areas and archaeological sites can be explained with similar geological settings of the regions; this effect made the interpretation of the results more difficult and sometimes uncertain;
- the same phenomenon also appeared in the radiogenic isotopic results; yet the Troian sediments and locally produced ceramics showed different data than the samples from Thrace and the Balkans;
- considering these results, one can state that 82 of 90 sherds from Troia and from the Balkans were with certainty or with high probability produced locally;

- 3 of the 6 sherds from the South Bulgaria (Ovcarovo) showed clear affinities with the North Bulgarian (Sborianovo) vessel fragments and sediments, thus I assumed that they originated in North Bulgaria and were transported from there to the South;
- further 4 sherds from Araptepe (north Turkish Thrace) and from Menekşe Cataği (the northern coast of the Sea of Marmara) showed clearly different petrographic and/or chemical properties from the local geological and archaeological materials, thus they belonged with certainty to non-locally produced vessels;
- in order to find the place of origin of these sherds, they were analysed with the NAA and EMPA. Although there are some supposed places of origin, due to the lack of comparative data and materials the exact origin of these vessels could not be determined. Their suggested, but not certain, places of origin could be the southern Strandja Massive, the andesite vulcanite dominated area of the southern Thrace Basin and the (southern) Rhodope Mts;
- one of greatest problems posed in this work was to filter out the chemical influence of temper on chemical and isotope geochemical composition. I could show that the non-plastic inclusions or added temper rich in trace elements (e.g. volcanites, magmatites) in special cases (isotopic data) can influence the bulk chemical composition of the clayey raw material of the sherds, and thus complicate the interpretation of the data. **Consequently, in case of coarse wares, only the combined use of petrographic and geochemical analyses can give effective provenance;**
- raw materials used for the ceramic production were mainly silty-sandy clays and/or river sediments. In some cases tempering of the clayey paste was carried out using natural (sandy) materials. Crushing of rocks in order to use as temper and the use of very fine-grained clays or levigated materials can be excluded;
- based on the clay mineral content (XRD data), the analysed sherds were grouped into three groups, indicating each one different, but relatively low maximum firing temperature, which are: in case of chlorite content: (550) 600-650 °C, 10Å phyllosilicate and calcite content: 700-750 °C and 10Å phyllosilicate content: 800-850 °C;
- the firing-cooling procedure took place mostly under reducing atmosphere; the fact is well reflected by the greyish-black colour of the samples.

My results are in good accordance with former archaeological studies, but they also provide new data which can serve as a basis for the future archaeological studies concerning the problem of the origin of the Knobbed ware from Troia and the Balkans. Although I have been able to determine that some sherd analysed in this study were not produced locally, **I was not able to identify any vessel fragment in Troia, which could certainly be of foreign origin. Thus the results of my thesis do not confirm the hypothesis of a common origin of the Troian and the Balkan Knobbed ware.** The

presence of single not locally produced sherds in Bulgaria and in some Thracian settlements can be regarded as an isolated phenomenon. In all other cases the explanation offered in this study for the spreading of the Buckelkeramik in the area of the Balkans and the north-west Anatolia is a transfer of technological solutions rather than import of the ready-made vessels. This supposition is also supported by the common production techniques (raw materials, firing temperature and condition) of the sherds analysed from the different archaeological sites.

## 8.2. Archaeological discussion of the results

Although, as it has been stated above in Chapter 1, it is impossible to draw conclusions on the ethnic change based solely on pottery, the results deriving from the presented study call for an archaeological interpretation. Cautious archaeological conclusions can be drawn from the obtained results of complex petrologic and chemical analysis of the Knobbed ware, keeping in mind that additional archaeological evidence, as well as further archaeological studies (especially the above mentioned dissertation of Pavol Hnila) may alter the picture.

On the basis of the analyses carried out in frames of the presented study it is clearly visible that the Knobbed ware in Troia was produced locally. The one sherd which produced unclear picture (the sample TR-20) is statistically insignificant in this study and it does not contradict clearly the obtained results.

Instead of import of pottery we observe in Troia clear import of technology of production, involving entirely new potters' skills. To make vessels in the Knobbed ware tradition the potters have to know how to form vessels in hand (a technique completely different than operation of a wheel), and how to decorate them with knobs and complicated incised patterns.

The fact of local production of the Knobbed ware in Troia is an argument supporting the hypothesis of the immigration of the new population in Troia after the destructions at the beginning of Troia VIIb2 (possibly preceded by another wave of immigrants at the beginning of Troia VIIb1, connected with the appearance of the "Barbarian" ware; this subject is beyond the scope of the present study). **It has to be stressed that although such theories have been already proposed by Blegen *et al.* (1958), the presented study is the first presentation of the geological and chemical data which provide indisputable evidence for the local production of the Knobbed ware in Troia. By now the local vs. foreign production was merely a subject of speculation.**

The existence of locally produced Knobbed ware in the same archaeological context as the locally produced wheelmade wares in Troia (e.g. the Grey Minyan ware) may suggest possible coexistence of the new and local ethnic element at the site; the people who represented different production tradition (reflected by the technology of production) and who used pottery in different ways (reflected by the new shapes). The character of this coexistence (if it indeed took place) cannot be determined on the

base of such scanty material, but what calls for attention is the fact that in Troia in the same houses complete functional sets executed in both Knobbed ware tradition and in local wheelmade tradition have been found (Guzowska, *et al.*, 2003).

In other sites being subject of the presented study we can see the same overall pattern: in most cases the Knobbed ware has been locally produced at the place of find. The other analysed sites cannot be compared to Troia concerning the size and cultural importance; no previous archaeological hypothesis interpreting the presence of the Knobbed ware in Thrace has been elaborated by archaeologists. In these cases we cannot discuss the possible ethnic change, for the lack of archaeological data supporting this hypothesis. However, the spreading of the new pottery tradition and technology of production from the Balkans through Thrace to the north western Anatolia may reflect the movement of the immigrants.

All the above presented archaeological interpretations have character of a speculation. As stressed many times above in the course of the study, more archaeological data are necessary for the stable conclusions about the possible immigration of the new population in Troia and in Thrace in the period of the appearance of the Knobbed ware.

### **8.3. General observations concerning the provenance analysis of coarse wares**

During the course of the study several methodological questions have been posed and answered concerning the provenance analysis of coarse wares. Some important observations can be made which refer to the uncertainties connected with this type of studies:

- 1) In provenance analysis it is always easier to establish whether a sherd is not locally produced than to prove positively its locally origin. In case of the areas with complex geological setting or by comparing the materials of different areas with similar geological build-up sufficient discrimination of the sherds can be problematic.
- 2) To carry out effective provenance analysis in the above mentioned situations, the complex and complementary petrographic and chemical analyses are needed, with special attention paid to the geological patterns of the study areas. But notwithstanding the extensive sampling of comparative materials (sediment samples, etc.), larger chemical variety must always be taken in the account.
- 3) Optical microscopic analysis is one of the most useful and indispensable methods in effective provenance studies. In several cases chemical data could only be explained using the petrographic information of the materials.

4) Considering the behaviour of different elements, the use of PAAS-normalised multi-element plots is a powerful method to characterise the sherds, the sediments, and the bulk geological properties of the area which provided the raw materials for the pottery production.

5) Although trace element-rich non-plastic inclusions (e.g. volcanites, magmatites, etc.) can strongly influence the bulk composition of the sherd, and consequently the provenance of the vessel, in case of local sediments and non-plastic inclusions originating from the same geological formation or parent rock(s) no substantial differences were observed between the chemistry of the bulk material (the whole sherd) and the chemical composition of the temper-free sample (cf. the sherd TR-7).

Isotopic values seem to be more sensitively influenced by the non-plastic inclusions (cf. the sherd *E9.158.1*), than the elementary composition, which suggests, that clayey matrix and sandy temper have most probably belonged to different geological formations and/or parent rocks (e.g. polymict, mixed, fluvial sediment).

6) In optimal case, the microchemical analysis (NAA, EMPA) of mineral and rock fragments, found in coarse wares can provide useful information about their chemical properties, which allows the direct comparison of the data to (geo)chemical information of their possible parent rocks, thus to the possible place of origin. Therefore, various effects (e.g. tempering, alteration of ceramics, firing processes, etc.), which can influence the results of provenance can be automatically filtered.

7) The simultaneous use of different analytical methods allowed in most cases for identification of the places of origin of the archaeological ceramics. The sherds from vessels produced locally and non-locally are with high probability distinguishable. Most similarities found in their mineral and petrographic as well as chemical composition were caused by the similar geological properties and raw materials of the different regions. These factors, which also caused and lead to some uncertainties in the provenance of some archaeological fragments, can only be filtered out with more detailed geochemical databases, information, and comparative archaeological materials.

#### **8.4. Open questions resulting from this study**

Notwithstanding the most cautious sampling of the geological comparative materials, due to the above mentioned natural effects (natural variability of sediments, complexity of the geology of the study areas, etc.) some question remained open in the dissertation. Below I would like to suggest some guidelines for the possible future research which can base on the complex petrochemical analytical methods and approach already developed in this study:

- completing the chemical database (main and trace elements) of sediments with more samples from localities with the most uncertain chemical features (e.g. Strandja Massive and central Bulgarian sites);
- completing the archaeological database with the complex geoarchaeological analysis of further Knobbed ware sherds, especially from archaeological places from the Balkans, southeast Romania (Babadag), as well as Greece;
- the exact origin of the sherd TR-20 (its local production) can be confirmed or disproved by more accurate chemical (REE and isotopic composition) comprehensive analysis with locally produced sherds from Menekşe Çatağı and surrounding areas;
- for provenance analysis, in case of coarse wares containing lots of (not altered) volcanite fragments, the use of electron microprobe analysis can be recommended.

## LITERATURE

- Adan-Bayewitz, D. & Perlman, I. (1985): Local pottery provenience studies: A role of clay analysis. – *Archaeometry*, **27**, 203-217.
- Anthony, D.W. (1990): Migration in Archaeology: The Baby and the Bathwater. – *American Anthropologist* **92**, 895-914.
- Anthony, D.W. (1997): Prehistoric Migrations as a Social Process. – In: Chapman, J., Hamerow, H. (eds.) Migrations and Invasions in Archaeological Explanation. *British Archaeological Reports International Series* 664, Oxford, 21-32.
- Anthony, D.W. (2000): Comment to S. Burmeister. – In: Burmeister, S. Archaeology and Migration. Approaches to an Archaeological Proof of Migration. *Current Anthropology* **41** (4), 554-555.
- Arai, S. (1992): Chemistry of chromian spinel in volcanic rocks as a potential guide to magma chemistry. – *Mineralogical Magazine*, **56**, 173-184.
- Arnold, D.E. (1972): Mineralogical analyses of ceramic materials from Quinua, department of Ayacucho, Peru. – *Archaeometry*, **14**, 93-102.
- Badre, L. (1998): Late Bronze and Iron Age Imported Pottery from the Archaeological Excavations of Urban Beirut. – In: Karageorghis, V. and Stampolidis, N. (eds.) *Proceedings of the International Symposium Eastern Mediterranean: Cyprus-Dodecanese-Crete 16th-6th cent. B.C.* Athens, 73–84.
- Balla, M. (1981): Római korú „terra sigillata” kerámiák vizsgálata korszerű anyagvizsgálási Módszerekkel [*Scientific analyses of roman terra sigillata – in Hungarian*]. – Diplomamunka (ELTE TTK), Budapest.
- Bayne, N. (2000). The Grey Wares of North-West Anatolia in the Middle and Late Bronze Age and the Early Iron Age and their Relation to the Early Greek Settlements. – *Asia Minor Studien*, **37**, Bonn.
- Barbin, V., Ramseyer, K. & Decrouez, D. (1992): Cathodoluminescence of white marbles: an overview. – *Archaeometry*, **34**, 175-183.
- Béarat, H., Dufuornier, D. & Nouet, Y. (1992): Alteration of ceramics due to contact with seawater. – *Archaeologica Polona*, **30**, 151-162.
- Becks, R. & Thumm, D. (2001): Untergang der Stadt in der Frühen Eisenzeit - Das Ende aus Archäologischer Sicht. – In: Theune-Großkopf, B., Seidel, M., Kastl, G., Kempa, M., Redies, M., Wais, A. (eds.) *Troia-Traum und Wirklichkeit; Begleitband zur Ausstellung „Troia – Traum und Wirklichkeit, Stuttgart-Braunschweig-Bonn“*, 419-424.
- Bingöl, E., Akyürek, B. & Korkmazer, B. (1973): Geology of the Biga Peninsula and some characteristics of the Karakaya Formation. – *Proceedings of the Congress on Earth Sciences*, Ankara, 70-76.
- Birgül, O., Diksic, M., & Yaffe L. (1977): Activation analysis of Turkish and Canadian clays and Turkish pottery. – *Journal of Radioanalytical Chemistry*, **39**, 45-62.
- Birkle, P. (1993): Petrologie, Geochemie und Geochronologie des miozänen Magmatismus auf der Biga Halbinsel (Ezine, NW-Türkei). – Diplomarbeit, Geowissenschaftliche Fakultät, Universität, Tübingen.
- Birkle, P. & Satır, M. (1994): Geological Aspects of the Use of Kestanbol Quartz-Monzonite Intrusion (Troas/Turkey) as Constructing Material in Archaeological Sites around the Mediterranean Sea. – *Studia Troica*, **4**, 143-155.
- Birgül, O., Diksic, M. & Yaffe, L. (1977): Activation analysis of Turkish and Canadian clays and Turkish pottery. – *Journal of Radioanalytical Chemistry*, **39**, 45-62.

- Blegen, C., Caskey J.L. & Rawson, M. (1953) Troy. Vol. III, The sixth settlement. – Princeton.
- Blegen, C.W., Boulter, C.G., Caskey, J.L. & Rawson, M. (1958): Troy IV. Settlements VIIa, VIIb and VIII. – Princeton.
- Bloedow, E.F. (1985): Handmade burnished ware or “Barbarian” pottery and Troy VIIb. – *La Parola del Passato, Rivista di Studi Antichi*, **40**, 161-199.
- Bonchev, E. (1971): Problemina Bulgarskata geotektonika (Problems of Bulgarian geotectonics). – Drzhavno Izdodvkie Tekhnika, Sofia .
- Boyanov I., Kozhoukharov, D., Yanev, Y., Goranov, A., Russeva, M. & Shilyafova. Z. (1989): Geological Map of Bulgaria at 1:100000 scale. Haskovo Map Sheet, Sofia.
- Böhm, K. & Hagn, H. (1988): Archäometrische Untersuchungen an jungsteinzeitlicher Keramik Südbayerns. – Vortäge des 6. Niederbayerischen Archäologentages, 15-55.
- Brindley, G.W. & Brown, G. (1980): Crystal structures of clay minerals and their X-ray diffraction. – *Mineralogical Society*, Monograph, **5**.
- Burmeister, A., Goedicke, C., Hennicke, H.W., Kleinmann, B., Knoll, H., Maggetti, M., Rottländer, R. & Schneider G. (1989): Naturwissenschaftliche Kriterien und Verfahren zur Beschreibung von Keramik. – *Acta Praehistorica et Archaeologica*, **21**, 7-39.
- Buxeda I Garrigós, J., Kilikoglou, V. & Day, P.M. (2001): Chemical and mineralogical alteration of ceramics from late bronze age kiln at Kommos, Crete: The effect on the formation of a reference group. – *Archaeometry*, **43**, 349-371.
- Buxeda I Garrigós, J., Mommsen, H & Tzolakidou, A. (2002): Alterations of Na, K and Rb concentrations in Mycenaean pottery and a proposed explanation using X-ray diffraction. – *Archaeometry*, **43**, 349-371.
- Carter, S.W., Wiegand, B., Mahood, G.A. & Dudas, F.O. (2004): Strontium isotopic analysis as a tool for ceramic provenance research. – 34<sup>th</sup> International Symposium on Archaeometry, Zaragoza, Spain, Abstract.
- Catling H.W., & Catling E.A. (1981): “Barbarian” pottery from the Mycenaean settlement at the Menelaion, Sparta. – *Annual of the British School at Athens*, **76**, 71-82.
- Catling, R.W.V. (1998): The typology of the Protogeometric and Subprotogeometric pottery from Troia and its Aegean context. – *Studia Troica*, **8**, 151-187.
- Chandler, G.M. (2001): Comparative petrographic analysis of sherds from five Minoan sites in Western Crete. – In: Bassiakos Y., Aloupi, E., Facorellis, Y. (eds.) *Archaeometry Issues in Greek Prehistory and Antiquity*, 379-395.
- Chatalov, G.A. (1988): Recent developments in the geology of the Strandzha zone in Bulgaria. – *Bulletins of the Technique University of Istanbul*, **41**, 433-465.
- Chichikova, M. (1968): Keramika ot starata zeliazna epoha v Trakia. – *Archeologija* (Sofia) **10** (4), 15-27.
- Cultrone, G., Rodriguez-Navarro, C., Sebastian, E., Cazalla, O. & De La Torre, M.J. (2001): Carbonate and silicate phase reactions during ceramic firing. – *European Journal of Mineralogy*, **13**, 621-634.
- Çağlayan, A.M., Şengün, M. & Yurtsever, A. (1988): Main fault systems shaping the Istranca Massif, Turkey. – *Journal of Pure and Applied Sciences, Series A, Geosciences*, **21**, 145-154.
- Dabovski, C., Harkovska, A., Kamenov, B., Mavrudchiev, B., Stanisheva-Vassileva, G. & Yanev, Y. (1991): A geodynamic model of the Alpine magmatism in Bulgaria. – *Geologica Balcanica*, **21** (4), 3-15.
- Deer, W.A., Howie, R.A. & Zussman, J. (1978): Single-Chain Silicates. – *Rock forming minerals*.

- Deger-Jalkotzy, S. (1977): Fremde Zuwanderer im Spätmykenischen Griechenland: Zu einer Gruppe handgemachter Keramik aus den Myk. IIIC Siedlungsschichten von Aigeira. – Österreichische Akademie der Wissenschaften, Wien
- Deger-Jalkotzy, S. (1983): Das Problem der “Handmade Burnished Ware” von Myk. III C. – In: Deger-Jalkotzy, S. (ed.) *Akten des Symposiums von Stift Zwettl. Griechenland, die Ägäis und die Lewante während der “Dark Ages”, vom 12 bis 9 Jh. v. Chr.*, 11-14 Oktober, 1980. Wien, 161-178.
- Dimitrov, D.P. (1968): Troia VIIIb2 i balkanskite trakijski i mizijski plemena. – *Archeologija*, **10** (4), 1-15.
- Dimitrov, D.P. (1971): Troia VIIIb2 und die Thrakischen und mösischen Stämme auf dem Balkan. – In: *Studia Balcanica*, V. L’ Ethnogenèse des peuples balkaniques, Sofia, 63-78.
- Di Pierro, S. (2003): Matrix-temper separation of Neolithic ceramics: an experimental approach to characterize the original raw materials and determine their provenance. – In: Di Pierro, S. – Serneels, V. – Maggetti, M. (eds.) *Ceramic in the Society, Proceedings of the 6<sup>th</sup> European Meeting on Ancient Ceramics*. Fribourg, Switzerland, 109-131.
- Felts, W.M. (1942): A petrographic examination of potsherds from ancient Troy. – *American Journal of Archaeology*, **46**, 237-244.
- Filipov, L. (1990): Geological Map of Bulgaria at 1:100000 scale. Isparih Map Sheet, Sofia.
- Folk, R.L. (1959): Practical petrographic classification of limestones. – *Bulletin, American Association of Petroleum Geologists*, **43**, 1-38.
- Foose, R.M. & Manheim, F. (1975): Geology of Bulgaria: a Review. – *Bulletin, American Association of Petroleum Geologists*, **59**, 303-335.
- French, E. & Rutter, J.B. (1977) The Handmade Burnished Ware of the Late Helladic IIIC Period: Its modern historical context. – *American Journal of Archaeology*, **81**, 111-112.
- García-Heras, M., Blackman, M. J., Fernández-Ruiz, R. & Bishop, R.L. (2001): Assessing ceramic compositional data: a comparison of total reflection X-ray fluorescence and instrumental neutron activation analysis on Late Iron Age Spanish Celtiberian ceramics. – *Archaeometry*, **43**, 325-347.
- GEOLOGICAL MAP OF TURKEY 1: 500.000, Sheet Istanbul (1964). – Institute of Mineral Research and Exploration, Ankara.
- Gherdán, K. (1999): Északnyugat-magyarországi bronzkori és vaskori kerámiák archeometriai vizsgálata [*Archaeometrical analysis of Bronze and Iron Age ceramics from Northwest Hungary – in Hungarian*]. – Diplomamunka, ELTE, Manuscript.
- Gherdán, K., Szakmány, Gy., Weiszburg, T. & Ilon, G. (2002): Petrological investigation of bronze and iron age ceramics from West Hungary: Vaskersztes, Velem, Sé, Gőr. – In: Kilkoglou, V., Hein, A., Maniatis, Y. (eds.) *BAR International Series 1011*, 305-312.
- Giacomini, F. (2003): The Roman tile-factories in Switzerland: the case of the Vindonissa legionary camp (1<sup>st</sup> Century A.D.). – In: Di Pierro, S., Serneels, V., Maggetti, M. (eds.) *Ceramic in the Society, Proceedings of the 6<sup>th</sup> European Meeting on Ancient Ceramics, Fribourg, Switzerland*, 145-162.
- Glowacki, D.M., Neff, H. & Glascock, D. (1995): Characterization of Mesa Verde black on white ceramics from southwestern Colorado using NAA. – *Journal of Radioanalytical and Nuclear Chemistry*, **196** (2), 215-222.
- Goldstein, S.J., O’Nions, R.K. & Hamilton, P.J. (1984): A Sm-Nd isotopic study of atmospheric dusts and particulates from major river systems. – *Earth and Planetary Science Letters*, **70**, 221-236.
- Goldstein, S.J. & Jacobsen, S.B. (1988): Nd and Sr isotopic systematics of river water suspended material. Implications for crustal evolution. – *Earth and Planetary Science Letters*, **87**, 249-265.

- Gomez, B., Neff, H., Rautman, M.L., Vaughan, S.J. & Glascock, M.D. (2002): The source of Bronze Age and Roman pottery from Cyprus. – *Archaeometry*, **44**, 23-36.
- Goren, Y. (1995): Shrines and ceramics in Chalcolithic Israel: The view through the petrographic microscope. – *Archaeometry*, **37**, 287-305.
- Götze, J. & Zimmerle, W. (2000): Quartz and silica as guide to provenance in sediments and sedimentary rocks. – In: Aigner, T., Cross, T., Wright, V.P. (eds.) *Contributions to Sedimentary Geology*, **21**.
- Gunneweg, J. & Mommsen, H. (1990): Instrumental neutron activation analysis and the origin of some cult objects and Edomite vessels from the Horvat Qitmit shrine. – *Archaeometry*, **32**, 7-18.
- Guzowska, M., Kuleff, I., Pernicka, E. & Satir, M. (2003): On the origin of Coarse Wares of Troia VII. – In: Wagner, G.A., Pernicka, E., Uerpmann, H.P. (eds.) *Troia and the Troad, Scientific Approaches*, 233-249.
- Hagn, H. (1983): Archäometrische Untersuchungen an körniger Keramik im Vergleich mit anderen bayerischen Produktionsstätten. – *Der Storchenturm*, **35**, 33-78.
- Hall, M., Maeda, U. & Hudson, M. (2002): Pottery production on Rishri Island, Japan: Perspectives from X-ray fluorescence studies. – *Archaeometry*, **44**, 213-228.
- Hancock, R.G.V. (1985): Neutron activation analysis of ceramics: problems with Titanium and Calcium. – *Archaeometry*, **27**, 94-101.
- Harangi, Sz. (1993): MINPROG; User's Manual. – Department of Petrology and Geochemistry, Eötvös University, Budapest, Manuscript.
- Harbottle, G. (1976): Activation analysis in archaeometry. – *Radiochemistry*, **3**, 33-72.
- Hatcher, H. & Tite, M.S. (1995): A comparison of Inductively-Coupled Plasma Emission Spectrometry and Atomic Absorption Spectrometry analysis on standard reference silicate materials and ceramics. – *Archaeometry*, **27**, 83-94.
- Hänsel, B. (1976). Beiträge zur regionalen und chronologischen Gliederung der älteren Hallstattzeit an der unteren Donau. – Beiträge zur Ur- und Frühgeschichtlichen Archäologie des Mittelmeer-Kulturrums, Band **16**, Bonn.
- Hein, A., Tzolakidou, A. & Mommsen, H. (2002): Mycenaean pottery from the Argolid and Achaia – A mineralogical approach where chemistry leaves unanswered questions. – *Archaeometry*, **44**, 177-186.
- Hochstetter, A. (1984): Kastanas. Ausgrabungen in einem Siedlungshügel der Bronze- und Eisenzeit Makedoniens 1975-1979. Die handgemachte Keramik. Schichten 19 bis 1. – *Prähistorische Archäologie in Südosteuropa*, Band **3**, Berlin.
- Jaranoff, D. (1937): Le Tertiaire dans la région de Rodosto (Tekir-dağ). – *Revue de Géographie Physique et de Géologie Dynamique*, **10**, 151-156.
- Jones, R.E. (1986): Greek and Cypriot pottery. – The British School at Athens, Fitch Laboratory Occasional Paper, **1**, Athens.
- Kamenetsky, V.S., Crawford, A.J. & Meffre, S. (2001): Factors controlling chemistry of magmatic spinel; an empirical study of associated olivine, Cr-spinel and melt inclusions from primitive rocks. – *Journal of Petrology*, **42** (4), 655-671.
- Kamilli, D.C. & Lamberg-Karlovsky, C.C. (1979): Petrographic and electron microprobe analysis of ceramics from Tepe Yahya, Iran. – *Archaeometry*, **21**, 47-59.
- Karageorghis, V. (1986): "Barbarian" Ware in Cyprus. – In: Karageorghis, V. (ed.) *Acts of the International Archaeological Symposium, Cyprus between the Orient and Occident*. Nicosia, 246-253.

- Kardos, J., Zimmer, K., Kriston, L., Morozva, O., Träger, T. & Jerem, E. (1985): Scientific investigation of the Sopron-Krautacker Iron Age pottery workshop. – *Archaeometry*, **27**, 83-93.
- Kasztovszky, Zs., Mackowiak de Antczak, M., Antczak, A., Millan, B., Bermúdez, J. & Sajo-Bohus, L. (2004): Provenance study of Amerindian figurines with Prompt Gamma Activation Analysis. – *Nukleonika*, **49** (3), 107-113.
- Kayan, I. (1991): Holocene Geomorphic Evolution of the Besik Plain and Changing Environment of AncientMan. – *Studia Troica*, **1**, 79-96.
- Kayan, I. (1997): Geomorphological Evolution of the Ciplak Valley and Archaeological Material in the Alluvial Sediments to the South of the Lower City of Troia. – *Studia Troica*, **7**, 489-507.
- Kayan, I., Öner, E., Uncu, L., Hocaoglu, B., & Vardar, S. (2003): Geoarchaeological Interpretations of the „Troian Bay“. – In: Wagner, G.A., Pernicka, E., Uerpmann, H.P. (eds.) *Troia and the Troad, Scientific Approaches*, 379-401.
- Kerschner, M., Mommsen, H., Beier, T., Heimermann, A. & Hein, A. (1993): Neutron activation analysis of bird bowls and related archaic ceramics from Miletus. – *Archaeometry*, **35**, 197-210.
- Kilka, T. (1992): An example of study where the petrography prevails over the chemistry: the Bronze Age ceramics from Fiave (Italy). – *Doc. et Trav. IGAL*, **16**, 61-72.
- Kilikoglou, V., Maniatis, Y. & Grimanis, A.P. (1988): The effect of purification and firing of clays on trace element provenance studies. – *Archaeometry*, **30**, 37-46.
- Klenk, G. B. (1987): Geologisch-mineralogische Untersuchungen zur Technologie frühbronzezeitlicher Keramik von Lidar Höyük (Südost-Anatolien). – *Münchener Geowissenschaftliche Abhandlungen*, **8**.
- Knacke-Loy, O. (1994): Isotopengeochemische, chemische und petrographische Untersuchungen zur Herkunftsbestimmung der bronzezeitlichen Keramik von Troia. – *Heidelberger Geowissenschaftliche Abhandlungen*, **77**.
- Knacke-Loy, O., Satir, M. & Pernicka, E. (1995): Zur Herkunftsbestimmung der bronzezeitlichen Keramik von Troia: Chemische und isotopengeochemische (Nd, Sr, Pb) Untersuchungen. – *Studia Troica*, **5**, 145-175.
- Kopp, K., Pavoni, N. & Schindler, C. (1969): Geologie Thrakiens. IV: Das Ergene Becken. – *Beihefte zum Geologischen Jahrbuch*, **76**, 63-71.
- Koppenhöfer, D. (1997). Troia VII – Versuch einer Zusammenschau einschließlich der Ergebnisse des Jahres 1995. – *Studia Troica*, **7**, 295-353.
- Korfmann, M. (1988): Ausgrabungen an der Bucht von Troia. – *Tübinger Blätter*.
- Korfmann, M. (1991): Troia Reinigungs- und Dokumentationsarbeiten 1987, Ausgrabungen 1988-1989. – *Studia Troica*, **1**, 1-34.
- Korfmann, M. (1992): Troia - Ausgrabungen 1990-1991. – *Studia Troica*, **2**, 1-42.
- Korfmann, M. (1997): Troia - Ausgrabungen 1996. – *Studia Troica*, **7**, 1-72.
- Korfmann, M. (2000): Troia - Ausgrabungen 2000. – *Studia Troica*, **10**, 1-34.
- Korfmann, M. (2001): Der prähistorische Siedlungshügel Hisarlık; „Die zehn Städte Troias“- von unten nach oben. – In: Theune-Großkopf, B., Seidel, M., Kastl, G., Kempa, M., Redies, M., Wais, A. (eds.) *Troia-Traum und Wirklichkeit; Begleitband zur Ausstellung „Troia – Traum und Wirklichkeit, Stuttgart-Braunschweig-Bonn“*.
- Kozhoukharov D., Boyanov, I., Shilyafov, G. & Goranov, A. (1993): Geological Map of Bulgaria at 1:100 000 scale, Svilengrad Map Sheet, Sofia.

- Kozhoukharov D., Savov, S., Boyanov, I. & Shilyafov, G. (1994): Geological Map of Bulgaria at 1:100 000 scale. Topolovgrad Map Sheet, Sofia.
- Koukouli-Chrysanthaki, C. (1970): Proistoriki Thasos, Archaologiki Ephimeris, Chronika, 16-22.
- Koukouli-Chrysanthaki, C. (1982): Die frühe Eisenzeit auf Thasos. – In: Hänsel B (ed.) Südosteuropa zwischen 1600 und 1000 v. Chr. Berlin: 65-86. Prähistorische Archäologie in Südosteuropa, **Band 1**, Berlin, 119-143.
- Laterrier, J., Maury, R.C., Thonon, P., Girard, D. & Marchal, M. (1982): Clinopyroxene composition as a method of identification of the magmatic affinities of palaeo-volcanic series. – *Earth and Planetary Science Letters*, **59**, 139-154.
- Leake, B.E. (1978): Nomenclature of amphiboles. – *American Mineralogist*, **63** (11-12), 1023-1052.
- Lenaz, D., Kamenetsky, V.S. & Princivalle, F. (2003): Cr-spinel supply in the Brkini, Istrian and Krk Island flysch basins (Slovenia, Italy and Croatia). – *Geological Magazine*, **140** (3), 335-342.
- Maggetti, M. (1974): Mineralogie und antike Keramik. – *Bulletin de la Société Fribourg des Sciences Naturelles*, **63** (1), 45-57.
- Maggetti, M. & Heimann, R. (1979): Bildung und Stabilität von Gehlenit in römischer Feinkeramik. – *Schweizerische Mineralogische und Petrographische Mitteilungen*, **59** (3), 413-417.
- Maggetti, M. & Rossmann, M. (1981): Archaeothermometry of Kaolinitic Clays. – *Revue d'Archéométrie, Supplément*, **5**, 185-194.
- Maggetti, M., Schubiger, A. & Wytenbach, A. (1981a): Homogenität archäologischer keramischer Objekte. Teil II. Ergebnisse der Neutronenaktivierungsanalyse. – *Archäologie und Naturwissenschaften*, **2**, 21-32.
- Maggetti, M., Nungässer, W. & Berger, J. (1981b): Zur Herkunft der Fossilien in den Fundschichten und den keramischen Scherben der Cortailod-Kultur von Twann. – In: W.E. Stöckli (ed.) Die Cortailod-Keramik der Abschnitte 6 und 7. Die neolithischen Ufersiedlungen von Twann, **Band 10**, Staatlicher Lehrmittelverlag Bern, 42-43.
- Maggetti, M. (1982): Phase Analysis and its Significance for Technology and Origin. – In: J.S. Olin and A.D. Franklin (eds): *Archaeological Ceramics*, Smithsonian Institution, Washington, 121-133.
- Maggetti, M., Galetti, G. & Paunier D. (1989): Röntgenographische Phasenanalyse schweizerischer antiker Keramik. – In: F. Schweizer und V. Villiger (eds.) *Methoden zur Erhaltung von Kulturgütern*, P. Haupt, Bern, 209-214.
- Maggetti, M. (1994): Mineralogical and Petrographical Methods for the Study of Ancient Pottery. – In: Burrigato, F., Grubessi, O., Lazzarini, L. (eds) *1<sup>st</sup> European Workshop on Archaeological Ceramics*. Roma, Dipartimento Scienze della Terra, Università degli studi di Roma „La Sapienza“ 23-35.
- Maritan, L. (2004): Archaeometric study of Etruscan-Padan type pottery from the Veneto region: petrographic, mineralogical and geochemical-physical characterisation. – *European Journal of Mineralogy*, **16**, 297-307.
- Marro, C. (1978): Recherches en Archeocéramique; (a) recherches minéralogiques sur la céramique malaun ancienne, (b) essais de séparation d'agile et de dégraissant de céramique cuite. – Travail de diplôme, Université de Fribourg.
- Mason, B & Moore, C.B. (1982): *Principles of Geochemistry*. – John Wiley & Sons Inc.
- Mason, R.B. (1995): Criteria for the petrographic characterisation of stonepaste ceramics. – *Archaeometry*, **37**, 307-321.

- Mason, R.B. (2003): Trade and industry at Qual'at Halab: Petrographic analysis of Medieval pottery from the recent excavations at the Aleppo Citadel, Syria. – *The Old Potter's Almanach*, **11** (1), 1-5.
- Mazar, A. (1985): Excavations at Tell Qasile (Qedem 20). – Jerusalem.
- Mazo-Gray, V. & Alvarez, M. (1992): X-ray fluorescence characterization of Ming-dynasty porcelain rescued from a Spanish shipwreck. – *Archaeometry*, **34**, 37-42.
- Mc Lennan, S.M. (1989): Rare earth elements in sedimentary rocks: influence of provenance and sedimentary processes. – In: Lipin B.R. and McKay G.A. (eds.) *Geochemistry and mineralogy of rare earth elements, Reviews in Mineralogy*, **21**, 169-200.
- Middleton, A.P., Freestone, A.C. & Leese, M.N. (1985): Textural analysis of ceramic thin sections. Evaluation of grain sampling procedures. – *Archaeometry*, **27**, 64-74.
- Miller, R.G. & O'Nions, R.K. (1984): The provenance of crustal residence ages of British sediments in relation to paleogeographic reconstructions. – *Earth and Planetary Science Letters*, **68**, 459-470.
- Mommsen, H., Kreuser, A. & Weber, J. (1988): A method for grouping pottery by chemical composition. – *Archaeometry*, **30**, 47-57.
- Mommsen, H., Kreuser, A., Weber, J. & Podzuweit, C. (1989): Classification of Mycenaean pottery from Kastanas by neutron activation analysis. – In: Y. Maniatis (ed.) *Proceedings of the 25<sup>th</sup> International Symposium on Archaeometry*, Athens, 1986, 515-523.
- Mommsen, H., Diehl, U. & Podzuweit, C. (1992): Provenance determination of Mycenaean sherds found in Tell el Amarna by neutron activation analysis. – *Journal of Archaeological Sciences*, **19**, 295-302.
- Mommsen, H. (2001): Provenance determination of pottery by trace element analysis: Problems, solutions and applications. – *Journal of Radioanalytical and Nuclear Chemistry*, **247**, 657-662.
- Mommsen, H., Hein, A., Ittameier, D., Maran, J. & Dakorina, P. (2001): New Mycenaean pottery production centers from Eastern Central Greece obtained by Neutron Activation Analysis. – In: Bassiakos Y., Aloupi, E., Facorellis, Y. (eds.) *Archaeometry Issues in Greek Prehistory and Antiquity*, Athens, 343-354.
- Morimoto, N., Fabries, J., Ferguson, A.K., Ginzburg, I.V., Ross, M., Seifert, F.A. & Zussman, M. (1988): Nomenclature of pyroxenes. – *Mineralogical Magazine*, **52**, 535-550.
- Morintz, S. (1964): Quelques problèmes concernant la période ancienne de Hallstatt au Bas-Danube à la lumière des foilles de Babadag. – *Dacia (NS)*, **8**, 101-118.
- Mountjoy, P.A. (1997): Troia Phase VI<sub>f</sub> and Phase VI<sub>g</sub>: The Mycenaean Pottery. – *Studia Troica*, **7**, 275-294.
- Mountjoy, P.A. (1999): Troia VII Reconsidered. – *Studia Troica*, **9**, 295-346.
- Nedialkov, R. & Pe-Piper, G. (1998): Petrology of the volcanism in the southeastern part of the Momchilgrad-Arda volcanic region, southeastern Bulgaria. – *Acta Vulcanologica*, **10** (2), 243-253.
- Nelson, B.K. & DePaolo, D.J. (1988): Comparison of isotopic and petrographic provenance indicators in sediments from Tertiary continental basins of New Mexico. – *Journal of Sediment Petrology*, **58**, 348-357.
- Nemecz, E. (1973): *Agyagásványok [Clay minerals – in Hungarian]*. – Akadémiai Kiadó, Budapest.
- Nungässer, W., Maggetti, M. & Galetti, G. (1992): Analyse der Scherbensubstanz mit Mikroskop und Röntgenlicht. – In: Bill, J., Nungässer, W., Galetti, G. (eds.) *Liechtensteinische Keramikfunde der Eisenzeit. Jahrbuch des Historischen Vereins für das Fürstentum Liechtenstein*, **Band 91**, 119-165.
- Obenauer, K. (1936): Petrographische Untersuchung der Keramik. – In: Buttler, W. & Haberey W. (eds.) *Die bandkeramische Siedlung bei Köln*, Berlin/Leipzig, 123-129.

- Okay, A.I., Siyako, M. & Bürken, K.A. (1991): Geology and tectonic evolution of the Biga peninsula, northwest Turkey. – *Bulletins of the University of Istanbul*, **44**, 191-256.
- Okay, A.I., Satır, M., Maluski, H., Siyako, M., Monie, P., Metzger, R. & Akyüz, S (1996): Paleo- and Neo-Tethyan events in northwestern Turkey: Geologic and geochronologic constraints. – In: Yin, A., & Harisson, T.M. (eds.) *The Tectonic Evolution of Asia*, 420-441.
- Okay, A.I. & Satır, M. (2000a): Upper Cretaceous Eclogite-Facies Metamorphic rocks from the Biga Peninsula, Northwest Turkey. – *Turkish Journal of Earth Sciences*, **9**, 47-56.
- Okay, A.I. & Satır, M. (2000b): Coeval plutonism and metamorphism in a latest Oligocene metamorphic core complex in northwest Turkey. – *Geological Magazine*, **137**, 495-516.
- Okay, A.I., Satır, M., Tüysüz, O., Akyüz, F. & Chen, F. (2001): The tectonics of the Strandja Massif: late-Variscian and mid-Mesozoic deformation and metamorphism in the northern Aegean. – *International Journal of Earth Sciences*, **90**, 217-233.
- Orton, C., Tyers, P. & Vince, A. (1993): Pottery in archaeology. – *Cambridge Manuals in Archaeology*, 269 p.
- Peacock, D.P.S. (1969): The scientific analysis of ancient ceramics: a review. – *World Archaeology*, **1**, 375-389.
- Picon, M. (1973): Introduction à l'étude technique des céramiques sigillées de Lezoux, Centre de recherches sur les techniques gréco-romaines, Lyon, 1-135.
- Picouet, P., Maggetti, M., Piponnier, D. & Schvoerer, M. (1999): Cathodoluminescence Spectroscopy of Quartz Grains as a Tool for Ceramic Provenance. – *Journal of Archaeological Sciences*, **26**, 943-949.
- Pilides, D. (1992) Handmade Burnished Ware in Cyprus: an attempt at its interpretation. – In: Ιωαννιδης ΓΚ (ed.) Αφιέρωμα στο Βασο Καραγιωργη. Κυπριακai Σπουδai ΝΔ - ΝΕ (54-55), Λευκοσια, 179-189.
- Pilides, D. (1994) Handmade burnished wares of the Late Bronze Age in Cyprus. – Paul Åström Verlag, Jonsered.
- Powers, M.C. (1953): A new roundness scale for sedimentary particles. – *Journal of Sediment Petrology*, **23**, 117-119.
- Richards, T.W. (1895): The composition of Athenian pottery. – *Journal of the American Chemical Society*, **17**, 152-154.
- Rollinson, H.R. (1993): Using Geochemical Data: Evaluation, Presentation, Interpretation. – Longman Scientific & Technical, New York, 352 p.
- Rottländer, R.C.A. (1989): Verwitterungserscheinungen an Keramik, Silices und Knochen. – Tübingen.
- Rye, O.S. (1981): Pottery technology – Principles and reconstructions. – *Taraxacum*, Washington.
- Rutter, J. (1975): Ceramic Evidence for Northern Intruders in Southern Greece at the Beginning of the Late Helladic III C Period. *American Journal of Archaeology* **79**, 17-32.
- Savov, S., Dabovski, C. & Budurov, K. (1995): New data on the stratigraphy of the Tethyan Triassic in the Strandzha Mts., SE Bulgaria. – *Geologica Balcanica*, **25** (5-6), 33-42.
- Schliemann, H. (1881): Ilios. Stadt und Land der Trojaner. – Brockhaus, Leipzig
- Schmidt, H. (1902): Die Keramik der verschiedenen Schichten. – In: Dörpfeld, W. (ed.) Troja und Ilion. Ergebnisse der Ausgrabungen in den vorhistorischen und historischen Schichten von Ilion 1870-1894. Beck & Barth, Athen, 243-319.
- Schneider, G. (1978). Anwendung quantitativer Materialanalysen auf Herkunftsbestimmungen antiker Keramik. – *Berliner Beiträge zur Archäometrie*, **3**, 63-122.

- Schneider, G., Burmester, A., Goedicke, C., Hennicke, H.W., Kleinmann, B., Knoll, H., Maggetti, M. & Rottländer, R. (1989): Naturwissenschaftliche Kriterien zur Beschreibung von Keramik. – *Acta Praehistorica et Archaeologica*, **21**, 7-39.
- Schubert, P. (1984): Der "Kleine Hafner" (Zürich): Mineralogisch-petrographische und chemische Analyse neolithischer Keramik. – *Fortschritte der Mineralogie*, **62** (1), 219-221.
- Schubert, P. (1986): Petrographic modal analysis, a necessary complement to chemical analysis of ceramic coarse ware. – *Archaeometry*, **28**, 63-122.
- Schubert, P. (1987): Die mineralogische - petrographische und chemische Analyse der Keramik. – P.J. Suter, Zürich "Kleiner Hafner", Tauchgrabungen 1981-1984. *Berichte der Zürcher Denkmalpflege, Monographien* **3**, 114-125.
- Shepard, A. (1956): *Ceramics for the Archaeologist*. – Washington, D. C., Carnegie Institution.
- Sengör, A.M.C. & Yılmaz, Y. (1981): Tethyan evolution of Turkey: a plate tectonic approach. – *Tectonophysics*, **75**, 181-241.
- Spataro, M. (2002): The first farming communities of the Adriatic: pottery production and circulation in the Early and Middle Neolithic. – *Società per la Preistoria e Protostoria della Regione Friuli-Venezia Giulia*, **9**, Trieste.
- Stefanovich, M. (1974): The Possible Origins of Knobbed Ware in Troy VIIb2. – *Thracia*, **3**, 101-105.
- Stimmel, C.A., Pilon, J. & Hancock, R.G.V. (1986): Problems in Coarse Ware Analysis. – In: Olin, J. S. & Blackman, M. J. (eds.) *Proceedings of the 24<sup>th</sup> International Symposium on Archaeometry*, Washington D. C., Smithsonian Institution Press, 407-417.
- Székány, Gy. (1996): Petrographical investigation in thin section of some potsherds. – In: Makkay, J., Starnini, E., Tulok, M. (eds.) *Società per la preistoria e protostoria della regione Friuli-Venezia giulia, Quaderno*, **6**, 143-150.
- Székány, Gy. (1998): Insight into the manufacturing technology and the workshops: evidence from petrographic study of ancient ceramics. – In: Költö, L. & Bartosiewicz, L. (eds.) *Archaeometrical research in Hungary*, **II**, 77-83.
- Székány, Gy. & Kustár, R. (2000): Untersuchung von Keramikproben aus dem spätbronzezeitlichen Hügel von Isztimér-Csöpuszta. – *Alba Regia*, **XXIX**, 55-60.
- Taylor, S.R. & McLennan S.M. (1985): *The Continental Crust: its Composition and Evolution*. – Blackwell Scientific Publications.
- Thierrin-Michael, G. (1991): Römische Weinamphoren: Mineralogische und petrographische Untersuchungen zur Klärung ihrer Herkunft und Herstellungsweise. – *Nachrichten der Schweizerischen Mineralogischen und Petrographischen Gesellschaft*, **9**.
- Thorez, J. (1975): *Phyllosilicates and clay minerals; a laboratory handbook for their X-ray diffraction analysis*. – Belgium.
- Tite, M.S. & Maniatis, Y. (1975): Examination of ancient pottery using the scanning electron microscope. – *Nature*, **257**, 122-123.
- Tite, M.S. & Bimson, M. (1986): Faience: an investigation of the microstructures associated with the different methods of glazing. – *Archaeometry*, **28**, 69-78.
- Tite, M.S., Kilikoglou, V. & Vekinis, G. (2001): Strength, toughness and thermal shock resistance of ancient ceramics, and their influence on technological choice. – *Archaeometry*, **43**, 301-324.

- Tzankov, V., Spasov, K. & Bogdanov, B. (1968): Yubilee Geologicheski Sbornik (Jubilee geological volume). – Bulg. Akad. Nauk., Izd. (Publishing house of Bulgarian Academic Sciences).
- Tzankov Tz., Nakov, R., Nedjalkov, N. & Angelova, D. (1992): Geological Map of Bulgaria at 1:100000 scale. Nova Zagora Map Sheet, Sofia.
- Tzankov Tz., Filipov, L. & Katzkov, N. (1995): Geological Map of Bulgaria at 1:100 000 scale. Stara Zagora Map Sheet, Sofia.
- Üşümezsoy, Ş. (1982): Igneous and metamorphic geology and mineralization of Istranca region. – *Istanbul Yerbilimleri*, **3**, 277-294.
- Von der Crone, M. (1993): The influence of seawater to the bleaching by firing ceramic masses: chemical results. – *Schweizerische Mineralogische und Petrographische Mitteilungen*, **73** (1), (Abstract).
- Wagner, G.A., Pernicka, E., Uerpmann, H.P. (2003): Troia and the Troad, Scientific Approaches. – Springer.
- Wedepohl, K.H., Correns, C.W., Shaw, D.M., Turekian, K.K. & Zeman, J. (1970): Handbook of Geochemistry, II-2. – Springer.
- Wedepohl, K.H., Correns, C.W., Shaw, D.M., Turekian, K.K. & Zeman, J. (1972): Handbook of Geochemistry, II-3. – Springer.
- Wedepohl, K.H., Correns, C.W., Shaw, D.M., Turekian, K.K. & Zeman, J. (1974): Handbook of Geochemistry, II-4. – Springer.
- Wedepohl, K.H., Correns, C.W., Shaw, D.M., Turekian, K.K. & Zeman, J. (1978): Handbook of Geochemistry, II-5. – Springer.
- Whitbread, I.K. (1986): The characterisation of argillaceous inclusions in ceramic thin sections. – *Archaeometry*, **28**, 79-88.
- Whitbread, I.K. (1992): Petrographic Analysis of Barbarian Ware from the Menelaion, Sparta. – In: Sanders, J.M. (ed.) *Filolakon. Laconian Studies in Honour of Hector Catling*. London, 297-306.
- Whitbread, I.K. (2001): Petrographic analysis of Middle Bronze Age pottery from Lerna, Argolid.- In: Bassiakos Y., Aloupi, E., Facorellis, Y. (eds.) *Archaeometry Issues in Greek Prehistory and Antiquity*, Athens, 367-377.
- White, W.M (2001): Radiogenic isotope geochemistry. – Geochemistry (online publication, <http://www.geo.cornell.edu/geology/classes/Chapters/Chapter08.pdf>), 318-362.
- Yanev, Y. (1998): Petrology of the Eastern Rhodopes Paleogene Acid Volcanics, Bulgaria. – *Acta Vulcanologica*, **10** (2), 265-277.
- Yanev, Y., Innocenti, F., Manetti, P. & Serri, G. (1998): Upper Eocene-Oligocene Collision-related Volcanism in Eastern Rhodopes (Bulgaria) - Western Thrace (Greece): Petrogenetic Affinity and Geodynamic Significance. – *Acta Vulcanologica*, **10** (2), 279-291.
- Yılmaz, Y., Genç, Ş.C., Yiğizbaş, E., Bozcu, M. & Yılmaz, K. (1995): Geological evolution of the late Mesozoic continental margin of Northwestern Anatolia. – *Tectonophysics*, **243**, 155-171.
- Yılmaz, Y. & Polat, A. (1998): Geology and evolution of the Thrace volcanism, Turkey. – *Acta Vulcanologica*, **10**, 293-303.
- Zöldföldi, J. & Satır, M. (2003): Provenance of the White Marble Building Stones in the Monument of Ancient Troia. – In: Wagner, G.A., Pernicka, E., Uerpmann, H.P. (eds.) *Troia and the Troad, Scientific Approaches*, 203-222.

**APPENDIX 1. ARCHAEOLOGICAL DESCRIPTION AND PHOTOGRAPHS OF THE SHERDS FROM TROIA, CHAL, DIADOVO, PSHENITSEVO, AND KIRILOVO. (THE COLOUR DESCRIPTION WAS CARRIED OUT ACCORDING TO THE MUNSEL SCALE).**

Nr.	Site	Arch. Nr.	Description (What fragment; dimensions (th. = thickness) colour of the sherd; surface; decoration)	Picture
TR-1	Troia	A7.1242.8	Body sherd; max. th. 20 mm, min. th. 10 mm; in: 10YR 5/2 greyish brown, out: 10YR 5/1 grey; surface unburnished; no decoration preserved	
TR-2	Troia	A7.1254.21	Body sherd; 11 mm; in: 5YR 6/6 reddish yellow, core: GLEY 1 2.5/N: black, out: 5YR 6/6 reddish yellow; surface burnished; no decoration preserved	
TR-3	Troia	D9.2969.1	Body sherd; th. 9 mm, in: 10YR 5/3 brown , out: 10YR 2/1 black; surface burnished; no decoration preserved	
TR-4	Troia	D9.2973.40	Body sherd of an opened vessel; th. 10 mm, in: 10YR 5/1 grey, out: 10YR 4/1 dark grey; surface burnished; no decoration preserved	
TR-5	Troia	D9.3007.15	Body sherd of a closed vessel; th. 9 mm; in: 7.5YR 6/3 light brown, core: GLEY 1 2.5/N black, out: 7.5YR 5/5 brown; surface unburnished; no decoration preserved	
TR-6	Troia	D9.3049.15	Body sherd of a closed vessel; th. 11 mm; in: 10YR 4/1 dark grey , out: 10YR 3/1 very dark grey; surface burnished; no decoration preserved	
TR-7	Troia	D9.3053.23	Handle fragment; th. 17 mm; 10YR 5/1 grey; surface unburnished; decoration of shallow incised ribs	X
TR-8	Troia	D9.3062.12	Body sherd; th. 6 mm; in: 10YR 4/1 dark grey , out: 10YR 5/2 greyish brown; surface burnished; no decoration preserved	
TR-9	Troia	D9.3065.1	Body sherd of an opened vessel; th. 7 mm; in: 10YR 4/1 dark grey , out: 10YR 3/1 very dark grey; surface burnished; zone in widdle body: decorated with incised groups of diagonal lines	X
TR-10	Troia	D9.3065.2, D9.3076.8	Body sherd of an opened vessel; th. 8 mm; in: 10YR 2/2 very dark brown, out: 10YR 2/2 very dark brown; surface burnished; no decoration preserved	
TR-11	Troia	D9.3086.59	Body sherd of an opened vessel; th. 10 mm; in: 10YR 5/2 greyish brown, out: 10YR 4/2 dark greyish brown; surface burnished; no decoration preserved	
TR-12	Troia	D9.3086.89	Body sherd of an opened vessel; max. th. 10 mm, min. th. 8 mm; in: 10YR 4/1 dark grey , out: 10YR 3/1 very dark grey; surface burnished; no decoration preserved	
TR-13	Troia	D9.3086.107	Body sherd of an opened vessel; th. 12 mm, in: 10YR 4/1 dark grey , out: 10YR 4/1 dark grey; surface burnished in and out; no decoration preserved	
TR-14	Troia	D9.3092.30	Handle of a vessel; th. 19 mm; 10YR 4/1 dark grey; surface burnished; no decoration preserved	X
TR-15	Troia	D9.3092.55	Body sherd of a closed vessel; max. th. 25 mm, min. th. 11 mm; in: 10YR 3/2 very dark greyish brown , out: 10YR 6/4 light yellowish brown; surface burnished; no decoration preserved	
TR-16	Troia	D9.3098.31 D9.3098.96	Body sherd of a closed vessel; max. th. 23 mm, min. th. 8 mm; in: 10YR 6/1 grey , out: 10YR 4/1 dark grey; surface burnished; no decoration preserved	

TR-17	Troia	D9.3130.7	Body sherd of an opened vessel; th. 8 mm; in: GLEY 1 2.5/N black, out: GLEY 1 2.5/N black; surface burnished; no decoration preserved	
TR-18	Troia	D9.3130.18	Body sherd of an opened vessel; th. 7 mm; in: GLEY 1 4/N dark grey , out: 10YR 5/3 brown; surface burnished; no decoration preserved	
TR-19	Troia	E8.148.3	Body sherd of an opened vessel; th. 11 mm; in: 10YR 4/1 dark grey, out: 10YR 3/1 very dark grey; surface burnished; no decoration preserved	
TR-20	Troia	E8.148.6	Body sherd of an opened vessel; th. 10 mm; in: GLEY 1 2.5/N black, out: 10YR 4/1 dark grey; surface burnished; no decoration preserved	
TR-21	Troia	E8.148.37	Body sherd of a closed vessel; th. 10 mm; in: 10YR 5/3 brown, out: 10YR 4/2 dark greyish brown; surface burnished; no decoration preserved	
TR-22	Troia	E9.724.18	Body sherd of a closed vessel; th. 10 mm; in: 10YR 4/1 dark grey, out: 10YR 4/1 dark grey; surface burnished; no decoration preserved	
TR-23	Troia	E9.876.11	Body sherd of an opened vessel; th. 7 mm; in: 10YR 4/1 dark grey, out: 10YR 4/1 dark grey; surface burnished; no decoration preserved	
TR-24	Troia	K4.470.14	Body sherd; th. 12 mm, in: 10YR 5/1 grey, out: 10YR 5/1 grey; surface burnished; no decoration preserved	
TR-25	Troia	KL 16/17.522.11	Body sherd of a closed vessel; max. th. 11 mm, min. th. 8 mm; in: GLEY 1 2.5/N black, out: GLEY 1 2.5/N black; surface burnished; no decoration preserved	
TR-26	Troia	KL 16/17.522.14	Handle fragment; th. 13 mm, width: 32 mm; 10YR 3/2 very dark greyish brown; surface burnished; no decoration preserved	X
TR-27	Troia	KL 16/17.713.6	Body sherd; th. 6 mm, in: 10YR 5/1 grey , out: 10YR 6/1 grey; surface burnished; no decoration preserved	X
TR-28	Troia	Z7.344.1	Body sherd; th. 8 mm; in: 10YR 6/3 pale brown, out: 10YR 4/1 dark grey; surface burnished; no decoration preserved	
A-1	Avşa (Manastir mevkii)	62	Base fragment; max. th. 13 mm, min. th. 6 mm, base diameter: 63 mm; in: GLEY 1 2.5/N black, out: GLEY 1 2.5/N black; surface burnished; no decoration preserved	
MCE-1	Menekşe Çatağı eastern settlement		Body sherd of an opened vessel; th. 13 mm; in: GLEY 1 2.5/N black, out: GLEY 1 2.5/N black; surface burnished; no decoration preserved	
MCE-2	Menekşe Çatağı eastern settlement		Body sherd of an opened vessel; th. 9 mm; in: 10YR 1 6/2 light brownish grey, out: GLEY 1 4/1 dark greenish grey; surface burnished; no decoration preserved	
MCE-3	Menekşe Çatağı eastern settlement		Base fragment; th. 10 mm; in: 10YR 5/2 greyish brown, out: 10YR 4/1 dark grey; surface burnished; no decoration preserved	
MCE-4	Menekşe Çatağı eastern settlement		Handle fragment; th. 18 mm, width: 28 mm; out: 10YR 4/1 dark grey; surface burnished; no decoration preserved	
MCE-5	Menekşe Çatağı eastern settlement		Body sherd; th. 7 mm; in: 10YR 6/2 light brownish grey, out: GLEY 1 2.5/N black; surface burnished; no decoration preserved	

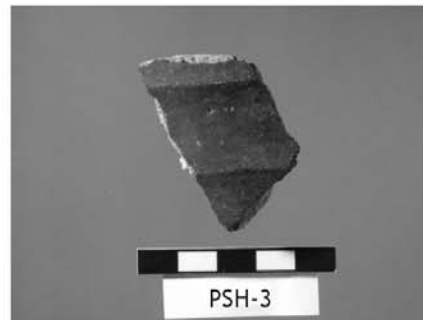
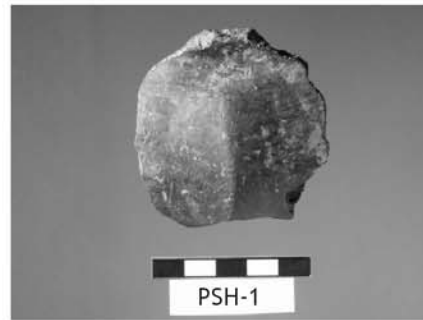
MCW-1	Menekşe Çatağı western settlement	39L/22	Rim fragment; th. 10 mm; in: GLEY 1 2.5/N black, out: GLEY 1 2.5/N black; surface burnished; no decoration preserved	
MCW-2	Menekşe Çatağı western settlement	39L/32	Body sherd; th. 5 mm; in: 10YR 5/8 yellowish brown, out: 10YR 5/8 yellowish brown; surface burnished; no decoration preserved	
MCW-3	Menekşe Çatağı western settlement	39L/35	Rim fragment; max. th. 6 mm, min. th. 3 mm; in: 10YR 4/3 brown, out: 10YR 6/3 pale brown; surface burnished; no decoration preserved	
MCW-4	Menekşe Çatağı western settlement	39L/47	Body sherd; th. 6 mm; in: 10YR 3/2 very dark greyish brown, out: 10YR 2/1 black; surface burnished; no decoration preserved	
MCW-5	Menekşe Çatağı western settlement	39L/49	Body sherd; th. 9 mm; in: 10YR 4/4 dark yellowish brown, out: 10YR 5/6 yellowish brown; surface burnished; no decoration preserved	
AK-1	Ağaçköprü	B3/4a	Body sherd of a closed vessel; th. 12 mm; in: 10YR 4/1 dark grey, out: GLEY 1 2.5/N black; surface unburnished; no decoration preserved	
AK-2	Ağaçköprü	B3/4b	Body sherd of a closed vessel; th. 14 mm; in: 10YR 5/3 brown, out: GLEY 1 2.5/N black; surface unburnished; no decoration preserved	
AT-1	Araptepe	B4/2a	Body sherd of a closed vessel; th. 7 mm; in: 10YR 3/2 very dark greyish brown, out: 10YR 2/1 black; surface unburnished; no decoration preserved	
AT-2	Araptepe	B4/2b	Body sherd of an opened vessel; th. max: 15 mm, min: 7 mm; in: 10YR 5/1 grey, out: GLEY 1 2.5/N black; surface burnished; no decoration preserved	
CM-1	Cevizlik Mevkii	B4/67a	Body sherd of a closed vessel; th. 7 mm; in: 10YR 5/3 brown, out: GLEY 1 2.5/N black; surface unburnished; no decoration preserved	
CM-2	Cevizlik Mevkii	B4/67b	Body sherd; th. max: 14 mm, min: 9 mm; in: 10YR 4/1 dark grey, out: 10YR 3/1 very dark grey; surface burnished; no decoration preserved	
CM-3	Cevizlik Mevkii	B4/67c	Body sherd; th. 7 mm; in: 10YR 3/2 very dark greyish brown, out: 10YR 2/1 black; surface burnished; no decoration preserved	
CM-4	Cevizlik Mevkii	B4/67d	Rim fragment; th. 7 mm; in: 10YR 3/2 very dark greyish brown, out: 10YR 2/1 black; surface unburnished; no decoration preserved	
DH-1	Demirlihanlı Mezarlığı	B3/IIa	Body sherd of a closed vessel; th. 9 mm; in: 10YR 2/1 black, out: 10YR 2/1 black; surface partially burnished; no decoration preserved	
DH-2	Demirlihanlı Mezarlığı	B3/IIb	Body sherd of an opened vessel; th. 11 mm; in: GLEY 1 3/N very dark grey, out: GLEY 1 3/N very dark grey; surface burnished; no decoration preserved	
DH-3	Demirlihanlı Mezarlığı	B3/IIc	Body sherd of an opened vessel; th. 10 mm; in: 10YR 5/2 greyish brown, out: GLEY 1 3/N very dark grey; surface burnished; no decoration preserved	

HM	Hamam Mevkii	A3/14	Body sherd of a closed vessel; th. 12 mm; in: 10YR 2/2 very dark brown, out: GLEY 1 3/N very dark grey; surface burnished; no decoration preserved	
YK-1	Yedigöz Kemerli	B3/5a	Body sherd of an opened vessel; th. 11 mm; in: GLEY 1 3/N very dark grey, out: GLEY 1 3/N very dark grey; surface burnished; no decoration preserved	
YK-2	Yedigöz Kemerli	B3/5b	Body sherd; th. 9 mm; in: 10YR 4/1 dark grey, out: 10YR 5/2 greyish brown; surface burnished; no decoration preserved	
YK-3	Yedigöz Kemerli	B3/5c	Body sherd of an opened vessel; th. 8 mm; in: 10YR 4/1 dark grey, out: 10YR 5/2 greyish brown; surface burnished; decorated with ribs	
YK-4	Yedigöz Kemerli	B3/5d	Body sherd of an opened vessel; th. 8 mm; in: GLEY 1 3/N very dark grey, out: GLEY 1 3/N very dark grey; surface burnished; no decoration preserved	
YK-5	Yedigöz Kemerli	B3/5e	Body sherd of an opened vessel; th. 8 mm; in: GLEY 1 3/N very dark grey, out: GLEY 1 3/N very dark grey; surface burnished; no decoration preserved	
OVC-1	Ovcarovo		Body sherd; th. 7 mm; in: in: GLEY 1 3/N very dark grey, out: GLEY 1 3/N very dark grey; surface unburnished; no decoration preserved	
OVC-2	Ovcarovo		Body sherd of a closed vessel; th. 14 mm; in: 7.5YR 6/4 light brown, out: 7.5YR 4/4 brown; surface burnished; no decoration preserved	
OVC-3	Ovcarovo		Body sherd of a closed vessel; th. 5 mm; in: GLEY 1 3/N very dark grey, out: GLEY 1 3/N very dark grey; surface burnished; no decoration preserved	
OVC-4	Ovcarovo		Rim fragment; th. 8 mm; in: 10YR 4/2 dark greyish brown, out: 10YR 4/2 dark greyish brown; surface unburnished; no decoration preserved	
OVC-5	Ovcarovo		Body sherd; th. 12 mm; in: 10YR 5/2 greyish brown, core: 10YR 2/1 black, out: 10YR 6/4 light yellowish brown; surface unburnished; no decoration preserved; sherd in a very fragmentary state	
OVC-6	Ovcarovo		Body sherd of a closed vessel; th. 8 mm; in: 10YR 2/1 black, out: 10YR 2/1 black; surface unburnished; no decoration preserved	
CH-1	Chal		Body sherd of a closed vessel; th. 11 mm; in: 10YR 5/4 yellowish brown, out: 10YR 3/1 very dark grey; surface unburnished; no decoration preserved; sherd in a very fragmentary state;	
CH-2	Chal		Body sherd; th. 10 mm; in: 10YR 3/1 very dark grey, out: 10YR 3/1 very dark grey; surface unburnished; incised decoration of running spiral	X
CH-3	Chal		Body sherd; th. 8 mm; in: 10YR 4/3 brown, out: 10YR 3/1 very dark grey; surface unburnished; incised decoration of inverted triangles filled with lines of dots	
CH-4	Chal		Body sherd of an opened vessel; th. 12 mm; in: 10YR 3/1 brown, out: 10YR 3/1 very dark grey; surface unburnished; no decoration preserved; sherd in a very fragmentary state;	
CH-5	Chal		Body sherd; th. 8 mm; in: 10YR 4/1 dark grey, out: 10YR 3/1 very dark grey; surface unburnished; no decoration preserved; sherd in a very fragmentary state	

CH-6	Chal		Body sherd of a closed vessel; th. 7 mm; in: 10YR 6/3 pale brown, out: 10YR 3/1 very dark grey; surface burnished; no decoration preserved; sherd in a very fragmentary state	
DIA-1	Diadovo		Rim fragment; th. 10 mm; in: GLEY 1 3/N very dark grey, core: 10YR 3/6 dark yellowish brown, out: GLEY 1 3/N very dark grey; surface burnished; decoration inside on rim, triangles filled with parallel lines pressed with a pointed triangular tool	X
DIA-2	Diadovo		Rim fragment; th. 12m; in: 10YR 3/1 very dark grey, out: 10YR 4/2 dark greyish brown; surface burnished; decoration: alternating spiral inside a circle and groups of two diagonal strokes pressed with a pointed rectangular tool	X
DIA-3	Diadovo		Body sherd of an opened vessel; th. 9 mm; in: GLEY 1 3/N very dark grey, out: GLEY 1 3/N very dark grey; surface burnished; decorated zone in middle body bordered with double incised encircling line, inside the zone: alternating spiral inside a circle and groups of two diagonal strokes pressed with a pointed rectangular tool	X
DIA-4	Diadovo		Handle and body fragment; th. body 5 mm, th. handle 9 mm, width handle 15 mm; in: GLEY 1 3/N very dark grey, out: GLEY 1 3/N very dark grey; surface burnished; decoration in middle body above carination rectangles formed by lines of small sharp incisions, filled with small concentric circles	X
DIA-5	Diadovo		Rim fragment of an opened vessel; th. 12 mm; in: GLEY 1 3/N very dark grey, out: GLEY 1 3/N very dark grey; surface burnished; decoration outside on rim, triangles filled with parallel lines	X
DIA-6	Diadovo		Rim fragment of an opened vessel; th. 8 mm; in: GLEY 1 3/N very dark grey, out: GLEY 1 3/N very dark grey; surface burnished; decorated with knobs and shallow pressed diagonal lines	X
DIA-7	Diadovo		Rim fragment of an opened vessel; th. 7 mm; in: 10YR 2/1 black, out: 10YR 2/1 black; surface burnished; decoration: alternating spiral inside a circle and groups of two diagonal strokes pressed with a pointed rectangular tool	X
DIA-8	Diadovo		Rim fragment of an opened vessel; th. 8 mm; in: 10YR 4/1 dark grey, out: 10YR 5/1 grey; surface burnished; decoration: alternating spiral inside a circle and groups of two diagonal strokes (also on the rim) pressed with a pointed rectangular tool	X
DIA-9	Diadovo		Body sherd; th. 9 mm; in: GLEY 1 3/N very dark grey, out: 10YR 3/1 very dark grey; surface burnished; buckel decoration	X
DIA-10	Diadovo		Body sherd; th. 10 mm; in: 10YR 6/1 grey, out: GLEY 1 3/N very dark grey; surface burnished; decoration: knobs with shallow pressed diagonal lines	X
DIA-11	Diadovo		Body sherd of an opened vessel; th. 8 mm; in: GLEY 1 3/N very dark grey, out: GLEY 1 3/N very dark grey; surface burnished; knobs and incised decoration: triangles filled with raws of small incisions, running spirals, parallel and diagonal lines	X
DIA-12	Diadovo		Handle fragment; diameter 18 mm; 2.5Y 4/1 dark grey; surface burnished; decoration: spiral ribs	X

DIA-13	Diadovo		Handle fragment; th. 18 mm, width 23 mm; in: 10YR 6/1 grey; surface burnished; decoration: two incised lines along the handle	X
PSH-1	Pshenitsevo		Body sherd; th. 6 mm; in: GLEY 1 3/N very dark grey, out: GLEY 1 3/N very dark grey; surface unburnished; decoration: knobs	X
PSH-2	Pshenitsevo		Rim fragment; th. 8 mm; in: GLEY 1 3/N very dark grey, out: GLEY 1 3/N very dark grey; surface burnished; no decoration preserved	X
PSH-3	Pshenitsevo		Body sherd; th. 5 mm; in: GLEY 1 3/N very dark grey, out: GLEY 1 3/N very dark grey; surface burnished; knobs and incised decoration: carination	X
KIR-1	Kirilovo		Body sherd; th. 7 mm; in: GLEY 1 3/N very dark grey, out: GLEY 1 3/N very dark grey; surface unburnished; decorated zone bordered by wide incision and a ledge and filled with shallow, incised, diagonal lines	X
KIR-2	Kirilovo		Body sherd; th. 5 mm; in: 7.5YR 6/8 reddish yellow, out: GLEY 1 3/N very dark grey; surface unburnished; sherd in a very fragmentary state	
KIR-3	Kirilovo		Body sherd of an opened vessel; th. 5 mm; in: 7.5YR 6/8 reddish yellow, out: 10YR 3/1 very dark grey; surface burnished; incised decoration of parallel strokes forming unidentified motif	X
SBO-1	Sborianovo		Body sherd; th. 9 mm; in: GLEY 1 3/N very dark grey, out: GLEY 1 3/N very dark grey; surface unburnished; sherd in a very fragmentary state	
SBO-2	Sborianovo		Body sherd; th. 8 mm; in: 7.5YR 6/8 reddish yellow, out: GLEY 1 3/N very dark grey; surface burnished; sherd in a very fragmentary state	
SBO-3	Sborianovo		Body sherd with handle fragment; th. 8 mm, th. handle: 12 mm, width handle 19 mm; in: 10YR 5/2 greyish brown, out: 10YR 7/2 light grey; surface burnished; no decoration preserved, sherd in a very fragmentary state	





**APPENDIX 2. GEOLOGICAL SAMPLES ANALYSED IN THIS STUDY. (SAMPLES NR. 1-20 AFTER KNACKE-LOY, 1994)**

Nr.	Archaeological site	Sample locality	Sample Nr.	Sample
1	Troia	Akköy	R6*	Neogene claymarl
2	Troia	Akköy	R10*	Potter's clay
3	Troia	Karamenderes river	R14*	River sediment
4	Troia	Karamenderes river	R16*	River sediment
5	Troia	Karamenderes river	R18*	River sediment
6	Troia	borehole KT 45	K8*	Clayey sand
7	Troia	borehole KT 45	K10*	Clay
8	Troia	borehole KT 45	K12*	Clay
9	Troia	borehole KT kk, K1	K22*	Sandy, clayey soil
10	Troia	borehole KT 11 c	K26*	Clay with sand
11	Troia	borehole KT 41 b	K31*	Clay with sand
12	Troia	borehole KT 41 b	K33*	Clay
13	Troia	borehole KT 41 b	K35*	Clay
14	Troia	borehole KT 42	K39*	Clay with sand
15	Troia	borehole KT 42	K42*	Clay with sand
16	Troia	borehole KT 43	K52*	Clay
17	Troia	borehole KT 43	K53*	Silty clay
18	Troia	Tevfikiye	R12*	Loam (Dümrek river)
19	Troia	Tevfikiye	R12/2*	Loam (Dümrek river)
20	Troia	Kumkale	R13*	Loam (Dümrek river)
21	Troia	Karamenderes river	Tr-1a	Medium to coarse sand
22	Troia	Karamenderes river	Tr-1b	Silty sand
23	Troia	Dümrek river	Tr-2a	Medium to coarse sand
24	Troia	Dümrek river	Tr-2b	Silty sand
25	Menekşe Çatağı	Tekirdağ	Mc-1	Neogene clay
26	Menekşe Çatağı	Tekirdağ	Mc-2	Silty clay
27	Menekşe Çatağı	Tekirdağ	Mc-3	Clay
28	Menekşe Çatağı	Menekşe Çatağı	Mc-4	Clay (river sediment)
29	Menekşe Çatağı	Menekşe Çatağı	Mc-5	Marl
30	Menekşe Çatağı	Menekşe Çatağı	Mc-6	Clayey soil
31	Menekşe Çatağı	Menekşe Çatağı	Mc-7	Clay
32	Menekşe Çatağı	Menekşe Çatağı	Mc-8	Pebbles
33	North Turkish Thrace	Arnavutköy	Ntt-1	Sandy river sediment
34	North Turkish Thrace	Yeniköy	Ntt-2	Fine sand (river sediment)
35	North Turkish Thrace	Yeniköy	Ntt-3	Silty sand
36	North Turkish Thrace	Anliyence Devesi	Ntt-4	Silt (river sediment)
37	North Turkish Thrace	Lalapaşa	Ntt-5	Sandy clay (river sediment)
38	North Turkish Thrace	Süleycik Deresi	Ntt-6	Clayey sand (river sediment)
39	North Turkish Thrace	Büyük Gerdelli	Ntt-7	Silty clay (river sediment)
40	North Turkish Thrace	Akardere	Ntt-8	Soil + clayey sand
41	North Turkish Thrace	Hasköy	Ntt-9	Sandy soil
42	North Turkish Thrace	Demirhanlı	Ntt-10	Sand (river sediment)
43	North Turkish Thrace	Hasanağa	Ntt-11	Silty clay
44	North Turkish Thrace	Hasanağa	Ntt-12	Sandy river sediment

\* data see in Knacke-Loy, 1994

<b>Nr.</b>	<b>Archaeological site</b>	<b>Sample locality</b>	<b>Sample Nr.</b>	<b>Sample</b>
45	Ovcarovo	Bulgarin	Ovc-1	Clayey silt + soil
46	Ovcarovo	Bulgarin	Ovc-2	Clayey soil
47	Ovcarovo	Ovcarovo	Ovc-3	Clayey soil
48	Ovcarovo	Ovcarovo	Ovc-4	Clayey silt
49	Ovcarovo	Ovcarovo	Ovc-5	Sandy clay
50	Ovcarovo	Ovcarovo	Ovc-6	Sandy clay (river sediment)
51	Chal	Chal	Ch-1	Clay
52	Chal	Chal	Ch-2	Clay
53	Chal	Chal	Ch-3	Clay (river sediment)
54	Chal	Malevo-Koren	Ch-4	Silty clay
55	Chal	Koren	Ch-5	Sand (river sediment)
56	Chal	Malik Izvor	Ch-6	Sandy clay
57	Chal	Koren-Malik Izvor	Ch-7	Sandy clay
58	Chal	Koren-Malik Izvor	Ch-8	Silty clay
59	Chal	Koren-Malik Izvor	Ch-9	Silt
60	Chal	Koren-Malik Izvor	Ch-10	Coarse sand (river sediment)
61	Kirilovo	Malaka verei	Kir-1	Soil
62	Kirilovo	Malaka verei	Kir-2	Clay
63	Kirilovo	Malaka verei	Kir-3	Clayey soil
64	Kirilovo	Elhovo	Kir-4	Clay (river sediment)
65	Kirilovo	Elhovo	Kir-5	Clayey soil
66	Kirilovo	Kirilovo	Kir-6	Soil
67	Diadovo-Pshenitsevo	Bereketzka tell	Dia-1	Clayey soil
68	Diadovo-Pshenitsevo	Bereketzka tell	Dia-2	Clay (river sediment)
69	Diadovo-Pshenitsevo	Pshenitsevo	Dia-3	Silty clay
70	Diadovo-Pshenitsevo	Korten	Dia-4	Clayey lime
71	Diadovo-Pshenitsevo	Banja	Dia-5	Clay
72	Diadovo-Pshenitsevo	Banja	Dia-6	Clay
73	Diadovo-Pshenitsevo	Padarevo	Dia-7	Silty clay
74	Diadovo-Pshenitsevo	Padarevo	Dia-8	Clay
75	Diadovo-Pshenitsevo	Zagorci	Dia-9	Clay
76	Diadovo-Pshenitsevo	Diadovo	Dia-10	Clay
77	Diadovo-Pshenitsevo	Diadovo	Dia-11	Clay
78	Diadovo-Pshenitsevo	Diadovo	Dia-12	Sandy clay
79	Diadovo-Pshenitsevo	Diadovo	Dia-13	Soil
80	Diadovo-Pshenitsevo	Diadovo	Dia-14	Sand (river sediment)
81	Sborianovo	Svestari	Sb-1	Clay
82	Sborianovo	Svestari	Sb-2	Clay (river sediment)
83	Sborianovo	Svestari	Sb-3	Clay
84	Sborianovo	Svestari	Sb-4	Clay
85	Sborianovo	Golan Porovec	Sb-5	Clay
86	Sborianovo	Zavet	Sb-6	Sandy clay (river sediment)
87	Sborianovo	Zavet	Sb-7	Sandy clay (river sediment)
88	Sborianovo	Malak Porovec	Sb-8	Clay
89	Sborianovo	Malak Porovec	Sb-9	Clay



Sample	CM-3	CM-4	DH-1	DH-2	DH-3	HM	YK-1	YK-2	YK-3	YK-4	YK-5	OVC-1	OVC-2	OVC-3	OVC-4
Matrix and pores	76.70	78.30	74.50	79.40	77.10	74.10	68.10	73.50	82.60	79.90	74.00	76.50	82.30	81.40	93.30
Non-plastic clasts	23.30	21.70	25.50	20.60	22.90	25.90	31.90	26.50	17.40	20.10	26.00	23.50	17.70	18.60	6.70
Clay temper, pellet		0.40	0.20	0.50		0.20									18.60
Monoquartz	51.40	63.10	39.60	37.50	34.70	48.20	50.20	42.20	55.60	57.60	44.40	27.80	37.20	23.30	48.80
Sparite															
Micrite															36.90
K-feldspar	24.80	20.20	27.50	9.70	9.50	10.20	6.80	11.30	13.10	9.10	16.50	23.50	20.40	29.90	
Plagioclase	1.90	1.00	0.20	2.10	2.00	3.40	1.00	3.30	1.20	1.00	1.60	2.30	0.60	1.00	
Pyroxene															
Hornblende	0.30		0.20			0.20	0.20		0.30	0.30	0.20				
Muscovite	0.20		0.30			6.40	0.30	0.10	0.40	0.20	0.30	1.70	0.20	0.70	3.70
Biotite	0.20		0.40			2.80	0.20	0.10	0.20	0.30	0.20	0.50		0.20	0.50
Epidote	1.30	0.20	0.20	0.20	0.20		0.60	0.10	0.20	1.00	0.30	0.40	0.20	0.20	
Garnet						1.70									
Olivine															
Opaque				1.50	0.50			0.20	0.20	0.20	0.20	0.40	0.60		10.10
Acidic-intermediate plutonite	0.50	2.30	9.90	5.20	0.30	12.40	25.50	3.50	6.70	1.70		26.20	6.30	33.30	
Basic-intermediate volcanite															
Intermediate-acidic volcanite															
Recrystallised volcanite			0.60		1.00										
Acidic volcanic glass										1.50					
Basic volcanic glass															
Chert (Chalcedony)				5.00	4.60	0.30									
Polycrystalline quartz	19.40	13.20	21.10	38.80	47.20	11.50	15.10	39.10	21.10	26.80	34.40	17.20	23.80	11.40	
Sandstone															
Phyllite															
Micaschist						2.90									
Serpentinite															
ARF							0.10	0.10	1.00	0.30	1.90		10.70		

Sample	DIA-2	DIA-3	DIA-4	DIA-5	DIA-6	DIA-7	DIA-8	DIA-9	DIA-10	DIA-11	DIA-12	DIA-13	SBO-1	SBO-2	SBO-3
Matrix and pores	79.90	76.70	90.90	71.60	84.50	80.90	74.70	86.30	82.80	84.20	80.00	68.10	75.70	96.80	96.60
Non-plastic clasts	20.10	23.30	9.10	28.40	15.50	19.10	25.20	13.70	17.20	15.80	20.00	31.80	24.30	3.20	3.40
Clay temper, pellet		20.90		1.00	6.60			0.70		4.60	1.60		20.30	76.60	73.90
Monoquartz	25.30	8.80	14.90	7.80	22.80	17.70	15.90	61.30	27.20	21.30	13.60	7.80	17.90	31.20	38.70
Sparite															
Micrite		10.20			5.60		2.30			3.50	1.00		78.20	62.00	35.30
K-feldspar	24.20	2.70	18.60	7.30	11.20	19.80	17.40	4.80	20.90	17.60	8.10	7.10	1.30	1.60	
Plagioclase	6.80	0.10	1.40	0.50	0.80	3.00	0.30	1.10	2.80	2.80	1.50	2.80			
Pyroxene															
Hornblende			2.90		0.30						0.10				
Muscovite	0.30	0.20		0.40	0.30	0.20	0.10	0.70	0.20	0.20	0.10	0.20		0.90	1.90
Biotite		0.50			1.50		0.10	1.40		0.40	0.30				
Epidote	0.30	0.10			0.30	0.10	0.10	0.30		0.10	0.10	0.10			
Garnet															
Olivine															
Opaque		0.10	1.40				0.20		0.40		0.20	0.50	2.60	4.30	24.10
Acidic-intermediate plutonite	26.40	52.90	4.30	57.80	23.20	59.20	62.60	18.60	12.30	54.10	9.10	76.70			
Basic-intermediate volcanite		1.50	1.00					8.70			14.60				
Intermediate-acidic volcanite															
Recrystallised volcanite					21.30										
Acidic volcanic glass									8.60						
Basic volcanic glass															
Chert (Chalcedony)		1.50					1.00				0.30				
Polycrystalline quartz	12.50	6.30	9.90	23.90	6.70				27.60		1.70				
Sandstone		3.80	45.60		6.00						33.30	4.80			
Phyllite		11.30									4.00				
Micaschist	4.20			2.30							1.70				
Serpentinite															
ARF											10.30				

Sample	OVC-5	OVC-6	CH-1	CH-2	CH-3	CH-4	CH-5	CH-6	KIR-1	KIR-2	KIR-3	PSH-1	PSH-2	PSH-3	DIA-1
Matrix and pores	86.90	96.20	76.80	83.40	81.70	82.80	79.30	79.30	83.60	88.60	85.20	78.70	85.10	82.60	83.50
Non-plastic clasts	13.10	3.80	23.20	16.60	18.30	17.20	20.70	20.70	16.40	11.40	14.80	21.30	14.90	17.40	16.50
Clay temper, pellet	63.70	51.20					11.20					0.50	24.90	0.30	2.60
Monoquartz	64.80	84.60	42.20	54.50	53.90	42.20	42.20	35.20	39.80	13.30	11.10	26.20	29.80	28.80	13.90
Sparite															
Micrite	32.20	10.40													
K-feldspar			18.10	10.10	27.20	13.10	7.50	15.10	16.30	33.80	38.20	24.20	17.70	38.20	24.10
Plagioclase			4.20	3.80	4.40	2.60	2.80	5.80	1.10	1.50		1.00	1.30	1.30	
Pyroxene															
Hornblende						0.20						0.10	0.40		
Muscovite	3.00	2.10	0.50	2.90		0.20		0.30	0.40			0.10	0.10		0.20
Biotite		0.80	0.50	0.40		1.30	1.00	0.20							0.20
Epidote			0.10	1.30		0.40		1.40		0.20		0.10		0.60	
Garnet															
Olivine						7.00									
Opaque		2.10	1.20		1.30	1.30	1.30			9.70	7.60	0.60		0.30	0.20
Acidic-intermediate plutonite			9.30	9.70	1.40	13.20	13.70	7.90	40.20	41.50	43.10	44.30	50.70	29.80	61.40
Basic-intermediate volcanite			7.30												
Intermediate-acidic volcanite															
Recrystallised volcanite															
Acidic volcanic glass															
Basic volcanic glass															
Chert (Chalcedony)			0.30				0.20	0.30							
Polycrystalline quartz			14.40	17.30	8.90	15.40	20.10	27.30	2.20			3.10		1.00	
Sandstone															
Phyllite			1.90						1.00			0.30			
Micaschist															
Serpentinite															
ARF					2.90	3.10		5.50							

Sample	DIA-2	DIA-3	DIA-4	DIA-5	DIA-6	DIA-7	DIA-8	DIA-9	DIA-10	DIA-11	DIA-12	DIA-13	SBO-1	SBO-2	SBO-3
Matrix and pores	79.90	76.70	90.90	71.60	84.50	80.90	74.70	86.30	82.80	84.20	80.00	68.10	75.70	96.80	96.60
Non-plastic clasts	20.10	23.30	9.10	28.40	15.50	19.10	25.20	13.70	17.20	15.80	20.00	31.80	24.30	3.20	3.40
Clay temper, pellet		20.90		1.00	6.60			0.70		4.60	1.60		20.30	76.60	73.90
Monoquartz	25.30	8.80	14.90	7.80	22.80	17.70	15.90	61.30	27.20	21.30	13.60	7.80	17.90	31.20	38.70
Sparite															
Micrite		10.20			5.60		2.30			3.50	1.00		78.20	62.00	35.30
K-feldspar	24.20	2.70	18.60	7.30	11.20	19.80	17.40	4.80	20.90	17.60	8.10	7.10	1.30	1.60	
Plagioclase	6.80	0.10	1.40	0.50	0.80	3.00	0.30	1.10	2.80	2.80	1.50	2.80			
Pyroxene															
Hornblende			2.90		0.30						0.10				
Muscovite	0.30	0.20		0.40	0.30	0.20	0.10	0.70	0.20	0.20	0.10	0.20		0.90	1.90
Biotite		0.50			1.50		0.10	1.40		0.40	0.30				
Epidote	0.30	0.10			0.30	0.10	0.10	0.30		0.10	0.10	0.10			
Garnet															
Olivine															
Opaque		0.10	1.40				0.20		0.40		0.20	0.50	2.60	4.30	24.10
Acidic-intermediate plutonite	26.40	52.90	4.30	57.80	23.20	59.20	62.60	18.60	12.30	54.10	9.10	76.70			
Basic-intermediate volcanite		1.50	1.00					8.70			14.60				
Intermediate-acidic volcanite															
Recrystallised volcanite					21.30										
Acidic volcanic glass								8.60							
Basic volcanic glass															
Chert (Chalcedony)		1.50					1.00				0.30				
Polycrystalline quartz	12.50	6.30	9.90	23.90	6.70				27.60		1.70				
Sandstone		3.80	45.60		6.00				3.10		33.30	4.80			
Phyllite		11.30									4.00				
Micaschist	4.20			2.30							1.70				
Serpentinite															
ARF											10.30				

**APPENDIX 4. TEXTURAL FEATURES OF THE KNOBBED WARE SHERDS ANALYSED IN THIS STUDY.**

Sample		TR-1	TR-2	TR-3	TR-4	TR-5
Colour of the groundmass	1 Nicol	brown- dark brown	orange- brown	brown- dark brown	dark brown	brown
	+ Nicols	dark brown	dark brown	(dark) brown	dark brown	brown
Isotropism of the groundmass		moderate- complete	poor- moderate	poor- complete	complete	poor- moderate
Texture		hiatal	serial (hiatal)	hiatal	hiatal	hiatal
Grain-size distribution	sorting	poor	poor	poor	poor	poor
Grain size maximum ( $\mu\text{m}$ )		4000	2400	2600	3000	4000
Roundness of the clasts		va-sr	va-sa	va-sr	va-sr	va-r
Sphericity of the clasts		1-4	1-4	1-4	1-5	1-4

Sample		TR-6	TR-7	TR-8	TR-9	TR-10
Colour of the groundmass	1 Nicol	brown-dark brown	black	(dark) brown	brown	brown-dark brown
	+ Nicols	(dark) brown	black	black	brown	(dark) brown
Isotropism of the groundmass		moderate- complete	complete	moderate- complete	poor	moderate- complete
Texture		serial	serial (hiatal)	hiatal	hiatal	hiatal (serial)
Grain-size distribution	sorting	poor	poor	poor	poor	poor
Grain size maximum ( $\mu\text{m}$ )		1400	2200	7000	1600	1800
Roundness of the clasts		va-sa	va-sr	a-sr	va-sa	sa-sr
Sphericity of the clasts		1-3	1-4	2-4	1-3	1-4

Sample		TR-11	TR-12	TR-13	TR-14	TR-15
Colour of the groundmass	1 Nicol	brown	brown	brown	brown	brown
	+ Nicols	(dark) brown	brown	dark brown	dark brown	dark brown
Isotropism of the groundmass		poor-good	poor	poor- moderate	good	good
Texture		serial	hiatal	hiatal	hiatal	hiatal
Grain-size distribution	sorting	poor	poor	poor	poor	poor
Grain size maximum ( $\mu\text{m}$ )		1400	1800	2400	3800	3800
Roundness of the clasts		va-r	va-sa	va-sr	va-sr	va-sr
Sphericity of the clasts		1-3	1-2	1-4	1-3	1-3

(va=very angular, a=angular, sa=subangular, sr=subrounded, r=rounded)

Sample		TR-16	TR-17	TR-18	TR-19	TR-20
Colour of the groundmass	1 Nicol	dark brown	dark brown	brown	orange	brown
	+ Nicols	black	black	brown	brown	dark brown
Isotropism of the groundmass		complete	complete	poor	poor	moderate-good
Texture		hiatal	hiatal	hiatal	serial	serial (hiatal)
Grain-size distribution	sorting	poor	poor	poor	mod.- poor	mod.- good
Grain size maximum ( $\mu\text{m}$ )		2700	2900	1700	1200	2000
Roundness of the clasts		a-r	a-sr	va-sr	va-sa	a-sr
Sphericity of the clasts		1-3	1-4	1-4	1-3	1-4

Sample		TR-21	TR-22	TR-23	TR-24	TR-25
Colour of the groundmass	1 Nicol	brown	brown	brown	brown	brown
	+ Nicols	dark brown	dark brown	dark brown	dark brown	dark brown
Isotropism of the groundmass		moderate	moderate-good	poor	poor	poor
Texture		hiatal	serial (hiatal)	hiatal	hiatal	serial
Grain-size distribution	sorting	poor	poor	poor	poor	poor
Grain size maximum ( $\mu\text{m}$ )		3000	1900	2200	1800	1500
Roundness of the clasts		a-sr	a-sr	a-r	a-r	va-sr
Sphericity of the clasts		1-3	1-4	1-4	1-4	1-5

Sample		TR-26	TR-27	TR-28	A-1	MCW-1
Colour of the groundmass	1 Nicol	brown	brown	brown	dark brown	brown
	+ Nicols	brown	dark brown	brown	black	dark brown
Isotropism of the groundmass		poor	good	poor	good	moderate-poor
Texture		serial	hiatal	hiatal	serial	serial
Grain-size distribution	sorting	poor	poor	poor	poor	moderate-good
Grain size maximum ( $\mu\text{m}$ )		1600	2200	1600	1800	1000
Roundness of the clasts		va-sr	va-sr	va-sr	va-sr	va-sr
Sphericity of the clasts		1-3	1-3	1-5	1-3	1-4

(va=very angular, a=angular, sa=subangular, sr=subrounded, r=rounded)

Sample		MCW-2	MCW-3	MCW-4	MCW-5	MCE-1
Colour of the groundmass	1 Nicol	yellowish-brown	brown	brown	brown	brown
	+ Nicols	brown	dark brown	dark brown	dark brown	dark brown
Isotropism of the groundmass		poor	moderate-poor	moderate-poor	poor	good
Texture		hiatal	serial	hiatal	serial	hiattal
Grain-size distribution	sorting	poor	moderate	poor	moderate	poor
Grain size maximum ( $\mu\text{m}$ )		1800	650	1600	1000	3400
Roundness of the clasts		va-sa	va-sa	a-sa	va-sr	
Sphericity of the clasts		1-2	1-3 (4)	1-2	1-2	va-sr

Sample		MCE-2	MCE-3	MCE-4	MCE-5	AK-1
Colour of the groundmass	1 Nicol	brown	brown	dark brown	dark brown	dark brown
	+ Nicols	dark brown	dark brown	black	dark brown	dark brown
Isotropism of the groundmass		poor-moderate	moderate-good	complete	moderate-good	complete
Texture		serial (hiatal)	serial	hiatal	serial (hiatal)	hiatal
Grain-size distribution	sorting	mod.-poor	moderate	poor	mod.-poor	moderate
Grain size maximum ( $\mu\text{m}$ )		1400	1000	2500	1000	2000
Roundness of the clasts		a-r	va-sr	va-sr	va-sr	va-sa
Sphericity of the clasts		1-3	1-2	1-4	2-3	1-3

Sample		AK-2	AT-1	AT-2	CM-1	CM-2
Colour of the groundmass	1 Nicol	dark brown, black	yellowish-brown	yellow	yellowish-brown	brown, dark brown
	+ Nicols	black	brown	yellowish-brown	brown, dark brown	dark brown
Isotropism of the groundmass		good	poor	poor	poor-moderate	poor
Texture		hiatal	serial	serial	hiatal	serial
Grain-size distribution	sorting	poor-moderate	poor	moderate	moderate-poor	moderate-poor
Grain size maximum ( $\mu\text{m}$ )		2800	1600	1800	2000	1800
Roundness of the clasts		va-sr	va-sa	va-sa	a-r	va-sr
Sphericity of the clasts		1-4	1-3	1-2	1-4	1-3

(va=very angular, a=angular, sa=subangular, sr=subrounded, r=rounded)

Sample		CM-3	CM-4	DH-1	DH-2	DH-3
Colour of the groundmass	1 Nicol	brown, dark brown	brown	brown-dark brown	brown - dark brown	dark brown
	+ Nicols	dark brown	dark brown	dark brown	dark brown	dark brown
Isotropism of the groundmass		poor-moderate	moderate	moderate-(complete)	moderate (complete)	complete
Texture		serial (hiatal)	serial (hiatal)	hiatal	serial	serial (hiatal)
Grain-size distribution	sorting	moderate-poor	poor-moderate	poor	moderate	moderate (poor)
Grain size maximum ( $\mu\text{m}$ )		3400	2000	2600	1500	1500
Roundness of the clasts		a-sa	va-sa	va-sa	va-sr	va-sr
Sphericity of the clasts		2-3	1-3	1-3	1-3	1-3

Sample		HM	YK-1	YK-2	YK-3	YK-4
Colour of the groundmass	1 Nicol	brown	brown	dark brown	brown-dark brown	brown
	+ Nicols	dark brown	dark brown	dark brown	dark brown	dark brown
Isotropism of the groundmass		moderate	poor	moderate-good	poor-good	poor
Texture		hiatal	hiatal	serial (hiatal)	hiatal	serial
Grain-size distribution	sorting	poor	poor	moderate	poor	poor
Grain size maximum ( $\mu\text{m}$ )		3600	4400	2900	1700	1800
Roundness of the clasts		va-sr	va-r	a-sa	va-sr	va-sa
Sphericity of the clasts		1-3	1-4	1-3	1-3	1-2

Sample		YK-5	OVC-1	OVC-2	OVC-3	OVC-4
Colour of the groundmass	1 Nicol	brown	brown	yellow	brown	brown
	+ Nicols	dark brown	dark brown	brown	dark brown	dark brown
Isotropism of the groundmass		moderate	moderate	poor	moderate-good	moderate
Texture		serial (hiatal)	hiatal	hiatal	hiatal	serial
Grain-size distribution	sorting	poor	poor	poor	poor	good
Grain size maximum ( $\mu\text{m}$ )		2200	2700	3400	3600	1000
Roundness of the clasts		va-sa	va-sa	va-sr	va-sa	va-r
Sphericity of the clasts		1-3	1-3	1-3	1-3	1-5

(va=very angular, a=angular, sa=subangular, sr=subrounded, r=rounded)

Sample		OVC-5	OVC-6	CH-1	CH-2	CH-3
Colour of the groundmass	1 Nicol	brown	brown	yell.-brown	brown	brown
	+ Nicols	dark brown	dark brown	brown-dark brown	dark brown	brown
Isotropism of the groundmass		complete	moderate	moderate	complete	poor
Texture		serial	serial	serial	hiatal/serial	serial/hiatal
Grain-size distribution	sorting	moderate	mod./good	poor	poor	moderate
Grain size maximum ( $\mu\text{m}$ )		1800	700	1800	1600	1700
Roundness of the clasts		a-r	a-r	va-sr	va-sa	va-a
Sphericity of the clasts		2-4	1-4	1-3	1-3	1-4

Sample		CH-4	CH-5	CH-6	KIR-1	KIR-2
Colour of the groundmass	1 Nicol	(dark) brown	yell.- brown	brown	brown	orange-brown
	+ Nicols	dark brown	brown-dark brown	dark brown	dark brown	brown
Isotropism of the groundmass		mod.- poor	poor - complete	moderate	moderate	poor-moderate
Texture		hiatal	hiatal	serial (hiatal)	hiatal	serial
Grain-size distribution	sorting	poor	poor	mod.- poor	poor	moderate
Grain size maximum ( $\mu\text{m}$ )		1900	2000	1400	3300	1000
Roundness of the clasts		va-sr	va-sa	va-sa	ra-sa	va-sa
Sphericity of the clasts		1-4	1-3	1-3	1-4	1-3

Sample		KIR-3	DIA-1	DIA-2	DIA-3	DIA-4
Colour of the groundmass	1 Nicol	Orange-brown	yellow-brown	yellow-brown	yellow-brown	yellow
	+ Nicols	brown-dark brown	brown	brown	brown	brown
Isotropism of the groundmass		poor-complete	moderate-poor	poor-moderate	poor	poor
Texture		serial (hiatal)	hiatal	hiatal (serial)	hiatal	serial
Grain-size distribution	sorting	moderate	poor	poor	poor	poor-moderate
Grain size maximum ( $\mu\text{m}$ )		1400	2500	1800	3600	1000
Roundness of the clasts		va-sr	va-sr	va-sa	va-sa	va-sa
Sphericity of the clasts		1-4	1-4	1-3	1-4	1-4

(va=very angular, a=angular, sa=subangular, sr=subrounded, r=rounded)

Sample		DIA-5	DIA-6	DIA-7	DIA-8	DIA-9
Colour of the groundmass	1 Nicol	yellow	brown	yellow-brown	yellow	brown
	+ Nicols	brown	dark brown	brown	brown	dark brown
Isotropism of the groundmass		poor	complete	complete-moderate	poor	moderate-good
Texture		hiatal	hiatal	hiatal	hiatal	serial/hiatal
Grain-size distribution	sorting	poor	poor	poor	poor	moderate
Grain size maximum ( $\mu\text{m}$ )		3800	220	2600	3300	1200
Roundness of the clasts		va-sa	va-sr	va-sa	va-sa	va-sa
Sphericity of the clasts		1-3	1-4	1-3	1-3	1-4

Sample		DIA-10	DIA-11	DIA-12	DIA-13	PSH-1
Colour of the groundmass	1 Nicol	brown	brown-yellow	brown	yellow-brown	brown
	+ Nicols	dark brown	brown	dark brown	brown	dark brown
Isotropism of the groundmass		moderate	poor	good	poor	good
Texture		hiatal	hiatal	serial	hiatal	hiatal
Grain-size distribution	sorting	poor	poor	poor	poor	poor
Grain size maximum ( $\mu\text{m}$ )		2200	1800	1700	4600	3800
Roundness of the clasts		va-sr	va-sr	va-r	va-sa	va-sr
Sphericity of the clasts		1-4	1-4	1-4	1-3	1-4

Sample		PSH-2	PSH-3	SBO-1	SBO-2	SBO-3
Colour of the groundmass	1 Nicol	yellow	yellow	brown	orange-brown	brown
	+ Nicols	brown	brown	dark brown	(dark) brown	dark brown
Isotropism of the groundmass		poor	poor-moderate	good-moderate	poor-complete	moderate-good
Texture		hiatal	hiatal	serial	serial	serial
Grain-size distribution	sorting	poor	poor	poor	moderate	moderate
Grain size maximum ( $\mu\text{m}$ )		2000	1800	2500	1200	1000
Roundness of the clasts		va-sr	va-sr	a-r	sa-r	sa-r
Sphericity of the clasts		1-4	1-4	1-4	1-4	1-4

(va=very angular, a=angular, sa=subangular, sr=subrounded, r=rounded)

**APPENDIX 5. MEASURED ELEMENTS, NUMBER OF THE STANDARDS APPLIED, STANDARD DEVIATION ( $3\sigma$ ), DETECTION LIMIT, AND STANDARD CONCENTRATIONS OF THE X-RAY FLUORESCENCE (XRF) ANALYSIS.**

Element	Nr. of Standards	Standard Deviation ( $3\sigma$ )	Detection Limit	Standard Concentrations
SiO <sub>2</sub>	30	± 0.1367 %	240 ppm	34.46 to 88.2 %
TiO <sub>2</sub>	29	± 0.0149 %	12 ppm	0.01 to 3.78 %
Al <sub>2</sub> O <sub>3</sub>	30	± 0.1660 %	244 ppm	0.03 to 59.27 %
Fe <sub>2</sub> O <sub>3</sub>	31	± 0.0569 %	180 ppm	0.08 to 25.70 %
MnO	22	± 0.22 ppm	5 ppm	0.0 to 0.35 %
MgO	29	± 0.139 %	88 ppm	0.03 to 39.37 %
CaO	32	± 0.0978 %	48 ppm	0.04 to 21.36 %
Na <sub>2</sub> O	27	± 0.0613 %	75 ppm	0.04 to 6.54 %
K <sub>2</sub> O	30	± 0.0301 %	24 ppm	0.01 to 1.39 %
P <sub>2</sub> O <sub>5</sub>	28	± 0.0087 %	14 ppm	0.01 to 1.39 %
Ba	22	± 0.34 ppm	11 ppm	0 to 4000 ppm
Ce	23	± 7 ppm	10 ppm	1 to 421 ppm
Co	21	± 1.6 ppm	1.6 ppm	1 to 210 ppm
Cr	28	± 12 ppm	3.5 ppm	3 to 2750 ppm
Eu	25	± 0 ppm	0.0 ppm	0 to 4 ppm
La	16	± 6 ppm	5.1 ppm	2 to 200 ppm
Nb	22	± 6 ppm	3.8 ppm	1 to 270 ppm
Nd	26	± 3 ppm	3.2 ppm	0 to 190 ppm
Ni	19	± 9 ppm	3.3 ppm	2 to 2040 ppm
Pb	28	± 3 ppm	10.3 ppm	2 to 54 ppm
Rb	31	± 8 ppm	2.9 ppm	0 to 3600 ppm
Sm	25	± 1 ppm	2.1 ppm	0 to 33 ppm
Sr	27	± 4 ppm	3.0 ppm	0 to 1375 ppm
Th	20	± 2 ppm	5.1 ppm	1 to 180 ppm
U	15	± 2 ppm	0.6 ppm	0 to 84 ppm
V	24	± 5 ppm	2.6 ppm	1 to 527 ppm
Y	23	± 3 ppm	1.8 ppm	0 to 184 ppm
Yb	28	± 0 ppm	0.2 ppm	0 to 17 ppm
Zn	28	± 10 ppm	3.0 ppm	10 to 1502 ppm
Zr	14	± 12 ppm	8.5 ppm	11 to 780 ppm

## APPENDIX 6. X-RAY FLUORESCENCE (XRF) ANALYSIS DATA OF GEOLOGICAL SAMPLES.

Sample	Me-1	Me-2	Me-3	Me-4	Me-5	Me-6	Me-7	Ntt-1	Ntt-2	Ntt-3	Ntt-4	Ntt-5	Ntt-6	Ntt-7	Ntt-8	Ntt-9	Ntt-10	Ntt-11	Ntt-12	Ove-1	Ove-2
<b>SiO<sub>2</sub> (wt %)</b>	62.02	58.23	64.69	56.85	49.01	72.83	56.24	58.08	72.96	63.74	58.16	63.47	63.50	70.52	69.13	74.33	53.67	45.21	47.66	71.19	65.57
<b>TiO<sub>2</sub> (wt %)</b>	0.76	0.82	0.85	0.81	0.93	0.56	0.76	0.68	0.54	0.66	0.34	0.65	0.83	0.59	0.61	0.46	0.75	0.48	0.67	0.62	0.55
<b>Al<sub>2</sub>O<sub>3</sub> (wt %)</b>	11.87	12.33	14.18	15.60	18.55	11.92	17.90	13.35	12.21	16.61	7.42	17.30	16.44	13.13	14.35	12.85	14.85	9.45	13.72	14.07	14.20
<b>Fe<sub>2</sub>O<sub>3</sub> (wt %)</b>	5.20	4.81	6.18	7.36	9.99	2.56	4.67	4.79	2.85	4.69	2.25	3.14	5.36	2.93	3.23	2.45	5.84	3.86	7.44	3.11	3.51
<b>MgO (wt %)</b>	2.92	2.24	2.56	3.07	4.85	0.75	0.98	2.17	1.02	2.90	1.66	1.82	2.14	1.06	1.27	0.86	2.47	2.46	4.67	0.73	1.23
<b>CaO (wt %)</b>	6.29	8.13	1.83	3.11	3.80	2.69	4.05	6.82	2.65	1.70	21.00	3.19	1.77	2.29	2.41	1.24	5.85	17.91	9.88	1.25	3.12
<b>Na<sub>2</sub>O (wt %)</b>	1.68	1.26	1.26	0.76	0.52	2.82	3.09	1.41	2.75	1.20	0.39	3.87	2.02	2.84	3.33	2.73	1.16	1.22	0.76	3.24	2.43
<b>K<sub>2</sub>O (wt %)</b>	1.77	2.01	1.95	2.39	3.08	3.07	2.90	2.32	2.26	1.94	1.17	2.32	2.70	2.50	2.70	2.64	2.12	1.55	2.26	3.34	2.94
<b>P<sub>2</sub>O<sub>5</sub> (wt %)</b>	0.14	0.14	0.08	0.30	0.10	0.12	0.43	0.18	0.12	0.08	0.09	0.15	0.16	0.13	0.19	0.06	0.21	0.11	0.14	0.12	0.35
<b>Ba (ppm)</b>	444.10	419.00	355.30	445.60	507.40	542.60	544.80	497.20	492.80	497.50	207.70	816.10	689.00	555.70	564.80	544.10	468.00	318.00	378.40	500.00	535.30
<b>Co (ppm)</b>	32.10	16.40	22.10	26.40	37.00	8.60	12.77	16.40	8.90	8.80	1.20	7.80	26.70	9.90	9.60	7.60	25.30	14.90	32.10	9.20	10.90
<b>Cr (ppm)</b>	258.30	92.50	231.80	230.90	211.60	28.10	23.60	53.63	30.65	49.20	26.40	10.27	60.45	46.49	56.16	18.98	157.80	273.20	300.50	7.10	10.75
<b>Ni (ppm)</b>	217.70	34.00	113.20	129.40	184.80	0.00	11.40	25.14	10.87	16.34	0.00	0.00	28.90	19.56	13.13	12.34	93.90	119.20	306.90	0.00	6.61
<b>Rb (ppm)</b>	152.20	89.50	71.70	104.00	107.50	103.20	133.70	102.60	81.80	99.00	47.80	100.60	125.60	93.70	101.70	106.20	113.60	59.20	110.90	144.50	130.40
<b>Sr (ppm)</b>	167.50	148.30	184.50	143.80	143.30	241.30	244.40	324.70	269.10	294.90	208.50	535.90	165.50	228.00	246.40	211.40	209.60	215.00	225.10	130.90	193.50
<b>V (ppm)</b>	180.80	99.20	101.00	119.50	144.90	56.30	847.00	97.80	70.00	87.00	41.50	71.90	98.10	61.20	67.50	54.00	111.70	73.00	142.10	60.20	68.50
<b>Y (ppm)</b>	28.80	41.20	28.20	33.30	32.40	40.40	37.70	28.20	26.10	17.60	17.60	26.00	41.60	32.20	33.60	32.90	33.90	19.70	24.50	31.70	28.70
<b>Zn (ppm)</b>	131.40	65.30	57.90	69.40	94.70	20.30	55.20	72.40	24.80	40.10	27.40	48.50	58.60	30.30	35.50	25.20	78.70	44.20	89.70	22.90	60.20
<b>Zr (ppm)</b>	85.30	256.60	163.10	170.00	117.20	290.10	335.80	183.10	234.30	210.10	82.60	239.80	257.80	283.70	303.00	312.00	164.10	102.30	84.20	175.50	182.40
<b>Ce (ppm)</b>	83.00	80.50	48.70	57.50	68.30	109.40	75.20	71.20	46.30	60.70	42.30	75.30	88.50	58.50	71.60	70.20	83.90	40.80	49.00	43.10	59.40
<b>Eu (ppm)</b>	0.90	0.80	0.70	0.80	0.80	1.00	1.00	1.10	0.80	0.80	0.80	1.40	1.00	0.80	0.90	0.80	1.00	0.80	1.10	0.50	0.80
<b>La (ppm)</b>	43.80	42.40	30.50	30.90	38.60	59.40	66.40	42.80	35.10	39.90	34.20	54.20	38.10	32.60	34.70	37.90	45.30	25.70	36.30	20.40	34.40
<b>Nb (ppm)</b>	13.90	20.70	13.80	15.10	12.40	15.90	33.50	0.00	0.00	15.00	0.00	0.00	21.80	15.90	19.10	0.00	14.80	0.00	0.00	12.10	16.70
<b>Nd (ppm)</b>	37.30	35.60	33.80	26.30	37.20	48.40	76.40	31.70	23.80	24.30	21.60	32.50	34.60	29.60	30.40	31.40	37.40	17.50	21.20	25.00	30.80
<b>Pb (ppm)</b>	26.90	24.90	13.80	26.90	16.50	20.30	33.80	37.50	23.30	25.90	9.60	34.10	40.50	29.30	25.30	21.50	36.30	12.50	16.20	22.20	25.30
<b>Sm (ppm)</b>	5.80	6.30	3.30	5.70	5.20	7.50	6.50	5.80	3.70	2.50	2.30	5.20	7.10	5.00	4.80	5.60	6.90	4.40	7.10	3.10	5.00
<b>Th (ppm)</b>	18.60	17.60	10.20	12.30	9.80	21.10	15.60	13.80	10.00	18.40	6.60	18.20	21.30	14.10	12.70	18.20	17.80	9.50	10.30	11.40	14.40
<b>U (ppm)</b>	0.00	0.00	0.00	0.00	0.00	0.00	0.00	0.00	0.00	1.30	0.00	0.00	0.00	0.00	0.00	0.00	0.00	0.00	0.00	0.00	0.00
<b>Yb (ppm)</b>	3.10	3.50	2.40	3.10	3.10	3.20	3.30	2.40	2.00	1.30	1.40	2.10	3.50	2.50	2.60	2.40	3.10	1.70	2.60	2.70	2.50
<b>Sum (%)</b>	94.79	102.97	103.26	98.55	97.55	100.87	103.21	102.47	100.11	102.97	93.04	102.80	102.88	102.66	100.09	103.59	102.54	100.66	102.43	103.18	103.03
<b>LOI (wt %)</b>	0.92	3.22	7.96	4.32	5.33	1.2	4.33	9.76	2.65	6.45	26.92	3.19	5.28	3.85	3.15	2.54	13.1	17.72	13.3	2.23	6.28

Sample	Ove-3	Ove-4	Ove-5	Ove-6	Ch-1	Ch-2	Ch-3	Ch-4	Ch-5	Ch-6	Ch-7	Ch-8	Ch-9	Kir-1	Kir-2	Kir-3	Kir-4	Kir-5	Kir-6	Dia-1	Dia-2
<b>SiO<sub>2</sub> (wt %)</b>	58.24	67.98	69.57	56.24	69.40	65.08	62.45	73.21	71.44	57.88	52.55	77.06	72.66	63.48	72.83	68.14	60.62	60.34	52.86	55.71	55.50
<b>TiO<sub>2</sub> (wt %)</b>	0.71	0.52	0.43	0.76	0.49	0.61	0.42	0.46	0.51	0.84	1.21	0.45	0.61	0.71	0.56	0.95	0.41	0.61	0.69	0.70	0.70
<b>Al<sub>2</sub>O<sub>3</sub> (wt %)</b>	17.16	15.70	14.70	17.90	13.91	15.18	11.29	13.26	12.61	21.36	23.62	11.34	13.61	14.30	11.92	12.64	10.63	14.84	13.43	13.85	13.74
<b>Fe<sub>2</sub>O<sub>3</sub> (wt %)</b>	4.37	2.95	3.44	4.67	3.86	4.74	3.76	3.00	2.85	6.86	7.52	2.63	3.08	6.00	2.56	3.66	2.48	4.79	5.66	5.40	5.23
<b>MgO (wt %)</b>	1.50	1.21	1.44	0.98	2.04	2.47	2.19	1.02	1.21	1.24	1.25	0.50	0.57	1.69	0.75	1.05	0.87	1.34	1.90	2.00	1.99
<b>CaO (wt %)</b>	4.07	1.86	3.12	4.05	1.52	1.79	1.61	1.18	2.53	0.35	0.36	0.43	0.55	2.07	2.69	3.98	8.72	5.12	9.46	8.31	8.52
<b>Na<sub>2</sub>O (wt %)</b>	3.05	3.69	2.43	3.09	2.13	2.54	0.99	1.52	2.89	0.95	0.88	2.13	2.92	1.46	2.82	3.19	2.19	1.51	1.40	1.01	1.06
<b>K<sub>2</sub>O (wt %)</b>	2.88	3.52	2.70	2.90	2.56	2.49	2.16	2.36	2.56	3.88	4.12	2.29	2.37	2.25	3.07	2.32	2.67	2.31	2.76	2.14	2.15
<b>P<sub>2</sub>O<sub>5</sub> (wt %)</b>	0.43	0.13	0.40	0.43	0.11	0.15	0.19	0.04	0.15	0.12	0.12	0.06	0.07	0.29	0.12	0.20	0.15	0.09	0.88	0.17	0.18
<b>Ba (ppm)</b>	529.00	472.10	666.70	544.80	708.10	684.20	509.80	667.30	626.30	757.30	803.70	345.70	384.20	435.80	542.60	451.80	468.40	475.20	411.60	624.70	694.80
<b>Co (ppm)</b>	12.20	8.60	10.60	12.77	19.60	21.70	12.70	10.60	10.10	15.30	15.60	9.00	9.90	21.50	8.60	11.80	7.50	15.80	17.20	19.60	17.50
<b>Cr (ppm)</b>	17.43	14.17	14.60	23.60	63.70	69.70	74.30	55.00	88.70	89.70	106.40	43.70	54.80	61.50	28.10	58.60	25.20	52.50	46.10	70.30	70.20
<b>Ni (ppm)</b>	10.10	0.00	6.91	11.40	93.70	11.50	60.70	24.40	15.20	27.80	31.70	1.60	9.40	21.90	0.00	6.10	0.40	16.80	13.10	31.80	30.10
<b>Rb (ppm)</b>	143.10	150.80	144.40	133.70	106.40	112.70	102.00	97.40	149.40	165.60	95.70	100.50	92.50	103.20	77.70	93.30	107.20	87.00	95.60	95.50	
<b>Sr (ppm)</b>	245.10	231.00	144.60	244.40	323.10	315.90	314.30	168.60	276.80	75.50	85.70	65.40	83.00	347.30	241.30	327.00	266.20	187.90	327.80	253.20	269.50
<b>V (ppm)</b>	82.70	64.60	77.50	847.00	78.00	94.80	78.90	57.80	60.90	126.40	139.60	49.70	59.90	143.90	56.30	89.90	53.60	113.80	139.50	119.50	123.00
<b>Y (ppm)</b>	38.30	27.40	26.60	37.70																	

Sample	Dia-3	Dia-4	Dia-5	Dia-6	Dia-7	Dia-8	Dia-9	Dia-10	Dia-11	Dia-12	Dia-13	Sb-1	Sb-2	Sb-3	Sb-4	Sb-5	Sb-6	Sb-7	Sb-8	Sb-9
<b>SiO<sub>2</sub> (wt %)</b>	58.77	75.40	71.57	76.39	69.40	63.03	41.84	57.44	57.25	57.37	57.38	55.87	58.23	58.94	57.66	58.92	58.38	57.68	54.73	86.52
<b>TiO<sub>2</sub> (wt %)</b>	0.69	0.20	0.44	0.22	0.20	0.77	0.51	0.68	0.69	0.63	0.65	0.79	0.82	0.80	0.83	0.84	0.89	0.84	0.76	0.40
<b>Al<sub>2</sub>O<sub>3</sub> (wt %)</b>	13.01	12.36	13.76	14.15	13.74	15.36	10.16	13.39	13.44	12.06	12.06	11.94	12.33	11.84	12.27	13.01	13.98	12.95	11.74	8.00
<b>Fe<sub>2</sub>O<sub>3</sub> (wt %)</b>	5.14	1.18	3.08	5.59	6.36	5.59	4.45	5.12	4.95	4.69	4.50	4.58	4.81	4.54	4.68	5.03	5.50	5.03	4.61	1.02
<b>MgO (wt %)</b>	2.18	0.53	0.80	0.98	0.94	2.18	2.32	2.21	2.22	2.17	2.55	2.30	2.24	2.28	1.55	2.07	1.85	1.84	1.90	0.45
<b>CaO (wt %)</b>	5.92	1.81	0.96	4.53	4.25	3.15	19.44	7.71	7.54	9.12	5.72	9.77	8.13	8.20	7.25	6.93	6.77	8.21	11.08	0.12
<b>Na<sub>2</sub>O (wt %)</b>	1.27	1.60	2.39	1.28	0.90	1.90	1.19	1.09	1.13	1.17	1.24	1.27	1.26	1.44	1.10	1.25	0.74	0.88	1.19	0.00
<b>K<sub>2</sub>O (wt %)</b>	1.87	2.79	3.52	1.56	2.51	2.34	1.23	2.58	2.60	2.46	1.81	1.95	2.01	1.95	2.15	2.10	1.94	1.88	1.82	0.66
<b>P<sub>2</sub>O<sub>5</sub> (wt %)</b>	0.15	0.04	0.08	0.09	0.09	0.16	0.09	0.12	0.13	0.14	0.20	0.12	0.14	0.15	0.25	0.14	0.11	0.11	0.13	0.03
<b>Ba (ppm)</b>	420.00	510.10	890.10	439.00	529.20	554.50	441.60	429.00	765.50	394.30	439.40	440.50	419.00	430.70	442.60	465.90	470.60	463.00	405.70	105.30
<b>Co (ppm)</b>	16.70	1.50	7.80	12.20	15.60	19.40	13.90	18.90	18.50	15.50	15.70	14.80	16.40	14.60	16.20	16.60	19.50	16.70	15.20	1.60
<b>Cr (ppm)</b>	67.40	22.60	33.00	55.20	85.70	79.40	49.90	64.70	69.60	68.30	66.30	87.60	92.50	93.10	92.90	97.40	104.70	97.40	91.70	47.00
<b>Ni (ppm)</b>	24.50	34.60	23.50	44.60	33.20	27.40	16.90	24.00	25.20	18.70	20.00	32.40	34.00	32.30	33.30	36.80	41.40	35.20	35.80	0.00
<b>Rb (ppm)</b>	93.30	89.50	128.00	76.70	93.80	109.90	51.40	85.40	87.60	84.70	96.60	87.00	89.50	85.30	100.20	101.00	104.40	97.80	85.60	36.30
<b>Sr (ppm)</b>	388.10	179.30	281.90	235.80	236.70	254.80	428.50	215.60	235.60	221.50	402.20	163.00	148.30	158.70	144.60	132.00	137.50	149.70	131.30	18.90
<b>V (ppm)</b>	113.70	76.40	62.70	85.80	129.40	119.30	107.90	111.50	112.80	105.30	90.80	86.90	99.20	91.90	91.20	98.70	115.20	106.30	93.20	59.80
<b>Y (ppm)</b>	28.80	19.40	26.00	19.80	21.40	34.20	18.10	31.60	31.20	29.80	28.90	39.60	41.20	42.30	39.80	41.40	43.20	40.30	37.70	40.50
<b>Zn (ppm)</b>	66.00	7.20	33.70	24.70	23.00	75.40	46.90	56.70	62.10	55.40	62.40	60.90	65.30	59.60	70.70	67.80	69.50	64.40	61.80	23.90
<b>Zr (ppm)</b>	195.60	116.30	214.60	151.20	164.90	218.20	124.70	193.80	219.20	214.00	215.10	236.00	256.60	261.80	230.40	247.80	249.60	249.50	226.30	276.90
<b>Ce (ppm)</b>	65.30	0.00	72.70	0.00	0.00	85.80	56.00	82.30	75.10	75.50	72.80	65.60	80.50	73.20	72.80	72.70	88.80	79.50	68.20	35.70
<b>Eu (ppm)</b>	1.20	0.30	0.90	0.70	0.70	1.00	1.20	0.70	1.00	1.00	1.10	0.90	0.80	0.90	0.90	0.90	0.80	0.90	0.80	0.30
<b>La (ppm)</b>	46.90	24.40	34.50	32.20	71.90	43.70	38.10	36.80	33.50	40.90	49.90	33.00	42.40	37.70	39.70	34.70	41.90	36.50	33.40	26.40
<b>Nb (ppm)</b>	0.00	0.00	13.40	0.00	0.00	15.90	0.00	14.60	16.50	0.00	0.00	19.00	20.70	20.10	21.20	21.20	22.10	21.50	18.30	13.40
<b>Nd (ppm)</b>	30.40	19.30	25.40	15.30	14.20	33.30	20.60	30.80	27.80	30.30	23.70	43.10	35.60	38.40	38.30	38.50	33.80	38.30	28.60	15.30
<b>Pb (ppm)</b>	23.10	16.30	27.30	17.30	22.20	26.60	16.20	29.10	20.70	21.20	31.90	18.30	24.90	21.80	20.50	24.30	21.50	26.40	28.00	19.70
<b>Sm (ppm)</b>	5.30	0.00	4.60	2.50	3.00	5.80	2.80	3.40	5.80	6.10	3.30	6.20	6.30	6.60	7.20	7.30	6.50	6.90	6.30	3.30
<b>Th (ppm)</b>	14.80	7.60	16.80	4.10	4.00	16.40	9.60	12.40	10.00	8.80	11.90	12.10	17.60	12.20	13.20	14.20	12.20	17.10	15.00	12.10
<b>U (ppm)</b>	0.00	2.20	0.00	0.80	1.70	0.00	0.00	0.00	0.00	0.00	0.00	0.00	0.00	0.00	0.00	0.00	0.00	0.00	0.00	0.00
<b>Yb (ppm)</b>	2.40	0.60	2.00	0.70	0.70	3.00	1.40	2.60	2.50	2.40	2.40	3.30	3.50	3.50	3.40	3.50	3.70	3.40	3.10	3.20
<b>Sum (%)</b>	100.12	100.40	94.50	99.68	99.20	104.39	101.08	109.07	103.66	100.67	103.52	100.68	102.97	100.30	102.92	101.86	102.32	100.50	103.93	100.25
<b>LOI (wt %)</b>	10.99	3.36	7.50	3.54	3.6	6.12	17.89	17.1	10.46	10.45	13.82	11.27	9.98	10.14	12.49	9.16	9.7	11.03	12.63	3.03

## APPENDIX 7. X-RAY FLUORESCENCE (XRF) DATA OF THE SHERDS.

Sample	TR-1	TR-2	TR-3	TR-4	TR-5	TR-6	TR-7	TR-8	TR-9	TR-10	TR-11	TR-12	TR-13	TR-14	TR-15
SiO <sub>2</sub> (wt %)	68.18	58.59	66.85	61.61	60.06	65.71	65.55	61.34	65.41	66.15	64.98	60.74	59.64	64.60	65.55
TiO <sub>2</sub> (wt %)	0.51	0.52	0.62	0.85	0.57	0.56	0.62	0.71	0.70	0.60	0.71	0.74	0.56	0.56	0.55
Al <sub>2</sub> O <sub>3</sub> (wt %)	11.57	12.56	16.07	18.52	12.72	18.31	18.12	17.10	16.79	17.74	16.78	16.28	11.56	13.39	10.95
Fe <sub>2</sub> O <sub>3</sub> (wt %)	3.85	5.46	4.74	7.86	4.85	4.01	4.43	6.32	4.83	4.26	5.88	6.37	4.09	3.94	3.62
MnO (wt %)	0.08	0.08	0.12	0.13	0.06	0.04	0.11	0.14	0.07	0.06	0.09	0.08	0.07	0.08	0.08
MgO (wt %)	1.41	1.62	1.40	3.12	2.62	1.12	1.32	1.67	1.21	1.16	1.42	2.72	1.54	1.46	1.60
CaO (wt %)	5.17	8.76	1.22	1.61	9.01	1.64	1.48	3.15	1.98	1.32	1.85	2.88	8.41	5.92	5.59
Na <sub>2</sub> O (wt %)	1.28	1.30	1.90	3.86	0.78	2.37	2.64	1.85	2.04	2.34	1.79	1.42	0.93	1.36	1.04
K <sub>2</sub> O (wt %)	3.36	3.00	3.69	2.08	3.33	3.70	3.46	3.67	3.22	3.60	3.19	3.44	3.19	3.32	3.27
P <sub>2</sub> O <sub>5</sub> (wt %)	0.36	0.20	0.22	0.33	0.12	0.23	0.10	0.25	0.14	0.08	0.16	0.14	0.11	0.16	0.25
Ba (ppm)	1022.40	818.60	892.30	549.50	886.30	935.10	860.50	1078.30	875.60	888.70	777.40	766.50	798.40	997.90	854.30
Co (ppm)	12.10	15.00	19.30	27.70	13.00	7.30	13.10	17.20	13.90	11.10	17.20	21.50	11.20	12.10	10.70
Cr (ppm)	98.10	308.10	130.60	261.60	87.10	54.40	54.60	67.90	68.80	54.80	85.50	156.60	97.00	85.00	94.40
Ni (ppm)	45.10	133.50	65.80	114.00	46.80	17.50	18.20	29.80	28.30	19.10	39.20	112.00	43.20	36.10	37.00
Rb (ppm)	79.60	63.40	92.00	57.50	75.90	104.40	98.20	111.30	94.40	99.20	79.20	93.30	72.50	83.90	74.70
Sr (ppm)	241.70	231.70	179.60	286.60	224.30	214.10	182.80	230.50	221.30	190.10	215.30	202.10	185.00	200.00	192.50
V (ppm)	74.80	94.50	89.40	177.10	94.20	60.90	70.30	122.30	90.10	76.10	118.10	116.60	80.50	83.60	77.40
Y (ppm)	24.10	20.70	29.60	28.50	22.10	24.10	33.30	30.00	31.00	27.20	27.30	26.20	24.90	26.10	27.10
Zn (ppm)	55.70	60.50	62.80	92.00	73.20	64.00	61.80	122.30	75.70	65.70	85.30	89.30	57.30	49.40	48.30
Zr (ppm)	150.80	137.90	194.60	139.50	115.80	216.00	211.00	154.10	194.30	211.80	173.50	135.20	142.40	165.40	174.80
Ce (ppm)	59.00	61.70	73.90	57.20	71.80	57.20	79.40	79.30	76.00	71.40	85.10	62.60	65.00	72.30	56.10
Eu (ppm)	0.90	0.90	0.70	1.10	0.80	0.80	0.90	0.90	0.90	0.80	0.70	0.80	0.70	0.70	0.80
La (ppm)	29.90	33.60	34.30	43.10	30.40	27.20	37.30	44.30	31.90	34.50	29.60	40.00	28.00	30.80	28.20
Nb (ppm)	0.00	0.00	16.60	0.00	0.00	11.50	19.60	16.90	16.00	18.40	14.20	13.50	0.00	0.00	14.60
Nd (ppm)	25.00	33.70	28.80	25.80	32.60	26.10	34.10	40.10	31.80	24.50	30.80	31.70	33.30	32.90	31.70
Pb (ppm)	31.50	22.90	34.80	20.30	37.70	33.90	28.70	74.60	33.50	32.40	30.30	28.10	33.80	34.60	31.30
Sm (ppm)	5.10	4.40	4.30	4.60	3.80	5.00	6.20	4.60	5.20	5.00	3.10	4.10	4.30	4.10	5.20
Th (ppm)	11.70	14.90	16.10	10.10	19.30	24.00	18.20	24.50	17.60	18.00	14.80	15.30	15.30	15.80	11.70
U (ppm)	0.00	0.00	0.00	0.00	0.00	0.00	0.00	0.00	0.00	0.00	0.00	0.00	0.00	0.00	0.00
Yb (ppm)	2.00	1.90	2.50	2.60	2.10	2.00	2.80	2.80	2.60	2.20	2.40	2.50	2.20	2.20	2.20
Sum (wt %)	100.71	100.18	101.45	101.06	94.31	97.87	100.96	99.74	100.23	100.73	100.59	99.18	98.55	100.42	99.97
LOI	4.73	7.89	4.42	0.89	8.34	2.29	2.96	3.31	3.67	3.24	3.54	4.18	8.29	5.43	7.30

Sample	TR-16	TR-17	TR-18	TR-19	TR-20	TR-21	TR-22	TR-23	TR-24	TR-25	TR-26	TR-27	TR-28	MCE-1	MCE-2
SiO <sub>2</sub> (wt %)	68.66	62.85	65.37	57.64	70.30	66.13	66.68	64.27	68.82	68.51	65.70	58.99	65.91	68.03	70.34
TiO <sub>2</sub> (wt %)	0.59	0.62	0.54	0.54	0.69	0.76	0.72	0.50	0.74	0.63	0.66	0.50	0.62	0.55	0.75
Al <sub>2</sub> O <sub>3</sub> (wt %)	12.55	16.56	19.05	10.01	14.77	16.18	14.71	12.36	14.81	13.09	17.23	11.28	17.15	16.16	13.46
Fe <sub>2</sub> O <sub>3</sub> (wt %)	4.10	5.10	4.15	3.49	5.31	6.58	6.90	4.22	5.54	4.30	4.80	4.07	4.00	4.79	5.90
MnO (wt %)	0.08	0.07	0.03	0.09	0.10	0.12	0.13	0.06	0.13	0.07	0.10	0.08	0.06	0.05	0.12
MgO (wt %)	1.90	1.30	1.04	1.90	1.88	2.52	3.62	2.78	1.59	1.57	1.23	2.74	1.06	0.96	2.00
CaO (wt %)	5.35	4.23	1.16	13.23	1.64	1.32	2.39	6.09	2.68	4.04	1.92	9.85	1.65	2.12	1.65
Na <sub>2</sub> O (wt %)	1.15	1.70	2.21	1.03	2.19	3.26	1.46	1.56	1.63	1.48	2.10	0.88	2.35	2.45	1.19
K <sub>2</sub> O (wt %)	3.12	2.92	3.91	2.36	2.23	1.86	2.37	3.17	2.94	2.81	3.07	2.86	3.24	2.62	1.76
P <sub>2</sub> O <sub>5</sub> (wt %)	0.12	0.18	0.13	0.11	0.10	0.12	0.11	0.17	0.12	0.11	0.13	0.12	0.12	0.15	0.12
Ba (ppm)	903.60	1454.60	834.20	1128.40	592.20	932.00	950.20	890.40	808.20	754.30	886.20	1349.00	1259.50	1058.50	784.00
Co (ppm)	13.70	11.90	6.70	10.40	20.60	23.20	33.70	11.60	18.80	12.30	14.70	10.40	9.40	8.90	24.60
Cr (ppm)	114.20	76.00	45.80	99.40	256.00	195.70	470.60	79.60	112.20	112.80	61.90	82.40	51.60	48.70	277.30
Ni (ppm)	40.80	27.90	10.30	40.40	111.70	109.20	251.40	46.40	65.40	43.00	27.90	41.50	16.50	39.70	140.20
Rb (ppm)	86.90	74.00	98.30	62.20	91.20	60.10	68.70	80.60	93.70	64.90	83.80	73.60	102.70	71.00	68.50
Sr (ppm)	212.40	191.10	161.70	302.20	195.60	289.30	245.30	291.40	245.30	263.50	210.50	340.50	260.20	346.70	134.60
V (ppm)	94.30	92.80	64.20	60.70	98.40	137.30	119.70	80.00	113.40	96.00	87.50	76.60	70.80	91.70	118.10
Y (ppm)	26.30	31.60	24.00	24.00	30.70	24.00	29.30	19.80	28.70	27.70	33.40	19.70	29.70	21.50	27.40
Zn (ppm)	52.90	56.10	60.00	47.50	57.80	72.10	75.30	60.40	72.60	55.70	67.10	58.20	55.50	54.10	61.20
Zr (ppm)	167.60	174.90	204.20	170.70	167.40	141.90	179.60	106.00	144.80	171.40	200.90	132.30	223.80	138.20	136.10
Ce (ppm)	69.40	65.90	60.90	66.10	61.20	46.30	73.10	60.70	61.00	61.30	76.90	53.10	67.00	52.30	51.60
Eu (ppm)	1.00	0.80	0.60	1.00	0.90	1.00	0.90	1.00	0.90	1.00	0.80	1.30	0.80	1.10	0.80
La (ppm)	33.80	24.20	19.50	31.80	37.30	28.40	36.20	34.10	40.40	36.30	40.70	29.20	25.20	33.70	28.90
Nb (ppm)	0.00	14.40	19.40	0.00	15.10	0.00	16.50	0.00	0.00	0.00	17.80	0.00	18.60	0.00	13.50
Nd (ppm)	31.10	26.20	27.90	33.70	30.60	20.30	34.90	23.20	34.00	28.40	37.80	29.30	24.80	24.30	28.80
Pb (ppm)	32.50	26.50	26.10	19.30	27.20	21.20	37.60	38.30	40.20	36.80	36.10	31.80	27.70	28.40	21.60
Sm (ppm)	6.80	5.10	3.70	4.10	5.10	4.10	4.10	4.90	3.90	5.40	4.80	6.10	3.90	4.30	4.90
Th (ppm)	15.60	17.10	20.00	11.10	11.80	9.80	14.60	18.80	13.10	16.20	20.00	16.80	19.00	19.30	10.90
U (ppm)	0.00	0.00	0.00	0.00	0.00	0.00	0.00	0.00	0.00	0.00	0.00	0.00	0.00	0.00	0.00
Yb (ppm)	2.20	2.80	2.00	2.00	2.70	2.10	2.50	1.80	2.60	2.40	2.90	1.80	2.40	1.90	2.50
Sum (wt %)	100.95	100.90	101.19	90.61	101.19	101.15	101.23	101.63	101.59	99.16	100.06	91.62	99.69	100.80	101.10
LOI	3.14	5.13	3.42	2.60	1.81	2.11	1.89	6.25	2.40	2.36	2.91	1.60	3.32	2.73	3.60

Sample	MCE-3	MCE-4	MCE-5	MCW-1	MCW-2	MCW-3	MCW-4	MCW-5	AK-1	AK-2	AT-1	AT-2	CM-1	CM-2	CM-3
SiO <sub>2</sub> (wt %)	71.80	76.20	75.13	73.00	60.91	70.14	66.86	68.73	67.02	66.81	65.59	54.18	64.07	67.14	66.61
TiO <sub>2</sub> (wt %)	0.63	0.53	0.58	0.47	0.68	0.73	0.74	0.72	0.59	0.67	0.66	0.76	0.70	0.59	0.72
Al <sub>2</sub> O <sub>3</sub> (wt %)	12.55	11.86	11.26	12.73	18.68	12.50	12.84	12.10	16.13	15.74	16.54	19.21	16.15	15.52	16.39
Fe <sub>2</sub> O <sub>3</sub> (wt %)	5.34	4.25	3.86	3.58	6.25	5.53	5.49	5.01	4.82	4.80	5.17	8.86	5.14	4.49	5.08
MnO (wt %)	0.08	0.05	0.08	0.05	0.12	0.10	0.07	0.06	0.08	0.06	0.06	0.08	0.06	0.06	0.08
MgO (wt %)	1.35	1.54	1.10	1.07	1.92	2.15	2.62	2.27	1.41	1.15	1.39	4.28	1.35	0.86	1.36
CaO (wt %)	1.74	1.22	1.18	1.24	4.23	1.47	3.00	2.92	1.94	1.77	2.40	5.89	2.03	1.69	2.11
Na <sub>2</sub> O (wt %)	1.19	1.14	1.08	1.35	1.94	1.46	1.41	1.55	1.72	1.61	2.15	0.69	1.99	1.55	2.30
K <sub>2</sub> O (wt %)	1.73	1.49	2.53	2.90	1.03	1.90	1.93	1.82	2.97	2.74	2.72	2.14	2.57	2.60	2.87
P <sub>2</sub> O <sub>5</sub> (wt %)	0.18	0.10	0.36	0.16	0.13	0.25	0.24	0.12	0.49	0.90	0.53	0.30	1.31	1.45	0.77
Ba (ppm)	918.20	600.90	778.20	761.40	466.40	676.50	548.00	503.30	1586.90	1819.50	1507.10	1765.30	2284.00	2234.60	1684.50
Co (ppm)	19.80	14.90	14.60	13.00	16.80	23.30	24.60	19.80	16.00	14.10	14.60	26.40	14.40	13.80	15.30
Cr (ppm)	230.30	195.40	177.60	64.30	8.70	296.60	254.20	226.80	51.50	24.20	24.20	315.60	30.60	16.10	34.90
Ni (ppm)	111.00	96.10	84.40	41.90	10.00	132.60	142.70	123.00	50.30	33.80	34.50	69.80	36.00	27.50	28.10
Rb (ppm)	56.40	50.80	79.90	93.30	32.90	73.40	82.50	77.10	86.60	71.30	76.10	62.90	79.20	66.30	86.20
Sr (ppm)	139.10	116.10	129.70	216.90	261.50	168.20	167.30	155.00	252.20	229.40	248.50	297.90	256.80	240.30	252.20
V (ppm)	102.50	70.90	84.10	71.40	107.10	118.10	124.80	97.30	105.00	91.50	89.10	222.20	89.30	89.80	95.20
Y (ppm)	25.30	21.80	28.60	25.10	26.90	25.90	26.60	27.20	27.90	28.20	30.40	22.90	36.70	26.60	35.70
Zn (ppm)	47.10	34.20	43.40	39.10	57.40	69.30	76.70	68.90	57.90	55.30	59.70	96.90	71.60	43.90	63.20
Zr (ppm)	117.40	111.60	166.20	138.00	136.70	145.90	150.80	144.70	157.60	176.60	160.10	93.40	239.10	182.60	266.00
Ce (ppm)	45.80	37.70	52.40	55.80	0.00	49.20	55.20	54.00	73.40	66.50	82.10	88.00	85.70	53.90	82.50
Eu (ppm)	0.70	0.60	0.70	0.80	1.00	0.70	0.70	0.80	0.90	0.90	1.00	1.10	1.00	0.80	0.90
La (ppm)	22.10	21.30	22.80	32.90	24.30	24.70	31.20	21.80	27.00	14.70	25.00	22.30	9.40	1.10	22.90
Nb (ppm)	0.00	0.00	0.00	11.70	0.00	0.00	14.40	12.70	13.00	15.00	13.50	0.00	19.60	15.80	21.90
Nd (ppm)	24.30	16.10	27.80	28.70	23.00	21.10	28.40	27.70	25.50	26.40	30.60	16.00	32.90	24.10	36.10
Pb (ppm)	18.10	11.40	21.10	26.60	9.60	15.30	14.70	14.60	37.00	27.60	32.40	31.40	30.10	22.00	29.10
Sm (ppm)	4.40	3.80	4.90	5.10	4.00	3.80	4.10	5.20	4.50	4.90	5.90	5.20	5.90	4.10	4.50
Th (ppm)	7.10	6.30	8.80	12.90	2.60	12.20	7.60	8.70	17.90	14.00	17.00	13.10	18.90	10.50	16.20
U (ppm)	0.00	0.00	0.00	0.00	0.00	0.00	0.00	0.00	0.00	0.00	0.00	0.00	0.00	0.00	0.00
Yb (ppm)	2.20	1.80	2.40	2.10	2.40	2.30	2.30	2.40	2.40	2.40	2.70	2.30	3.10	2.20	2.90
Sum (wt %)	100.50	100.41	99.80	99.75	100.06	100.47	101.24	99.66	101.56	101.03	101.68	101.08	100.13	101.23	101.18
LOI	3.73	1.89	2.49	3.04	4.06	4.07	5.88	4.19	4.14	4.51	4.22	4.37	4.42	4.97	2.61

Sample	CM-4	DH-1	DH-2	DH-3	HM	YK-1	YK-2	YK-3	YK-4	YK-5	OVC-1	OVC-2	OVC-3	OVC-4	OVC-5
SiO <sub>2</sub> (wt %)	66.04	71.72	70.27	66.95	64.60	68.78	69.67	64.67	67.10	72.25	66.41	66.40	66.62	57.44	65.15
TiO <sub>2</sub> (wt %)	0.57	0.56	0.61	0.57	0.76	0.67	0.58	0.73	0.68	0.63	0.56	0.65	0.63	0.92	0.92
Al <sub>2</sub> O <sub>3</sub> (wt %)	15.25	14.00	14.70	15.89	16.52	14.86	13.93	16.04	15.14	14.12	16.43	16.07	17.16	15.62	15.20
Fe <sub>2</sub> O <sub>3</sub> (wt %)	4.29	4.02	4.04	4.62	5.89	4.59	4.21	5.56	5.04	3.98	4.34	4.33	4.84	6.35	6.01
MnO (wt %)	0.06	0.08	0.06	0.07	0.07	0.05	0.12	0.13	0.08	0.08	0.07	0.04	0.07	0.11	0.10
MgO (wt %)	0.96	0.99	1.50	1.33	1.58	1.51	1.12	1.61	1.36	1.14	1.27	0.58	1.09	0.88	1.58
CaO (wt %)	1.92	1.71	2.22	2.21	2.20	1.99	1.61	2.14	2.29	1.56	2.07	1.78	2.14	5.07	3.93
Na <sub>2</sub> O (wt %)	1.71	1.55	1.75	1.94	1.58	1.51	1.42	1.61	1.34	1.71	1.88	0.98	1.87	0.70	0.89
K <sub>2</sub> O (wt %)	2.66	2.52	2.05	2.92	1.90	2.83	2.79	3.04	2.26	2.71	3.44	2.79	2.87	1.42	2.25
P <sub>2</sub> O <sub>5</sub> (wt %)	1.80	0.16	0.13	0.43	0.50	0.53	0.77	0.65	0.79	0.28	0.31	0.32	0.26	1.82	0.37
Ba (ppm)	2192.60	1713.80	1355.60	2226.20	1246.90	1929.20	2211.70	1674.70	2662.90	1205.20	1315.10	1358.50	1132.50	736.70	669.40
Co (ppm)	13.60	12.90	14.00	13.00	15.10	13.70	15.40	17.80	15.10	13.40	10.60	11.60	12.00	17.30	19.00
Cr (ppm)	28.40	55.90	21.50	48.30	37.10	26.10	8.60	46.90	21.40	20.40	12.60	28.30	25.90	94.10	97.90
Ni (ppm)	26.60	35.10	23.50	34.70	29.10	23.70	20.90	34.90	21.10	19.50	13.10	18.90	15.90	58.40	51.50
Rb (ppm)	68.60	64.30	56.60	93.80	46.30	77.50	78.50	86.60	53.60	86.30	104.60	83.20	94.70	37.60	80.50
Sr (ppm)	282.50	164.00	179.70	267.50	203.40	219.60	231.60	236.80	252.00	207.20	186.20	153.70	212.00	137.90	111.90
V (ppm)	78.20	79.70	72.20	101.80	111.10	86.70	86.80	102.00	97.00	74.00	82.30	87.70	94.70	127.60	112.80
Y (ppm)	30.10	28.30	29.80	28.00	24.80	30.30	24.90	33.20	28.10	34.10	23.60	26.20	26.30	45.30	46.30
Zn (ppm)	61.20	42.10	49.20	56.10	70.60	62.70	49.90	76.50	60.90	43.60	59.00	43.30	54.60	81.90	80.20
Zr (ppm)	193.70	165.30	196.70	188.40	144.60	173.30	179.80	193.80	158.90	234.00	131.90	161.30	161.30	244.70	248.30
Ce (ppm)	63.40	65.60	59.00	77.60	56.50	67.40	56.50	74.00	56.40	69.00	57.70	61.00	69.30	84.20	85.30
Eu (ppm)	0.90	0.70	0.90	0.90	0.80	0.90	0.80	1.00	0.90	0.80	0.80	0.70	0.90	1.00	0.80
La (ppm)	8.40	15.30	20.60	16.80	13.90	11.80	5.10	24.70	0.00	21.60	21.70	13.70	29.00	41.60	42.40
Nb (ppm)	14.90	0.00	16.10	0.00	13.20	11.80	0.00	20.20	13.40	16.40	16.00	17.60	18.00	23.10	21.50
Nd (ppm)	27.00	27.90	26.90	34.70	22.10	26.70	28.00	38.00	22.30	33.80	24.00	30.50	32.80	41.10	39.60
Pb (ppm)	26.70	23.20	24.30	43.30	24.40	24.80	25.90	27.20	22.50	20.20	31.30	31.30	20.20	29.90	28.00
Sm (ppm)	4.00	3.30	6.10	4.80	3.90	4.80	3.60	5.20	4.10	4.90	5.60	4.70	6.20	7.30	6.90
Th (ppm)	13.00	11.90	15.30	24.90	12.30	11.60	12.90	14.90	11.00	13.70	16.90	17.60	13.10	15.40	19.30
U (ppm)	0.00	0.00	0.00	0.00	0.00	0.00	0.00	0.00	0.00	0.00	0.00	0.00	0.00	0.00	0.00
Yb (ppm)	2.60	2.50	2.40	2.40	2.20	2.70	1.90	2.90	2.50	2.80	2.00	2.20	2.20	4.00	4.00
Sum (wt %)	100.69	97.57	101.85	101.23	100.25	97.63	99.91	100.29	100.93	100.69	101.55	100.08	100.07	100.49	100.98
LOI	5.11	4.10	4.31	3.98	4.44	3.95	3.38	3.84	4.49	2.00	4.57	5.92	2.31	9.98	4.42

Sample	OVC-6	CH-1	CH-2	CH-3	CH-4	CH-5	CH-6	DIA-1	DIA-2	DIA-3	DIA-4	DIA-5	DIA-6	DIA-7	DIA-8
SiO <sub>2</sub> (wt %)	57.98	70.11	66.62	66.96	54.25	67.43	68.85	67.71	67.50	63.99	58.67	68.79	68.20	68.65	70.50
TiO <sub>2</sub> (wt %)	0.86	0.40	0.96	0.45	0.63	0.56	0.45	0.62	0.46	0.71	0.84	0.52	0.73	0.53	0.52
Al <sub>2</sub> O <sub>3</sub> (wt %)	17.15	15.51	14.73	15.86	13.31	14.96	15.42	15.29	14.73	17.16	17.98	14.97	16.34	16.25	12.58
Fe <sub>2</sub> O <sub>3</sub> (wt %)	7.05	3.58	5.69	3.90	4.72	4.73	3.61	4.45	3.75	6.67	8.56	4.17	6.09	4.37	3.90
MnO (wt %)	0.09	0.03	0.12	0.03	0.09	0.04	0.05	0.07	0.05	0.12	0.10	0.02	0.11	0.06	0.07
MgO (wt %)	1.15	0.99	1.86	1.03	1.21	0.92	0.83	1.30	0.96	2.15	2.40	0.82	2.13	1.03	1.26
CaO (wt %)	4.20	1.69	4.28	1.73	2.25	1.59	1.86	1.10	0.77	2.43	2.57	0.85	2.03	0.73	3.21
Na <sub>2</sub> O (wt %)	0.59	1.88	1.18	1.91	1.50	1.34	1.92	1.82	2.07	1.36	2.03	1.58	1.80	1.80	1.52
K <sub>2</sub> O (wt %)	1.83	2.79	2.26	2.62	1.90	2.10	2.80	3.64	3.41	3.18	2.84	2.88	2.72	3.40	3.10
P <sub>2</sub> O <sub>5</sub> (wt %)	0.90	0.31	0.13	0.29	0.15	0.43	0.26	0.12	0.17	0.16	0.14	0.16	0.18	0.11	0.13
Ba (ppm)	961.80	904.20	499.30	887.90	721.90	841.40	744.50	570.70	660.40	650.40	432.10	780.80	570.30	533.20	511.80
Co (ppm)	17.80	7.80	18.80	8.90	12.40	12.80	9.10	12.70	9.50	21.50	23.60	10.10	19.40	10.50	13.70
Cr (ppm)	100.40	75.60	92.30	59.70	90.40	70.50	51.90	70.50	52.10	108.10	61.80	57.60	85.10	65.50	61.30
Ni (ppm)	67.60	45.60	52.30	35.30	64.30	28.90	18.30	24.80	19.90	61.90	30.10	20.40	38.20	26.20	21.50
Rb (ppm)	75.70	104.80	108.90	105.80	77.60	88.30	119.40	123.40	96.30	88.90	41.10	89.00	78.40	135.10	69.30
Sr (ppm)	103.80	225.60	117.20	209.30	179.60	103.40	240.00	158.70	136.30	208.80	416.20	147.00	242.60	126.70	137.90
V (ppm)	136.50	64.70	105.50	65.30	70.00	94.30	53.00	84.80	68.30	147.30	263.90	72.70	134.30	79.50	72.30
Y (ppm)	43.50	18.70	47.30	19.00	23.50	23.70	24.50	30.30	23.00	28.40	19.40	21.70	30.50	25.90	23.80
Zn (ppm)	95.30	46.20	75.00	46.10	52.10	43.50	39.60	53.50	43.60	85.60	87.80	41.60	76.70	54.40	46.40
Zr (ppm)	190.30	120.70	270.30	116.50	141.50	120.50	155.30	162.70	123.00	134.70	108.80	130.90	159.60	140.50	135.90
Ce (ppm)	99.60	64.40	78.80	63.80	41.20	66.70	66.40	69.00	61.20	84.60	73.50	59.00	81.20	60.00	64.10
Eu (ppm)	0.80	0.70	1.00	0.70	1.10	0.70	0.70	0.70	0.60	0.90	1.30	0.60	1.10	0.50	0.70
La (ppm)	41.40	38.10	41.30	35.40	28.30	30.70	41.60	42.40	32.60	46.90	55.00	33.30	48.40	32.20	33.30
Nb (ppm)	22.10	0.00	25.20	0.00	0.00	12.90	0.00	17.20	14.00	13.40	0.00	12.80	12.30	16.70	11.50
Nd (ppm)	44.70	14.50	48.10	29.60	24.80	27.80	36.40	29.30	22.60	26.90	21.90	26.70	35.40	28.30	27.40
Pb (ppm)	29.60	32.70	32.90	33.50	20.40	18.70	32.10	23.40	24.60	29.60	15.50	24.00	27.10	23.60	23.00
Sm (ppm)	5.40	3.60	8.90	3.20	7.10	6.00	3.40	5.70	4.30	4.80	4.30	3.60	6.20	3.70	5.40
Th (ppm)	19.80	16.20	17.10	17.50	14.40	13.50	18.00	11.30	12.90	15.30	7.50	11.60	12.70	12.60	10.10
U (ppm)	0.00	0.00	0.00	0.00	0.00	0.00	0.00	0.00	0.00	0.00	0.00	0.00	0.00	0.00	0.00
Yb (ppm)	4.00	1.60	4.00	1.60	2.20	2.10	2.10	2.70	2.00	2.60	1.90	1.80	2.70	2.30	2.00
Sum (wt %)	100.17	101.95	101.59	100.00	84.05	99.76	96.21	100.21	98.44	101.33	100.50	99.25	100.49	99.53	96.91
LOI	8.18	4.49	3.61	5.05	3.89	5.50	5.71	3.94	4.43	3.22	4.20	4.32	0.71	2.47	4.81

Sample	DIA-9	DIA-10	DIA-11	DIA-12	DIA-13	KIR-1	KIR-2	KIR-3	PSH-1	PSH-2	PSH-3	SBO-1	SBO-2	SBO-3
SiO <sub>2</sub> (wt %)	65.60	68.36	65.95	62.02	64.70	58.13	58.22	65.15	68.71	68.12	70.89	56.38	52.33	67.92
TiO <sub>2</sub> (wt %)	0.78	0.63	0.68	0.77	0.68	0.99	1.00	0.69	0.59	0.63	0.59	0.71	0.89	0.93
Al <sub>2</sub> O <sub>3</sub> (wt %)	15.26	14.86	15.47	17.51	15.45	17.74	17.92	15.02	14.47	14.66	14.57	13.83	17.05	14.67
Fe <sub>2</sub> O <sub>3</sub> (wt %)	5.68	4.61	5.14	7.78	6.07	8.13	8.15	4.83	4.44	5.15	4.28	5.71	7.17	5.73
MnO (wt %)	0.09	0.07	0.07	0.13	0.07	0.10	0.10	0.10	0.07	0.08	0.07	0.11	0.09	0.12
MgO (wt %)	1.70	1.26	1.39	2.78	1.59	1.30	1.31	1.25	1.19	1.47	1.27	0.88	0.74	1.56
CaO (wt %)	1.59	1.27	1.25	2.18	2.07	2.52	2.54	1.24	1.87	1.85	1.55	10.55	8.52	2.66
Na <sub>2</sub> O (wt %)	1.24	1.74	1.29	2.30	1.48	2.44	2.42	1.65	1.84	1.68	1.80	0.31	0.22	1.25
K <sub>2</sub> O (wt %)	3.31	3.31	3.97	2.51	2.98	3.20	3.11	3.98	2.82	2.33	2.74	0.82	0.80	2.35
P <sub>2</sub> O <sub>5</sub> (wt %)	0.14	0.19	0.14	0.14	0.22	0.50	0.42	0.32	0.31	0.54	0.44	0.79	1.17	0.36
Ba (ppm)	681.40	626.30	763.40	505.70	720.10	649.40	658.50	622.20	1096.70	1189.60	1034.60	680.00	768.60	718.10
Co (ppm)	15.50	12.60	14.00	22.60	18.10	20.20	21.80	14.80	13.30	14.50	13.20	16.00	18.60	19.50
Cr (ppm)	68.10	37.10	47.70	73.70	99.70	31.90	33.10	46.20	25.60	36.20	34.10	79.70	87.10	91.10
Ni (ppm)	23.10	28.50	29.00	44.30	39.00	23.00	21.40	26.30	27.50	36.90	27.20	60.30	61.50	51.40
Rb (ppm)	77.80	93.80	102.90	68.00	69.90	54.30	79.30	110.50	80.80	89.20	82.50	44.30	48.00	83.40
Sr (ppm)	166.40	201.50	144.00	344.50	181.40	294.50	290.00	197.30	328.00	350.80	316.50	142.60	159.10	113.00
V (ppm)	111.30	91.90	98.10	186.70	112.60	200.30	200.30	105.90	91.10	116.20	96.70	108.70	145.90	109.80
Y (ppm)	29.10	31.80	31.00	24.90	35.40	30.70	31.30	32.60	30.00	26.50	28.30	66.40	45.80	48.20
Zn (ppm)	65.80	55.70	54.00	82.70	62.20	72.50	73.90	83.00	54.30	58.60	49.10	93.30	103.60	84.70
Zr (ppm)	150.60	197.10	161.50	136.60	181.50	139.10	141.40	178.70	223.00	167.30	178.70	178.40	162.00	263.40
Ce (ppm)	62.90	77.20	72.50	84.20	68.20	85.60	74.40	76.10	83.20	67.80	76.60	94.20	90.00	81.20
Eu (ppm)	0.80	0.80	0.70	1.10	0.90	1.10	1.10	0.80	1.00	1.20	1.10	1.10	1.10	0.80
La (ppm)	30.20	41.20	33.40	52.10	32.90	44.30	45.70	44.80	38.20	36.10	41.60	59.20	47.90	36.90
Nb (ppm)	14.70	18.80	15.80	0.00	14.50	0.00	0.00	16.20	0.00	0.00	13.40	17.30	20.70	24.10
Nd (ppm)	31.30	32.90	34.60	33.10	33.90	26.50	22.90	40.50	29.60	28.60	25.30	62.40	48.50	45.80
Pb (ppm)	15.50	26.80	23.50	21.70	23.10	12.10	9.90	27.20	20.90	21.50	26.50	20.70	27.00	23.60
Sm (ppm)	5.70	5.40	5.40	4.10	6.00	4.50	5.30	5.20	4.10	6.00	5.40	8.70	8.60	6.70
Th (ppm)	11.50	16.90	13.50	10.80	12.50	7.10	10.70	12.40	16.10	10.00	10.90	14.70	18.10	14.20
U (ppm)	0.00	0.00	0.00	0.00	0.00	0.00	0.00	0.00	0.00	0.00	0.00	0.00	0.00	0.00
Yb (ppm)	2.60	2.70	2.80	2.40	3.20	2.90	2.90	2.90	2.50	2.30	2.30	6.40	4.30	4.10
Sum (wt %)	99.83	99.90	99.70	99.07	99.53	100.91	100.90	99.69	100.45	100.87	101.26	98.35	99.97	100.51
LOI	4.30	3.44	4.20	0.79	4.02	5.70	5.54	5.29	3.92	4.11	2.84	8.08	10.81	2.79

**APPENDIX 8. RADIOGENIC ISOTOPE DATA OF SEDIMENT SAMPLES AND THE SHERDS  
ANALYSED IN THIS STUDY.**

<b>Sediment</b>	$^{87}\text{Sr}/^{86}\text{Sr}$	$^{143}\text{Nd}/^{144}\text{Nd}$	<b>Sherd</b>	$^{87}\text{Sr}/^{86}\text{Sr}$	$^{143}\text{Nd}/^{144}\text{Nd}$
Mc-1	0.712515 ± 9	0.512284 ± 8	TR-8	0.708733 ± 7	0.51236 ± 10
Mc-5	0.711816 ± 7	0.512250 ± 9	E.9.158.1	0.707833 ± 9	0.512478 ± 9
Ntt-7	0.711782 ± 10	0.512238 ± 10	MCE-1	0.707333 ± 8	0.512232 ± 7
Ch-4	0.71063 ± 9	0.512317 ± 9	MCE-4	0.710605 ± 8	0.512258 ± 6
Dia-3	0.708422 ± 9	0.512255 ± 10	MCW-1	0.710775 ± 10	0.512223 ± 8
Dia-3*	0.710333 ± 9	0.512161 ± 10	MCW-2	0.706485 ± 9	0.512656 ± 9
Dia-10	0.709995 ± 7	0.512212 ± 8	CM-2	0.711962 ± 11	0.512210 ± 9
Dia-10*	0.708642 ± 7	0.512232 ± 8	CH-2	0.709014 ± 9	0.512270 ± 9
Sbo-6	0.715209 ± 9	0.512098 ± 9	CH-3	0.708685 ± 9	0.512327 ± 7
			CH-5	0.711878 ± 10	0.512259 ± 9
			DIA-1	0.714891 ± 10	0.512183 ± 10
			DIA-9	0.711475 ± 10	0.512261 ± 9
			SBO-3	0.718055 ± 10	0.512103 ± 9

\* decarbonatised sample

## APPENDIX 9. DATA OF THE ELECTRON MICROPROBE ANALYSIS (EMPA) OF THE SHERDS MCE-1 AND AT-2.

### Sherd MCE-1

K-fp/plag.	A/1	A/2	A/3	A/4	A/5	B/1	B/2	B/3	B/4	C/1	C/2
SiO <sub>2</sub> (wt %)	69.13	67.25	68.87	62.61	69.09	69.06	62.6	63.01	67.86	63.1	68.32
Al <sub>2</sub> O <sub>3</sub> (wt %)	19.26	18.91	19.29	17.77	19.31	19.22	17.96	18.59	19.39	17.47	20.15
CaO (wt %)	0.38	0.11	0.09	0	0.27	0.25	0	0.07	0.04	0	0.68
Na <sub>2</sub> O (wt %)	11.4	11.05	11.71	0	12.36	12	0.41	0.3	11.97	0.02	11.45
K <sub>2</sub> O (wt %)	0	0.18	0.21	15.15	0.02	0.17	15.98	15.28	0.07	14.93	0.06
<b>Total</b>	100.17	97.5	100.17	95.53	101.05	100.7	96.95	97.25	99.33	95.52	100.66
<b>Or</b>	0	1	1.2	<b>100</b>	0.1	0.9	<b>96.3</b>	<b>96.7</b>	0.4	<b>99.8</b>	0.3
<b>Ab</b>	<b>99.2</b>	<b>98.4</b>	<b>98.4</b>	0	<b>98.7</b>	<b>97.9</b>	3.7	2.9	<b>99.5</b>	0.2	<b>96.5</b>
<b>An</b>	0.8	0.6	0.4	0	1.2	1.2	0	0.4	0.1	0	3.2

K-fp/plag.	D/1	D/2	E/1	E/2	F/1	F/2	F/3	F/4	F/5	F/6	F/7
SiO <sub>2</sub> (wt %)	63.94	66.79	68.93	68.09	68.34	68.89	68.14	68.67	67.82	64.09	65.75
Al <sub>2</sub> O <sub>3</sub> (wt %)	18.85	18.95	19.95	19.17	20.14	19.51	19.98	18.84	19.99	17.28	17.48
CaO (wt %)	0.24	0.33	0.05	0.36	0.23	0.25	0.51	0.28	0.58	0.06	0.23
Na <sub>2</sub> O (wt %)	0.52	12.27	12.28	11.95	11.69	11.91	11.93	11.84	11.84	0.18	0.21
K <sub>2</sub> O (wt %)	14.37	0.15	0	0.06	0.04	0.1	0	0	0.07	16.24	15.97
<b>Total</b>	97.92	98.49	101.21	99.63	100.44	100.66	100.56	99.63	100.3	97.85	99.64
<b>Or</b>	<b>96.4</b>	0.8	0	0.4	0.2	0.5	0	0	0.4	<b>98.1</b>	<b>96.9</b>
<b>Ab</b>	2.3	<b>97.8</b>	<b>99.8</b>	<b>98</b>	<b>98.7</b>	<b>98.4</b>	<b>97.7</b>	<b>98.7</b>	<b>97</b>	1.6	1.9
<b>An</b>	1.3	1.4	0.2	1.6	1.1	1.1	2.3	1.3	2.6	0.3	1.2

amphibole	F/8
SiO <sub>2</sub> (wt %)	47.53
TiO <sub>2</sub> (wt %)	1.1
Al <sub>2</sub> O <sub>3</sub> (wt %)	5.64
FeO (wt %)	12.82
MnO (wt %)	1.09
MgO (wt %)	15.43
CaO (wt %)	10.6
Na <sub>2</sub> O (wt %)	1.29
K <sub>2</sub> O (wt %)	0.37
<b>Total</b>	95.87

## Sherd AT-2

pyroxene	1	2	3	4	5	6	7	8	9	10
SiO <sub>2</sub> (wt %)	51.86	51.93	50.44	50.5	51.11	50.77	48.12	48.64	51.93	52.65
TiO <sub>2</sub> (wt %)	0.25	0.27	0.24	0.36	0.35	0.16	0.51	0.67	0.18	0.29
Al <sub>2</sub> O <sub>3</sub> (wt %)	2.11	1.55	3.19	3.09	2.06	2.44	4.9	4.24	1.68	1.45
Cr <sub>2</sub> O <sub>3</sub> (wt %)	0.04	0.31	0.09	0.18	0.06	0.03	0	0	0.59	0.32
FeO (wt %)	6.64	4.87	7.06	7.84	6.55	6.59	8.39	9.23	4.77	4.68
MnO (wt %)	0.27	0.04	0.26	0.25	0.13	0.32	0.26	0.31	0.01	0
MgO (wt %)	15.62	16.17	14.9	15.05	15.08	15.38	13.85	14.29	17.15	17.17
CaO (wt %)	22.86	23.78	22.43	22.7	23.27	23.89	22.13	22.15	23.36	23.57
Na <sub>2</sub> O (wt %)	0.23	0.14	0.24	0.17	0	0.21	0.46	0.13	0.35	0.22
K <sub>2</sub> O (wt %)	0	0	0	0	0	0	0	0	0	0
<b>Total</b>	99.88	99.06	98.85	100.14	98.61	99.79	98.62	99.66	100.02	100.35

px/chromite	11	12	25	26	13	14	15	16	17
SiO <sub>2</sub> (wt %)	50.48	50.15	49.13	49.97	0.48	0.1	0.43	0.07	0.03
TiO <sub>2</sub> (wt %)	0.29	0.31	0.21	0.99	1.28	1.42	1.77	1.83	2.04
Al <sub>2</sub> O <sub>3</sub> (wt %)	3.07	3.38	4.73	4.06	9.81	10.29	10.33	10.6	10.38
Cr <sub>2</sub> O <sub>3</sub> (wt %)	0	0.11	0.1	0.08	28.97	27.96	21.42	20.48	21.73
FeO (wt %)	7.66	7.45	7.22	7.65	45.1	45.23	50.13	50.68	51.54
MnO (wt %)	0.1	0.22	0.25	0.45	0.54	0.36	0.56	0.75	0.64
MgO (wt %)	15.38	14.86	13.97	13.35	10.04	9.6	8.79	9.25	10.07
CaO (wt %)	23.12	23.26	23.38	23.03	0.08	0.11	0.1	0.16	0.05
Na <sub>2</sub> O (wt %)	0.19	0.08	0.36	0.58	0	0	0.02	0.71	0.15
K <sub>2</sub> O (wt %)	0	0	0	0	0	0	0	0	0
<b>Total</b>	100.29	99.82	99.35	100.16	96.3	95.07	93.55	94.53	96.63

K-fp/plag.	18	19	20	21	22	23	24	27
SiO <sub>2</sub> (wt %)	65.53	65.33	64.38	65.2	68.12	68.3	64.55	62.67
Al <sub>2</sub> O <sub>3</sub> (wt %)	22.54	22.03	17.53	17.81	19.42	19.62	18.65	19.45
CaO (wt %)	3.79	3.08	0.13	0	0.3	0.04	0.38	0.38
Na <sub>2</sub> O (wt %)	9.59	9.14	0.39	0.23	10.5	11.05	0.25	0.25
K <sub>2</sub> O (wt %)	0.11	0.07	16.18	16.25	0.27	0.09	15.28	15.24
<b>Total</b>	101.56	99.65	98.61	99.49	98.61	99.12	99.11	98.08
<b>Or</b>	0.6	0.4	<b>95.9</b>	<b>97.9</b>	1.7	0.5	<b>95.7</b>	<b>95.6</b>
<b>Ab</b>	<b>81.6</b>	<b>83.9</b>	3.5	2.1	<b>96.8</b>	<b>99.3</b>	2.4	2.4
<b>An</b>	<b>17.8</b>	<b>15.6</b>	0.6	0	1.5	0.2	1.9	2

**APPENDIX 10. DATA OF THE NEUTRON ACTIVATION ANALYSIS (NAA) OF THE SHERD TR-20, THE VOLCANITE FRAGMENTS IN THE SHERD MCE-1, AND THE BASALT SAMPLE MC-8.**

	TR-20	volcanite fragments (MCE-1)	basalt sample (Mc-8)
<b>As (ppm)</b>	11.0 ± 0.4	11.4 ± 0.4	33.6 ± 1.1
<b>Ba (ppm)</b>	726 ± 44	900 ± 40	1640 ± 90
<b>Ce (ppm)</b>	71.3 ± 2.3	21.6 ± 0.8	110 ± 4
<b>Co (ppm)</b>	19.2 ± 0.9	2.47 ± 0.12	27.2 ± 1.0
<b>Cr (ppm)</b>	271 ± 9	7.72 ± 0.73	84.4 ± 3.6
<b>Cs (ppm)</b>	5.83 ± 0.30	0.72 ± 0.08	1.48 ± 0.35
<b>Eu (ppm)</b>	1.41 ± 0.09	0.5 ± 0.04	1.72 ± 0.10
<b>Fe%</b>	3.92 ± 0.13	1.1 ± 0.04	4.62 ± 0.15
<b>Hf (ppm)</b>	6.43 ± 0.27	2.97 ± 0.13	7.58 ± 0.32
<b>K%</b>	1.78 ± 0.15	3.95 ± 0.14	2.40 ± 0.23
<b>La (ppm)</b>	31.82 ± 0.86	13.10 ± 0.4	54.5 ± 1.5
<b>Lu (ppm)</b>	0.37 ± 0.02	0.2 ± 0.01	0.23 ± 0.01
<b>Na%</b>	1.6 ± 0.05	0.29 ± 0.01	2.78 ± 0.09
<b>Nd (ppm)</b>	24 ± 5		28 ± 6
<b>Rb (ppm)</b>	86.9 ± 8.0	134 ± 9	99 ± 11
<b>Sb (ppm)</b>	0.95 ± 0.04	13.5 ± 0.4	1.43 ± 0.06
<b>Sc (ppm)</b>	13.88 ± 0.33	2.88 ± 0.10	14.7 ± 0.4
<b>Sm (ppm)</b>	6.19 ± 0.20	1.95 ± 0.06	7.73 ± 0.24
<b>Ta (ppm)</b>	0.72 ± 0.09	0.33 ± 0.05	
<b>Tb (ppm)</b>	0.74 ± 0.11		
<b>Th (ppm)</b>	12.7 ± 0.5	10.8 ± 0.3	18.2 ± 0.6
<b>U (ppm)</b>	2.9 ± 0.19	3.11 ± 0.14	3.6 ± 0.30
<b>Yb (ppm)</b>	2.81 ± 0.08	1.19 ± 0.04	1.64 ± 0.06
<b>Zn (ppm)</b>	78 ± 9	106 ± 8	76 ± 11

**CURRICULUM VITAE**

**Farkas Pintér**  
**Maros u. 20**  
**H-1122 Budapest, HUNGARY**

**27. 03. 1978:** born in Budapest

**1984-1992:** Primary school

**1992-1996:** High school

**1996-2001:** Eötvös University of Budapest, Institute of Geology

**2001:** M.A, Eötvös University; **Dissertation:** *Provenance Analysis and Investigation of Weathering Surfaces on „Red Marble“ Monuments from Hungary using Petrographic and Geochemical Methods*

**2001-2004:** DFG scholarship in the frame of the Graduate School „Anatolien und seine Nachbarn“ at the University of Tübingen, Germany

**Dissertation:** *Provenance study of the Early Iron Age Knobbed ware in Troia, NW Turkey and the Balkans. Petrographic and geochemical evidence*

**2005:** State Center for the Restoration and Conservation of Historic Monuments, Scientific Laboratory, Budapest, Hungary; assistant geologist.